LABORATORY EXPERIMENTS ON LAMINATION STRATIFICATION AND DESICCATION

by

Pierre Y. Julien and Yongjiang Lan

Colorado State University

Report CER89-90-PYL-YQL-15
Engineering Research Center
Colorado State University
Fort Collins, CO 80523
U.S.A.

May, 1990

Revised July, 1990

LABORATORY EXPERIMENTS ON LAMINATION STRATIFICATION AND DESICCATION

by

Pierre Y. Julien and Yongqiang Lan

Colorado State University

Report CER89-90-PYL-YQL-15
Engineering Research Center
Colorado State University
Fort Collins, CO 80523
U.S.A.

May, 1990

Revised July, 1990

"La plupart des erreurs des hommes ne viennent point tant de ce qu'ils raisonnent mal à partir de principes vrais, mais plutôt qu'ils raisonnent juste à partir de principes faux ou de jugements inexacts."

Lettre de Fenelon, dite de Port-Royal, pour l'éducation du Duc de Chevreuse.

Translation:

Man's foremost errors do not arise from false reasoning based on correct principles, but rather from correct reasoning based on incorrect principles or inexact judgement.

ACKNOWLEDGEMENTS

We are very grateful to M. Guy Berthault, who not only provided financial support for the experimental program, but manifested great enthusiasm during the review of the experimental program. This program of study has been completed with the thoughtful and dedicated assistance of Mr. Yi-Ching Chen who carried out early experiments, and Mr. Rodney Wittler who designed most of the experimental facilities. We also thank Mr. Nils R. Olsen and Mr. Yassen Raslan for their assistance in collecting data during the experiments and preparing photos for the reports, and Mrs. Jenifer Davis for patiently typing the manuscript.

FOREWORD

M. G. Berthault (1986, 1988) experimentally demonstrated that continuous settling of heterogeneous sediment mixtures in air and water causes a repetitive segregation of particles. The characteristic height of deposits increased with the difference in particle sizes, but does not depend on the rate of sedimentation. Sorting on inclined surfaces was found to remain parallel to the sloping bed. This mechanical process could explain the formation of laminae generally found in sedimentary rocks.

The report "Flood Deposits, Bijou Creek, Colorado, June, 1965" by McKee, Crosby and Berryhill (1967), showed that flood deposits are composed of more than 90% of horizontal strata characterized by vertical sorting, with laminae and stratification joints. After analyzing the report of Guy, Simons and Richardson (1986); "Summary of Alluvial Channel Data from Flume Experiments, 1956-1961", he undertook to experimentally investigate the Bijou Creek flood in laboratory flumes in order to observe the internal structure of deposits through the glassed flume walls.

Subsequent contacts with Dr. E.V. Richardson and then P.Y. Julien lead to the definition of the experimental program detailed in this report.

FOREWORD TO THE REVISED EDITION

The copies of several photographs, primarily those on stratification (Pictures 38-95), turned out very dark and without contrast. It has therefore been decided to prepare a revised edition which hopefully illustrates better the results of our experimental program. Among the few modifications: 1) a new set of photographs to replace Pictures 38-43; 2) the results of a very simple experiment on lamination in Appendix B; and 3) a comment from M. G. Berthault in Appendix C. It may also be worth noting that a video cassette of the experiments on lamination and stratification is available.

TABLE OF CONTENTS

LIST OF FIGURES

LIST OF TABLES

LIST OF PICTURES

LIST OF SYMBOLS

D_s	Diameter of particle
D_{10}	particle size of which 10% of mixture is finer
D_{25}	particle size of which 25% of mixture is finer
D_{50}	particle size of which 50% of mixture is finer
D_{75}	particle size of which 75% of mixture is finer
D_{90}	particle size of which 90% of mixture is finer
f	Darcy-Weisbach friction coefficient
Fr	Froude number
h	original depth of water in the cylinder or flow depth
h_u	flow depth on top of delta
h_d	flow depth downstream of delta
h_{eq}	flow depth at equilibrium (cm)
H	height of base deposit
H-Lam	horizontal lamination
H.L.	horizontal lamination
Q	flow discharge
S_w	water surface slope
U_*	friction velocity (cm/sec)
V_m	mean velocity (cm/sec)
V_s	surface velocity (cm/sec)
V_u	mean velocity on top of delta
V_d	mean velocity downstream of delta
V_{su}	surface velocity on top of delta
V_{sd}	surface velocity downstream of delta
V_{bu}	near-bed velocity on top of delta
V_{bd}	near-bed velocity downstream of delta
V_{meq}	mean velocity at equilibrium
V_{beq}	near-bed velocity at equilibrium
V_{seq}	surface velocity at equilibrium
τ_o of shear	bed shear stress (dynes/cm^2)
ξ_{eq}	water surface elevation at equilibrium (cm)
(84cm-H)	height of fall of particles
Particle shape	defined as the sphericity of particle
Fall velocity	descending velocity of particle in air or water
Cross-Lam	cross-lamination

I. INTRODUCTION

Several researchers have carried out extensive field and laboratory investigations on lamination processes under various flow regimes where bedforms of various shapes and sizes migrate in the downstream direction. Few studies, however, examined the internal structure of horizontal laminae seen in bed configurations with motion of sediment. Upper regime conditions are difficult to control because of the inherent hydraulic instability of open channel flows near critical flow conditions. For instance, McBride et al. (1975) stated, "we were unable to produce laminae during aggradation at plane bed conditions."

This study stems from the recent investigations of Berthault (1986, 1988). The primary objective of this experimental program is to examine the fundamental process of segregation of heterogeneous sediment mixtures under settling conditions, and under fluvial conditions of plane bed with sediment transport.

This study focuses on three primary aspects: 1) settling in air and water; 2) segregation under fluvial conditions; and 3) desiccation of alluvial deposits.

The facilities used in the Hydraulics Laboratory at the Engineering Research Center, Colorado State University, include a specifically designed settling column, a recirculating plexiglas flume, and a wide rectangular flume.

The square cylindrical plexiglas settling column allows the visualization of segregation of heterogeneous sand mixtures in air and water. Photographs are taken from the sides of the column and the characteristics of sorting of various mixtures with different densities, sizes and shapes are documented.

The recirculating plexiglass flume has been particularly designed for the analysis of lamination , stratification and desiccation processes under a wide variety of flow conditions. The flume recirculates both water and sediment in order to provide a constant supply of sediments under steady flow conditions during the course of each experiment. The slope of the channel is determined prior to each run in order to study the thickness of laminae and the angle of laminated deposits with the slope of the flume bed.

The wide rectangular flume allows the study of lamination processes under wide flow conditions not constrained by the wall effects of narrow flumes. This facility provides additional insight for processes that occurred under field conditions.

A key feature in this investigation is the use of sand mixtures with grains of different colors. Mixtures of natural black and white sediment particles of different sediment size, shape and specific gravity ensure a better visualization of the laminae besides providing an assessment of the distribution of different sediment particles.

This study is limited to horizontal lamination without bedforms under various conditions of discharge and slope for two different sediment mixtures. The superposition of deposits is induced by controlling the tailwater elevation which does not affect the lamination process and maintains a constant supply of sediment during the entire investigation.

Several partial reports have been produced on various aspects of this program: Julien and Chen (1989a), Julien and Chen (1989b), Julien and Lan (1989), and Julien and Lan (1990). The purpose of this report is to compile the most relevant material from these early reports, and present the synthesis of these partial reports completed with additional ideas, equipment and measurements that were carried out in the latter part of the research program.

The reader will find in the following, a review of pertinent literature, an analysis of settling of sand mixtures in a vertical cylinder, and a study of lamination, stratification and desiccation in recirculating flumes with complementary experiments in the wide rectangular flume. Numerous illustrations are provided in order to better visualize the results of our experiments.

II. SEDIMENTATION OF SAND MIXTURES

This modified version of the studies of Julien and Lan (1990) reports on the experiments of sedimentation of heterogranular mixtures in a rectangular vertical cylinder. Several types of heterogeneous sand mixtures are used for the experiments, with materials of different sizes, density and shape. Settling experiments were carried out in air and in water.

2.1 Literature Review on Lamination

Horizontal lamination in mixtures of sand particles is very common in many aqueous environments. Horizontal laminae are composed of many thin layers of slightly different grain sizes. Their dimensions range from fractions of a millimeter to several millimeters. Those thin laminae are always in different thicknesses and the finer laminae are often darker than coarser ones, due to relatively larger proportions of clay, mica, and heavy minerals (Bridge, 1978; McBride et al., 1975).

Berthault (1986, 1988) conducted series of experiments on the lamination characteristics in still water and running water conditions. These laminae resulted from spontaneous periodic and continuous grading process, which took place immediately following the deposit of the heterogranular mixture. From his experiments some lamination characteristics could be found. The thickness of laminae increased as the difference between
the size of particles became greater in still water, and the laminae thickness also increased with flow velocity of running water. Also, the slope of the surface has little influence on lamination and seems to favor it.

Few laboratory experiments of horizontal lamination have been obtained for unidirectional, upper flow regime flow conditions. However, from some observations, the horizontal laminae were formed under lower flow regime near critical flow condition. Paola et al. (1989), along with the experiments of Bridge and Best (1988), explained that lamination results from the superposition of two processes: 1) high-frequency erosion and deposition due to turbulence; and 2) migration of low-amplitude bed forms that is neither upper-regime nor lower-regime solely.

Regarding the upper-regime bed, some researchers invoke the interaction of sediment transport and turbulence to interpret the formation of horizontal lamination. Bridge (1978) proposed the "burst-sweep cycle" in the turbulent boundary layers to explain the vertical sorting that defines laminae. The bursting process, a quasi-cyclic sequence of fluid motion, caused temporal and spatial variation in bed shear and lift forces acting on sediment particles in motion over plane beds. It is an average deterministic sequence of ejection (burst) and sweep events repeated in space and time. Bursts will cause upward dispersion of the suspended load throughout the flow, also some of the saltating load will carry coarser grains due to higher shear stress. As bed shear stress decreases, the dispersed particles settle down by a "like-seeks-like" mechanism (Moss, 1963; and Kuenen, 1966) to deposit together and to form a laminated layer. According to this possible explanation, the repeated burst-sweep cycle forms laminae.

In the report of investigation in horizontal laminae formed under upper-regime plane bed by Cheel and Middleton (1986b) they suggested that the probable mechanism for the formation of FU (fining-upward) and CU (coarsening-upward) laminae was the burst-sweep process: 1) FU laminae formed by fallout of progressively finer sand bursted upward temporarily, and 2) CU laminae formed of sorting by dispersive pressure in a layer of high grain concentration produced by locally high shear stress developed beneath a sweep of high speed fluid approaching the bed.

They added that because of the arbitrary position of the units over which measurements were made, there may be some overlap of laminae so that the heavy minerals assigned to fining-upward laminae may actually be at the base of coarsening upward laminae. Allen (1984) created a model based on the larger coherent structures of the turbulent boundary layers to explain the formation of horizontal laminae from upper-regime plane bed. He assumed that the upper-regime plane bed occurred in a long bed wave of little height which was driven rapidly downstream and forced by the larger coherent turbulence structure to which they were coupled through a pattern of bed shear stress. Under steady uniform flow conditions each bed wave generated a normally graded lamina. This model provides one possible explanation for the origin of horizontal lamination at high sediment transport stages but is inadequate in describing the formation from flat bed in slow-moving bed forms (e.g. Smith 1971; McBride et al., 1975). Also, the larger coherent turbulent structure within outer region of boundary layers was different than Bridge's model (1978) within inner region of turbulent boundary layers.

In the experiments of Paola et al. (1989), the deposition of a lamina was usually initiated by a surge of high-concentration of coarser grains near the bed, which decelerated and rapidly stopped during a few tenths of a second. Subsequently, the fine grains were sieved from the flow as their saltation or rolling paths direct them into pockets in the pores created by the larger stationary grains. This process of selective removal of fine grains by smoothing the top of the bed: the effective friction angle between the bed surface and the larger grains was reduced while that of the fine grains trapped in the bed was decreased. This "glazing" process took place over several seconds and was not directly related to turbulent fluctuations. It differed with Bridge's model (1978).

Through the investigation of bedforms in the Platte River, Nebraska, Smith (1971) observed that horizontal laminae were produced by migration of thin sand sheets, i.e. low amplitude sand waves, with downstream foresets. They had very shallow to nearly horizontal stoss sides, steep foresets at the angle of repose. In cross section, the thinnest waves appeared as horizontal laminae, whereas the thicker waves showed readily discerned planar or cross-lamination. The most important factor controlling production of the thin flat-topped waves is the very shallow depths in which they formed. The Froude numbers range from 0.46 to 0.73 which were below unity. They produced internal horizontal stratification which is similar to upper-regime plane bed deposition except that the grains were differentiated into alternating coarse and fine lamination by sorting processes at the foreset.

Moreover, McBride et al. (1975) proposed a series of experiments to reproduce horizontal laminae under lower-regime bed. They found that lamination is observed as the result of the migration of very low-relief ripple and in-phase waves which produced thin laminae when coarser grains in the lee side of the bedforms buried finer grains in the stoss
side of the bedforms; the lack of avalanche face prevented cross-laminae from developing. Shallow depths also were essential to form the near horizontal laminae, because at greater flow depths, ripples developed avalanche faces and produced micro cross-laminae.

Bridge (1978) listed hypotheses formulated by various authors to explain the origin of near-horizontal lamination in unidirectional aqueous flow. Cheel and Middleton (1986b) summarized some research results on the formation of horizontal laminae under upper-regime bed conditions. Table 1 summarizes the various hypotheses attempting to explain horizontal lamination, also indicating those found in recent literature.

As stated by Allen (1984), many workers explaining such a combination of features, have qualitatively recognized the importance of some periodic or quasi-periodic phenomenon, either located in the flow or in the uppermost levels of the bed. Velocity pulses or, what amounts to the same thing, the passage of large eddies have had a wide appeal (Kuenen and Menard, 1952; Kuenen, 1953, 1957; Ten Haaf, 1956; Pettijohn, 1957, 1965; Bouma, 1962; Lombard, 1963; Allen, 1964). On the basis of field observations or laboratory experiments, other investigators have explained parallel laminations by the travel of extremely flat symmetrical to strongly asymmetrical bed waves (Jopling, 1964, 1966, 1967; Jopling and Walker, 1968; Smith, 1971; McBride et al., 1975; Allen, 1982), although not always in the context of an upper-stage plane bed. Unrug (1959) and Wood and Smith (1959) saw parallel laminations as caused by the segregation of the coarser grains into distinct clouds within the flow. Hsü (1959) attributed lamination to laminar flow at the bed. A "like-seeks-like" mechanism of grain sorting in the bedload layer was advocated by Moss (1962, 1963) and Kuenen (1965, 1966). A sorting process was also supported by Frostick and Reid (1977).

The idea that parallel lamination depended on a deterministic flow phenomenon achieved semi-quantitative expression under Bridge (1978), who proposed that each texturally defined lamina represented a cycle of bursting, in circumstances of net sediment accretion. The uplifting and eventually bursting streak was expected to advect bedload sediment into the outer parts of the flow, from whence grains were subsequently redeposited after sorting. The textural grading of the lamina was suggested to vary with the general coarseness of the sediment in transport and with the net deposition rate. A particularly appealing feature of Bridge's model is its apparent ability to predict the streamwise scale of a lamina from the burst period, dependent as pointed

Table 1. Summary of hypotheses explaining the origin of horizontal lamination

	Reference	Summary of Hypothesis
1.	Kuenen and Menard (1952) Kuenen (1953, 1957)	Velocity pulsations in turbidity current, perhaps with one sorting sorting by traction.
2.	Ksiazkiewicz (1952)	Diluted secondary turbidity currents suspended above bed.
3.	Ten Haaf (1956)	Sorting action of vortices by turbulence in turbidity currents.
4.	Hsü (1959)	Settling and laminar flow of fluidized sediment along bed.
5.	Unrug (1959) Wood and Smith (1959)	Settling from tail of turbidity current with a non-uniform concentration.
6.	Bouma (1962) & Lombard (1963)	Small turbulence eddies. Current velocity pulses with settling or traction.
7.	Moss (1963) Kuenen (1966)	Grains of similar susceptibility to transport tend to deposit together, i.e. spatial & temporal selection similar grains due to grain interaction under quasi-steady flow condition - the "like-seek-like" principle.
8.	Allen (1964)	Pulsating sediment supply due to separate large scale eddies. Upper regime plane bed.
9.	Walker (1965)	Intermittent supply of mixes sediment to top of viscous sublayer followed by differential settling through; for finer grained laminae. Coarser grained laminae under upper regime plane bed.
10.	Sanders (1965)	Settling and traction during current velocity fluctuation. Not upper regime plane bed.
11.	Jopling (1967)	Attributed laminae to the superposition of longitudinal segregations of bedload grains under aggradation of a upper regime plane bed.
12.	Pettijohn (1957, 1975)	Transitory phases or minor chance fluctuations in velocity of depositing current.
13.	Smith (1971) McBride et al. (1975)	Migration of very low relief bedforms (diminished ripples and dunes).
14.	Frostick and Reid (1977)	Combine the ideas of Pettijohn, Moss and Kuenen.
15.	Bridge (1978)	Described possible lamination formation due to the effect of single burst-sweep cycle on a plane bed.
16.	Hesse and Chough (1980)	Suggested that a horizontal lamination formed with multiple burst and sweep events on plane bed.
17.	Allen (1984)	Laminae form due to the shifting distribution of boundary shear stress as large eddies move down-stream over a plane bed.
18.	Bridge and Best (1988)	Laminae form by both migration of low-relief bedwaves and the turbulent bursting process.
19.	Paola, Wiele and Reinhart (1989)	Extremely low amplitude bedforms. Initial deposition from small scale turbulent fluctuations in shear stress followed by sieving out mechanism resulting in a smooth surface process termed glazing.

out on flow thickness and mean velocity. The difficulties - and they are critical - concern the transverse scale of the lamination and the volume of a typical lamina in relation to the burst from which it is supposed to have been largely deposited.

Bridge and Best (1988) concluded that: "it appears that laminae can be formed by both the migration of low-relief bedwaves and the turbulent bursting process, as recognized by Paola et al. (1989). Laminae formed by these two processes should be interposed, but will differ in lateral extent and thickness.

It is interesting to notice that Kuenen (1966) reported that: "current pulsations are so numerous that they should produce ten to a hundred times more laminae than are present." He also states in his abstract: "the selective concentration is due to the tendency of particles moving along the bottom to join stationary ones of equal weight, density and shape..." The principle of "like-seeks-like" dominates the accumulation of grains that are rolling over the bed between excursions into the saltating carpet. Kuenen (1966) also stated that "in spite of extremely uniform discharge without pulsation, lamination developed in nearly all experiments." Additionally, "Rolling of grain on this surface and selective accumulation becomes possible - the lamination begins to join... Lamination developed as soon as sufficient time was allowed for the required sorting to take place."

2.2 Experiments

2.2.1 Experimental Set Up

The experimental equipment particularly designed for this study is sketched in Figure 1 and also shown in Picture 1. The vertical cylinder is made of plexiglass with a dimension of 10 cm x 10 cm x 84 cm(height). The release of heterogranular mixtures from the square cone to the cylinder is well controlled by a precisely designed gate valve at the bottom of the cone. A valve is installed at either end of the cylinder to supply or drain water during and/or after experiments. The cone at the top is removable.

2.2.2 Sediment Mixtures Used in the Experiments

Ten types of sediments, varying in size, density, and shape, have been used in this study. The size distributions of these materials are shown in Figure 2 and some characteristics of these sands are listed in Table 2 where D_{10}, D_{25}, D_{50}, D_{75} and D_{90} represent the sizes of which 10%, 25%, 50%, 75% and 90% of the materials are finer, respectively. Not listed in Table 2 is the

sphericity of the particle which is difficult to define. Visual observations indicate that ERC #1, ERC #2, ERC #3, ERC #5, limestone #1, and limestone #2 are rounded, coal #1, coal #3, coal #4, B2040 and B3060 are angular, and the others are between rounded and angular.

With these many sediment samples ranging from very fine material to coarse sand size, we are able to obtain different types of mixtures for different purposes. In order to see the possible differences of lamination from differences in size, density, and shape, mixtures listed in Table 3 are proposed for this experiments. Generally, a mixture is composed of one white material and one black material for convenient observations. Also listed in Table 3 includes the conditions under which the experiments are conducted.

2.2.3 Experimental Procedure

After a designed mixture is well prepared in a certain container, the mixture is poured into the cone at the top of the cylinder. The control valve is then opened to let the mixture settle directly to the center of the cylinder. The rate of settling is controlled by the control valve. During the process of sedimentation, the cylinder is held stationary without vibration. Time spent in each run is recorded in order to determine the rate of deposition by dividing mixture volume by time. The process of sedimentation of different mixtures is also documented. At the end of each run, a few pictures in different directions are taken to illustrate the lamination phenomenon.

The experiments are conducted under two conditions, with or without water in the cylinder. Under both conditions, the fall (or settling) velocity of the particles influences the formation of laminae. To achieve this, a base, defined as the original height of sediment at the bottom of the cylinder before the start of each run is set before starting the run. This base can be replaced by several short wood logs in square shape (approximately 10 cm x 10 cm x 10 cm). Obviously, higher base reduces the fall velocity of particle when it impacts with the particles on the base and surely weakens the splashing of particles.

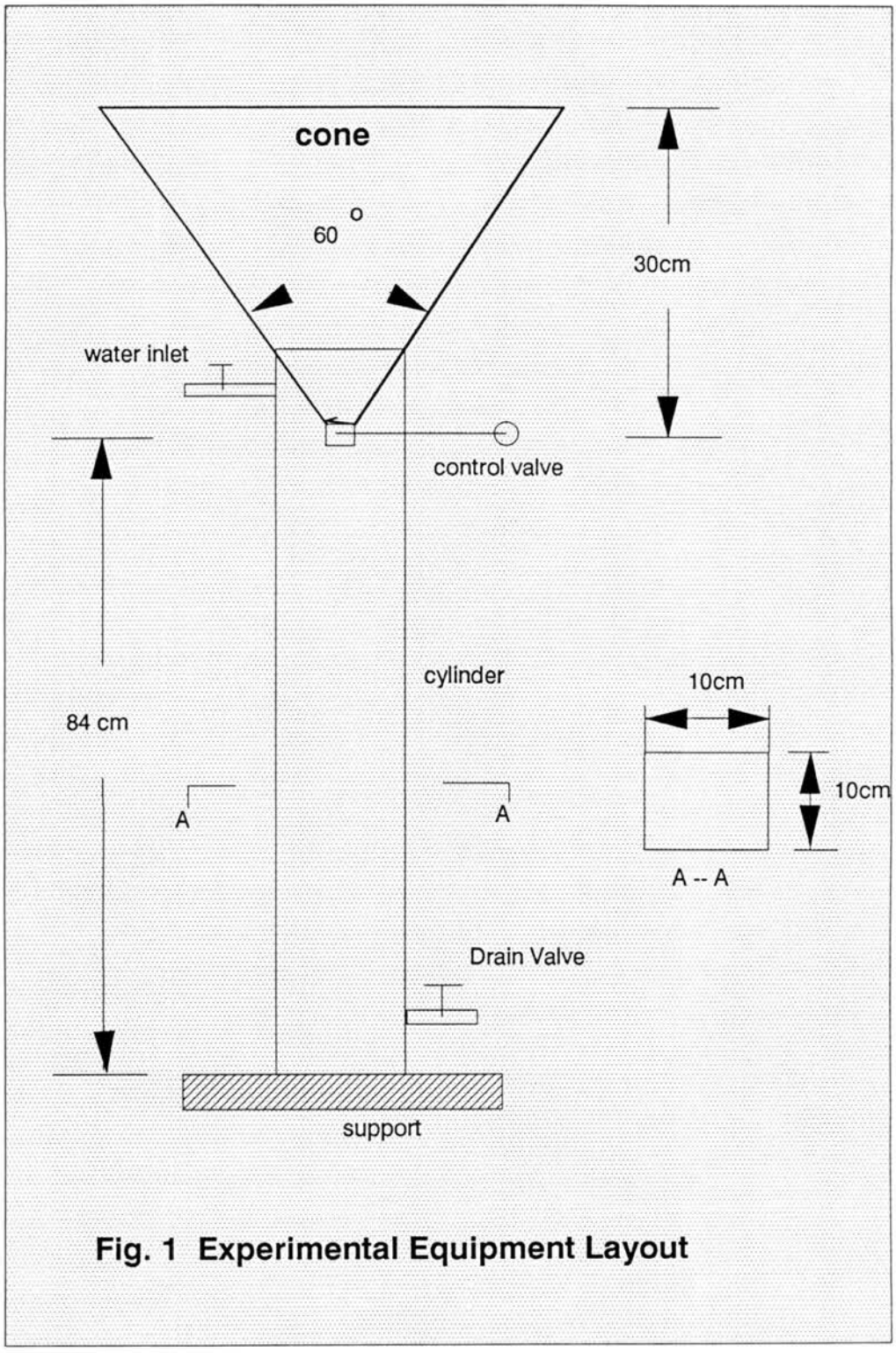

Fig. 1 Experimental Equipment Layout

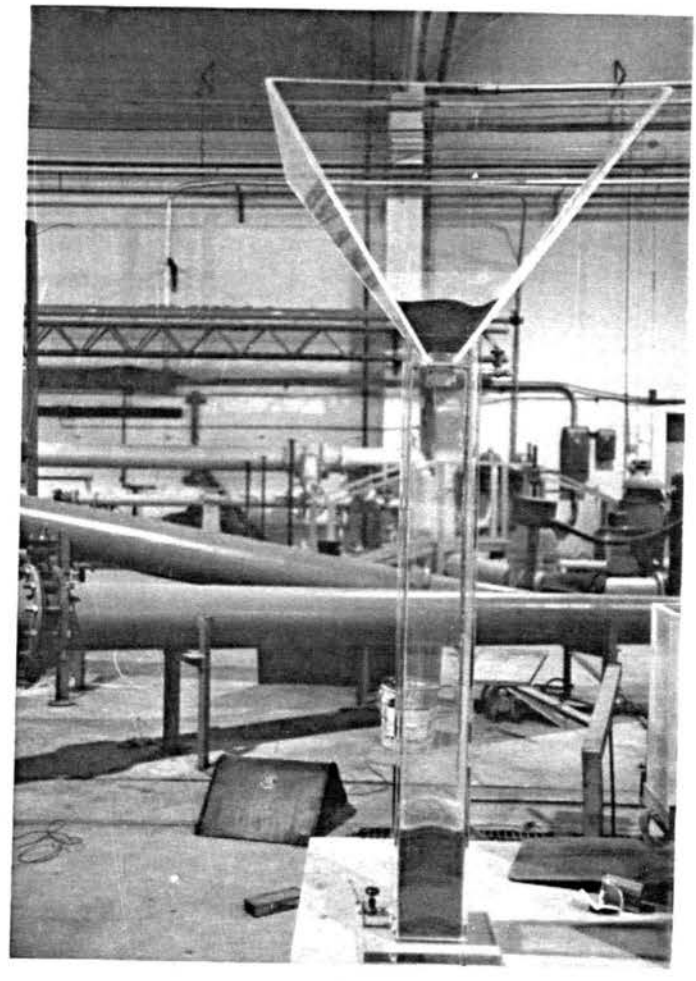

Picture 1. Experimental setup

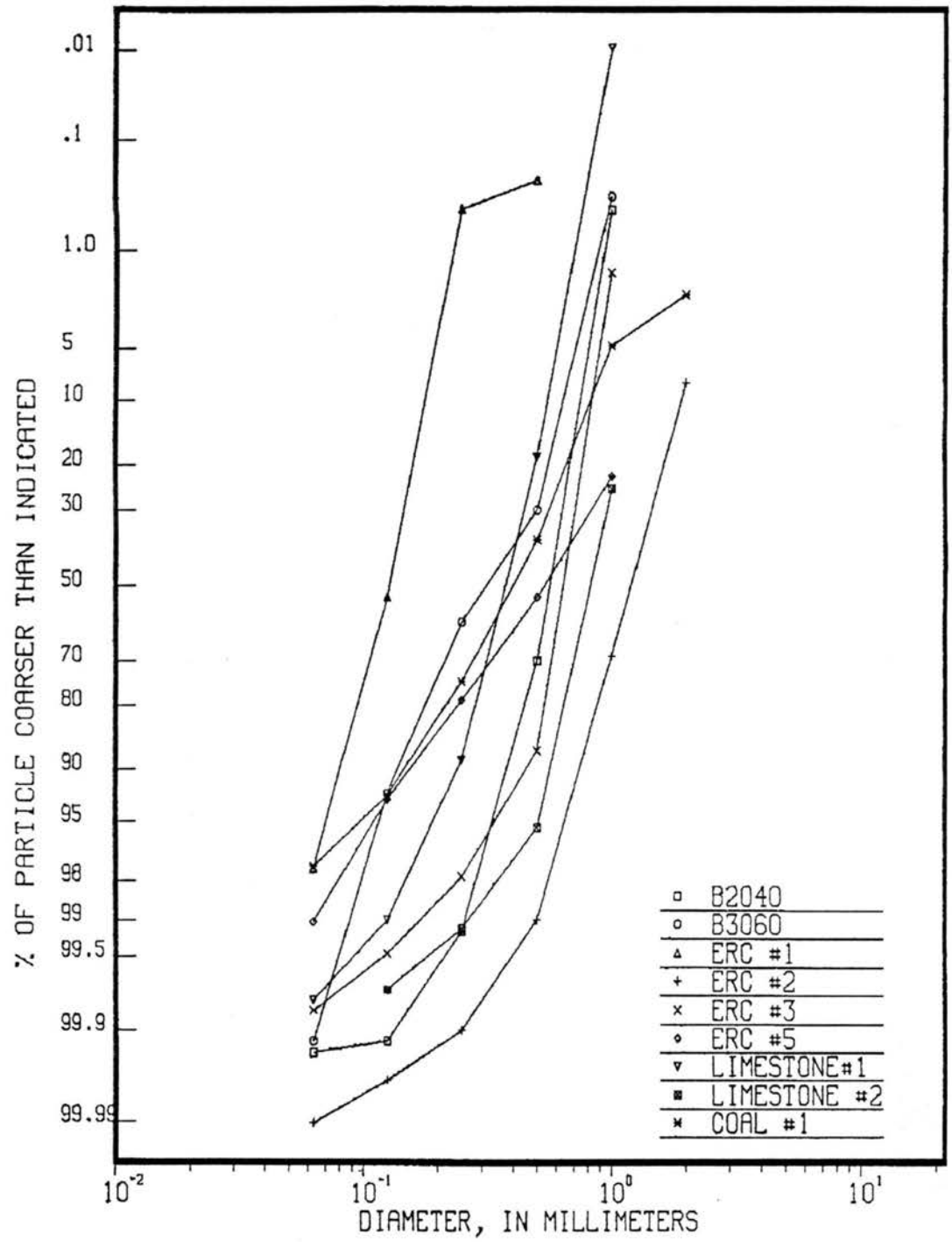

Figure 2. Size distribution curves for tested sands

Table 2. Characteristics of sands tested

Sand	Color	Density	Angle of repose (degree) in air	Angle of repose (degree) in water	Angularity	D_{10} (mm)	D_{25} (mm)	D_{50} (mm)	D_{75} (mm)	D_{90} (mm)
B2040	black	2.70	39.5	38	angular	.380	.480	.575	.670	.760
B3060	black	2.70	37	36	angular	.140	.205	.335	.550	.620
ERC #1	white	2.45	35	32	rounded	.084	.110	.130	.155	.180
ERC #2	white	2.65	37	34	rounded	.720	.900	1.200	1.500	1.900
ERC #3	white	2.65	37.5	35	rounded	.480	.550	.635	.730	.825
ERC #5	beige	2.65	42.5	35	rounded	.150	.290	.558	.970	
limestone#1	white	2.65					.310	.390	.470	
limestone#2	white	2.65	37	34	angular		.760	.910	1.005	
coal #1	black	1.30					.260	.410	.575	
coal #2	black	1.30	40	40	very angular			.250		
coal #3	black	1.30						.665		
coal #4	black	1.30						1.240		

Table 3. Sand mixtures and testing conditions

Mixture	Combination	Characteristics	In Air	In Water
1	B2040&ERC#3	similar size & density	yes	yes
2	ERC#1 & B3060	different size & similar density (fine sands)	yes	yes
3	ERC#1 & coal#1	different density, size and shape	yes	yes
4	ERC#3 & coal#3	similar size & different density & shape	yes	yes
5	limestone#1 & B3060	similar size, density & different shape	yes	yes
6	limestone#2 & coal#1	different size & shape, similar density	yes	yes
7	limestone#2 & B3060	different size & shape, same density, limestone much coarser	yes	no
8	ERC#2 & coal#1	different size, shape & density, lighter material, finer	yes	no
9	limestone#1 & coal#2	different density, size & similar shape	yes	yes
10	limestone#1 & B2040	same density, different shape & size	yes	yes

2.3 Experimental Results

A summary of experimental results from the present experiments is given in Tables 4 and 5 for those in air and in water, respectively. In these tables, 'proportion' means the volumetric ratio of one type of material over the other in the mixture, and 'rate of dep' denotes the rate of sedimentation of the mixture. Tables 4 and 5 give a general idea how different types of mixtures affect the formation of laminae. Detailed explanation of these two tables are given in the next two sections.

Table 4. Results of tests in air

Run #	Mixture	Proportion	Rate of Dep. (cm^3/s)	Observation	Pictures
1	1	1:1	2.05 & 5.76	no clear lamination	2, 3
2	2	1:1	9.14	clear lamination	4, 5, 6
3	2	1:1	9.14	clear lamination	7, 8, 9
4	3	1:1	7.00	clear lamination	10
5	4	1:1	4.01	no clear lamination	11
6	5	1:1	9.00	no lamination	12
7	6	1:1	5.20	no lamination	
8	7	1:1	9.00	no lamination	13
9	8	1:1	9.00	no lamination	14
10	9	1:1	3.44	no clear lamination	15
11	10	1:1	1.619	no clear lamination	16

Table 5. Results of tests in water

Run #	Mixture	Proportion	Rate of Dep. (cm^3/s)	Observation	Pictures
12, 13, 14, 15	2	1:1	9.14	no clear lamination	17, 18, 19, 20
16	2	1:1	0.384	no clear lamination	21, 22, 23
17	3	1:1	9.0	no lamination	24
18	4	1:1	0.797	clear lamination	25, 26, 27, 28
19	5	1:1	0.837	no clear lamination	29, 30, 31
20	10	1:1	0.759	clear lamination	32, 33, 34
21	1	1:1	1.02	no lamination	no picture
22	6	1:1	1.05	no lamination	no picture
23	7	1:1	0.90	no lamination	no picture
24	8	1:1	0.750	no lamination	no picture
24	9	1:1	1.30	no lamination	no picture

2.3.1 Sedimentation in Air

Detailed results from sedimentation experiments in air are presented in the following including observations of the sedimentation process and pictures.

Run #1

This run actually includes two tests, one at a higher rate of sedimentation with no base and the other at a lower rate with high base.

In the first test, the base height, denoted as H, is zero. The rate of sedimentation is 2.05 cm^3/sec. During the experiment, splashing of falling particles, when they impact with surface of deposit on the bottom, dominates the process due to high fall velocities of the particles. The jumping distance of particles can vary from zero to 5 centimeter, this is, from the center to the wall of the cylinder (see Figure 3 below). Rolling of one type of particles on the other is not obvious. And eventually, no lamina is formed (see Picture 2).

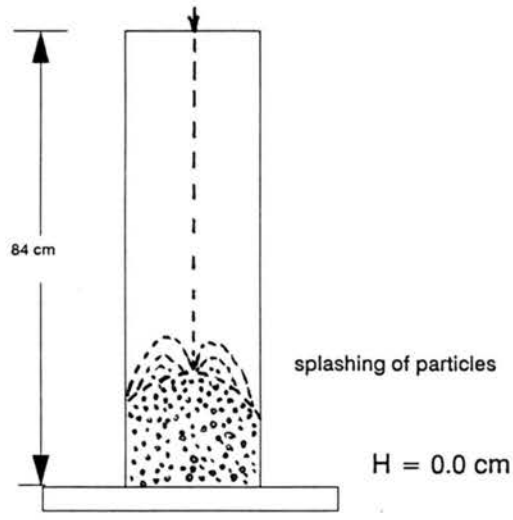

Figure 3. Positioning of cylinder for run #1

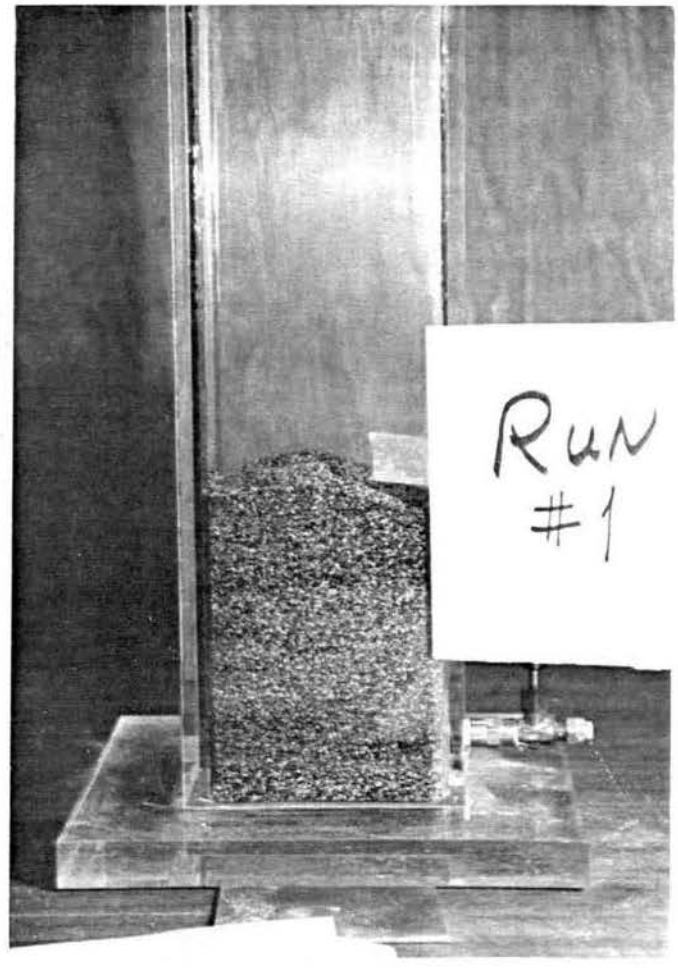

Picture 2. No clear laminae from run #1

Mixture #1: white ERC #3, D_{50} = 0.635 mm
and black B2040, D_{50} = 0.575 mm

In the second test, the height of the base is no longer zero but 61.5 cm. And the rate is 5.76 cm^3/sec. Consequently, the fall velocities of particles are dramatically reduced. The splashing of particles is much weakened. Meanwhile, a cone is well formed and landsliding occurs (see Figure 4). Again, no lamina is observed (see Picture 3).

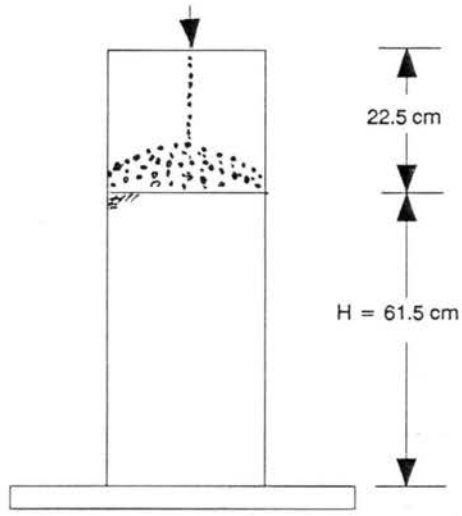

Figure 4. Positioning of cylinder for run #1 (2)

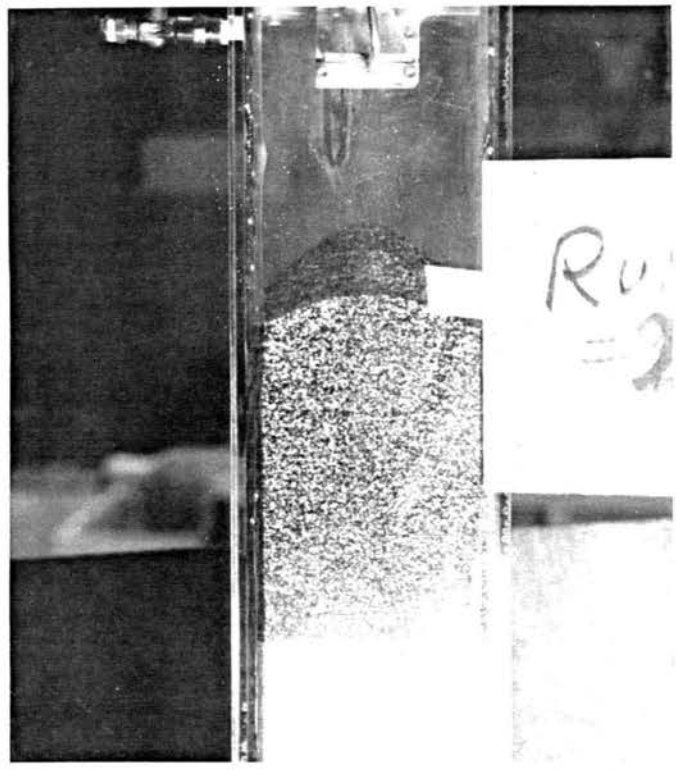

Picture 3. No clear laminae from run #1 (2)

Mixture #1: white ERC #3, D_{50} = 0.635 mm
and black B2040, D_{50} = 0.575 mm

Run #2

In this run, the height of the base is zero. And the rate is 9.14 cm^3/sec. Splashing of particles does not occur while landsliding is dominant. Rolling of black particles on the white particles before landsliding is observed. Consequently, clear laminae with thickness less that 0.5 cm are observed (see Picture 4, 5, and 6).

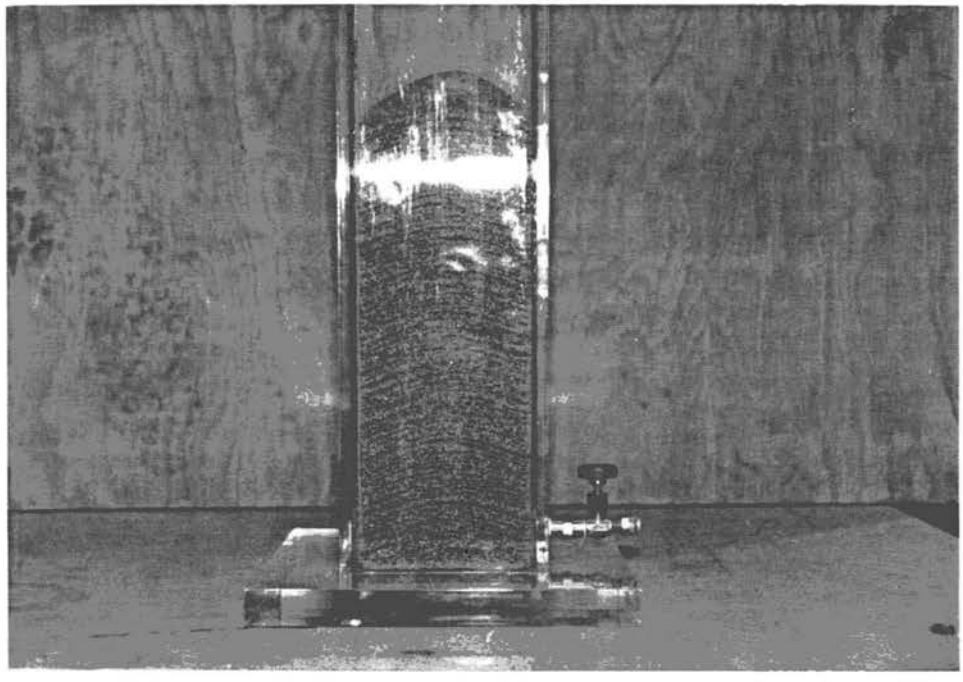

Picture 4. Clear laminae from run #2

Mixture #2: white ERC#1, D_{50} = 0.130 mm
and black B3060, D_{50} = 0.335 mm

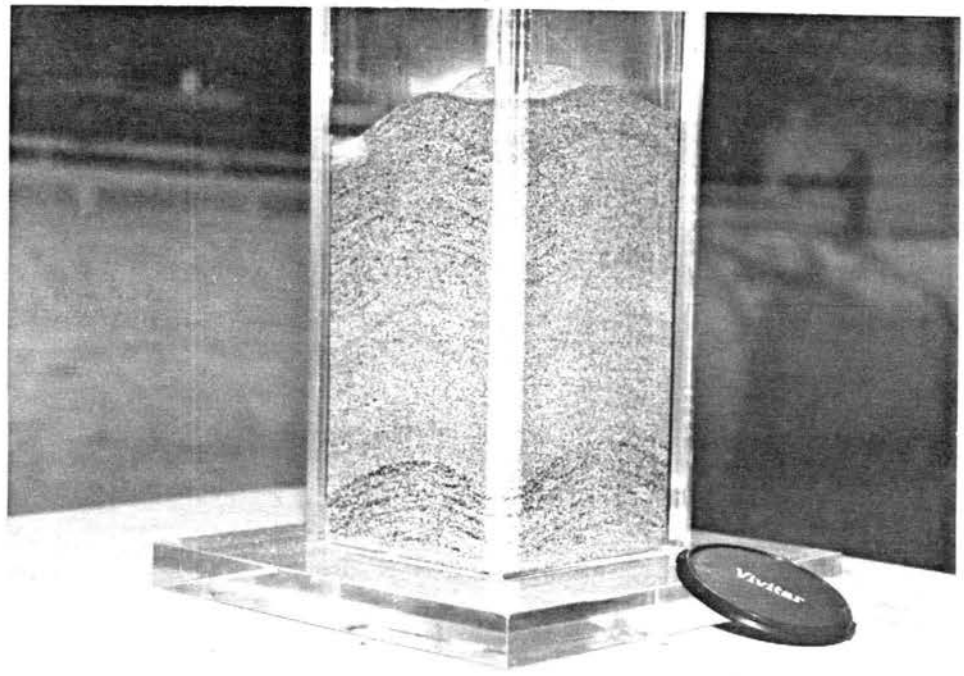

Picture 5. Clear laminae from run #2

Mixture #2: white ERC#1, D_{50} = 0.130 mm
and black B3060, D_{50} = 0.335 mm

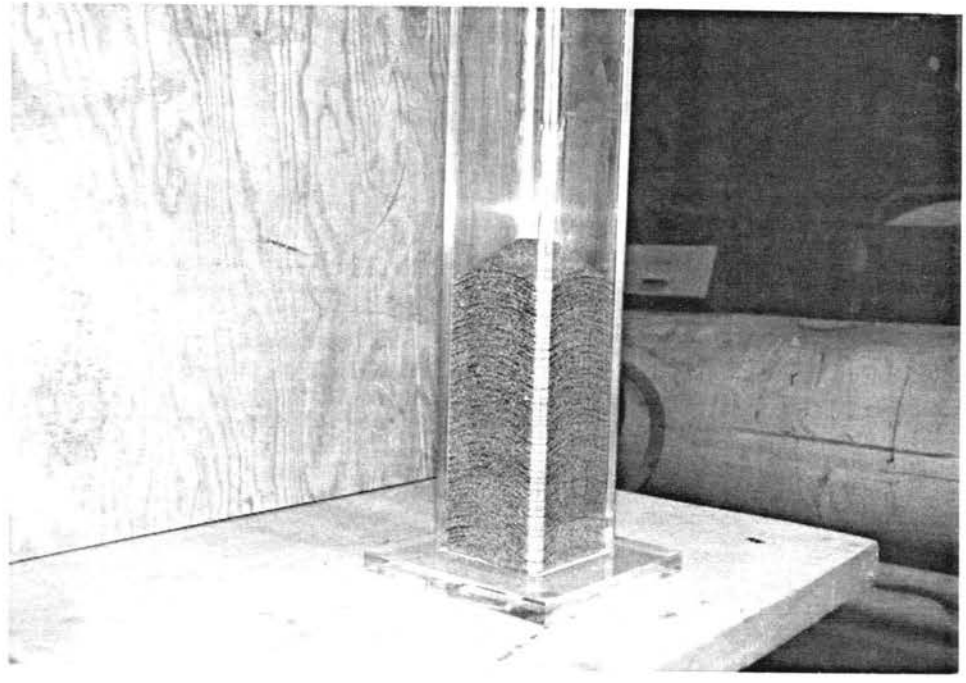

Picture 6. Clear laminae from run #2

Mixture #2: white ERC #1, D_{50} = 0.130 mm
and black B3060, D_{50} = 0.335 mm

Run #3

This run is under the same condition as in run #2 except that the cylinder is not straight up but a little inclined with an angle of approximately 5 degrees (see Figure 4). The purpose of this setup is to see the importance of rolling distance of the particles. Pictures 7, 8, and 9 are taken in directions of A, B, and C shown in Figure 4. From these pictures, it can be seen easily that a longer rolling distance produces clearer lamination. The thickness of the laminae, however, remains unaffected by the inclination angle.

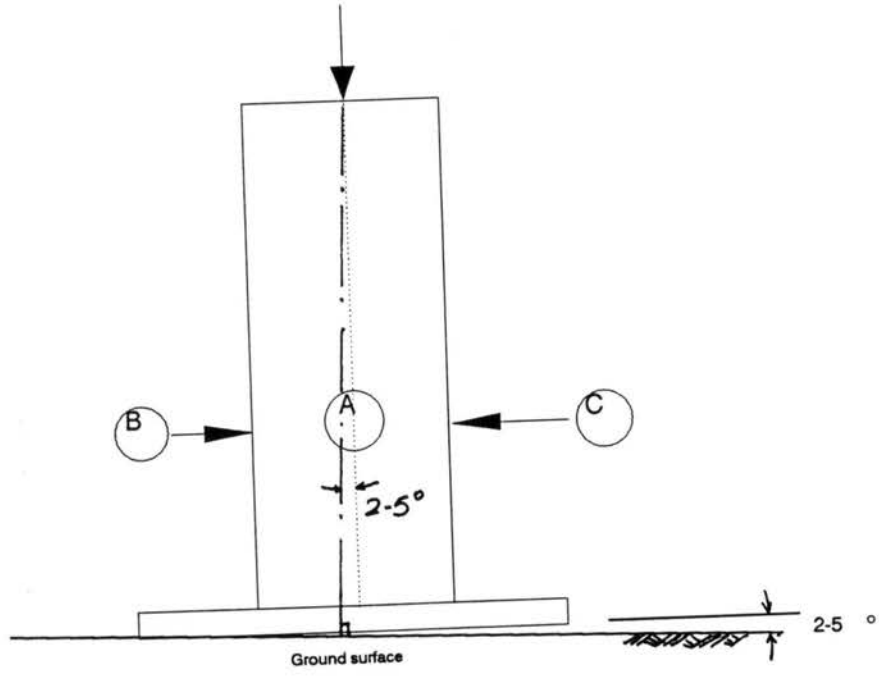

Figure 5. Positioning of cylinder for run #3

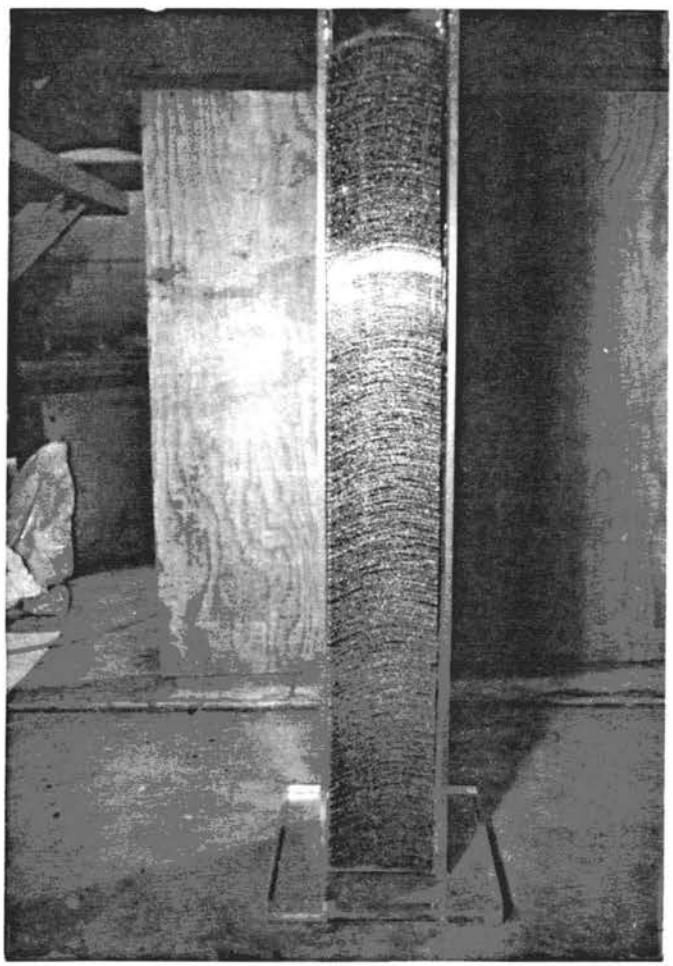

Picture 7. Clear laminae from run #3

Mixture #2: white ERC #1, D_{50} = 0.130 mm
and black B3060, D_{50} = 0.335mm

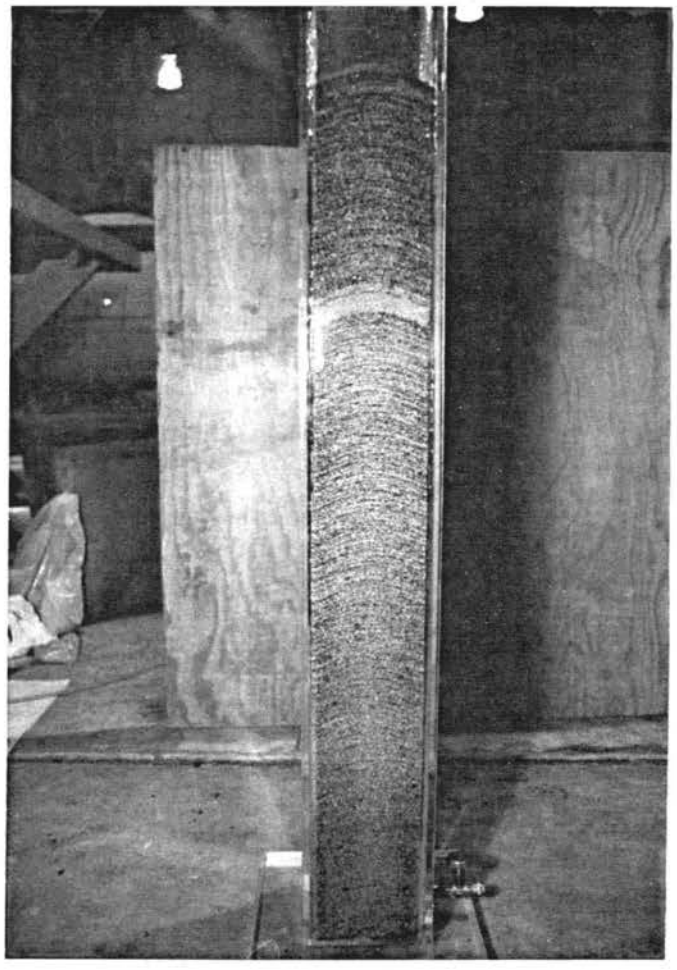

Picture 8. Laminae becomes clearer as deposit gets higher

Mixture #2: white ERC #1, D_{50} = 0.130 mm
and black B3060, D_{50} = 0.335mm

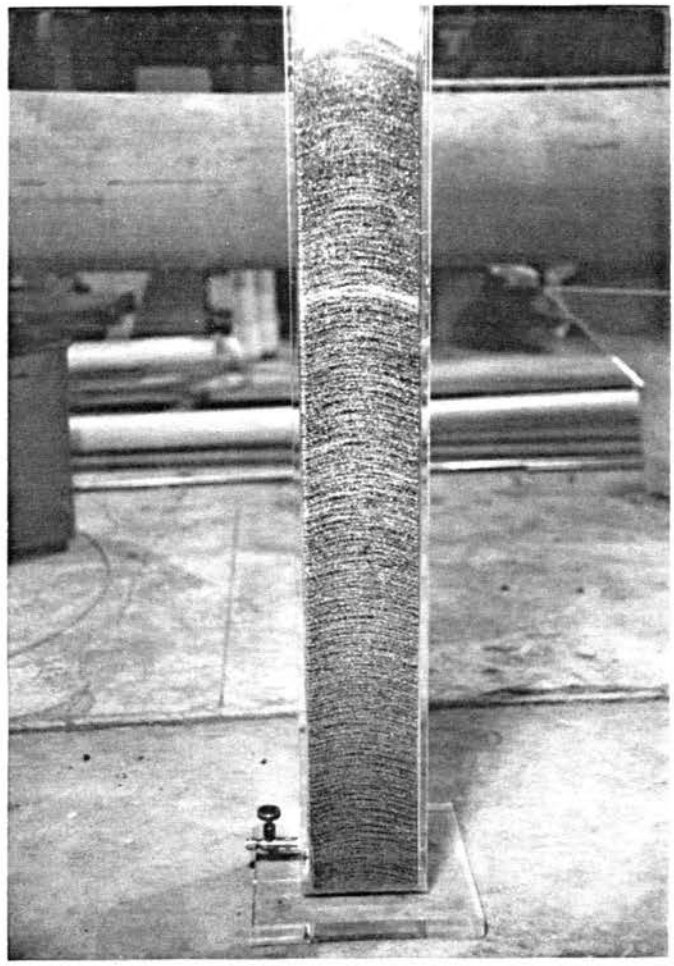

Picture 9. Clearer laminae from side far from the center

Mixture #2: white ERC #1, D_{50} = 0.130 mm
and black B3060, D_{50} = 0.335mm

Run #4

In this run, the height of the base is zero. And the rate is 7.00 cm^3/sec. Splashing of particles does not occur while landsliding is dominant. Rolling of black particles on the white particles before landsliding is observed. Consequently, clear laminae with thickness less than 0.5 cm are observed (see Picture 10).

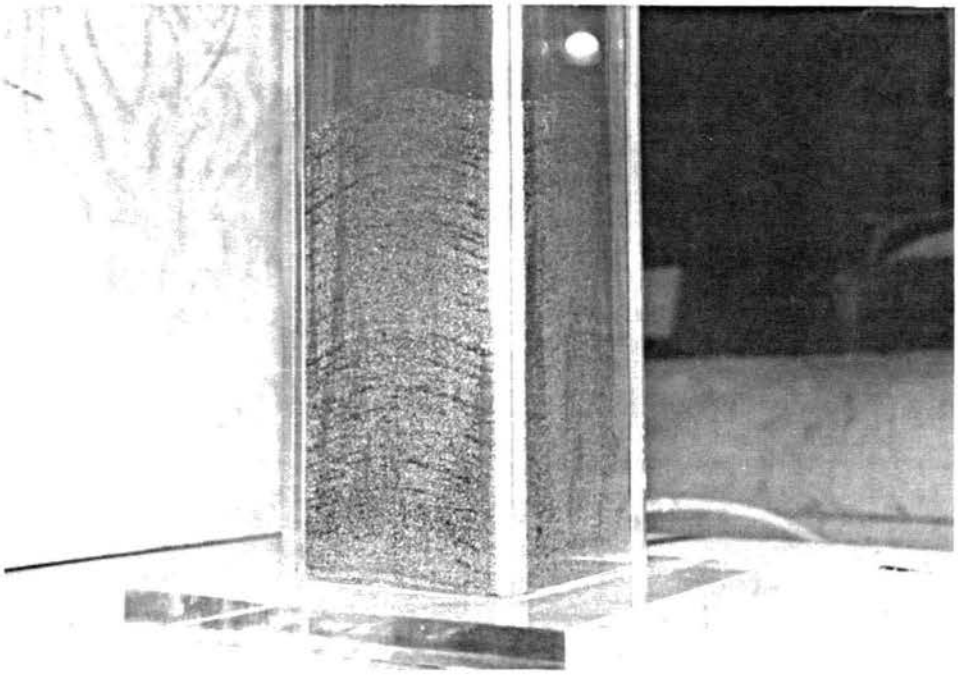

Picture 10. Clear laminae from run #4

Mixture #3: white ERC #1, D_{50} = 0.130 mm
and black B3060, D_{50} = 0.335 mm

Run #5

In this run, the height of the base is 63.5 cm, and the rate is 4.01 cm^3/sec. Consequently, the fall velocities of particles are dramatically reduced. The splashing of particles is weak. Meanwhile, a cone is well formed and landsliding occurs. No clear lamina is observed (see Picture 11).

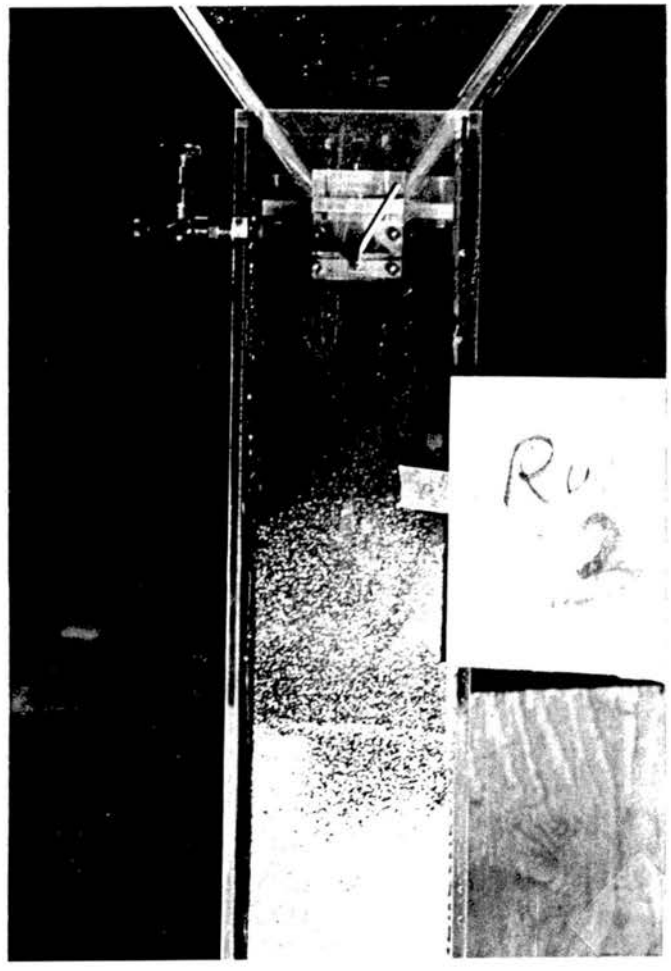

Picture 11. No clear laminae from run #5

Mixture #4: white ERC #3, D_{50} = 0.635 mm
and black coal #3, D_{50} = 0.665 mm

Run #6

In this run, the height of the base is zero, and the rate of sedimentation is 9.0 cm^3/sec. The splashing of particles is weak because both types of particles are fine materials. Meanwhile, a cone is well formed and landsliding occurs occasionally. Laminae is observed but not distinct (see Picture 12).

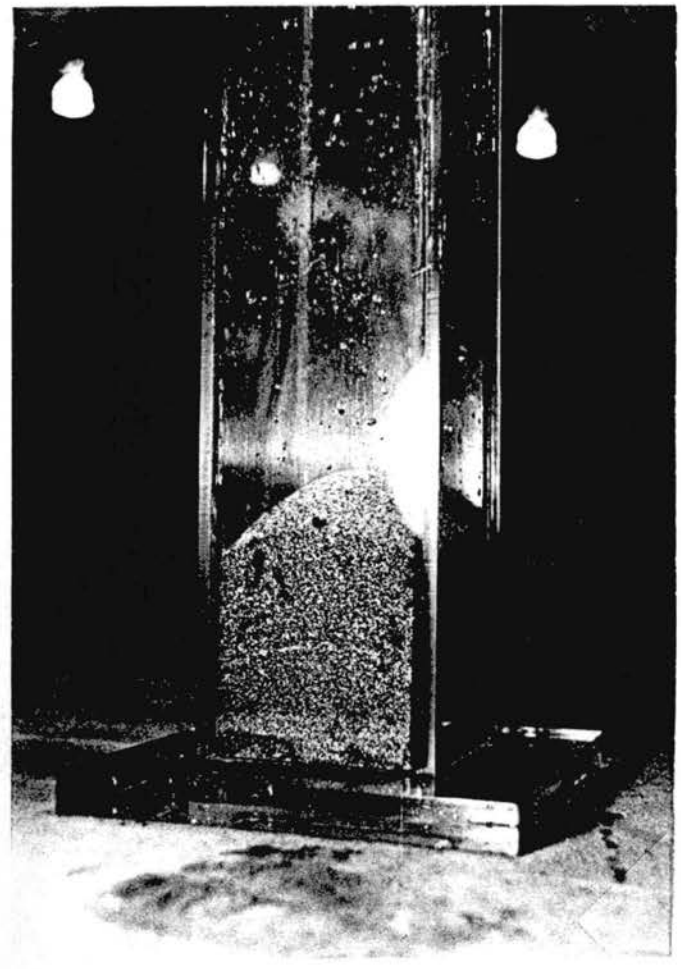

Picture 12. No laminae from run #6

Mixture #5: limestone #1, D_{50} = 0.390 mm
and black B3060, D_{50} = 0.335 mm

Run #7

Compared with run #6, the limestone used in this run is much coarser. Consequently, splashing of particles is dominant in the sedimentation process. Lighter material, coal, is pushed to the wall of the cylinder. No lamina is observed.

Run #8

The conditions in this run are the same as in run #6, except that the limestone is much coarser. The height of the base is zero, and the rate of sedimentation is 9.0 cm^3/sec. The splashing of limestone particles is strong and the cone is not well formed. Meanwhile, the black sand is pushed to the wall of the cylinder. Landsliding does not occur. Laminae are not observed (see Picture 13).

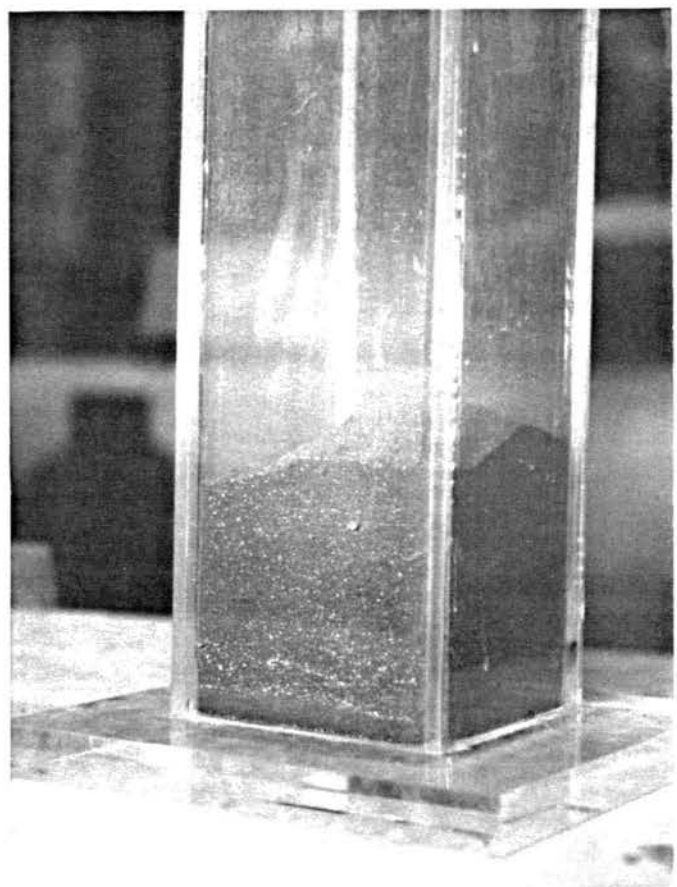

Picture 13. No clear laminae from run #8

Mixture #7: limestone #2, D_{50} = 0.910 mm
and black B3060 D_{50} = 0.335 mm

Run #9

In this run, the lighter material, namely coal, is much finer than the other material, ERC#2. The height of the base is zero, and the rate of sedimentation is 9.0 cm^3/sec. Splashing of particles is weak but no landsliding is observed, and the cone is not well formed. Meanwhile, the black coal is pushed to the wall of the cylinder. Laminae are not observed (see Picture 14).

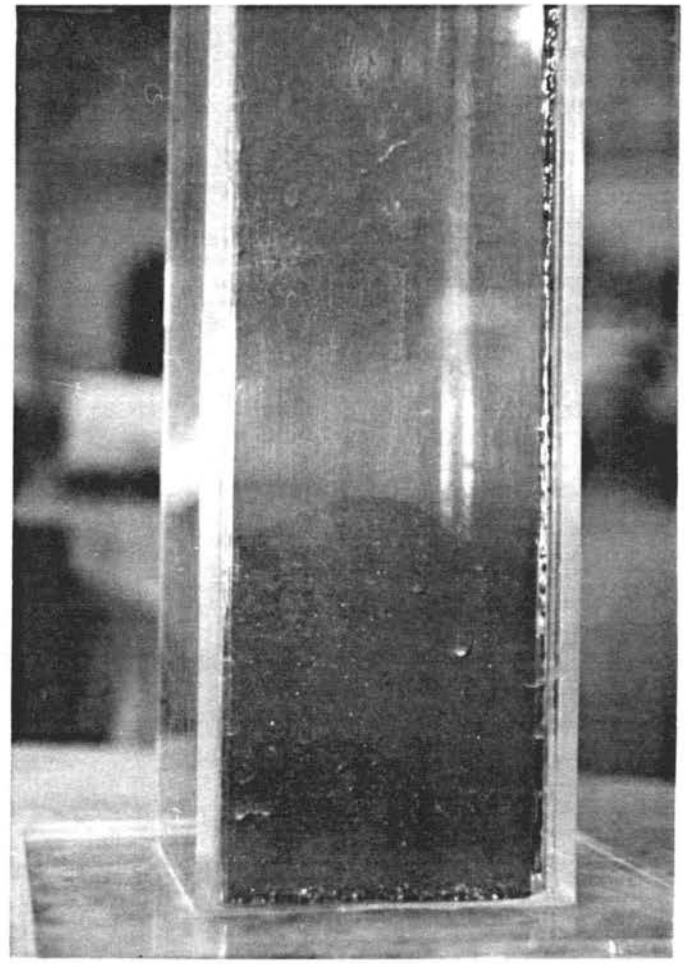

Picture 14. No laminae from run #9

Mixture #8: white ERC #2, D_{50} = 1.200 mm
and black coal #1, D_{50} = 0.410 mm

Run #10

In this run, the lighter material, namely coal, is coarser than the other material, limestone #1. The height of the base is zero, and the rate of sedimentation is 3.44 cm^3/sec. Splashing of particles is weak, and landsliding occurs but no distinct separation of black and white particles is observed. Rolling of one particle over the other is observed, but no clear lamina is formed (see Picture 15).

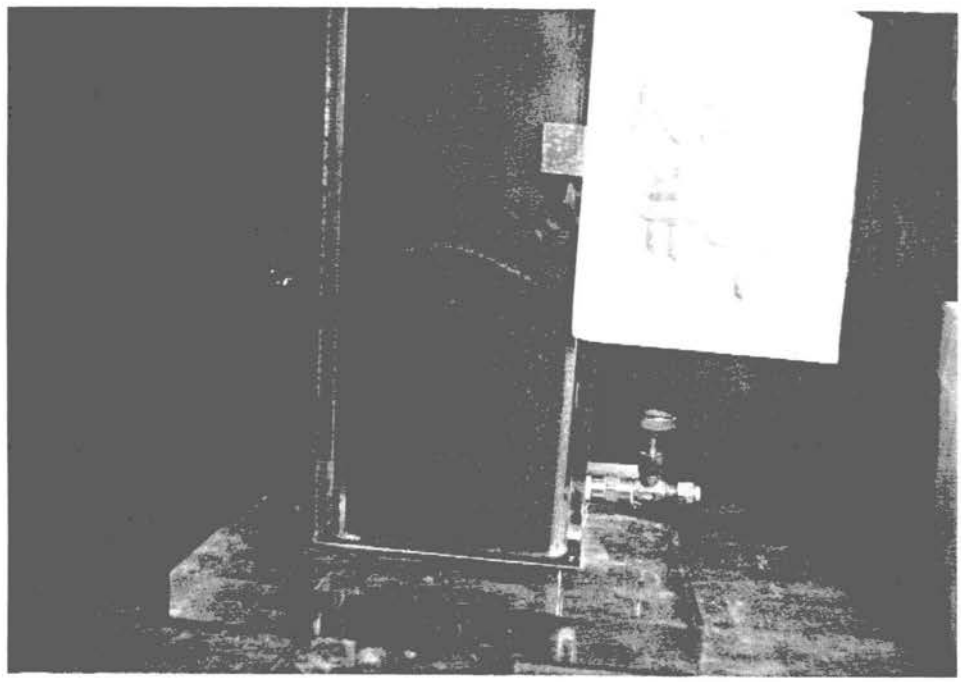

Picture 15. No clear laminae from run #10

Mixture #9: limestone #1, D_{50} = 0.390 mm
and black coal #2, D_{50} = 0.250 mm

Run #11

The height of the base is zero, the rate of sedimentation is 1.619 cm^3/sec., and splashing of particles is moderate. Landsliding occurs occasionally, but no distinct separation of black and white particles is observed. Rolling of one particle over the other is observed, but no clear lamina is formed (see Picture 16).

Picture 16. No clear laminae from run #11

Mixture #10: limestone #1, D_{50} = 0.390 mm
and black B2040, D_{50} = 0.575 mm

2.3.2 Sedimentation in Water

Run #12, 13, 14 and 15

The rate of sedimentation in these three runs is the same, 9.14 cm^3/sec. The only difference among these runs is the height of base and the original water depth. These conditions are summarized in Table 6. Laminae can be seen although not distinctly when the original water depth, h, is low (see Pictures 17, 19 and 20). When the original water depth is too high, no lamina is formed due to the uniform settling at the bottom of the cylinder (Picture 18).

Table 6. Experimental conditions for runs #12, 13, 14 and 15 (height in cm)

Run #	Height of Base cm	Original Water Depth, h cm	Picture #
12	0.0	35.00	17
13	0.0	68.50	18
14	65.0	6.50	19
15	10.0	5.00	20

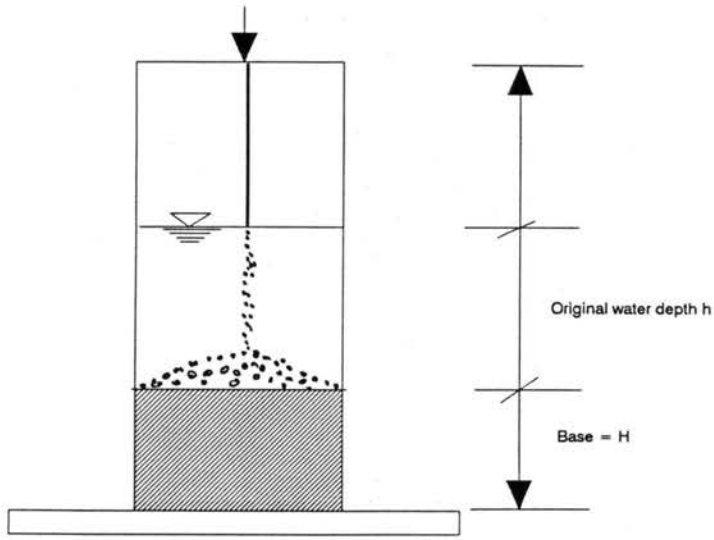

Figure 6. Definition of base height and original depth

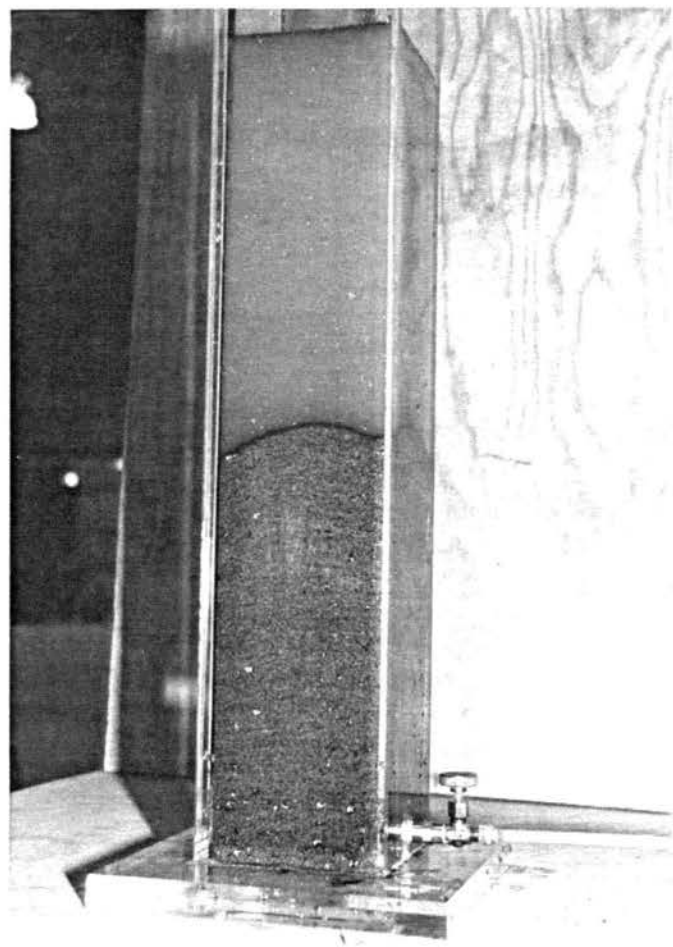

Picture 17. Laminae from run #12

Mixture #2: white ERC #1, D_{50} = 0.130 mm
and black B3060, D_{50} = 0.335 mm

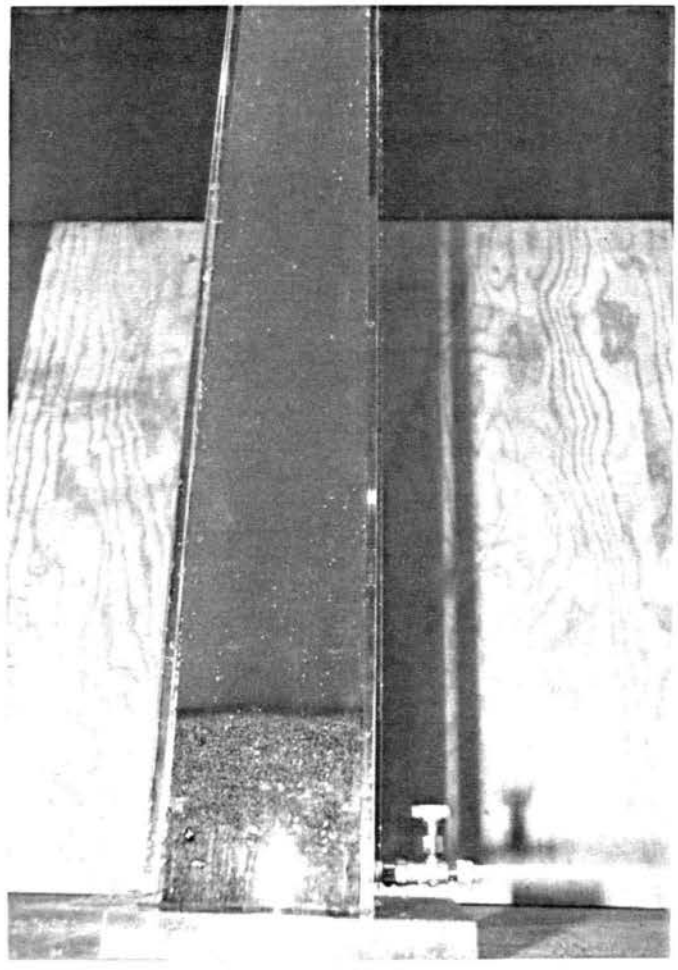

Picture 18. No laminae from run #13

Mixture #2: white ERC #1, D_{50} = 0.130 mm
and black B3060, D_{50} = 0.335 mm
H = 0.0, h = 35 cm

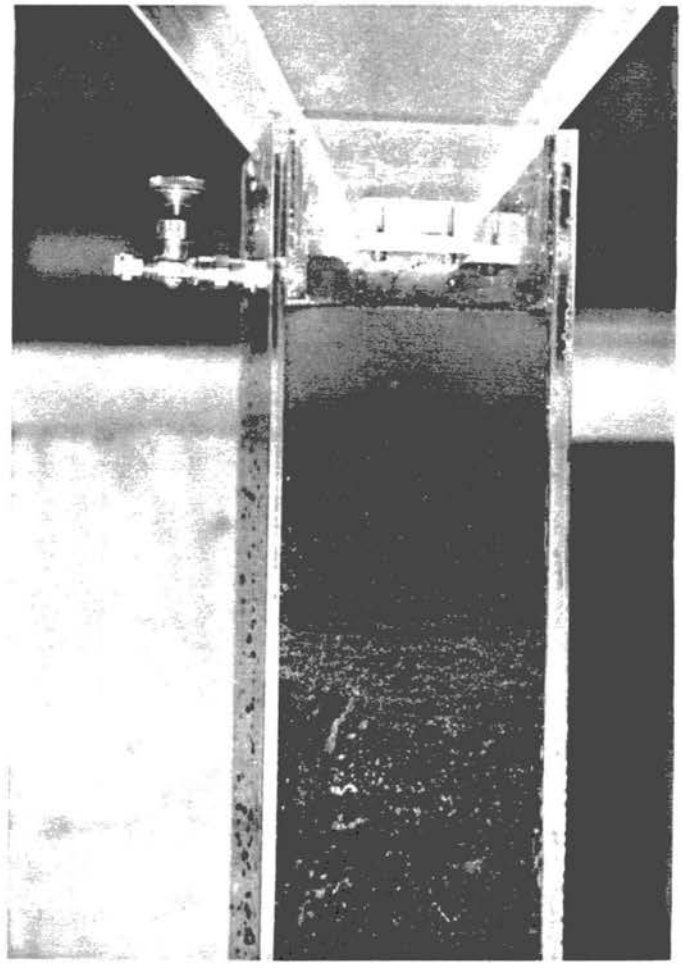

Picture 19. Laminae from run #14

Mixture #2: white ERC #1, D_{50} = 0.130 mm
and black B3060, D_{50} = 0.335 mm
H = 65.0 cm, h = 6.5 cm

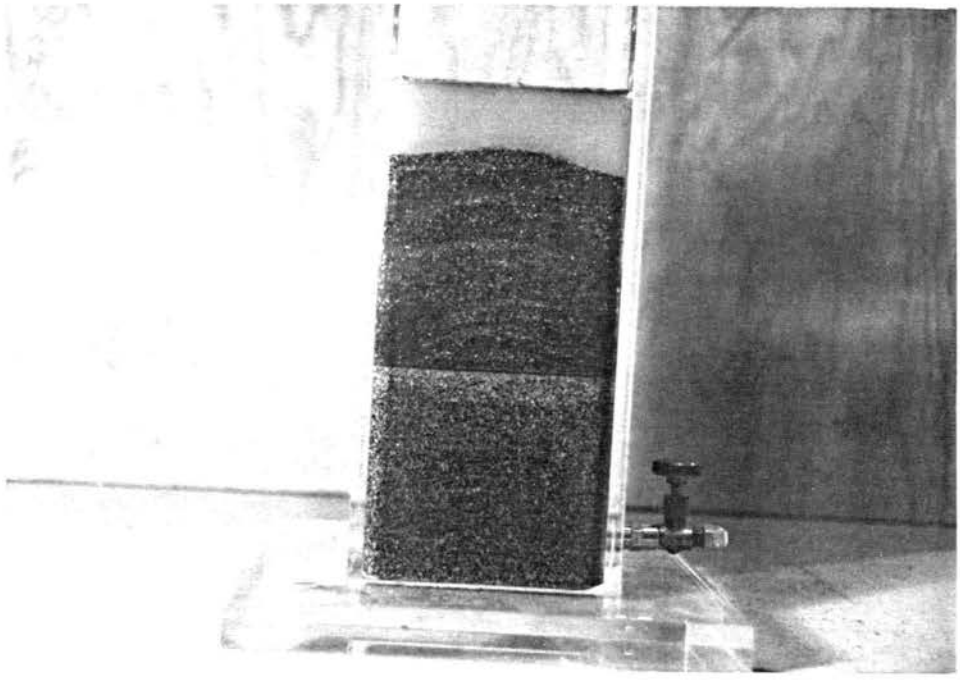

Picture 20. Laminae from run #15

Mixture #2: white ERC #1, D_{50} = 0.130 mm
and black B3060, D_{50} = 0.335 mm
H = 10.0 cm, h = 5.0 cm

Run #16

The mixture used in this run is the same as in runs #12-15. However, the rates of sedimentation are much lower, 0.384 cm^3/sec, 1.24 cm^3/sec, and 2.00 cm^3/sec, respectively. The original water depth is 62 cm, and base height is zero. The process of sedimentation can be seen in Pictures 21 and 22, taken at the water surface and bottom of cylinder, respectively. Laminae, although not clear, can be seen in Picture 23.

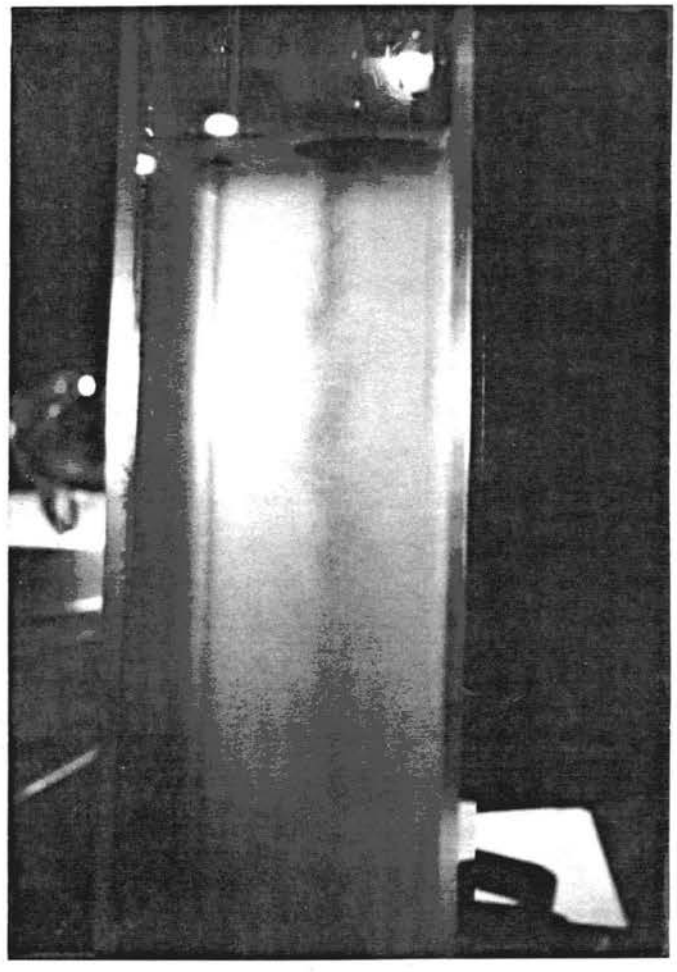

Picture 21. Sedimentation process at the water surface

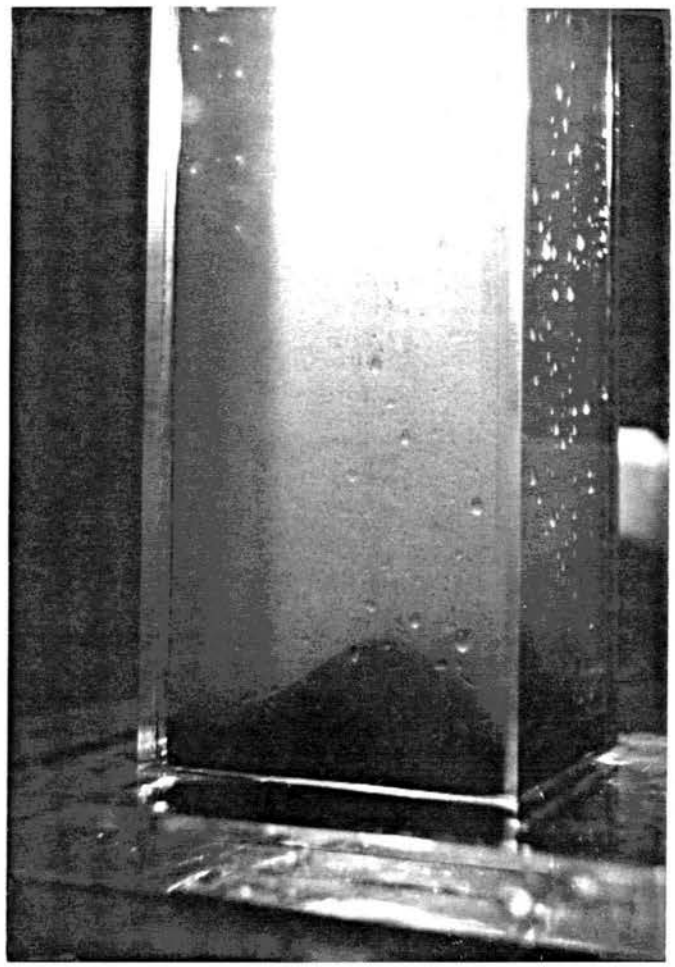

Picture 22. Sedimentation process at bottom of run #16

Picture 23. Laminae (not clear) from run #16

Mixture #2: white ERC #1, D_{50} = 0.130 mm
and black B3060, D_{50} = 0.335 mm
H = 0.0, h = 62 cm

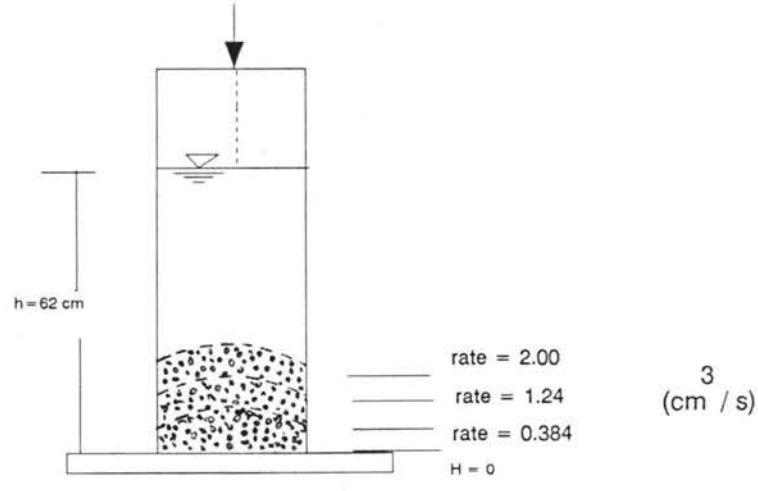

Figure 6. Explanation sketch for picture 23

Run #17

In this run, the height is zero and the original water depth is 79.2 cm. Since the settling velocity of coal is much smaller than that of the white sand, heavier materials deposited on the bottom of the cylinder first, and then both materials together. If there is a discontinuity during the process, a layer of coal, with thickness depending on the interval of discontinuity, would form. Otherwise, no lamina is observed (see Picture 24).

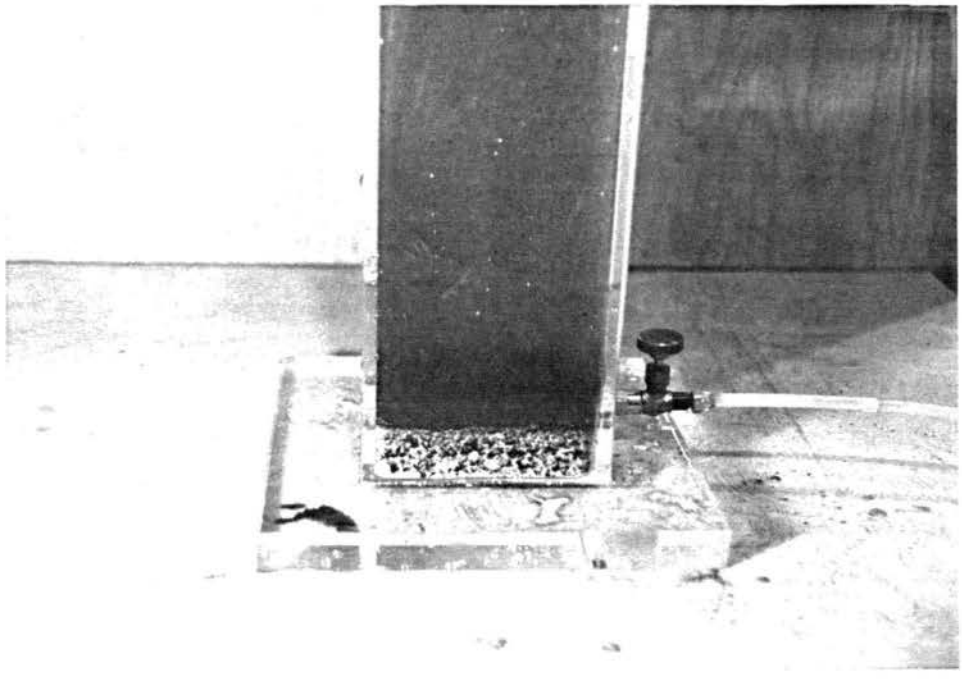

Picture 24. No laminae from run #17

Mixture #3: white ERC #1, D_{50} = 0.130 mm and black coal #1, D_{50} = 0.410 mm H = 0.0, h = 79.2 cm

Run #18

The base height is zero, and the original water depth is 60 cm in this run. Since the settling velocity of the white sand is much larger than that of coal, the settling of the white materials is straight down to the bottom while coal particles suspend in water up and down for a while and then settle down. The white sand, therefore, deposits at the center of the cylinder while the coal deposits around the cone from by white particles. This is demonstrated by Pictures 25 (taken during the process), and 26 (taken after the water is drained). Landsliding is observed during the process. Eventually, laminae are formed (see Pictures 27 and 28).

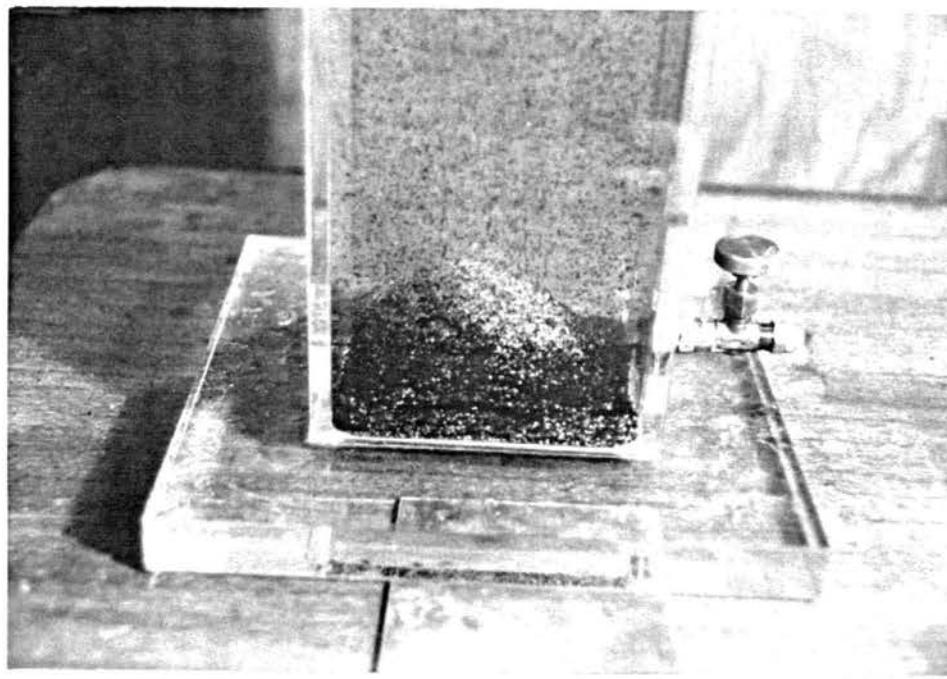

Picture 25. Sedimentation process in run #18

Mixture #4: white ERC #3, D_{50} = 0.635 mm
and black coal #3, D_{50} = 0.665 mm
H = 0.0, h = 60 cm

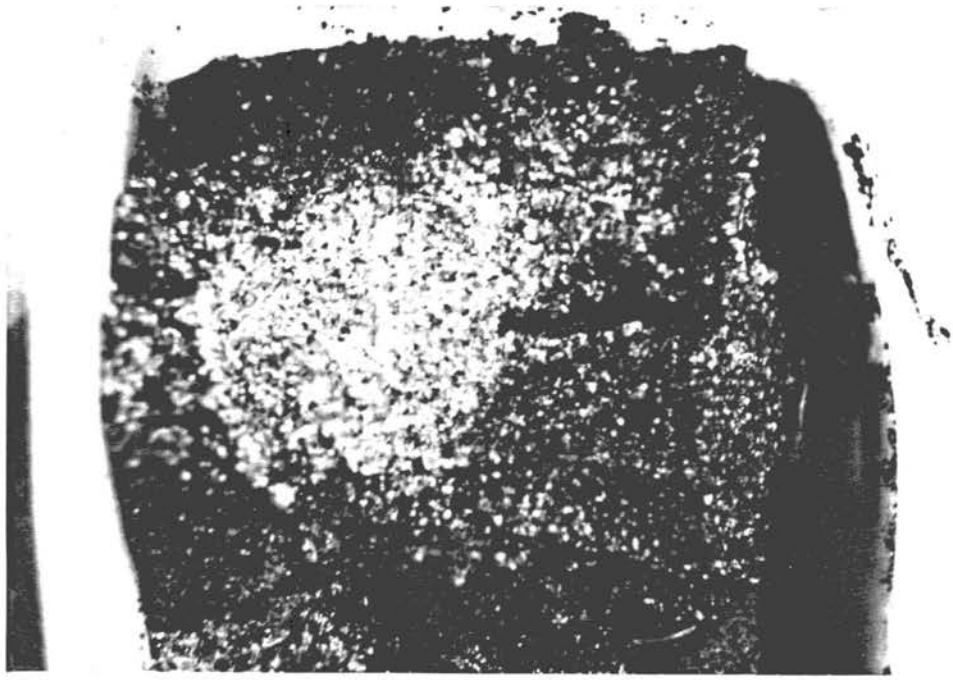

Picture 26. Centering of heavier materials (after)

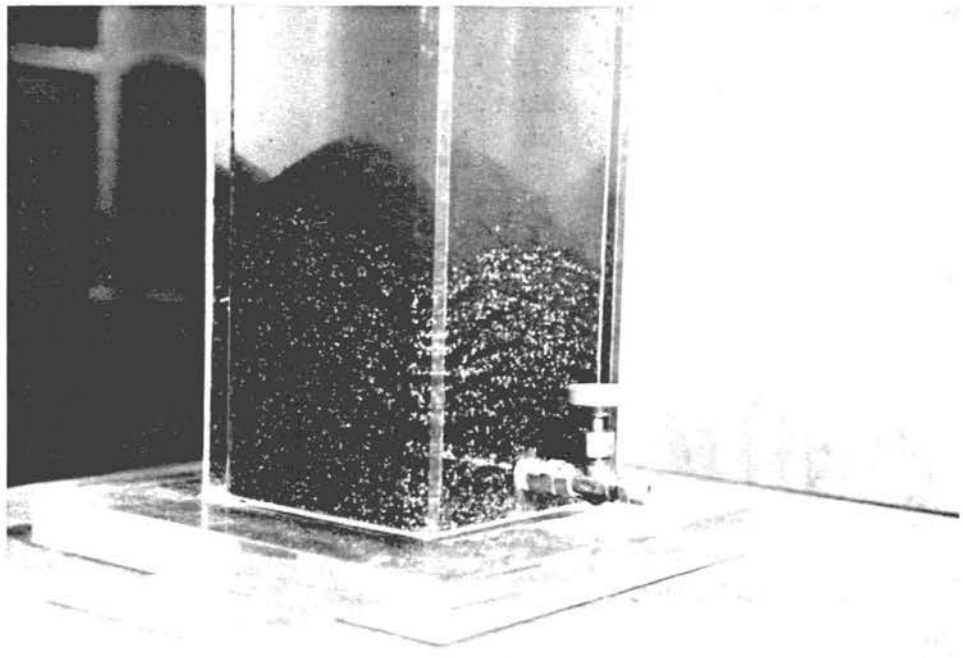

Picture 27. Clear laminae from run #18

Mixture #4: white ERC #3, D_{50} = 0.635 mm and black coal #3, D_{50} = 0.665 mm H = 0.0, h = 60 cm

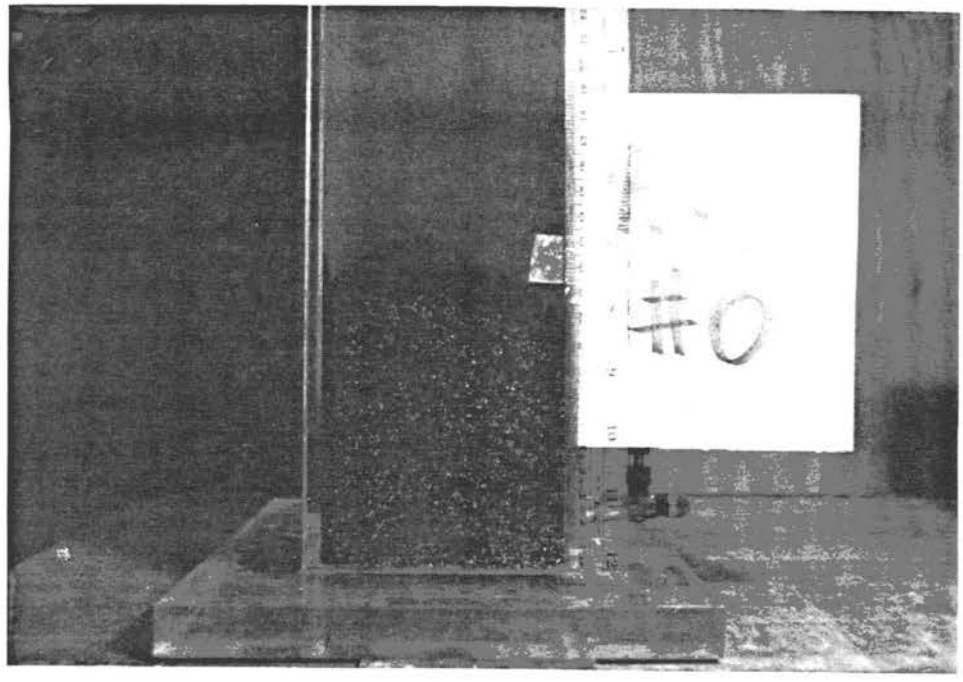

Picture 28. Clear laminae from run #18

Mixture #4: white ERC #3, D_{50} = 0.635 mm
and black coal #3, D_{50} = 0.665 mm
H = 0.0, h = 60 cm

Run #19

The base height is zero and original water depth is 59 cm in this run. Since particle settling velocities are small, particles suspend all over the cross-section. Landsliding occurs, but is not as dominant as in run #18. laminae are much clearer from the side wall farther from the center of cylinder (the cylinder stands at a little incline). This can be demonstrated from Pictures 29, 30, and 31, with reference from Figure 7.

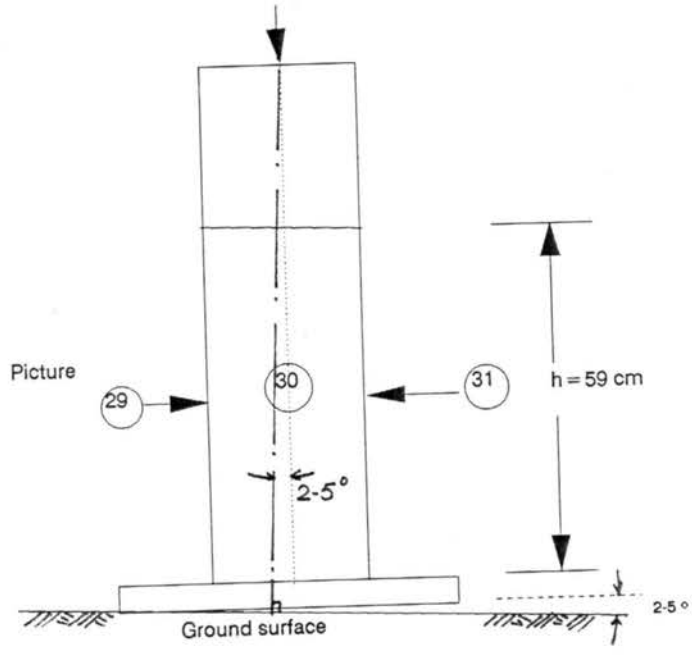

Figure 8. Positioning of cylinder for run #19

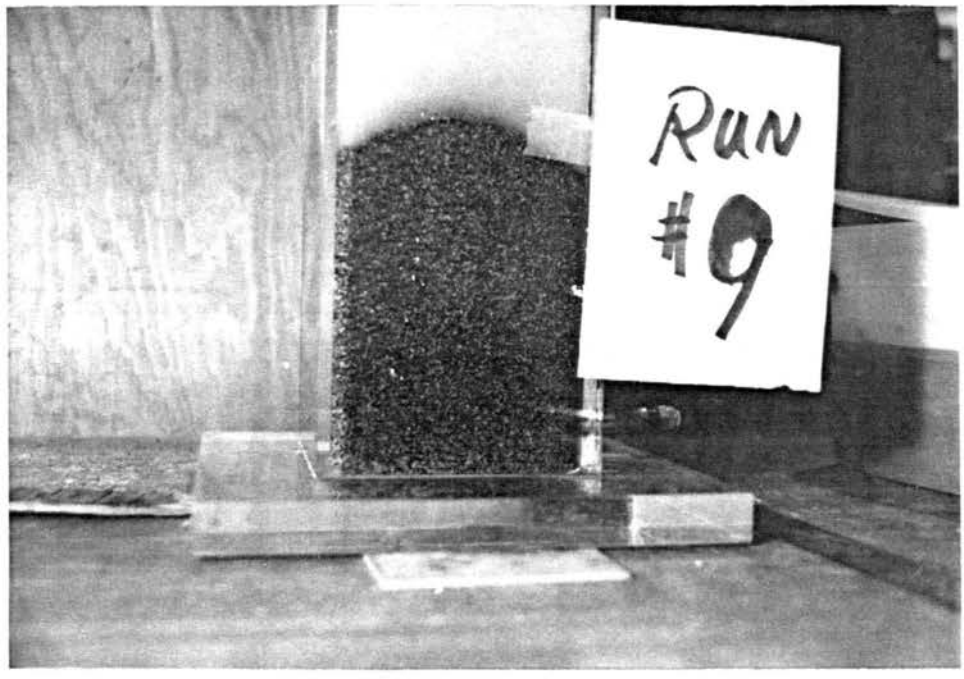

Picture 29. No clear laminae near the center (run #19)

Mixture #4: white ERC #3, D_{50} = 0.635 mm
and black coal #3, D_{50} = 0.665 mm
H = 0.0, h = 60 cm

Picture 30. Better laminae in frontal view (run #19)

Mixture #4: white ERC #3, D_{50} = 0.635 mm
and black coal #3, D_{50} = 0.665 mm
H = 0.0, h = 60 cm

Picture 31. Clearer laminae from the far side (run #19)

Run #20

The base height is zero and original water depth is 58 cm in this run. The rate of sedimentation is 0.759 cm^3/sec. A cone in water is well created. Landsliding appears to be stronger than that in the air because splashing of particles could not happen in water. The obvious segregation of black particles from the whites really causes the clear formation of laminae. Again, it is indicated from Pictures 32, 33 and 34 that longer distances from the crest produce clearer lamination.

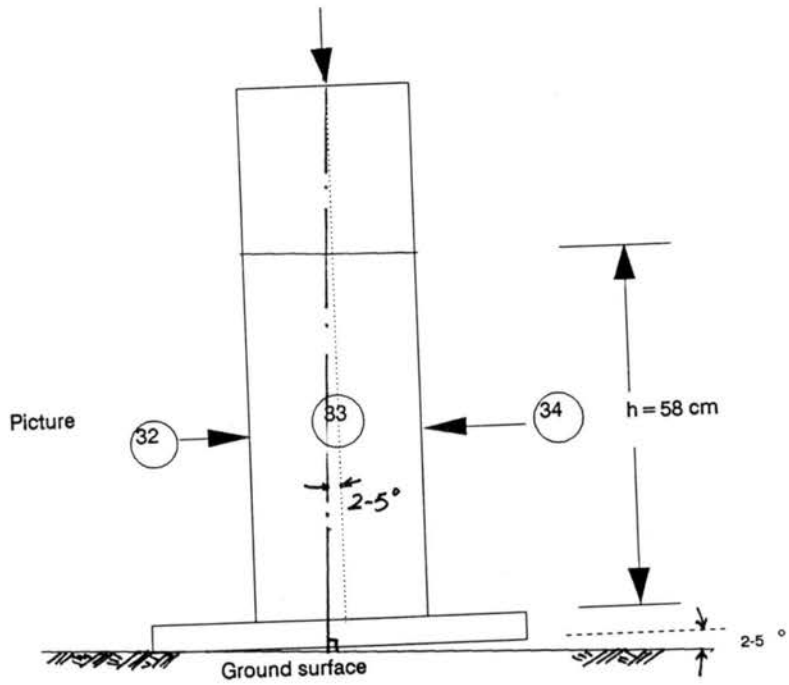

Figure 9. Positioning of cylinder for run #20

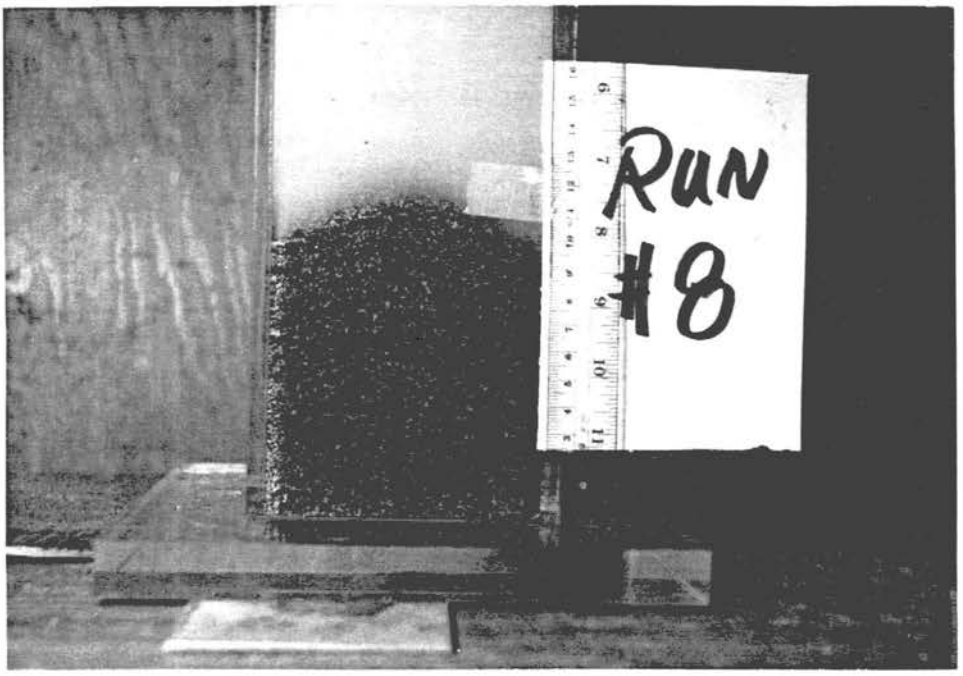

Picture 32. Laminae from the near side (run #20)

Mixture #10: limestone #1, D_{50} = 0.390 mm
and black B2040, D_{50} = 0.575 mm
H = 0.0, h = 58 cm

Picture 33. Good lamination in frontal view (run #20)

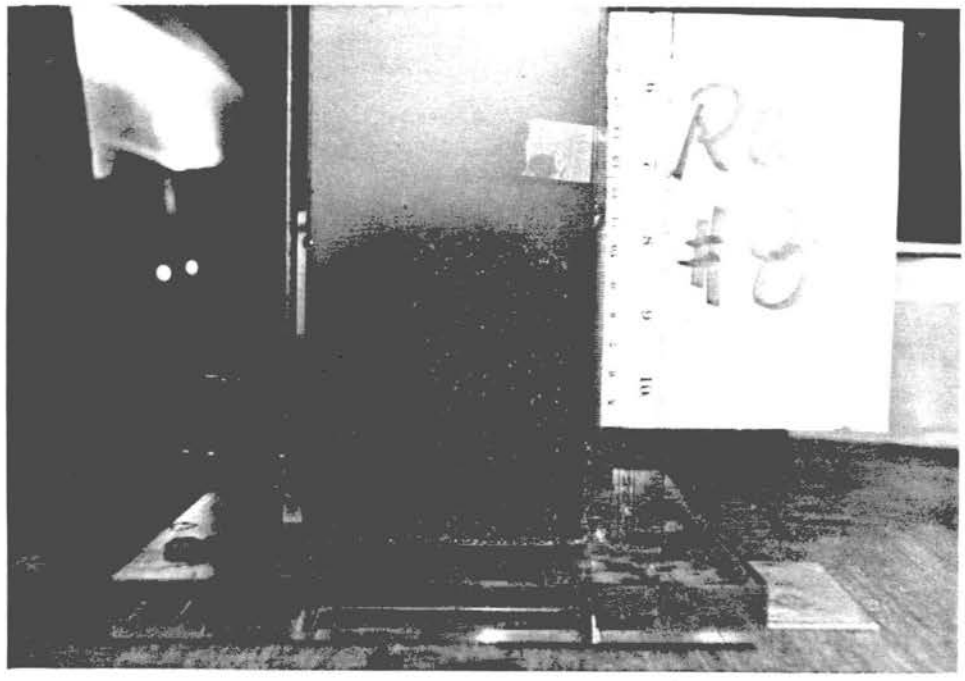

Picture 34. Clearer lamination from the far side (run #20)

Mixture #10: limestone #1, D_{50} = 0.390 mm
and black B2040, D_{50} = 0.575 mm
H = 0.0, h = 58 cm

Run #21

In this run, the base height is zero, and water depth is 55 cm. The rate of sedimentation is small, 1.02 cm^3/sec. Landsliding is dominant during the process, which is in contrast to the experiment in the air where splashing is dominant (run #1). Although the sizes of ERC #3 and B2040 are different, segregation of black and white particles during the landsliding is not observed. Obviously, no lamina is observed.

III. STRATIFIED DEPOSITS IN A NARROW LABORATORY FLUME

The structure, texture, and shape of sand material deposited provides a useful interpretation of the ancient deposits formed during floods. They also help in relating the types of structures in a recognizable flood deposit to the specific stage of flood deposition, or stream regime, and in distinguishing the deposits of a river channel from those of adjacent flood plains. A former investigation of the deposits of Bijou Creek flood, June 1965 (McKee et al., 1967), showed criteria that might be used in the recognition of flood deposits in ancient rocks and a study of sedimentation in terrestrial environments.

The proposed laboratory experiments in a small plexiglas recirculating flume are intended to examine the depositional characteristics of Bijou Creek sand under plane bed conditions with sediment motion. A recirculating plexiglass flume has been designed at the Engineering Research Center of Colorado State University for the analysis of deposition processes under a wide variety of flow conditions (Julien and Chen, 1989a, 1989b). This flume recirculates both water and sediment under steady flow conditions during the course of each experiment.

This study focuses on parallel lamination and delta formation processes without bed forms because horizontal deposits constituted 90% to 95% of all deposits of the Bijou Creek flood (McKee et al., 1967). Experiments are carried out under various flow conditions under different bed slopes. After each experiment, the sediment deposits were dried in the flume to examine the appearance of vertical cracks and stratification joints. The results of the desiccation experiments are reported in Section VI.

3.1 Literature Review on Bijou Creek Flood, June 1965

The heavy rains in June, 1965, caused floods of unusual magnitude in the area drained by the South Platte River. The floodwaters spread extensive, locally thick deposits of sand and mud along the South Platte River and its tributaries. It was a good opportunity to study the distribution, texture, composition, and structures of sediment deposits under flood conditions. The deposits of Bijou Creek, a tributary of the South Platte River, were investigated by McKee et al. (1967) in recognition of flood deposits in ancient rocks and in studies of sedimentation in terrestrial environments.

The geological environment of the area drained by Bijou Creek is underlain by the Pierre shale, Fox Hills sandstone, and Laramie Formation of Late Cretaceous age. These formations consist of poorly to moderately well consolidated shale, sandy shale, sandstone, and lignitic coal

beds; they contain little or no coarse material, in contrast to younger deposits of this area. The surface material is confined within the older alluvial deposits on the channel and flood plain (McLaughlin, 1946).

The local rainstorms across eastern Colorado and heavy rains at Bijou Creek drainage area caused a flood peak discharge of 466,000 ft^3/sec near the mouth of the creek, breaking the former observed peak discharge of 282,000 ft^3/sec. A mean velocity of 16.4 ft/sec was reported for the entire cross-sectional area, and velocities up to 21.8 ft/sec for the main channel were reported (McKee et al., 1967). The corresponding Froude number Fr = 0.6 is close to unity, which indicates near critical flow conditions. Four localities were studies along Bijou Creek, including East and West Bijou Creeks, for flood deposit of 1965 as shown on Figure 10. There were 75 trenches dug in this area with depths ranging from a few inches to 12 feet deep, and lengths from 2 to 12 feet. In each trench two vertical faces at right angles were planed and the structures were recorded by field sketches and photographs as shown in Figure 11. Measured thicknesses and angles of dip were recorded on the sketches. The investigated results in the report are summarized on Table 7 for each locality. The maximum measured thickness of deposits attributable to the flood was about 12 feet, and the thicknesses of 2 to 4 feet were common at all localities. However, within the main channel, most new deposits could not be distinguished from older ones as no soil or vegetation zone was present. The scouring and filling was continuously occurring in the cross-section during flow and may cause changes of 5 to 10 feet in elevation of the sediment-water interface during flooding.

At all localities sampled, the most abundant sediment was quartz sand of fine to coarse texture. Small amounts of silt and clay, mostly less than 2%, were intermixed with sand in some beds, and a few thin beds of silt, silty clay, and clay were noted in overbank deposits. Several samples from locality I contain 5% to 30% fine gravel and a few larger pebbles. However, samples for downstream localities yielded much less very coarse sediment. It was a sorting process along Bijou Creek from upstream to downstream.

On the flood plain, the newly-formed flood deposits were mostly flat bedded. Low to moderate-angle foreset bedding formed where receding water poured back into the main or subsidiary channels or where it swirled around the bases of large trees. Climbing-ripple laminae and convolute structures were well developed in limited area. Cut-and-fill structures were present, but common in overbank deposits. In channel deposits, both flat bedding and festoon cross-bedding were formed. Those depositional structures are similar to the sedimentary structures investigated in the deltaic plain of the Mississippi River (Coleman and Gagliano, 1965). The analysis of the sedimentary characteristics of flood deposits should be useful in

interpretation of depositional environments represented by ancient rocks. The flood plain deposits extended over several thousand feet in width and up to 12 feet in thickness, and were characterized by a variety of sedimentary structures accumulated during a few hours.

The strata of sand deposited by a violent flood contain dominantly horizontal layering characteristic of the upper stream regime. In contrast to the horizontal stratification of rapid flow characteristic, climbing-ripple lamination, convolute structures, festoon bedding, and scoured surfaces commonly result from the decrease of velocity during the waning stage of flood.

In contrast, texture of sand, although it may record rapid flow, relatively coarse grains, and decrease in velocity with finer grains, can be deceptive. Relatively slow, receding water may rework coarse sediments deposited earlier, and thus reverse a normal depositional sequence of texture. The medium to large-scale festoon cross-bedding and the megaripples, common to stream channels where flow is concentrated, contrast with the typical climb-ripple lamination and convolute structures of blanket deposits formed during the waning phase of flood plain deposition.

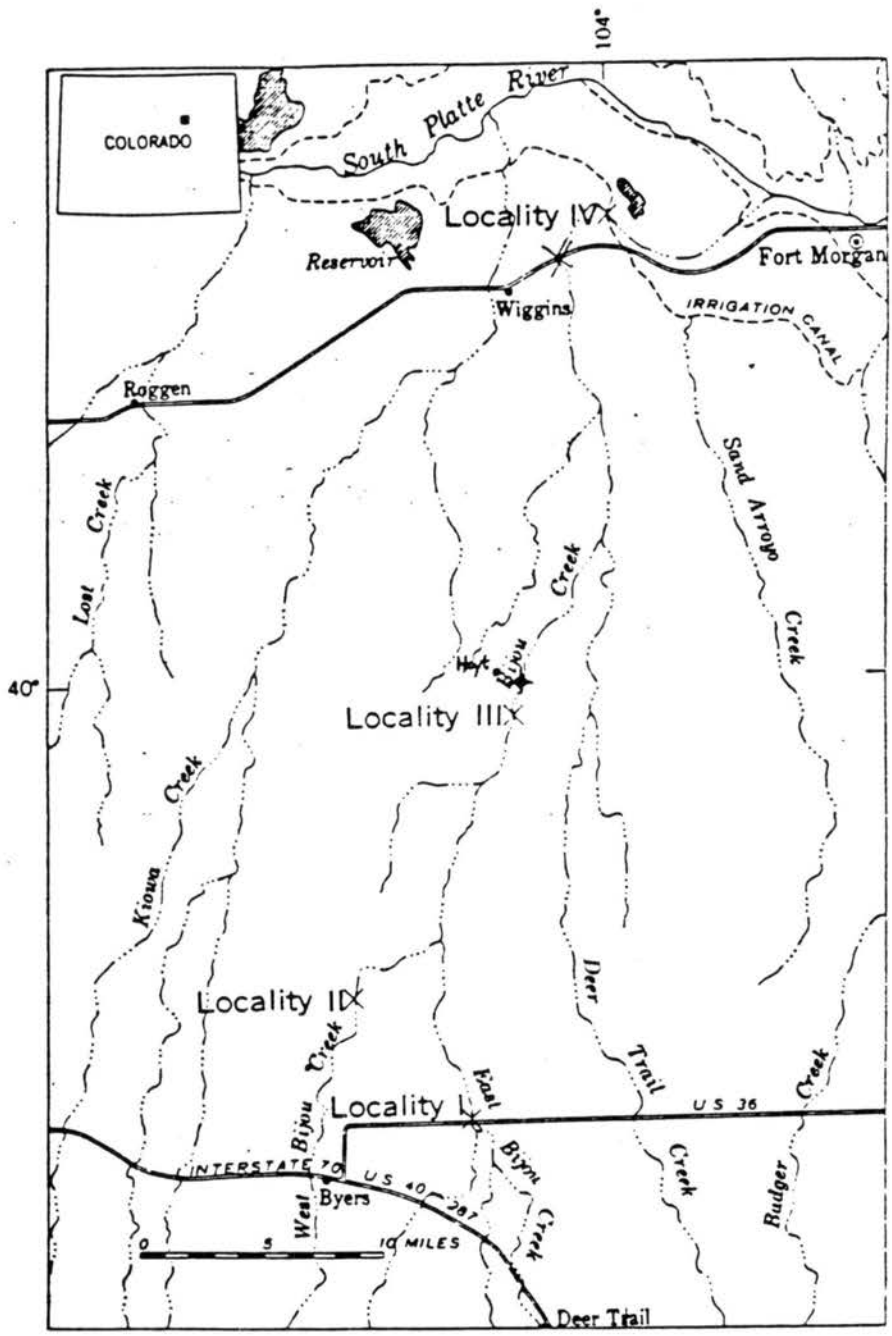

Figure 10. Index map of Bijou Creek, north of Byers, Colorado showing localities where flood deposits of June, 1965 were investigated (McKee et al., 1967).

Note: * showing locality of sand samples in this experiment.

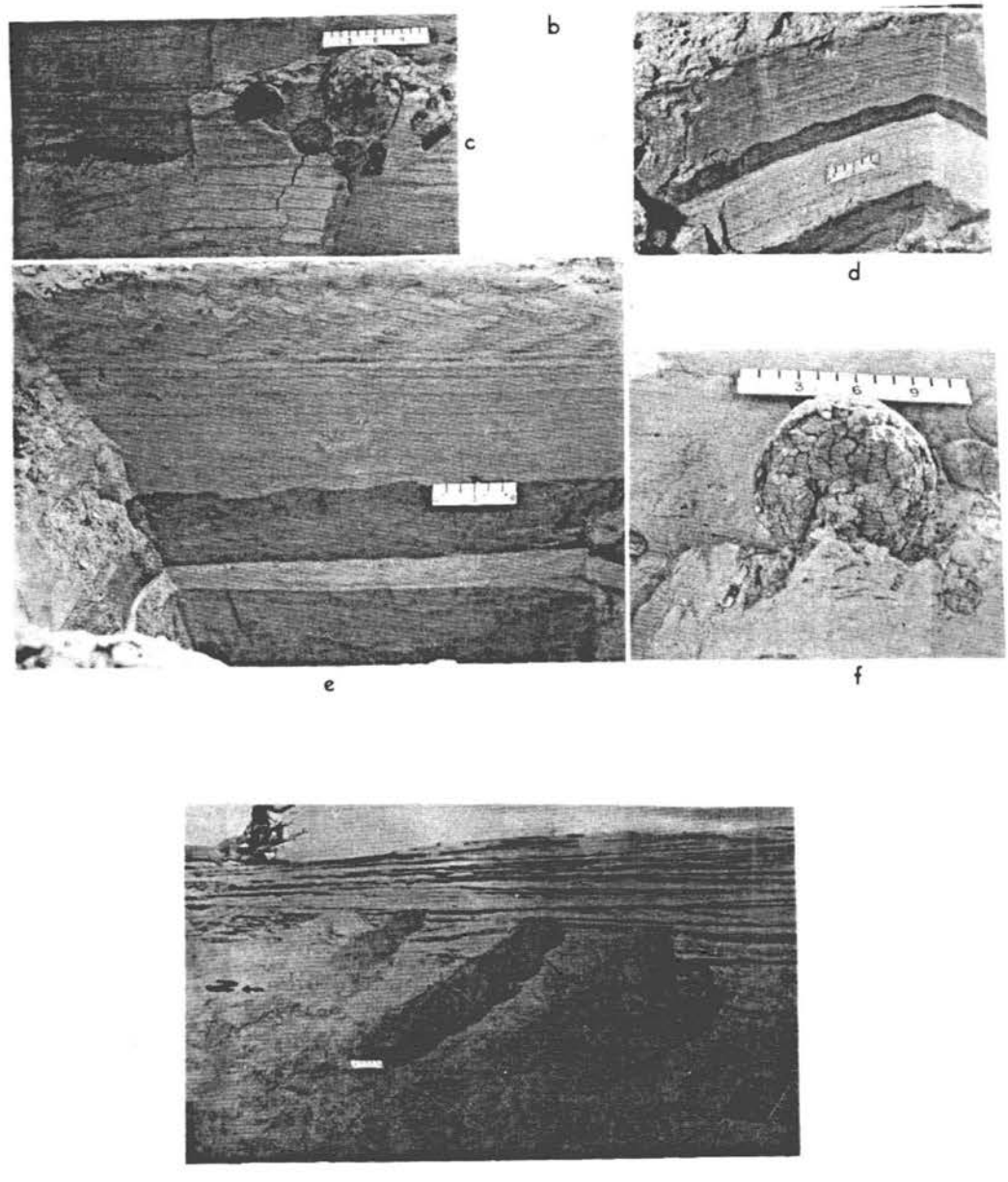

Figure 11. Sedimentary structures on West Bijou Creek
(from McKee et al., 1967)

Table 7. Summary of Bijou Creek flood deposits, June 1965

	Locality I	Locality II
Trench number	23	28
Thick-ness	*20-30 inches near cutbank along channel edge; *A maximum thickness of 40 inches in a trench; *In eastern 2/3 of the deposits, the sand maintain a thickness of 20 inches or more to within 100 ft of edge of deposition; *Northward (wooded area), the sand thinned irregularly across a distance of 1000 ft or more.	*Site A: A blanket ranging in thickness from 2 or ft near bank to 1 ft or less at down-current margin; *Site B: Thickness is greater than that in most of the flood deposits; 12 ft of thickness is the greatest thickness observed during study; *Site C: Depth to the preflood surface was not determined, but deposits ranging from m to coarsersand and including many mudba are exposed to 50 inches.
Struc-ture	*Dominately even-bedded, flat-lying or essentially horizontal strata; *Dips of less than 5 degree were most common; some were more than 10 degree; *Low-angle foreset bedding along outer margin and 28 degree steeper foresets around trees; *Small scale cut-and-fill near top of one trench; *2 examples of deformation that shallow V's bent downward in a zone of near flat-lying laminae were noted.	*Site A: Relatively thin overbank deposits consis almost entirely of flat, nearly horizonta strata; *site B: Several of which indicate a lower flow regime like climbing ripple laminae, fore sets forming tabular planar crossbeddir and convolute lamination; *Site C: Flat-lying layers of sand, sets of trough planar crossbeds in 5 ft thickness, clim ing ripple laminae near top layers, and layers or lenses of dominantly spherica mudballs.
Texture	*41% medium sand, 32% coarse sand and 14% fine sand in total 52 samples; *Sorting, according to the Payne scale, was fair in 50 sample, good in one, and poor in one; *Material larger than coarse sand was conspicuously present both within the bedded deposits and as a veneer over much of the surface of sand sheet. Very coarse sand and granules were interbedded with finer sand in some trenches; pebbles and cobbles up to 7 or 8 inches long were scattered through the sand and on the sand surface. *Small clay ball and large crumbling clay ball were exposed at upper surface of the sand deposit.	*Most in medium to fine dominant grain size amo 40 samples; *Site A: Medium to coarse grains in essentially horizontal strata; most in sorting of fa *Site B: 15 Of 24 samples in fine-grain; most of reminder are either slightly coarser or slightly finer; 21 samples in fair sortir 2 poor and 1 good; *Site C: 6 of 11 samples in medium grain size ar 8 samples in fair sorting and 3 in poor; *The dominant grain size in horizontal laminae ranges from very fine to very coarse; howeve ripple lamination and convolute structure are p dominantly fine to very fine grained.

Table 7 (continued)

	Locality III	Locality IV
Trench number	17	7
Thick-ness	*The sand sheet is a lens bisected by the stream channel; the thickness of sand on the east flood plain is 72 inches at cutbank but decreases uniformly eastward to the margin of the deposits; *Thickness is 17 inches at cutbank and increases ir regularly to 54 inches on west flood plain; *Thickness in main channel is unknown due to the difficulty in recognizing preflood surface.	*Two lens deposit on flood plain and main channel; *An asymmetrical lens on flood plain whose thickest part, near the north edge, is 34 inches; *Maximum thickness in main channel is unknown due to unrecognized preflood surface in a trench to 28 inches.
Structure	*Laminated, flat-lying to near flat-lying beds on flood plain; dips of less than 5 degree in common; deposition near margin has dips of more than 10 degree; *Both cut-and-fill crossbedded and horizontally laminated sand deposits fill main channel; *Climbing-ripple bedding and cut-and-fill bedding along secondary channel at outer edge of west flood plain; *Along east bank of main channel two types of erosional structure: wedge-shape beds at channel edge against truncated, laminated deposit before flood and faults that formed at still water when slices of sand along bank slumped to channel floor.	*Horizontal to nearly horizontal layer across flood plain; less 5 degree of dip in common; *A lower unit of laminated sand, a middle unit of virtually structureless sand that contains thick laminae locally, and a local thin upper unit of horizontally bedded to crossbedded sand that is absent in 3 trenches on the flood plain. *In the channel the part of sand deposit exposed by two units of crossbedded sand separated by a horizontal layered, laminated unit; the lower unit has cut-and-fill bedding of well developed festoon pattern; in upper unit the crossbedding is more tabular and wedge shaped, but still has festoon pattern; and the surface of channel is marked by a series of megaripples.
Texture	*The predominant grain size is medium, but the degree of sorting is only fair in most samples; *The coarsest material in deposit is in main channel and decreases in both outer margin of flood plain direction; *The coarser sand not only is largely in main channel but most is associated with cut-and-fill crossbedding.	*Coarse grains dominate at this locality; however, a range of medium to very coarse grain size more nearly typifies the deposit as a whole; the vertical variation in grain size is more apparent than lateral variation; *At this locality stratigraphic units could be recognized by differences in grain size more readily than by structure; lateral variation in grain size is also apparent; *The distinctiveness of two main units across flood plain in the upper coarse-grained unit ranges from nonlayered to crossbedded indicate an increase both in water velocity and in bed load of coarse material.

3.2 Principles of Open-Channel Flows

This section, compiled from Julien (1987), reviews some fundamentals of fluid mechanics. The major topics discussed are: kinematics of flow, equations of motion, turbulence, velocity profiles, rough versus smooth boundaries, specific energy equations, and backwater curves.

3.2.1 Kinematics of Flow

The most common orthogonal coordinate system is cartesian with linear coordinates (x, y, z).

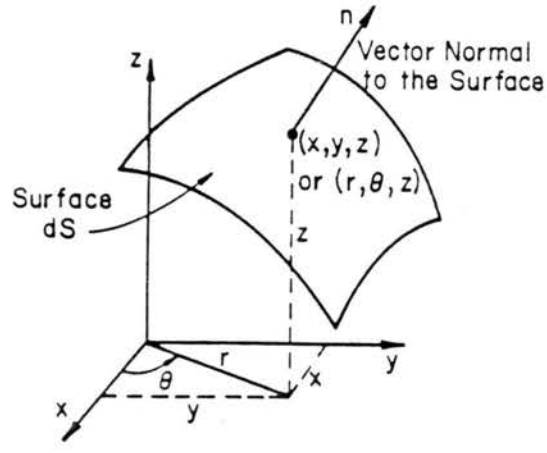

Figure 12. Cartesian system of coordinates

The rate of change in the position of a fluid element is a measure of its velocity. Velocity is defined as the ratio between the displacement **ds** and the corresponding increment of time. Velocity is a vector quantity. Its magnitude **V** can be evaluated from the square root of the sum of squares of its perpendicular components. The direction and the magnitude of the velocity vector vary both spatially and temporally.

A line tangent to the velocity vector at every point at a given instant is known as the stream line. The path of fluid element is the locus of the element through time. A streak line is defined as the line connecting all fluid elements that have passed successively at a point in space.

The differential velocity components at an infinitesimal distance (dx, dy, dz) from a point (x, y, z) are:

$$dv_x = \frac{\partial v_x}{\partial x}\,dx + \frac{\partial v_x}{\partial y}\,dy + \frac{\partial v_x}{\partial z}\,dz \tag{1}$$

$$dv_y = \frac{\partial v_y}{\partial x}\,dx + \frac{\partial v_y}{\partial y}\,dy + \frac{\partial v_y}{\partial z}\,dz \tag{2}$$

$$dv_z = \frac{\partial v_z}{\partial x}\,dx + \frac{\partial v_z}{\partial y}\,dy + \frac{\partial v_z}{\partial z}\,dz \tag{3}$$

3.2.2 Equations of Motion

The forces acting on a rectangular cubic element of fluid (dx, dy, dz) are considered. The internal forces, or body forces, per unit mass existing at the centrad of the element are written as g_x , g_y , g_z . The external forces per unit area are subdivided into normal and tangential stress components on each face of the element. The normal stresses, σ_x, σ_y, σ_z, are designated positive for tension. Six shear stresses, τ_{xy} , τ_{yx} , τ_{xz} , τ_{zx} , τ_{yz} , τ_{zy} , are distinguished with two orthogonal components acting on each face as shown in Figure 13. The first subscript indicates the direction of the normal to the face, and the second the direction of action with positive values along the x, y, and z coordinates.

When considering the moments of the shear stresses around the centroid, n a demonstrate the following identities. $\tau_{xy} = \tau_{yx}$, $\tau_{xz} = \tau_{zx}$, and $\tau_{yz} = \tau_{zy}$.

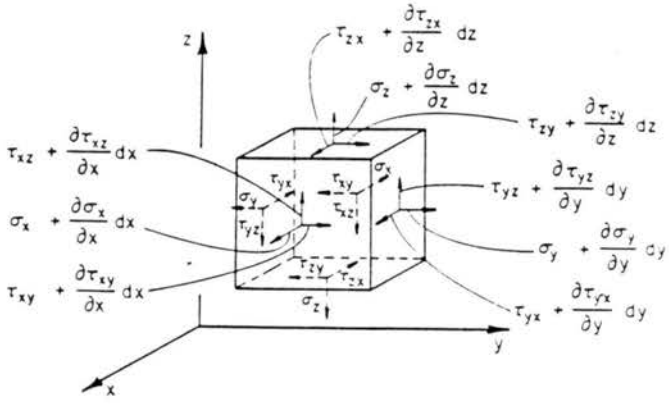

Figure 13. Normal and tangential stresses

The fluid element in Figure 13 is considered in equilibrium when the sum of the forces per unit mass in each direction x, y, and z is equal to the corresponding acceleration components a_x, a_y and a_z. After expanding the acceleration components a_x, a_y and a_z, the equation of motion in x-direction in rectangular coordinates can be written as:

$$\frac{\partial v_x}{\partial t} + v_x \frac{\partial v_x}{\partial x} + v_y \frac{\partial v_x}{\partial y} + v_z \frac{\partial v_x}{\partial z} = g_x - \frac{1}{\varrho} \frac{\partial p}{\partial x} + \frac{1}{\varrho} \left[\frac{\partial \tau_{xx}}{\partial x} + \frac{\partial \tau_{yx}}{\partial y} + \frac{\partial \tau_{zx}}{\partial z} \right] \tag{4}$$

Similar equations are obtained in the y and z direction.

3.2.3 Turbulence

Most flows encountered in fluvial systems are characterized by irregular velocity fluctuations indicating turbulence. The fluctuation superimposed to the principal motion is complex in its detail and still poses difficulties to mathematical treatment.

In describing turbulent flow in mathematical terms, it is convenient to separate the mean motion from the fluctuation. Denoting the time average of the v_x component by $\bar{v}_x$ and its fluctuation by v'_x, the pressure and velocity components are obtained similarly:

$$p = \bar{p} + p' \tag{5}$$

$$v_x = \overline{v_x} + v'_x \tag{6}$$

$$v_y = \overline{v_y} + v'_y \tag{7}$$

$$v_z = \overline{v_z} + v'_z \tag{8}$$

the time-averaged values at a fixed point in space are given by:

$$\overline{v_x} = \frac{1}{t_1} \int_{t_o}^{t_o + t_1} v_x \, dt \tag{9}$$

Taking the mean values over a sufficiently long interval of time t_1, the time-averaged values of the fluctuations are equal to zero, thus:

$$\overline{v_x'} = \overline{v_y'} = \overline{v_z'} = \overline{p'} = 0 \tag{10}$$

It is seen that both the time-averaged velocity components and the fluctuating components satisfy the equation of continuity, thus for incompressible fluids:

$$\frac{\partial \overline{v_x}}{\partial x} + \frac{\partial \overline{v_y}}{\partial y} + \frac{\partial \overline{v_z}}{\partial z} = 0 \tag{11}$$

$$\frac{\partial v_x'}{\partial x} + \frac{\partial v_y'}{\partial y} + \frac{\partial v_z'}{\partial z} = 0 \tag{12}$$

The velocity and pressure terms are substituted into the Navier-Stokes equation to give in the x direction:

$$\frac{\partial \overline{v_x}}{\partial t} + \overline{v_x}\frac{\partial \overline{v_x}}{\partial x} + \overline{v_y}\frac{\partial \overline{v_x}}{\partial y} + \overline{v_z} = g_x - \frac{1}{\varrho}\frac{\partial \overline{p}}{\partial x} + \nu \nabla^2 \overline{v_x} - \left[\frac{\partial \overline{v_x'^2}}{\partial x} + \frac{\partial \overline{v_x' v_y'}}{\partial y} + \frac{\partial \overline{v_x' v_z'}}{\partial z}\right] \tag{13}$$

In addition to the terms found in the Navier-Stokes equations, three additional terms involving the cross products of velocity fluctuations are added to the right-hand side. These additional stresses are known as Reynolds stresses, or apparent stresses, for turbulent flow. Generally speaking, these apparent stresses far outweigh the viscous components in turbulent flow.

3.2.4 Velocity Profiles

Since the no-slip condition prevails at solid boundaries, all turbulent components must vanish at the walls and they are very small in their immediate neighborhood. It follows that all apparent stresses become smaller than the viscous stresses of the Navier-Stokes equation. Therefore, in turbulent flows, laminar motion must persist in a very thin layer next to the wall. This is known as the laminar sublayer.

With analogy to the mean free path in the kinetic theory of gases, Prandtl imagined the mixing length concept which implies that the transverse velocity fluctuation v'_y is of the same order of magnitude as v'_x and can be written in the form:

$$\overline{v'_x} \sim \overline{v'_y} \sim \ell \frac{d\overline{v_x}}{dy} \tag{14}$$

in which ℓ denotes the Prandtl mixing length.

$$\overline{v'_x v'_y} \sim - \overline{|v'_x|}\ \overline{|v'_y|} \tag{15}$$

$$\overline{v'_x v'_y} \sim \ell^2 \left[\frac{d\overline{v_x}}{dy}\right]^2 \tag{16}$$

Following the Prandtl mixing length hypothesis, the shear stress can be written as:

$$\tau = \rho\, \ell^2 \left[\frac{d\overline{v_x}}{dy}\right]^2 + \mu \frac{d\overline{v_x}}{dy} \tag{17}$$

In turbulent flows, the first term of Eq. 17 outweighs the second term due to viscosity. Prandtl hypothezied that the mixing length is proportional to the distance from the boundary,

$$\ell = \kappa y \tag{18}$$

in which κ is the von Kàrmàn constant.

The shear stress in the region close to the wall remains relatively constant and with the use of the shear velocity u_*, one obtains:

$$\sqrt{\frac{\tau_o}{\rho}} = u_* = \kappa y \left[\frac{d\bar{v}_x}{dy}\right] \tag{19}$$

The variables $\bar{v}_x$ and y can be separated and integrated to yield the well-known logarithmic velocity distribution.

$$\frac{v_x}{u_*} = \frac{1}{\kappa} \ell n\, y + c_1 \tag{20}$$

in which c_1 is a constant of integration evaluated as a function of the distance y_o from the wall at which the velocity v_{xo} equals zero. Hence:

$$\frac{v_x}{u_*} = \frac{1}{\kappa} \ell n \frac{y}{y_o} \tag{21}$$

3.2.5 Rough Versus Smooth Boundaries

When the boundary roughness or sediment size d_s exceeds the laminar sublayer thickness, $\delta = 11.6\,\nu/u_*$, these elements protrude in the turbulent zone and the flow is described as turbulent over a rough boundary. In such a case, experiments indicate that the distance $y_o = d_s/30$ (when $u_* d_s/\nu > 70$).

It can be found from dimensional analysis that for turbulent flows over a smooth boundary, the distance y_o is proportional to the ratio ν/u_*. This has been verified with experiments that define $y_o = \nu/9u_*$.

By definition, the Darcy-Weisbach friction factor f is obtained from:

$$\tau_o = \frac{f}{8} \rho \bar{V}_x^2 \tag{22}$$

where $\bar{v}_x$ is the depth-averaged flow velocity, thus:

$$f = \frac{8\tau}{\rho \bar{V}_*^2} \tag{23}$$

3.2.6 Specific Energy

In rectangular flumes, the specific energy function E for flows with unit discharge q = Vy is:

$$E = y + \frac{q^2}{2gy^2} \tag{24}$$

Properties of the specific energy function are such that critical flow depth y_c corresponds to the minimum of the specific energy function E_{min} when $F_r = 1$. After substitutions, the resulting equation for gradually varied steady one-dimensional flow is:

$$\frac{dy}{dx} = \frac{S_o - S_f}{1 - F_r^2} \tag{25}$$

3.2.7 Backwater Curves

Gradually varied flows are classified depending on the slope and the position of the water surface relative to the critical depth y_c and the normal depth y_n, see Figure 14.

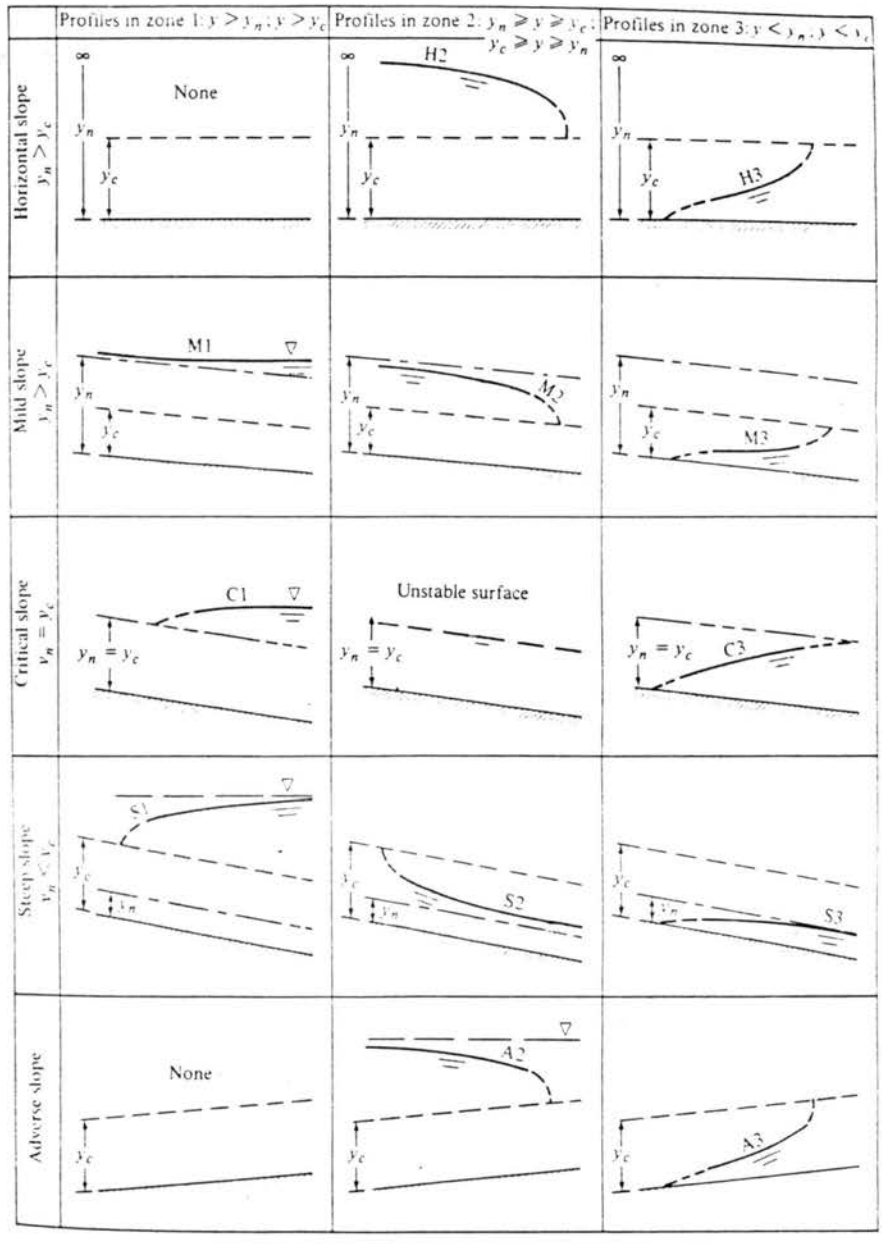

Figure 14. Classification of water-surface profiles of gradually varied flow. (from Robertson and Crowe, 1985)

From the general classification table of gradually varied flows, the most commonly seen type of backwater curve is the M-1, which involves downstream control of the water elevation. Such flow conditions can be simulated in laboratory flumes by controlling the tailwater elevation with tailgates. The M-1 backwater curve is favorable for sedimentation because the velocity and the shear stress decreases in the downstream direction. Additional experiments are carried out under adverse A-2 and horizontal H-2 slopes.

3.2.8 Incipient Motion of Noncohesive Sediment Particles

The flow of water around sediment particles exerts forces which tend to initiate their downslope motion. The resisting forces of noncohesive material relate to the weight of the particles. When the hydrodynamic forces acting on a single particle equal the resisting forces, threshold conditions are reached and the particle is impending incipient motion.

The forces acting on a sediment particle sketched in Figure 15 are the submerged weight, buoyancy, and the lift and drag forces.

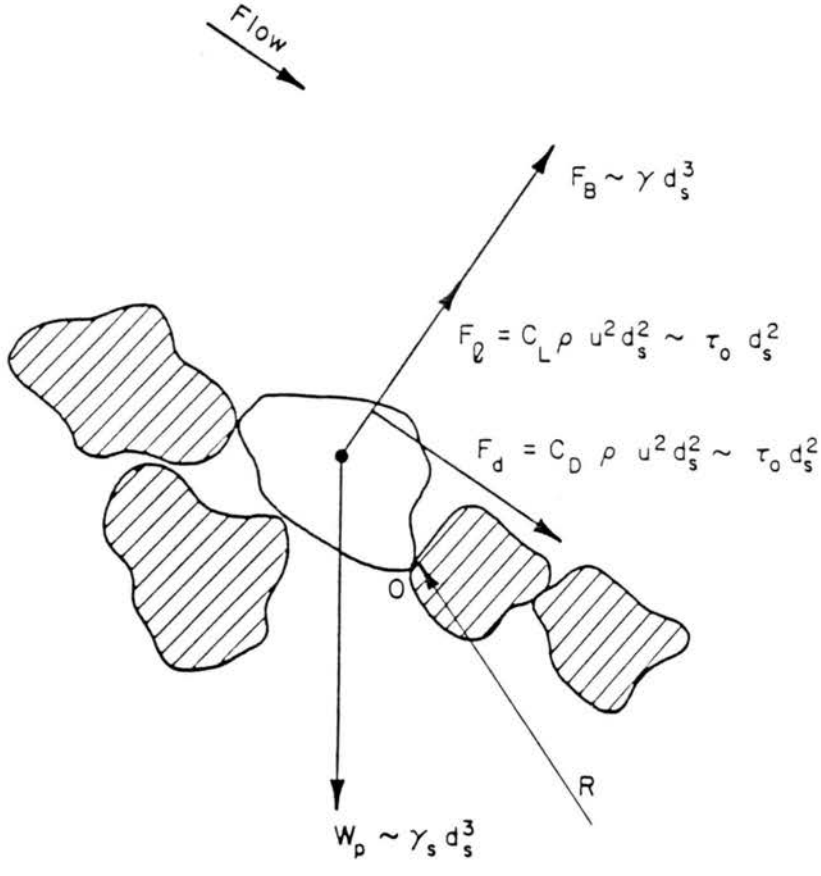

Figure 15. Force diagram for a single particle under steady uniform flow.

From the analysis of the hydrodynamic forces around a sphere, no lift force is present under creeping flow conditions. In turbulent flows, however, lift forces depend on the circulation around the particle and it is assumed that lift and drag forces are proportional. The sum of moments around the point of contact 0 can be written:

$$\tau_o = c_1 d_s^2 = c_2 (\gamma_s - \gamma) d_s^3 \qquad (26)$$

in which:
- τ_o is the bed shear stress,
- γ_s specific weight of a sediment particle,
- γ specific weight of the fluid,
- d_s sediment size, and
- c_1, c_2 product of moment arms and constants function of the shape of the particle and the geometry of the channel.

The ratio of the two moments in Equation 26 defines the Shields number τ_* which is a function of the laminar or turbulent flow conditions around the particle. The value of the Shields number corresponding to beginning of motion ($\tau_o = \tau_c$) becomes a function of the ratio of sediment size to the laminar sublayer thickness expressed either as d_s/δ or $u_* d_s/\upsilon$ (because $\delta = 11.6\ \upsilon/u_*$):

$$\tau_* = \frac{\tau_c}{(\gamma_s - \gamma) d_s} = f\left[\frac{u_* d_s}{\nu}\right] \qquad (27)$$

Early experiments by Shields (1936) led to the widely accepted diagram shown in Figure 16.

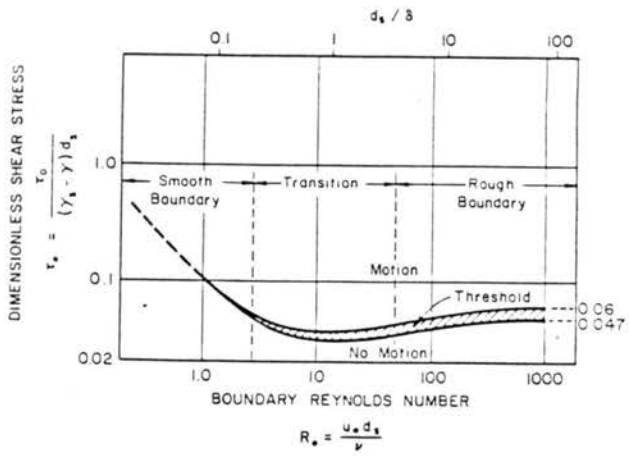

Figure 16. Shields diagram

Shields determined the threshold condition by measuring transport for values of the Shields parameter at least twice as large as the critical value and then extrapolated to the point of vanishing sediment transport. This indirect method avoids the implications of random variability of sediment and flow properties.

For turbulent flows over rough boundaries the critical shear stress becomes proportional to the sediment size since the threshold value of the Shields parameter remains constant.

Figure 18 shows data on critical velocity plotted against mean sediment size for quartz sediment in water (ρ_s = 2.65 g/cm^3) obtained from three sources. The data points and the curves of the upper limit, mean, and lower limit of the critical mean velocity are taken from the work of Hjulström (1935) who prepared the curves based on data of several workers. The curves are for flows with depths of at least 1m. In such fine sediments, cohesion is an important factor in determining critical conditions.

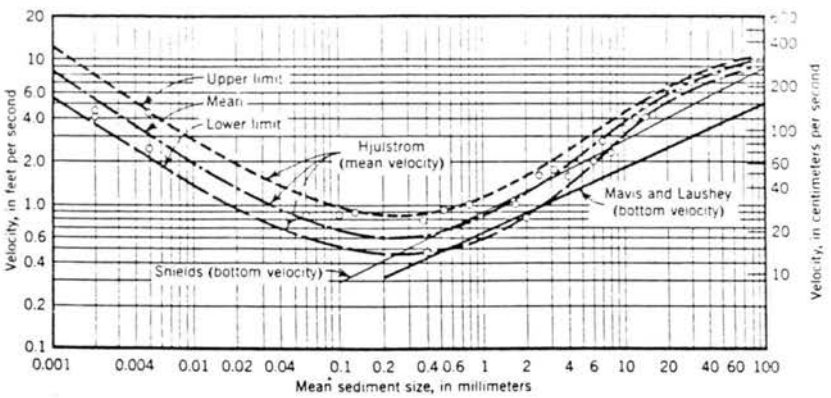

Figure 17. Critical water velocities

3.3 Experimental Procedure

3.3.1 Equipment

All the experiments are carried out in a tilting, recirculating flume: 0.15m wide, 0.15m deep, and 2.40m long, as sketched in Figure 19. The flow rate is controlled by a gate valve and measured by a Venturi orifice. The deposition of sand in the flume is controlled by small tailgates 0.15m wide and 0.02m high. In one experiment, a 0.04m high tailgate is also used. The depth of water and deposition is measured by an affixed ruler on the sidewall of the flume. The slope of the flume can be adjusted by a screw jack. The details on the experimental flume are shown in Figure 18 and a photograph of the flume is also presented in Picture 35.

Particular consideration in the design procedure has been given to the entrance condition of the flume. The return of water and sediment in the head water box needs to be carefully designed in order to ensure complete mixing of the sediment particles and constant inflow of sediment under steady flow conditions. The rounded entrance profile and the use of a movable plate shown on Picture 36 provided excellent feeding conditions into the plexiglas flume.

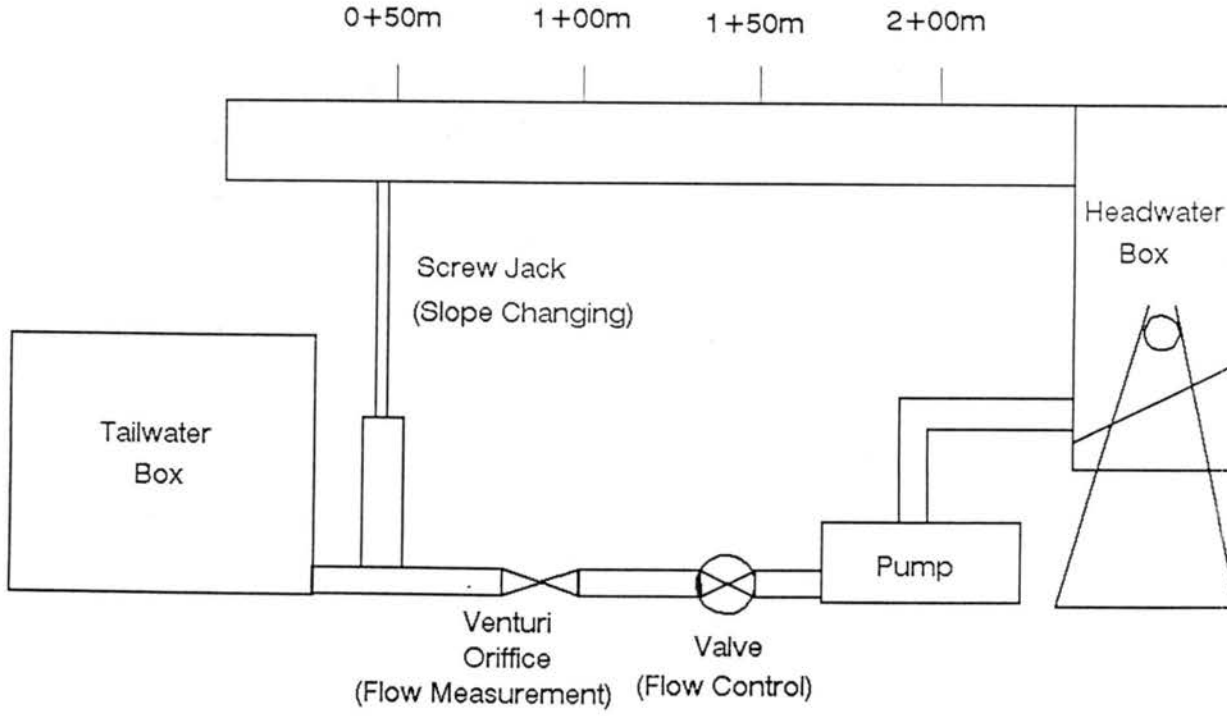

Figure 18. Recirculating flume

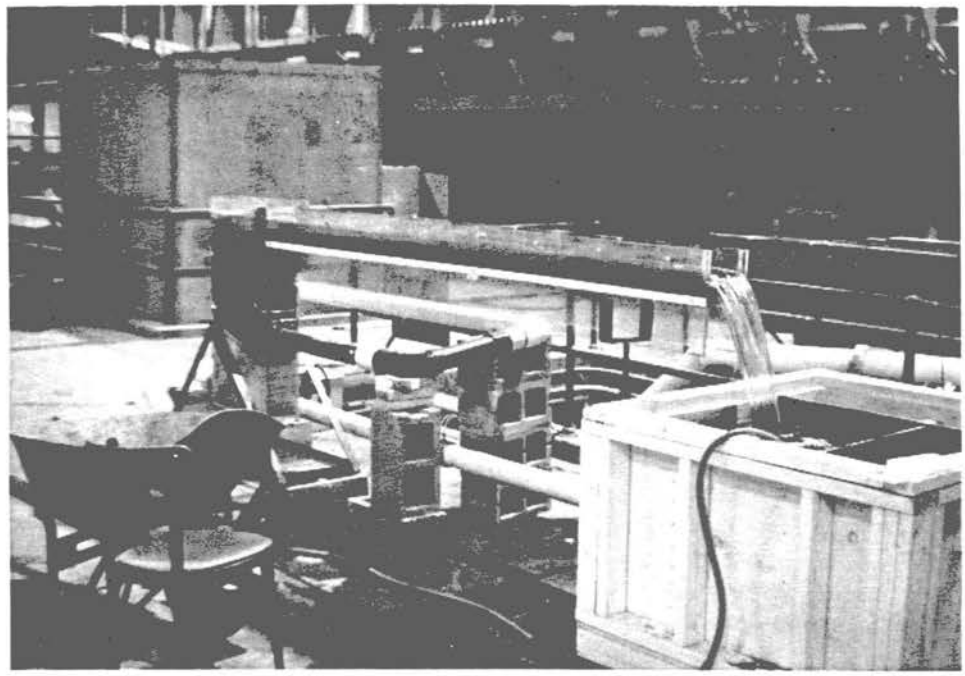

Picture 35. Experimental facilities (whole view)

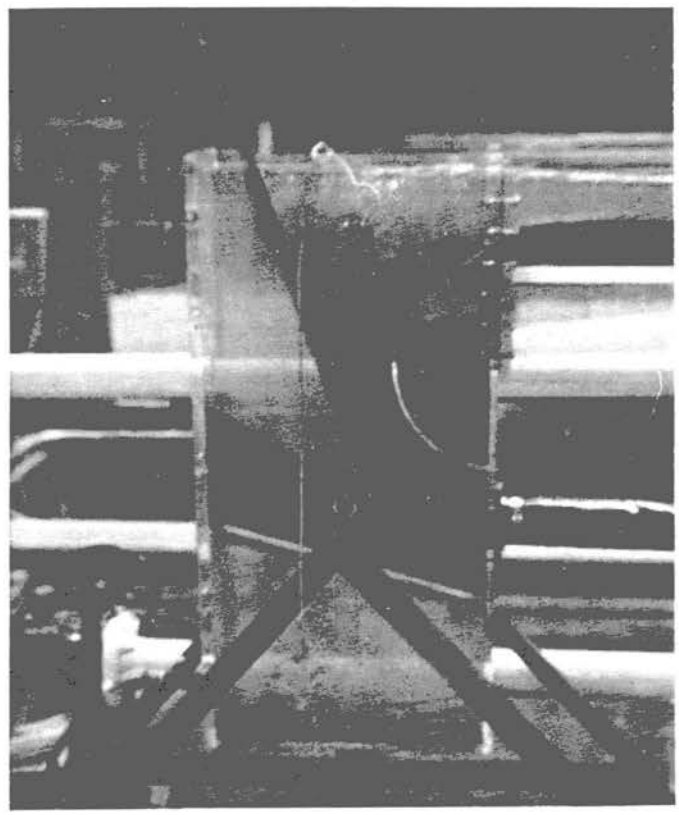

Picture 36. Headwater box

3.3.2 Sediment Mixtures

Four types of sands are readily available at ERC, out of which two white sands identified as ERC#2 and ERC#4 have been selected for this analysis. In order to clearly visualize the lamination process, two black sands with a specific gravity of 2.65 identified as B3060 and B2040 were obtained to prepare several mixtures. The characteristics of the original sands are summarized in Table 8.

Table 8. The original sand size distributions

Type	Color	D_{10}	D_{25}	D_{50}	D_{75}	D_{90}
B3060	black	0.14mm	0.205mm	0.335mm	0.55mm	0.62mm
B2040	black	0.38mm	0.48mm	0.575mm	0.67mm	0.76mm
ERC#2	white	0.72mm	0.90mm	1.20mm	1.50mm	1.90mm
ERC#4	white	0.094mm	0.13mm	0.16mm	0.19mm	0.24mm

From these original sands, four sand mixtures were prepared after sieving out the coarser fraction of one sand and the finer fraction of the second one. The four mixtures identified as SM-1, SM-2, SM-3, and SM-4 were analyzed in a preliminary study by Julien and Chen (1989), and the best two mixtures (SM-2 and SM-3) were considered in the following analysis. The characteristics of these two black and white mixtures are summarized in Table 9. Note that in the mixture SM-2, the coarse material is black and the fines are white. Conversely, the mixture SM-3 is comprised of coarse white particles mixed with fine black particles. The particle-size distributions of the original sands and the mixtures are shown on Figure 20 and 21.

Table 9. The composition of sand mixtures

Sand Mixture	Composition	Total Weight	D_{50}
• SM-2	B2040 & ERC #4 2.0mm-0.425mm:0.425mm-0.063mm 80kg : 80kg	160 kg	0.28 mm
• SM-3	B3060 & ERC #2 0.6mm-0.063mm:2.0mm-0.6mm 62kg : 82kg	144 kg	0.62 mm

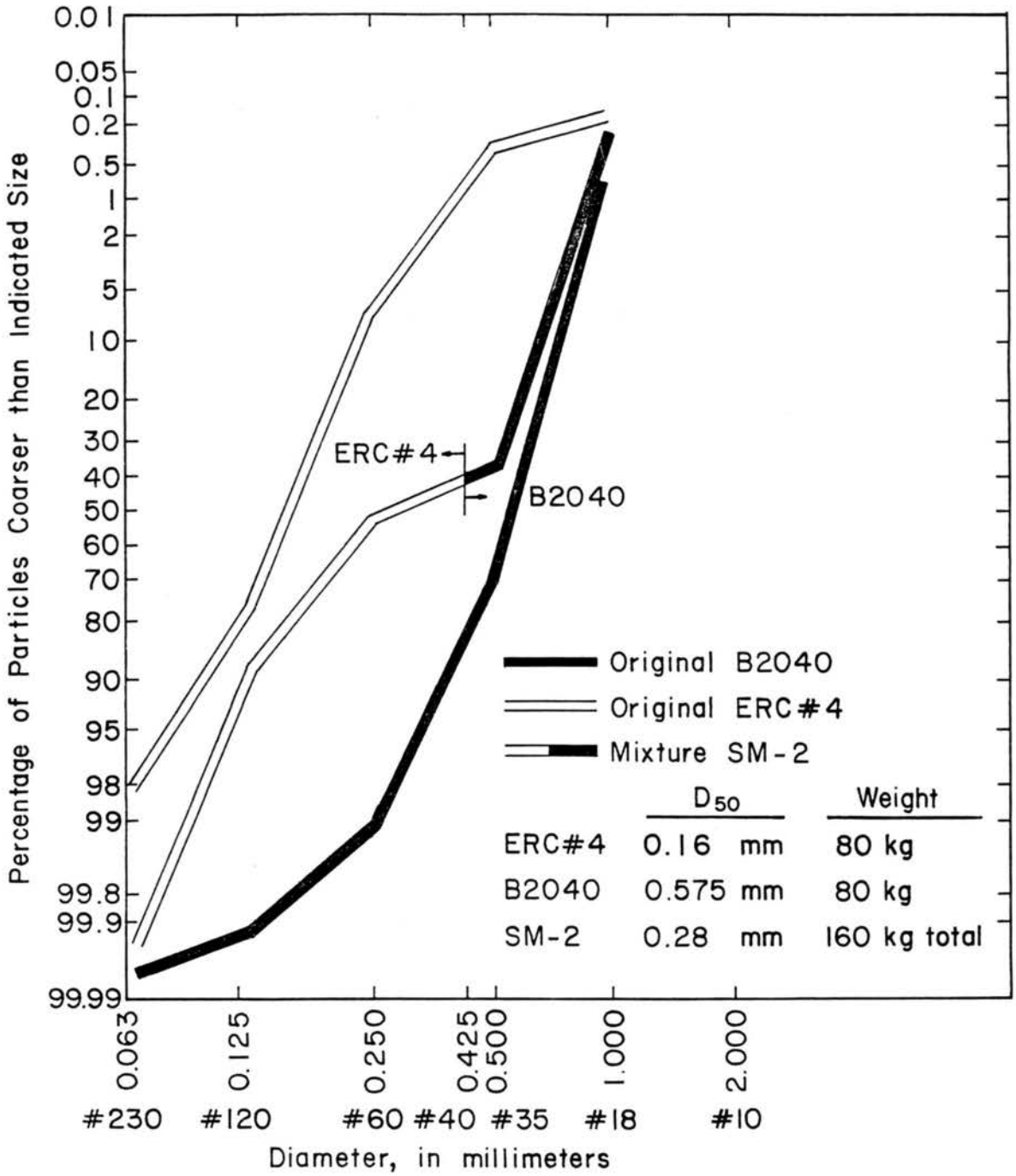

Figure 19. Particle-size distribution for sand mixture No. 2
(mixing B2040 sieve #10-#40 & ERC #4 sieve #40-#230)

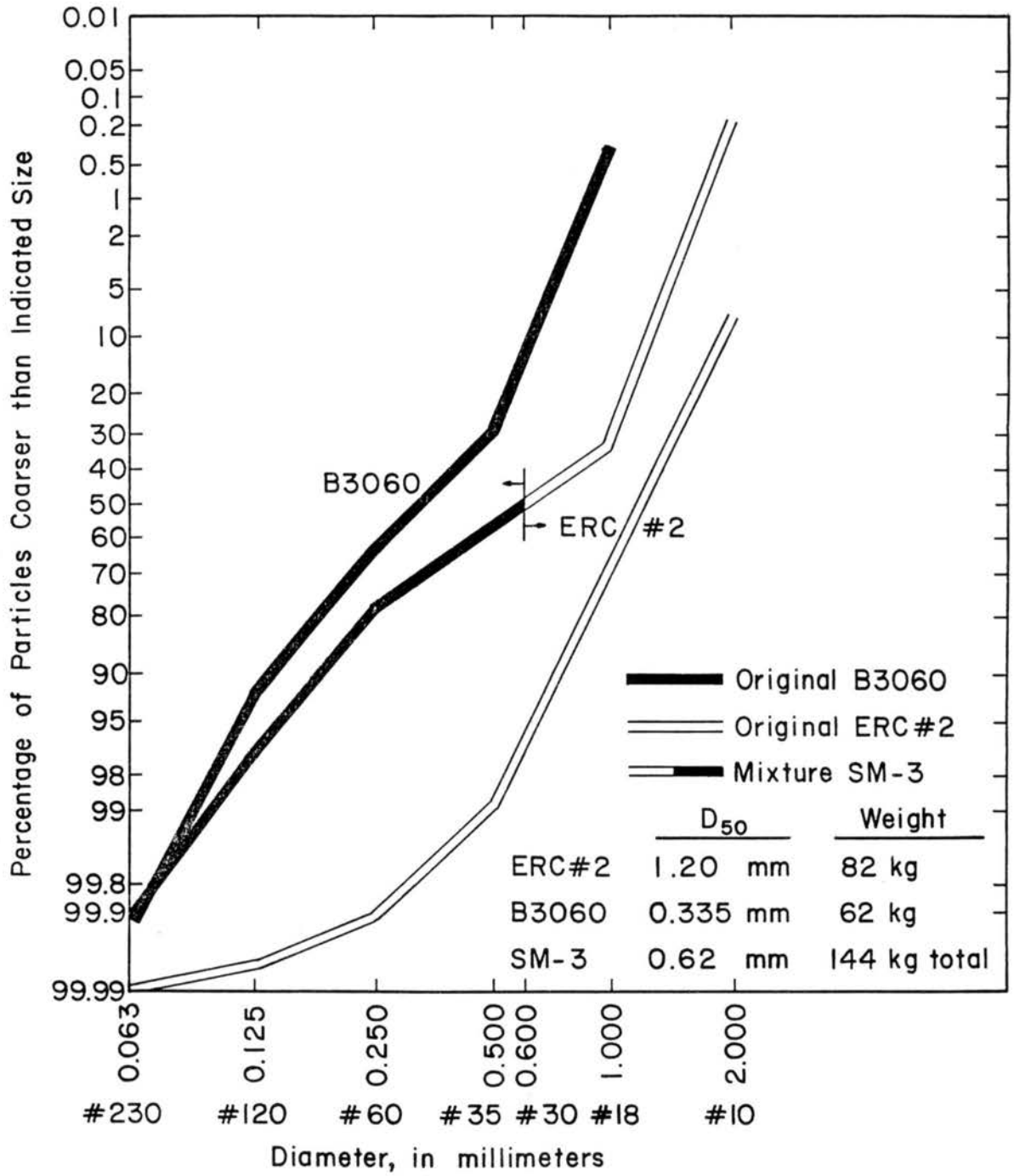

Figure 20. Particle-size distribution for sand mixture No. 3
(mixing B3060 sieve #30 - #230 & ERC #2 sieve #10 - #30)

3.3.3 Procedure

In this experimental program, five runs are detailed in Table 10 for two sand mixtures, i.e. four runs for SM-2 and one run for SM-3. In each run the flume slope is fixed and four constant values of flow discharge are selected for each of the four steps. Therefore, for each step we specify flume slope and flow discharge. The discharge increases slightly at each subsequent step. Two tailgates (2cm high) are used to control tailwater depth and sand deposition under three conditions, i.e. without tailgate, one tailgate, and two tailgates; but for Run SM-2D, we propose two different gate sizes (2cm & 4cm high) to study the effect of gate size.

Before each experiment, we set the flume slope (horizontal, positive, or adverse slope). For each step we adjust the valve to control the flow rate and fix the discharge. Firstly, the flow runs freely without gate control until the first deposition layer is formed. Sequentially, the first tailgate is inserted at the downstream end of the flume. We wait until the deposit layer is completely formed and equilibrium conditions are reached (about 20 to 30 minutes). Then, we measure the discharge, surface velocity, depth and record the configuration of laminae deposition. After the measurements are completed, the second gate is inserted to form the second layer of deposits and the procedure similar to the first gate is repeated. For the other steps and runs, the whole procedure is repeated. The detailed procedure is listed on a flow chart in Figure 22. The cross-section SEC1+00 has been selected for the comparison of the various sedimentation profiles.

Table 10. The runs and steps in the horizontal lamination experiment

Run	Step	Flume Slope	Tailgate Condition
1. SM-2A	1, 2, 3, 4	horizontal	without gate, add first gate, add second gate
2. SM-2B	1, 2, 3, 4	adverse slope (S= -0.005)	without gate, add first gate, add second gate
3. SM-2C	1, 2, 3, 4	positive slope (S= +0.005)	without gate, add first gate, add second gate
4. SM-2D	1, 2*	horizontal	without gate, add 1st small gate (2cm high), and 2nd large gate (4cm high)
5. SM-3A	1, 2, 3, 4	horizontal	without gate, add first gate, add second gate

* Note: The SM-2D experiment involves a larger tailgate which increases the water depth and causes overflow at larger discharges. Therefore, two steps were used to avoid excessive flow discharges.

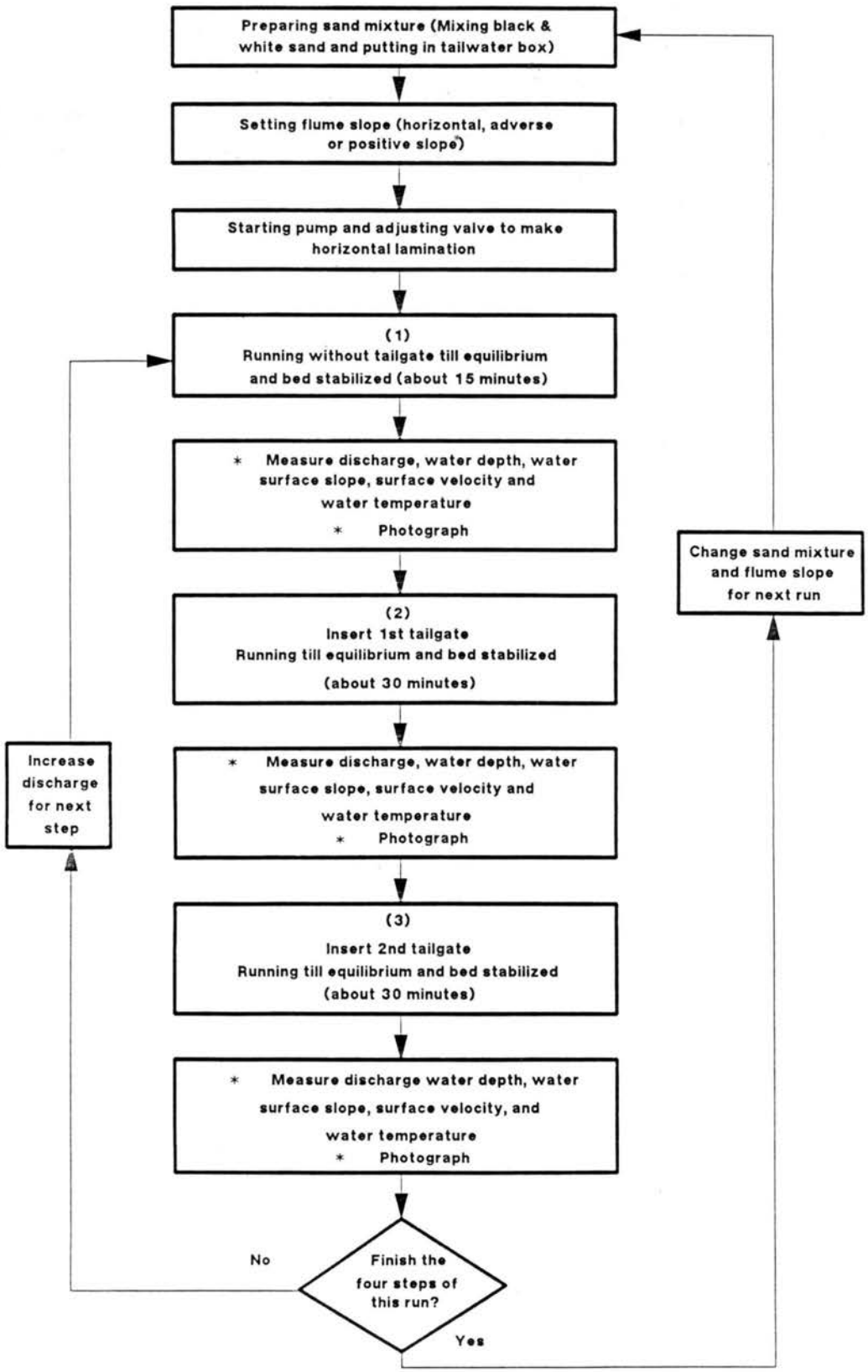

Figure 21. Flow chart for experimental procedure in each run

3.3.4 Data Measurement

During each step, several types of measurements are repeated to generate a data base of hydraulic conditions associated with the observed formations of laminae and stratified deposits.

The flow discharge is measured by a Venturi orifice shown in Figure 19. The manometer readings are transformed into discharge values through a calibrated chart. The water temperature is measured with a mercury thermometer.

The hydraulic characteristics of flow depth and flow velocity are measured with the water surface slope. The water depth is measured with a ruler affixed on the flume sidewall at several sections including SEC1+100 and others. The thickness of horizontal laminae deposits are measured from the ruler affixed on the flume sidewall at SEC1+00. The water surface slope is determined from the difference in water surface elevation between two points. The surface velocity is determined from average measurements of the travel time of a floating paper ball between two points. Average flow velocities are calculated form the discharge measurements and the cross-section area.

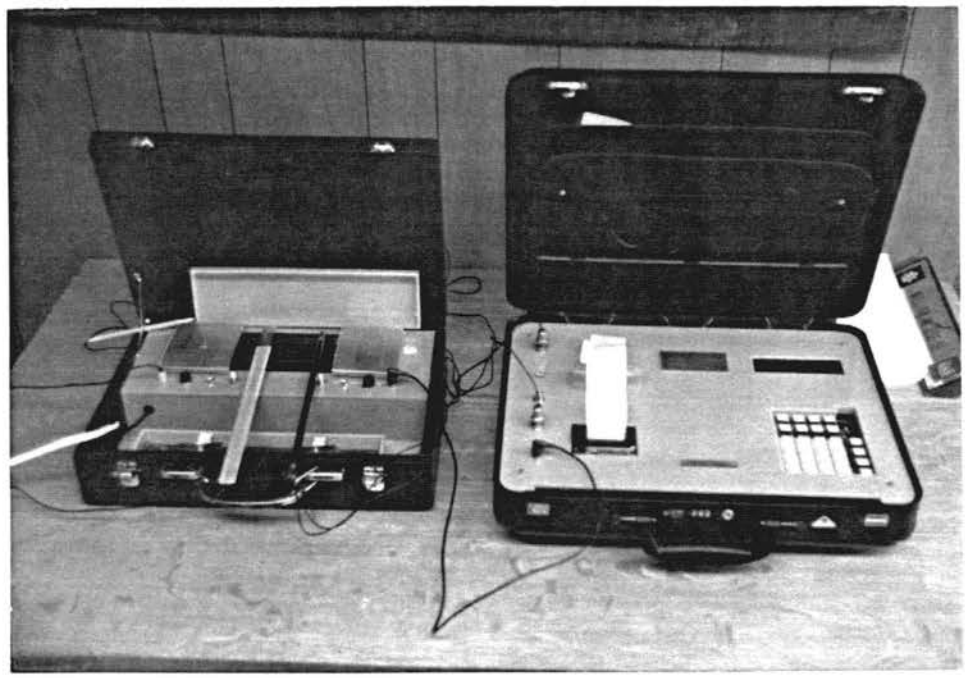

Picture 37. Ultrasonic Doppler Velocimeter (UDV-89)

Local velocity measurements are taken from a Ultrasonic Doppler Velocimeter Model UDV-89, shown in Picture 37. It's a multifunction flow meter mainly used to measure flow velocity in a clear fluid or in a muddy fluid. Besides, flow turbulence intensity, maximum/minimum velocity, velocity probability density distribution, velocity accumulative probability curve can be obtained by using the velocimeter.

The Ultrasonic Doppler Velocimeter measures the difference between the frequency of source wave transmitted and the frequency received after reflection from small particles moving with the fluid. The UDV-89 velocimeter is an easy operating velocimeter composed of a probe composed of the ultrasonic wave transmitter and the receiver, and a specific microcomputer system which analyzes the measurements and prints the results. In a sediment-laden flow, the particle producer is not needed. The measurement of velocity at a point can be accomplished in about 10 seconds. The UDV-90 velocimeter is best suited to laboratory one-dimensional flow measurement. It can take measurements of velocity in the range of 0.03-6.0 m/sec. with an accuracy of +0.003 m/sec. or 2% of reading, whichever is greater. The sediment concentration in the flow can be as high as 650 kg/m^3. To measure the velocity at a certain point, the Doppler probe is installed at about 5 cm downstream of the measuring point.

3.4 Experimental Results

This section presents the results of all the measured and calculated parameters for each run of the experimental program detailed in the previous section. One of the most interesting features of the experimental program is illustrated in Pictures 38-43 on the following pages. From the equilibrium conditions of mostly fine white sand particles on the bed, shown in Picture 38, the insertion of a tailgate induces a deltaic formation of coarse black particles which is shown to propagate downstream on Pictures 38 and 39.

Starting from steady uniform flow conditions, the introduction of a tailgate creates a perturbation which propagates upstream and increases the flow depth. During this short period with unsteady flow conditions (about 10 sec.) the flow depth increases and both velocity and shear stress decrease in the downstream direction. This induces settling of the particles held in suspension which forms a microscopic layer of sediments. As the inflow of sediments remains unchanged, the incoming particles deposit upstream where the flow condition drops below threshold condition. A delta comprised of the coarser traction of the sediment mixture soon develops and propagates in the downstream direction. The time sequence of the development of bed deposits can be sketched in Figure 22 as follows with time $t_1 < t_2 < t_3$:

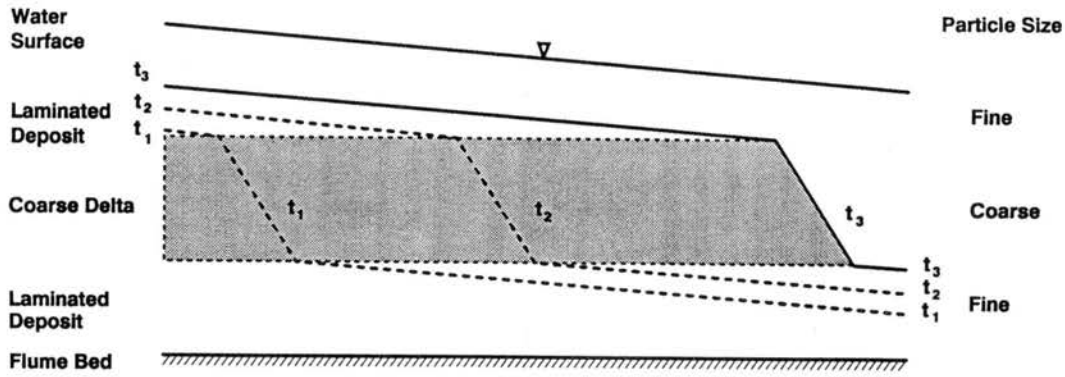

Figure 22. Deposition sequence for $t_1 < t_2 < t_3$

As the delta progresses, finer white particles are seen to segregate and deposit in the form of laminae on top of the coarse black particles as shown on Picture 40. The lamination process continues in time and the thickness of the overlying laminated white deposit increases gradually until equilibrium conditions are reached. After completion of the experiment, Picture 42 shows a detailed view of the lamination at the entrance section of the flume, while picture 43 illustrates the superposition of stratified and laminated deposits. It must be noticed that this experiment was carried out with a steady supply of water and sediment at the upstream end of the flume. A cross-sectional view of the deposit in the middle reach of the flume is shown in Picture 44. The following sub-section documents each of the five runs separately.

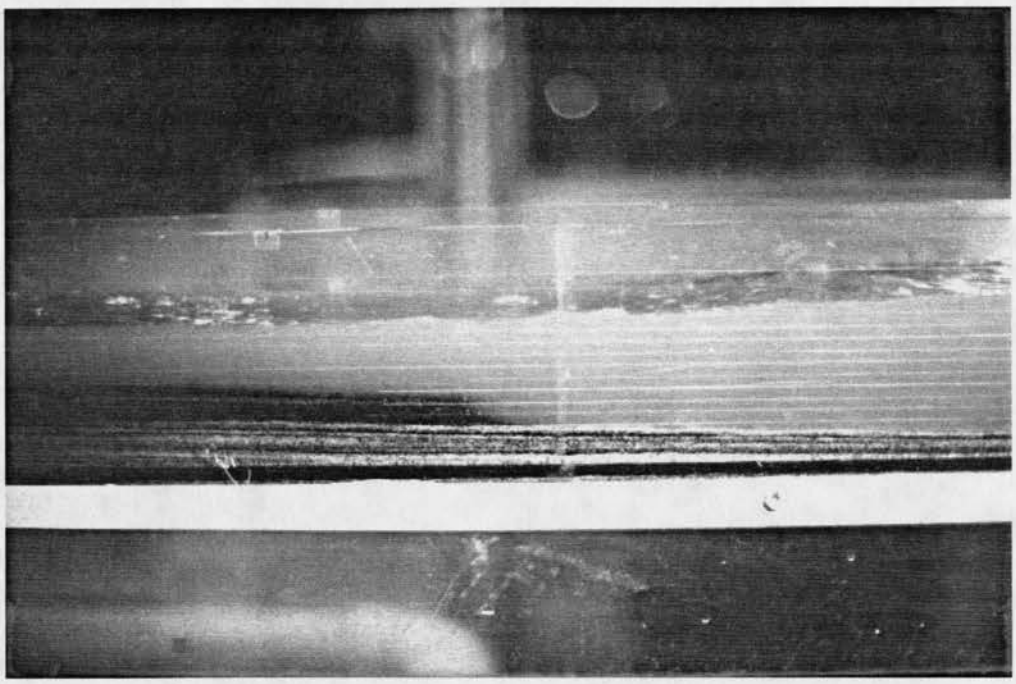

Picture 38. Delta propagation on laminated bed

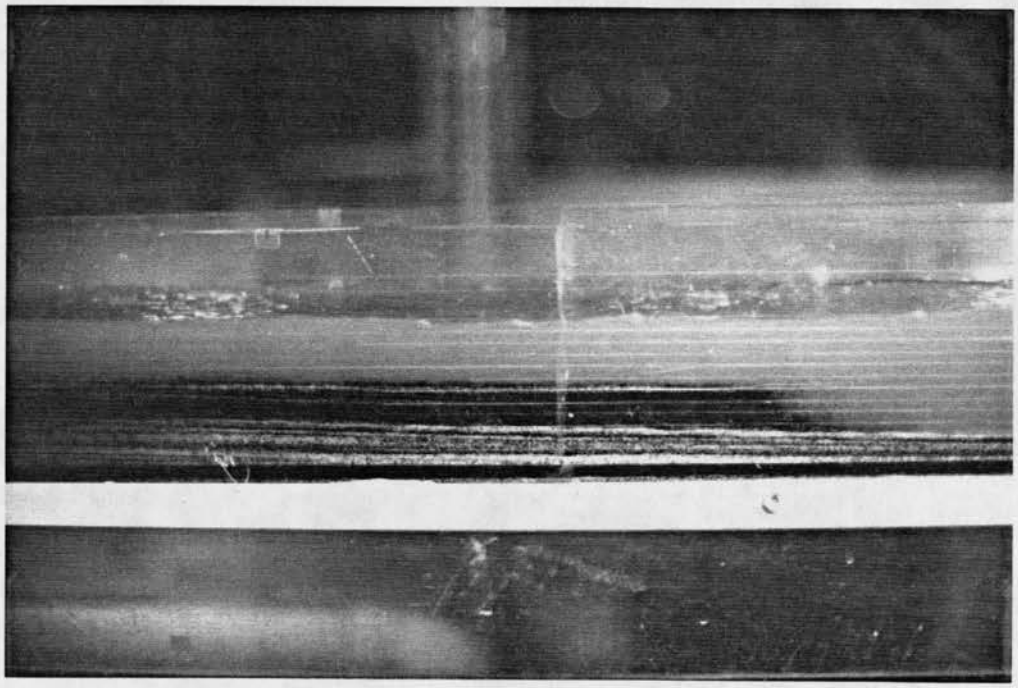

Picture 39. Delta propagation on laminated bed

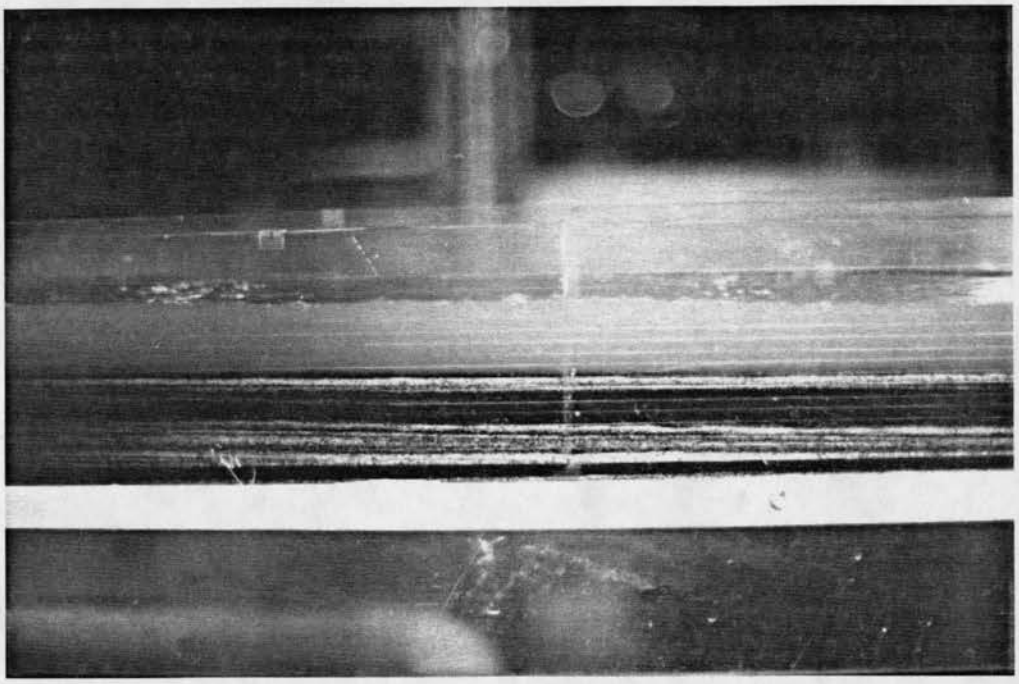

Picture 40. Laminae formation of white particles on top of delta

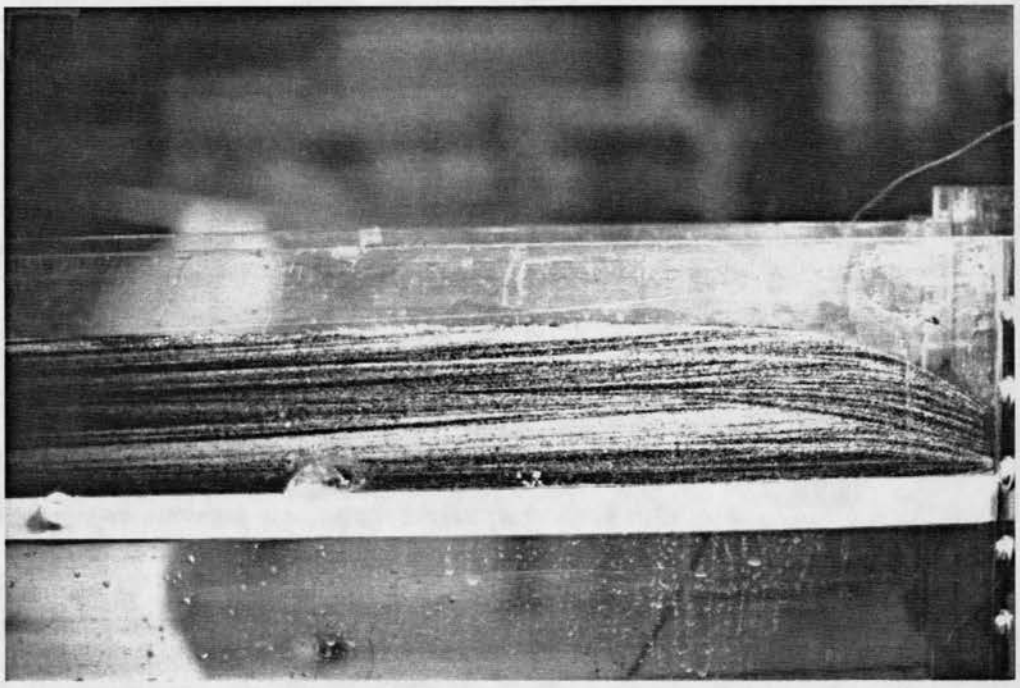

Picture 41. Detailed view of lamination at the entrance section (flow from right to left)

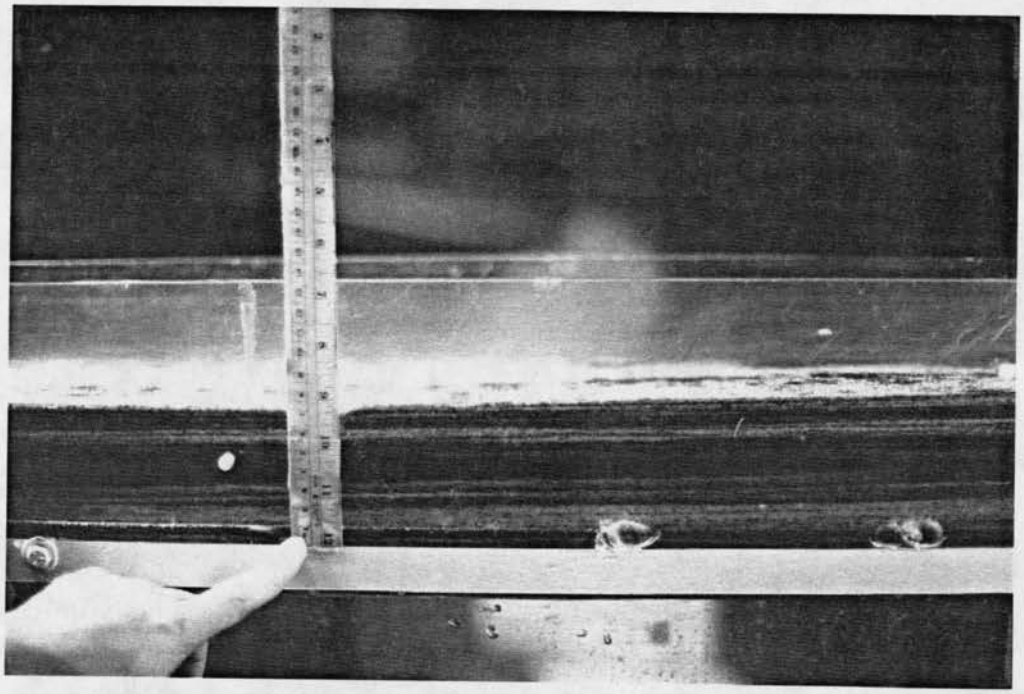

Picture 42. View of the deposit after completion of experiment (flow from right to left)

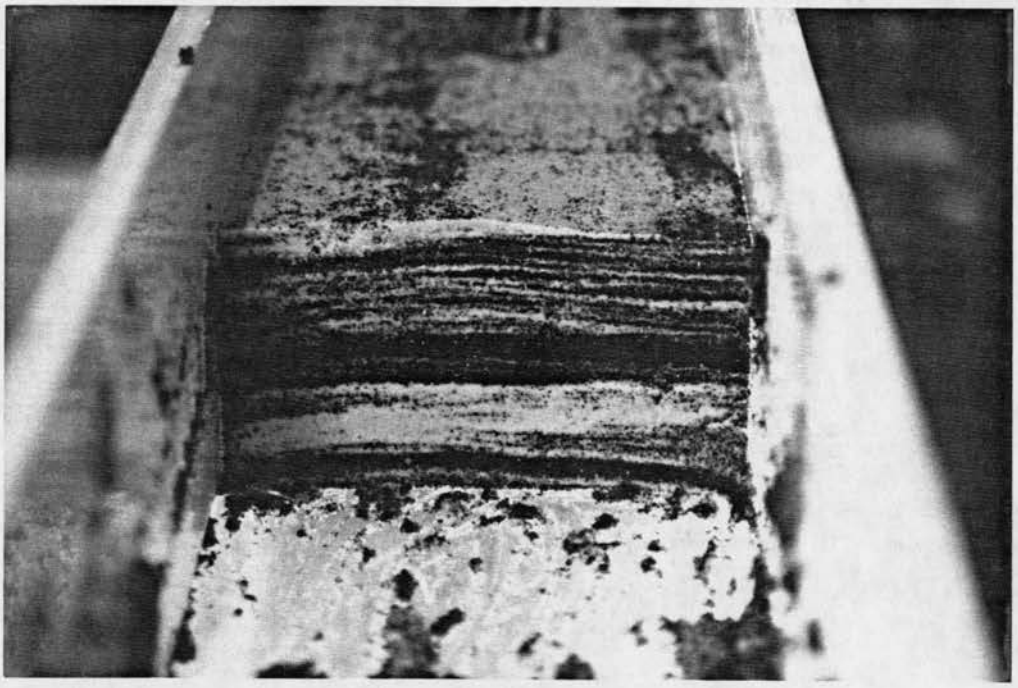

Picture 43. Cross-sectional view of deposit after the experiment

3.4.1 Run SM-2A

(1) Objective of this run: Examine the relationship between velocity and lamination thickness.

(2) Experimental conditions and data summary:

- Horizontal flume
- SM-2 sand mixture (B2040 & ERC #4), D_{50} = 0.28 mm
- Two small tailgates (2 cm high each).
- Two deposition for each step is shown on pictures as:
  - Step 1: Picture 44 and 45
  - Step 2: Picture 46 and 47
  - Step 3: Picture 48 and 49
  - Step 4: Picture 50 and 51
- The data for this run is summarized in Table 11 below.

Table 11. Data Summary for Run SM-2A

Run: SM-2A (Horizontal) D_{50} = 0.28mm

Step	Gate	Q cm^3/s	h cm	Vm cm/s	Vs cm/s	Sw	Shear $dyne/cm^2$	Fr	U* cm/s	f	H. Lam mm	Delta mm
SM2A-1	1st	2606	3.1	54.23	62.14	0.010	23.54	0.983	4.852	0.064	4	12
	2nd	2546	3.4	48.31	55.02	0.010	23.57	0.836	4.855	0.080	5	10
SM2A-2	1st	3536	3.7	61.65	73.54	0.011	29.08	1.023	5.392	0.061	9	7
	2nd	3470	3.9	57.40	64.96	0.011	30.12	0.928	5.488	0.073	8	8
SM2A-3	1st	4026	3.9	66.60	76.78	0.014	37.75	1.077	6.144	0.068	14	5
	2nd	3949	4.0	63.69	69.30	0.011	30.63	1.017	5.534	0.060	11	4
SM2A-4	1st	4548	3.9	75.23	82.83	0.015	40.29	1.216	6.438	0.056	16	5
	2nd	4480	4.1	70.49	76.54	0.012	33.76	1.112	5.810	0.054	12	2

Q = flow discharge; h+ water depth SEC1+00; Vm = mean velocity; Vs = surface velocity; Sw = water surface slope; shear = bed shear stress; Fr = Froude number; U* = friction velocity; f = friction coefficient; H.Lam = horizontal lamination.

Detailed velocity measurements were made with a Ultrasonic Doppler Velocimeter for SM2A under a constant flow rate of 2650 cm^3/s. In this run, flow depth, mean velocity, surface velocity, and near-bed velocity on top and downstream of the moving delta are measured, in order to examine the values of hydraulic parameters which control the formation of delta during the process of lamination. The results are listed in Table 12. The symbols in this table are explained as follows: h_{eq} ,ξ_{eq} = flow depth and water surface elevation at equilibrium; S_w = water surface slope at equilibrium; h_u, h_d = flow depth on top of delta and downstream of delta, respectively; V_u, V_d = mean velocity on top and downstream of delta, respectively; V_{su}, V_{sd} = surface velocity on top and downstream of delta, respectively; V_{bu}, V_{bd} = near-bed velocity on top and downstream of delta, respectively; and V_{meq}, V_{beq}, V_{seq} = mean, near-bed, surface velocity at equilibrium respectively. All measurements are under a constant discharge of 2650 cm^3/s.

Table 12. Detailed measurements of velocity during lamination

	h_{eq} cm	ξ_{eq} cm	S_w (%)	h_u cm	h_d cm	V_u cm/s	V_d cm/s	V_{su} cm/s	V_{sd} cm/s	V_{bu} cm/s	V_{bd} cm/s	V_{meq} cm/s	V_{beq} cm/s	V_{seq} cm/s
No gate	2.80	3.00	0.65									59.90	34.04	66.64
1st gate	2.90	5.08	0.65	3.20	4.80	52.40	34.95	57.54	37.65	33.31	15.68	59.89	33.45	73.56
2nd gate	2.97	7.05	0.70	3.25	5.20	53.20	33.25	61.39	41.84	39.08	21.50	57.55	26.17	71.88

Table 12 indicates that as a tailgate is introduced, the flow velocity decreases dramatically. A delta then starts to build up and move downstream as sediment from upstream continues to deposit on the toe of the delta. The high flow velocity on top of the delta and the low flow velocity downstream of the delta creates a separation zone downstream of the delta with high turbulent intensity. Accordingly, coarse particles can easily deposit on the front of the delta while most of the fine particles travel further downstream. As the delta moves downstream, the thickness of delta increases until it reaches equilibrium. Meanwhile, a thin layer of fine particles develops on top of the coarse particle and then coarse particles roll on top of this thin layer of fine materials. At equilibrium, the flow velocity is greater than the velocity on top of the delta during the process.

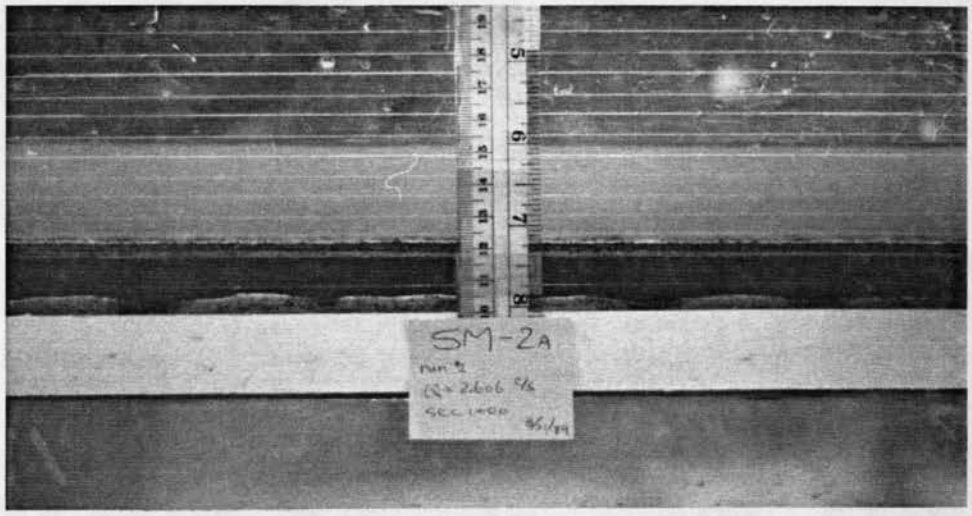

Picture 44. Run SM-2A, Step 1

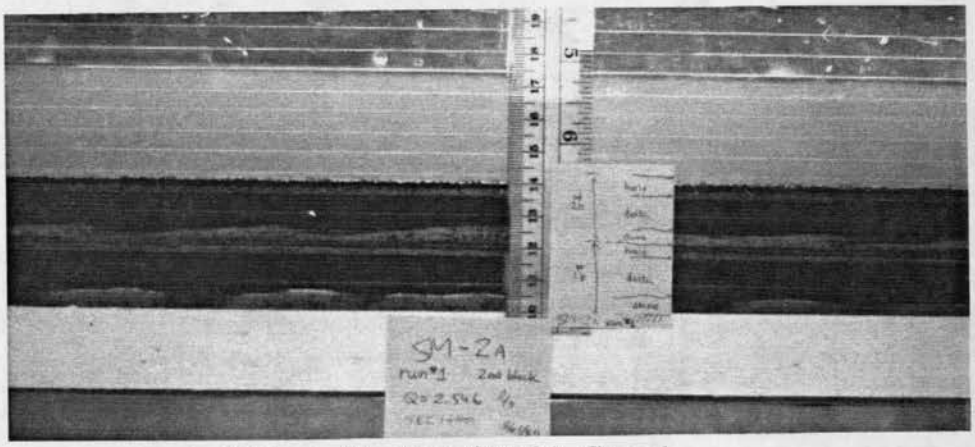

Picture 45. Run SM-2A, Step 1

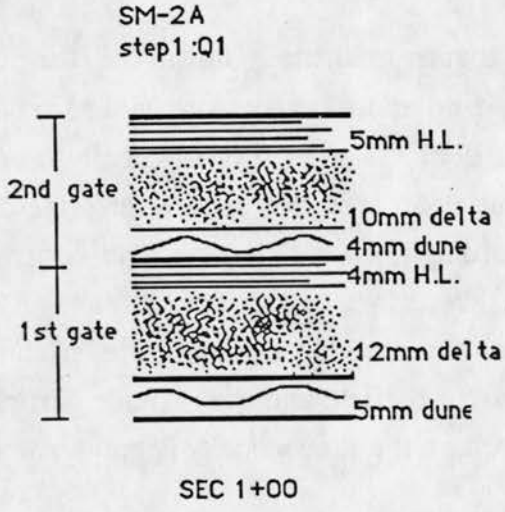

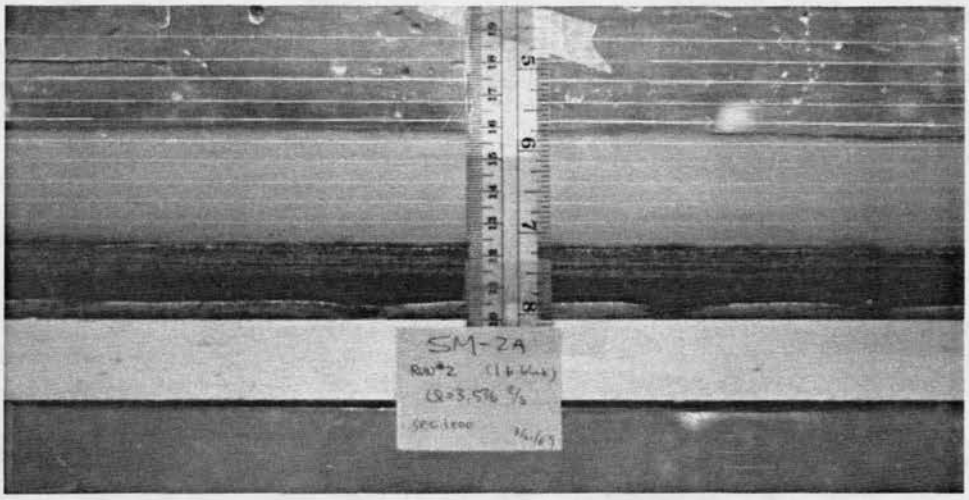

Picture 46. Run SM-2A, Step 2 (horizontal)

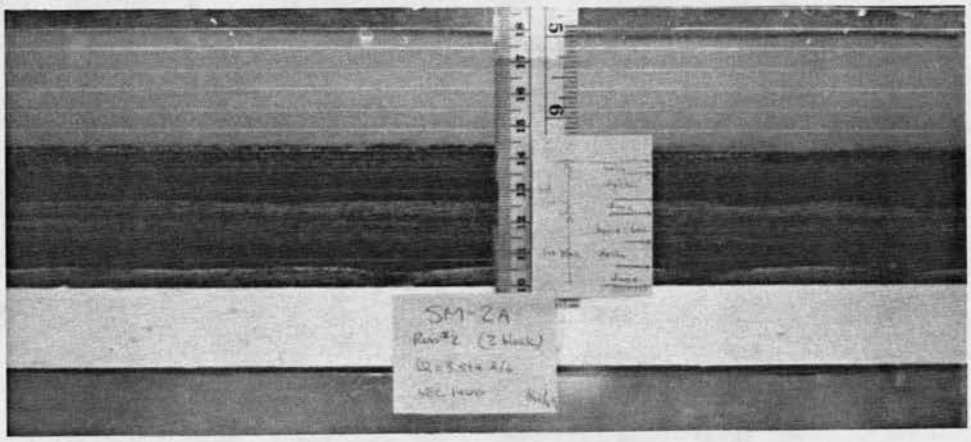

Picture 47. Run SM-2A, Step 2 (horizontal)

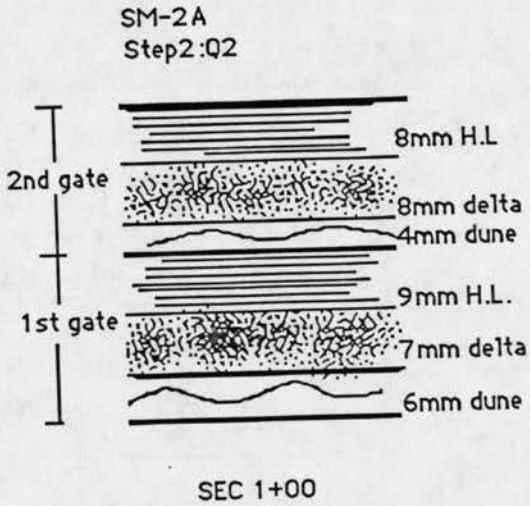

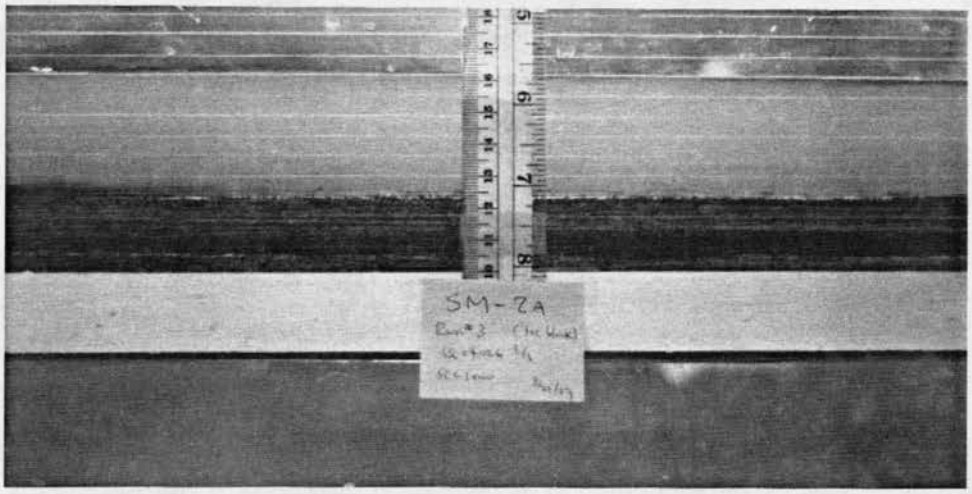

Picture 48. Run SM-2A, Step 3 (horizontal)

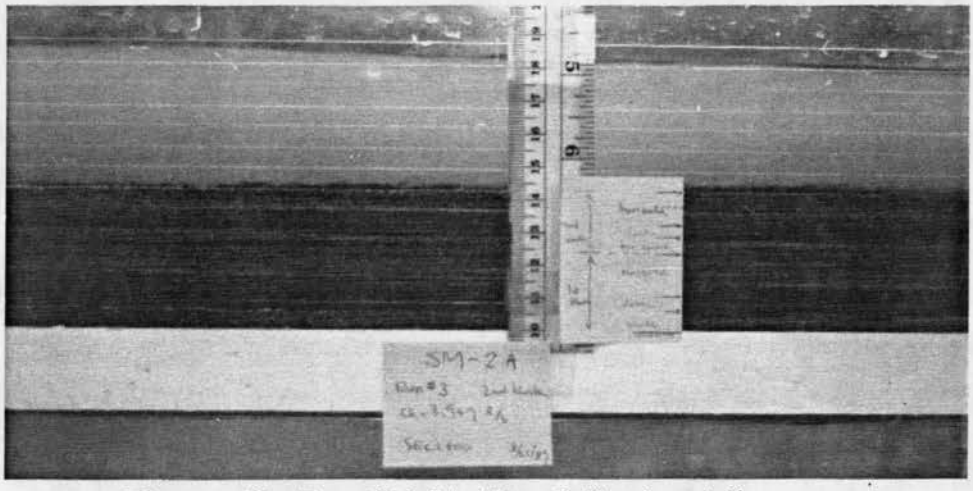

Picture 49. Run SM-2A, Step 3 (horizontal)

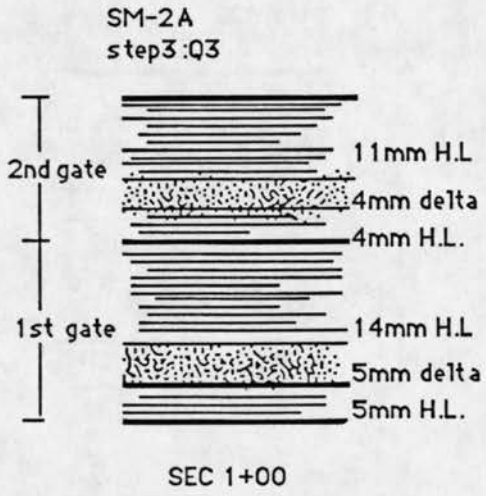

Picture 50. Run SM-2A, Step 4 (horizontal)

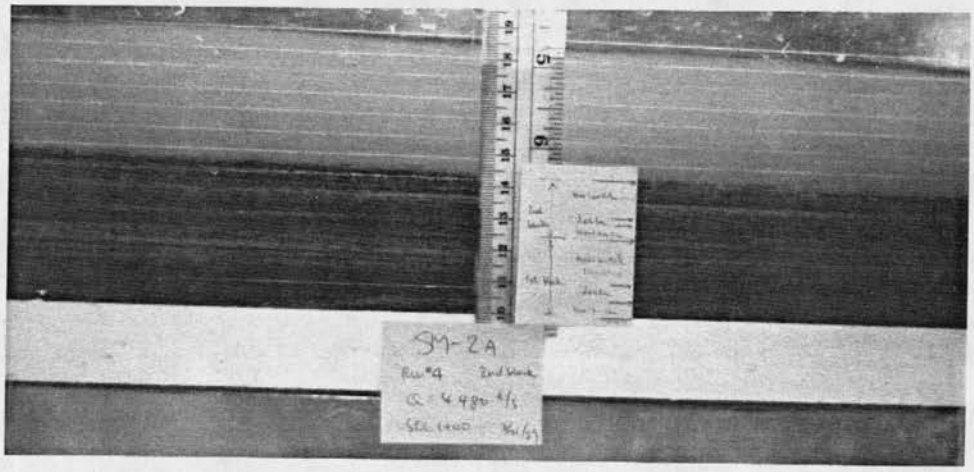

Picture 51. Run SM-2A, Step 4 (horizontal)

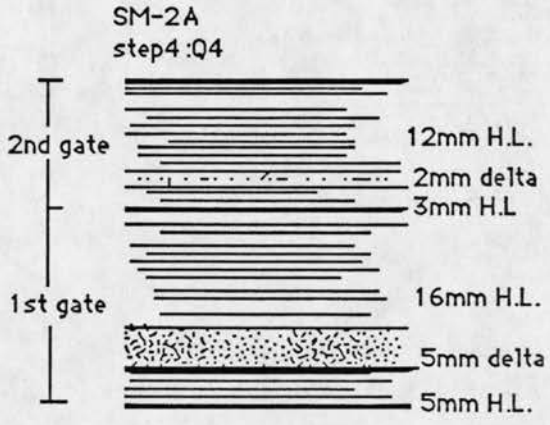

Comparing the horizontal lamination thickness under 1st gate condition from step 1 to 4 as shown in Figure 23, the thickness increased from 4mm, to 9mm, 14mm, and 16mm by increasing velocity. The corresponding delta thickness decreased from 12mm, to 7mm, 5mm, and 5mm, respectively. For the 2nd gate condition, the tendency was the same. The horizontal lamination thickness is therefore dependent to the flow velocity (or discharge). This phenomenon is similar to Berthault's experiment (1988).

From the observation of horizontal lamination we found that coarser particles (black) were rolling on the bed and also moving in saltation, but finer particles (white) deposited. This phenomenon is beyond the explanation of the Shields diagram.

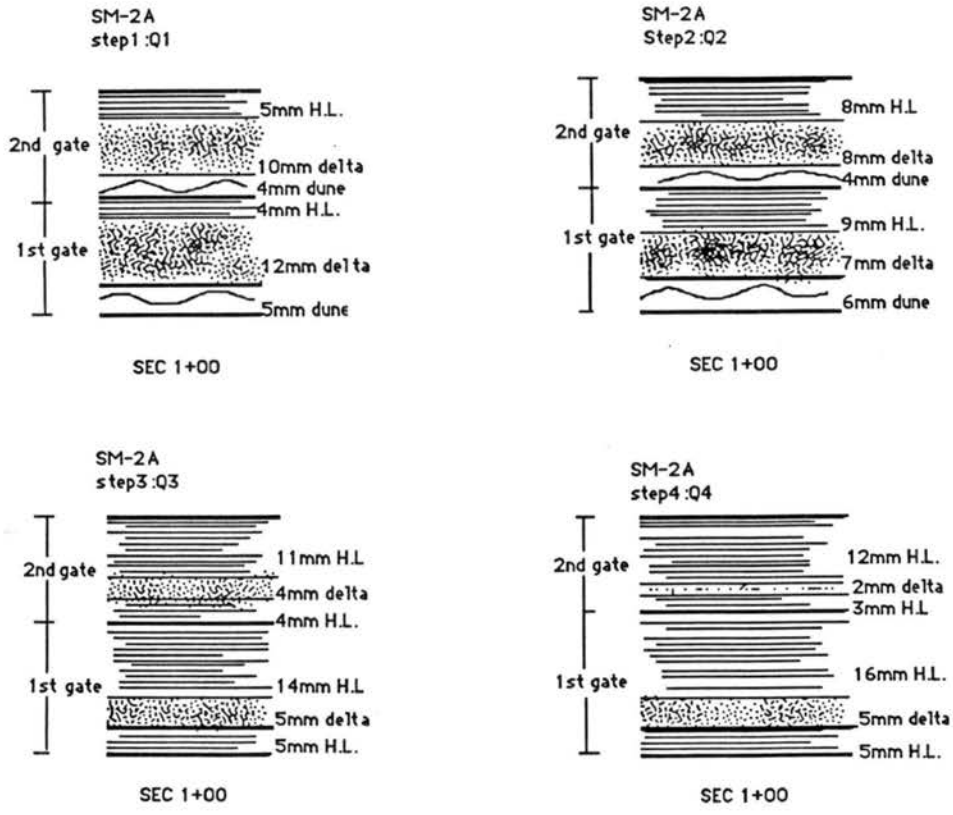

Figure 23. Deposition sketches for SM-2A (horizontal)

3.4.2 Run SM-2B

(1) Objective of this run: Examine the lamination slope referring to flume bed under the adverse slope conditions.

(2) Experimental conditions and data summary:

- Adverse flume slope (S = -0.005)
- SM-2 sand mixture (B2040 & ERC #4), D_{50} = 0.28 mm
- Two small tailgates (2 cm high each).
- Two deposition for each step is shown on pictures as:
  - Step 1: Picture 52, 53, and 54
  - Step 2: Picture 55 and 56
  - Step 3: Picture 57, 58 and 59
  - Step 4: Picture 60 and 61
- The data for this run is summarized in Table 13 below.

Table 13. Data summary for run SM-2B

Run: SM-2B (Adverse Slope S= -0.005) D_{50} = 0.28mm

Step	Gate	Q cm^3/s	h cm	Vm cm/s	Vs cm/s	Sw	Shear $dyne/cm^2$	Fr	U* cm/s	f	H. Lam mm	Delta mm
SM2B-1	no	3425	3.4	64.99	76.43	0.016	38.39	1.124	6.196	0.072	4	4
	1st	3380	4.0	54.51	67.25	0.013	35.96	0.870	5.997	0.096	8	6
	2nd	3334	4.0	53.77	66.24	0.011	30.76	0.858	5.546	0.085	7	12
SM2B-2	1st	3728	3.3	72.88	75.63	0.016	36.29	1.281	6.024	0.054	11	11
	2nd	3601	4.1	56.66	65.93	0.011	28.90	0.893	5.376	0.072	6	9
SM2B-3	no	3789	3.4	71.89	73.94	0.016	38.39	1.245	6.196	0.059	4	5
	1st	3665	3.8	62.22	71.69	0.012	31.48	1.019	5.611	0.065	8	6
	2nd	3644	4.0	58.77	66.40	0.012	32.52	0.938	5.703	0.075	7	8
SM2B-4	1st	4121	4.0	66.46	71.82	0.019	49.12	1.061	7.008	0.088	10	11
	2nd	3988	4.1	62.75	69.01	0.013	34.68	0.989	5.889	0.070	8	12

Q = flow discharge; h+ water depth SEC1+00; Vm = mean velocity; Vs = surface velocity; Sw = water surface slope; shear = bed shear stress; Fr = Froude number; U* = friction velocity; f = friction coefficient; H.Lam = horizontal lamination.

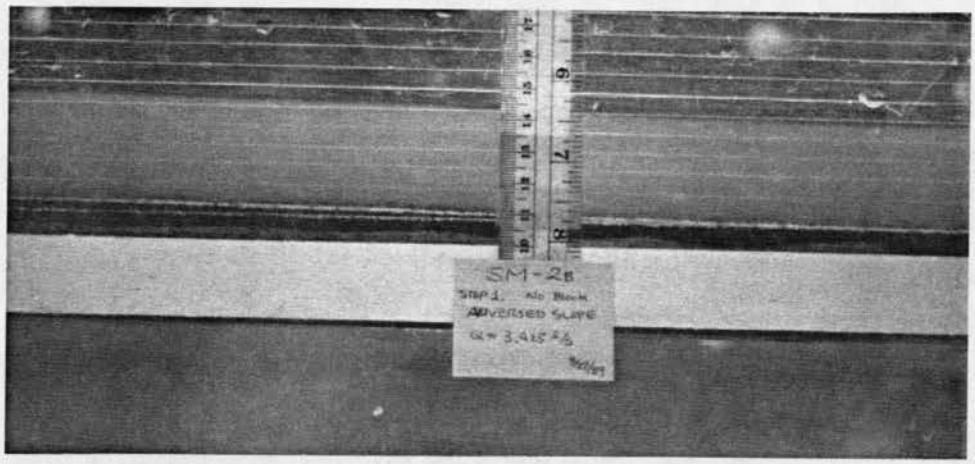

Picture 52. Run SM2-B, Step 1 (adverse slope)

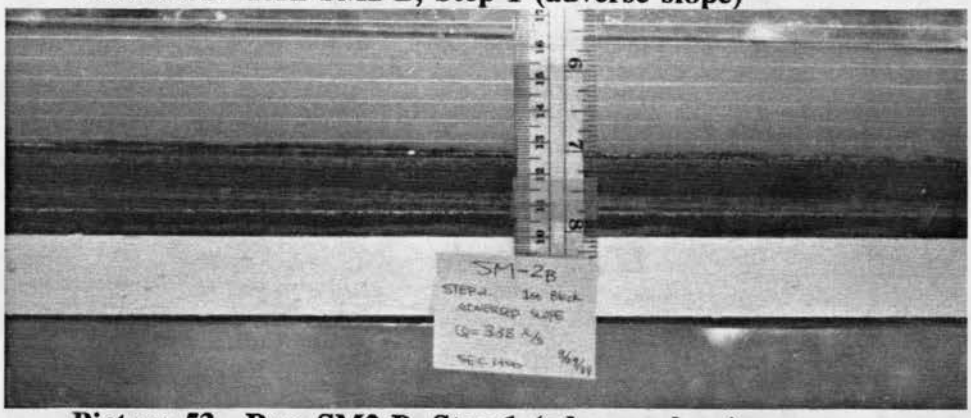

Picture 53. Run SM2-B, Step 1 (adverse slope)

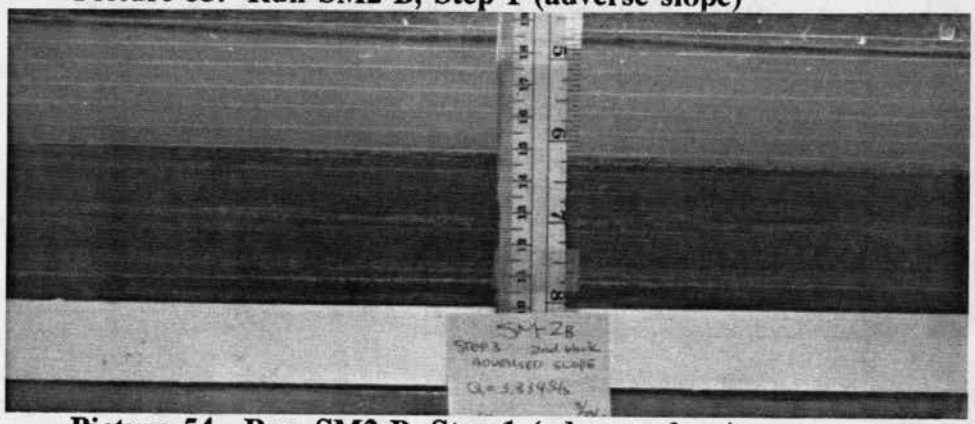

Picture 54. Run SM2-B, Step 1 (adverse slope)

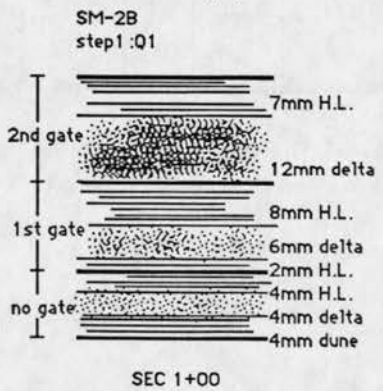

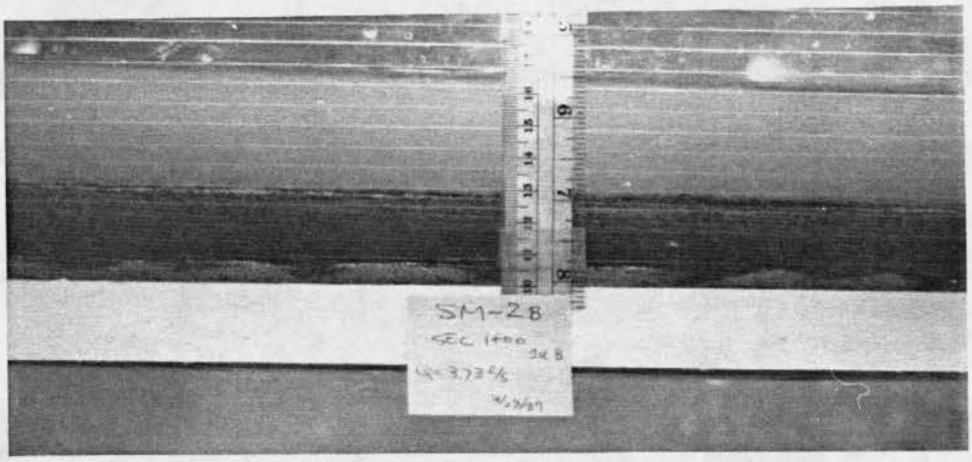

Picture 55. Run SM-2B, Step 2 (adverse slope)

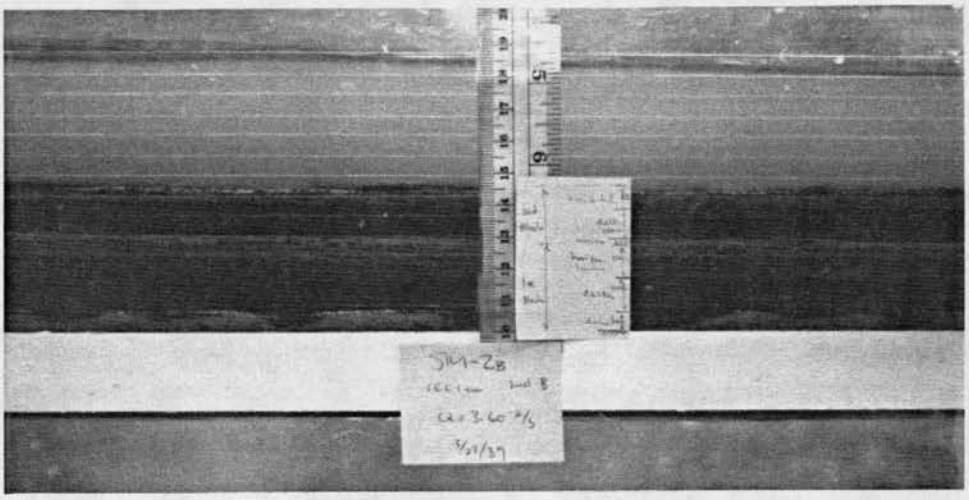

Picture 56. Run SM-2B, Step 2 (adverse slope)

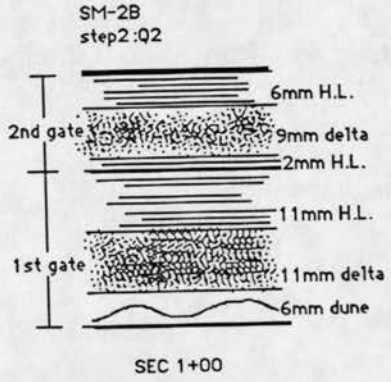

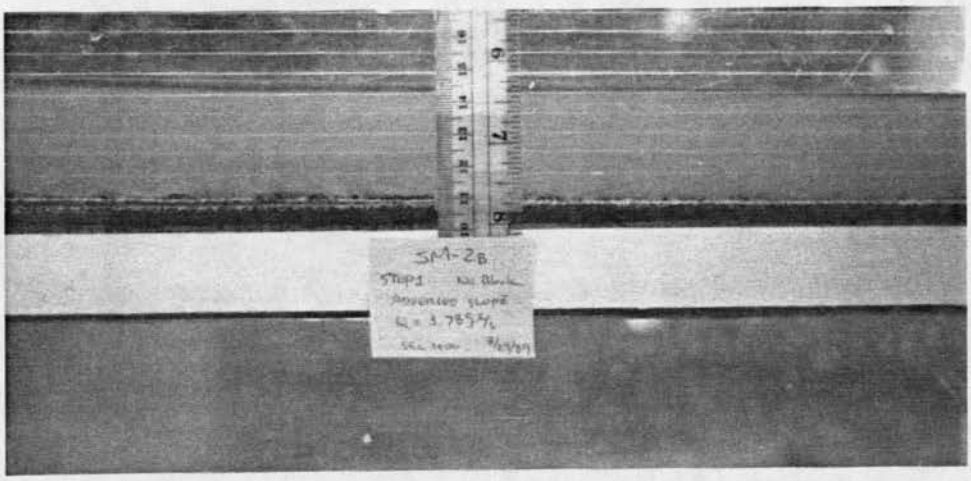

Picture 57. Run SM2-B, Step 3 (adverse slope)

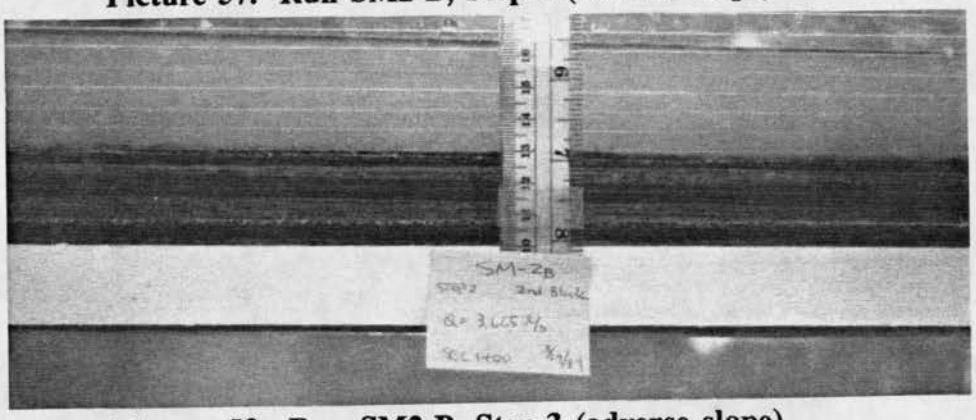

Picture 58. Run SM2-B, Step 3 (adverse slope)

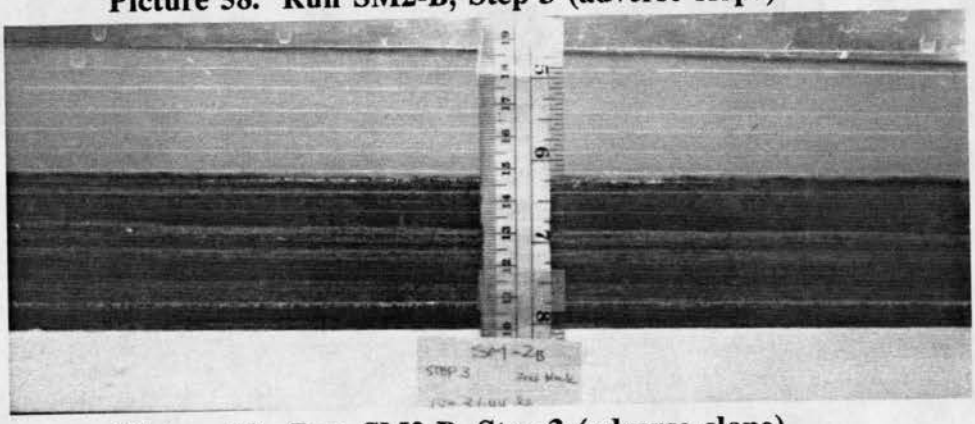

Picture 59. Run SM2-B, Step 3 (adverse slope)

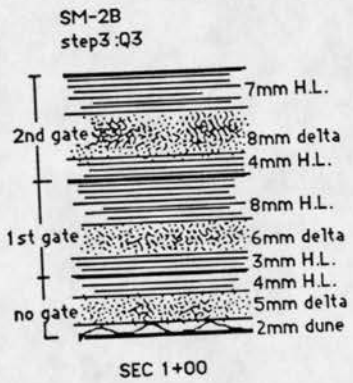

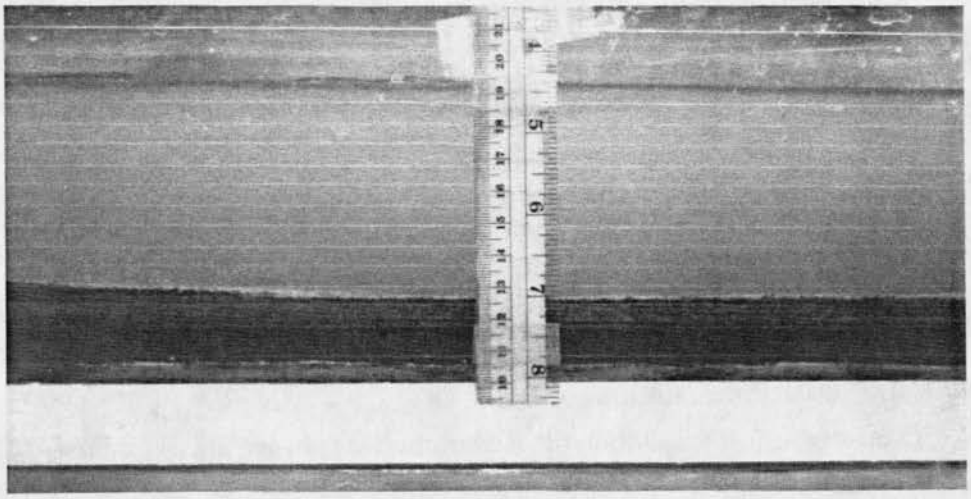

Picture 60. Run SM-2B, Step 4 (adverse slope)

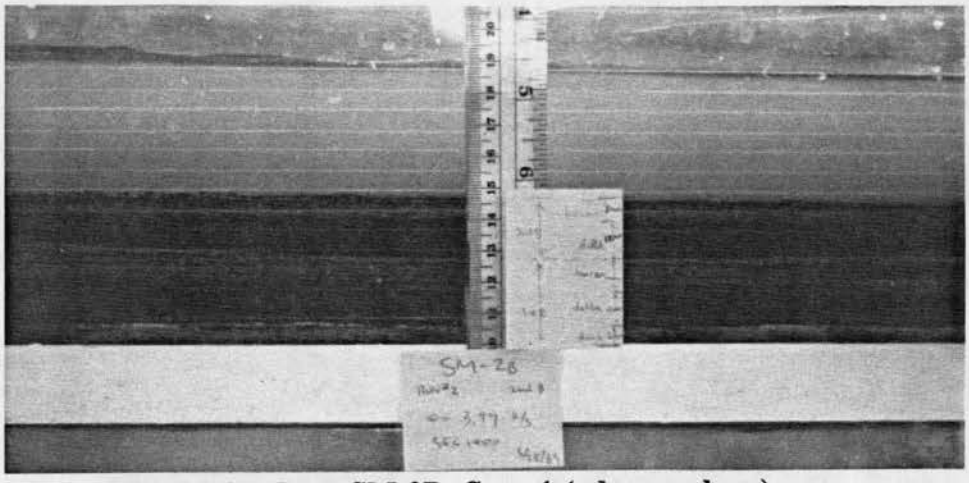

Picture 61. Run SM-2B, Step 4 (adverse slope)

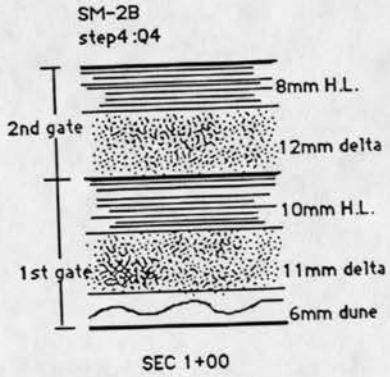

From the observation of laminae deposition we find that the horizontal lamination is subparallel to the previous deposit rather than the flume bed (as shown on Picture 62). It is similar to the results of Berthault's experiment (1988) in calm water the slope of the bed surface has little influence on lamination and seems to favor it.

In the observation of step 4 we could find a series of extremely low-relief sandwaves migrating as shown on Picture 63. The Froude number for this step is 0.989 which is nearly unity. This phenomenon is similar to the observation in Smith's report (1971) and the experiment of McBride et al. (1975). The extremely low-relief sandwave may contribute to the formation of horizontal lamination.

The deposition for each run is sketched as shown in Figure 24.

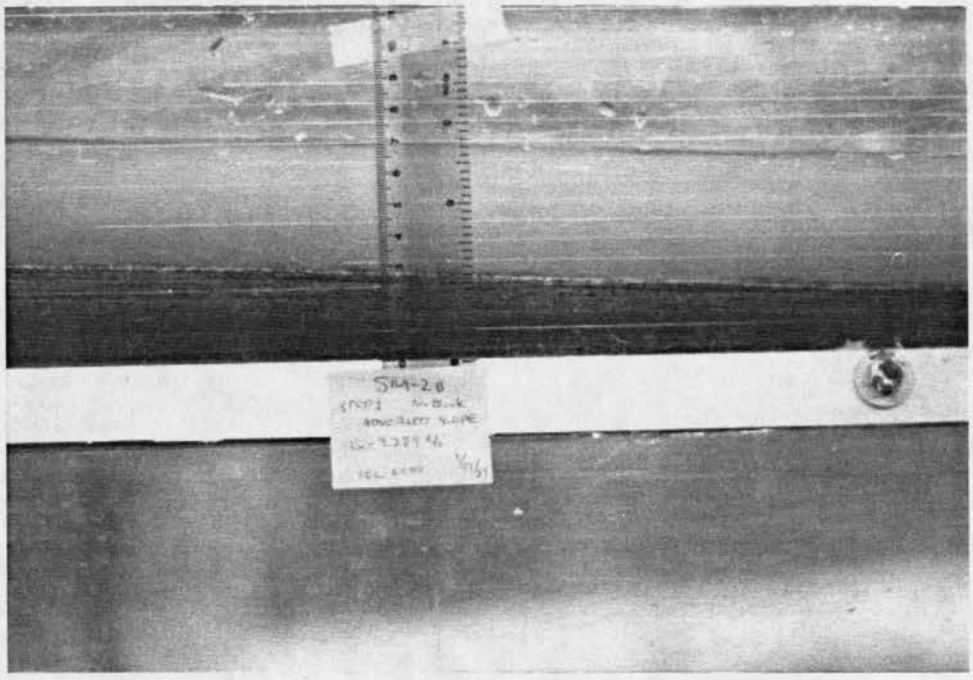

Picture 62. Horizontal lamination, Run SM-2B (adverse slope)

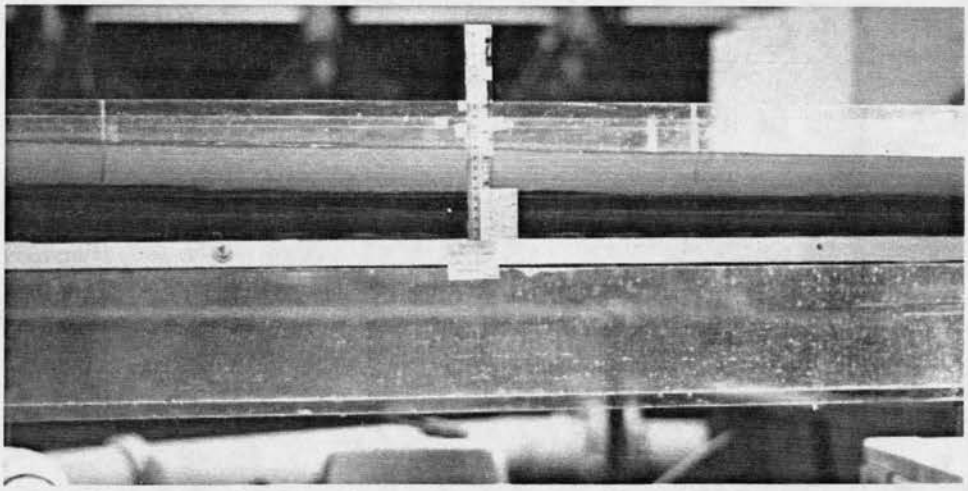

Picture 63. Very low-relief sandwaves migration, Run SM-2B (adverse slope)

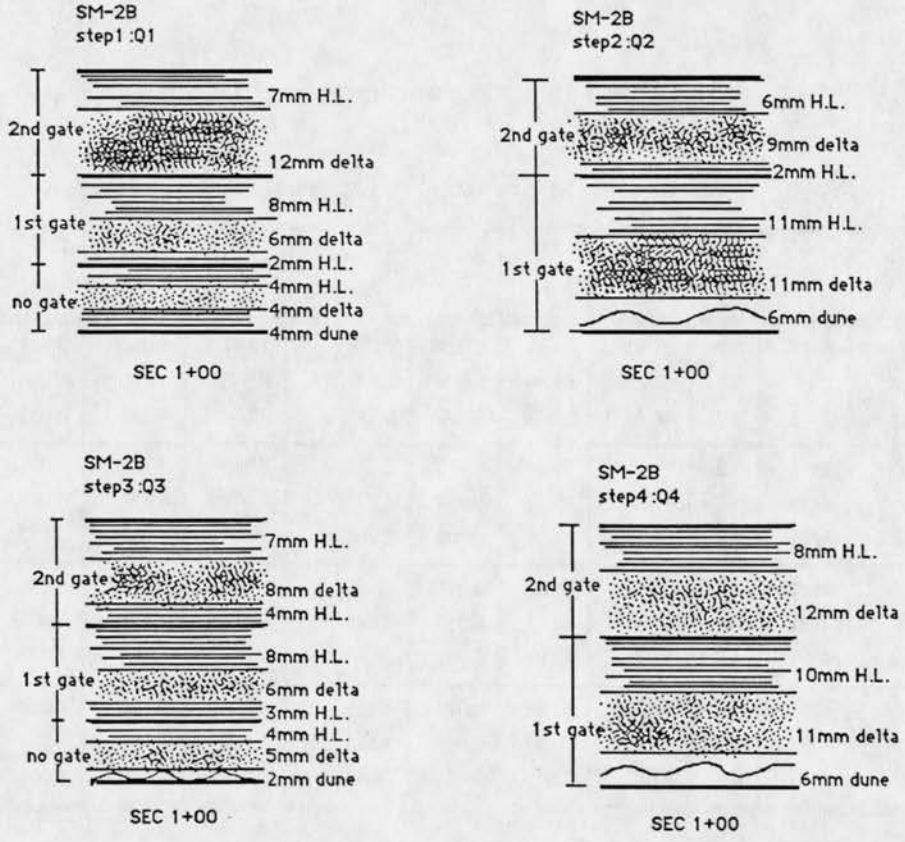

Figure 24. The deposition of SM-2B (adverse slope)

3.4.3 Run SM-2C

(1) Objective of this run: Examine the lamination slope referring to flume bed under the positive flume slope condition.

(2) Experimental conditions and data summary:

- Positive flume slope (S = -0.005)
- SM-2 sand mixture (B2040 & ERC #4), D_{50} = 0.28 mm
- Two small tailgates (2 cm high each).
- Two deposition for each step is shown on pictures as:

  Step 1: Picture 64, 65 and 66

  Step 2: Picture 67, 68 and 69

  Step 3: Picture 70, 71 and 72

  Step 4: Picture 73, 74 and 75
- The data for this run is summarized in Table 14 below.

Table 14. Data summary for run SM-2C

Run: SM-2C (Positive Slope S= -0.005) D_{50} = 0.28mm

Step	Gate	Q cm^3/s	h cm	Vm cm/s	Vs cm/s	Sw	Shear $dyne/cm^2$	Fr	U* cm/s	f	H. Lam mm	Delta mm
SM2C-1	no	3019	3.0	64.92	70.31	0.012	25.60	1.197	5.060	0.048	2	0
	1st	2887	3.5	53.21	65.90	0.009	21.45	0.908	4.631	0.060	9	6
	2nd	2778	3.7	48.43	56.45	0.007	17.37	0.804	4.168	0.059	6	8
SM2C-2	no	3558	3.2	71.73	79.88	0.013	29.03	1.280	5.388	0.045	2	0
	1st	3470	3.5	63.96	69.33	0.018	42.72	0.092	6.536	0.083	10	5
	2nd	3470	3.8	58.91	61.98	0.009	22.68	0.965	4.763	0.052	7	9
SM2C-3	no	4102	3.5	75.61	79.25	0.017	40.35	1.291	6.352	0.056	3	0
	1st	4121	4.0	66.46	74.81	0.013	33.81	1.061	5.815	0.061	12	5
	2nd	4007	4.5	57.44	62.90	0.009	25.68	0.865	5.033	0.061	7	5
SM2C-4	no	4514	3.8	76.63	83.84	0.016	40.18	1.255	6.338	0.054	3	0
	1st	4497	4.1	70.76	78.75	0.016	42.25	1.116	6.500	0.067	10	6
	2nd	4428	4.4	64.92	70.76	0.011	30.47	0.988	5.520	0.057	9	4

Q = flow discharge; h+ water depth SEC1+00; Vm = mean velocity; Vs = surface velocity; Sw = water surface slope; shear = bed shear stress; Fr = Froude number; U* = friction velocity; f = friction coefficient; H.Lam = horizontal lamination.

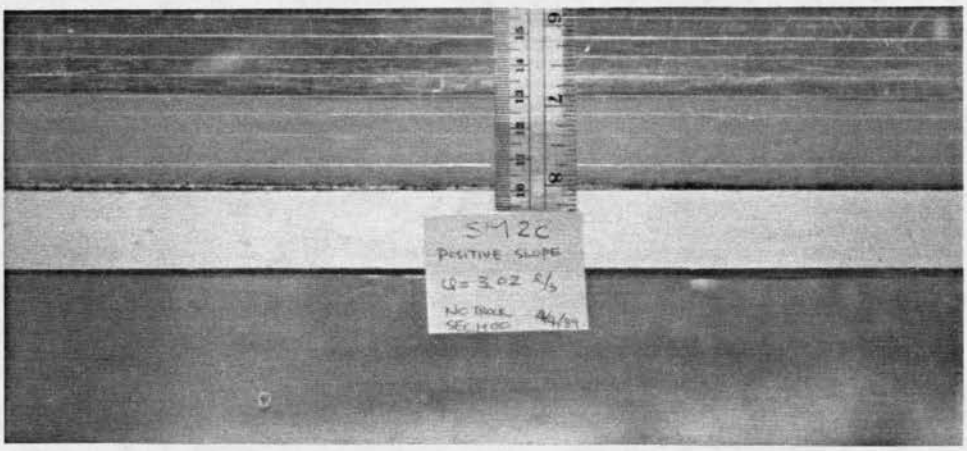

Picture 64. Run SM-2C, Step 1 (positive slope)

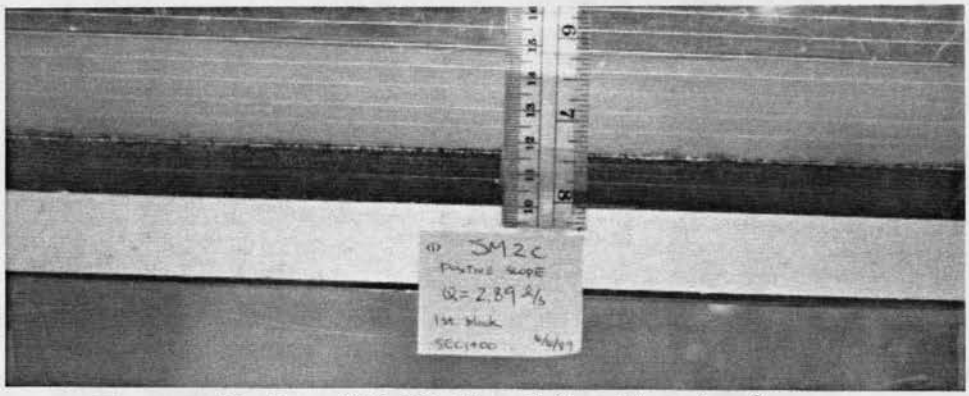

Picture 65. Run SM-2C, Step 1 (positive slope)

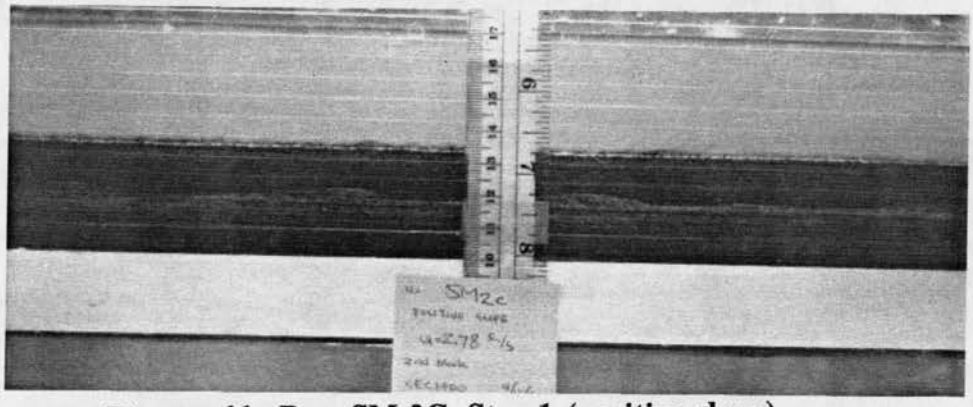

Picture 66. Run SM-2C, Step 1 (positive slope)

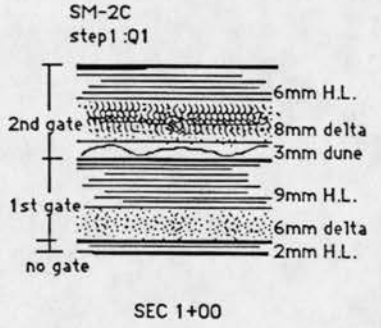

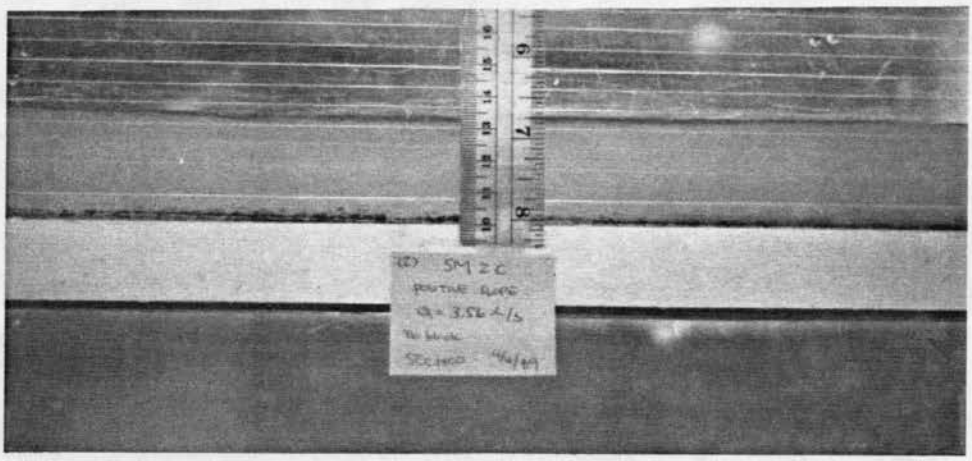

Picture 67. Run SM-2C, Step 2 (positive slope)

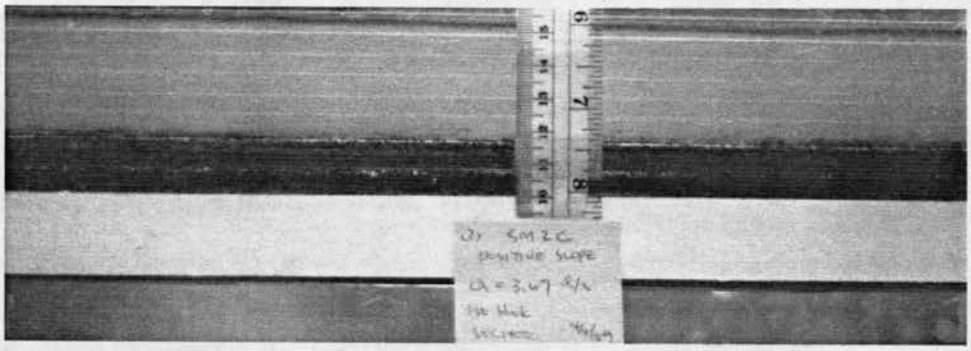

Picture 68. Run SM-2C, Step 2 (positive slope)

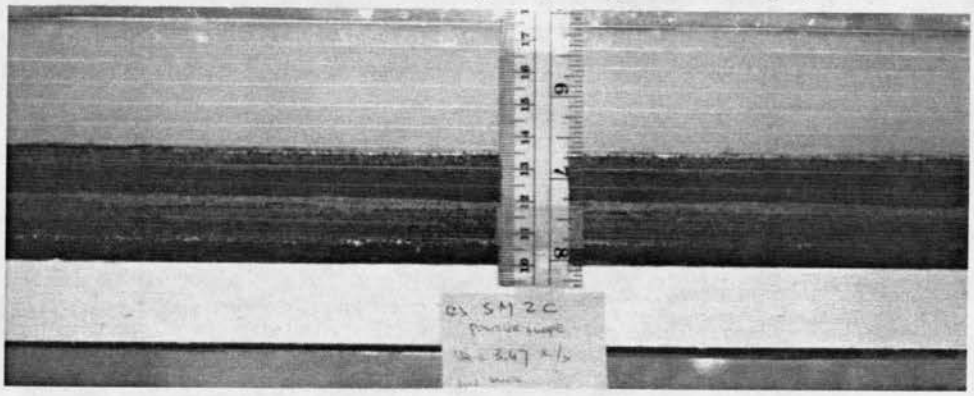

Picture 69. Run SM-2C, Step 2 (positive slope)

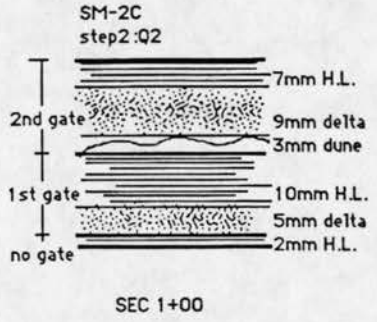

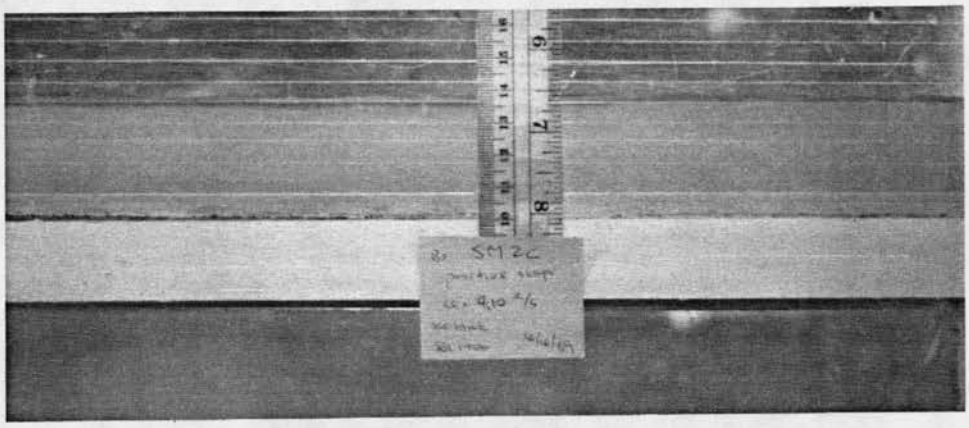

Picture 70. Run SM-2C, Step 3 (positive slope)

Picture 71. Run SM-2C, Step 3 (positive slope)

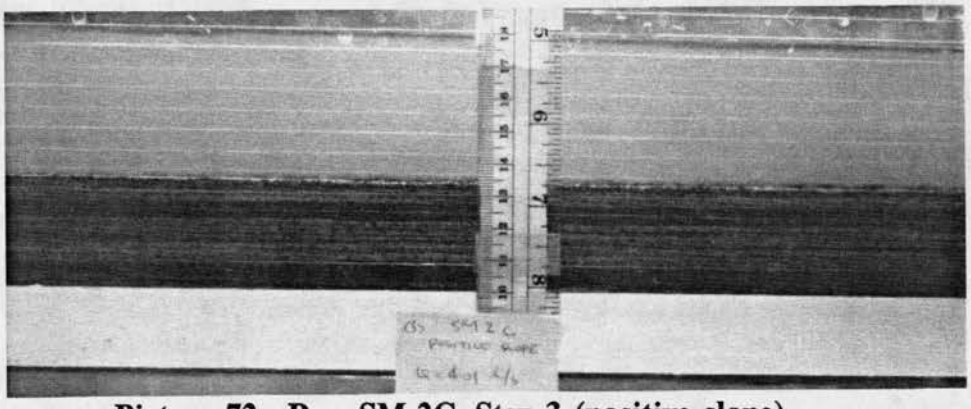

Picture 72. Run SM-2C, Step 3 (positive slope)

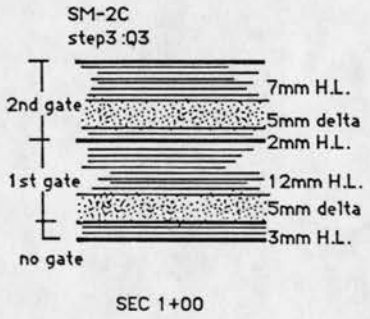

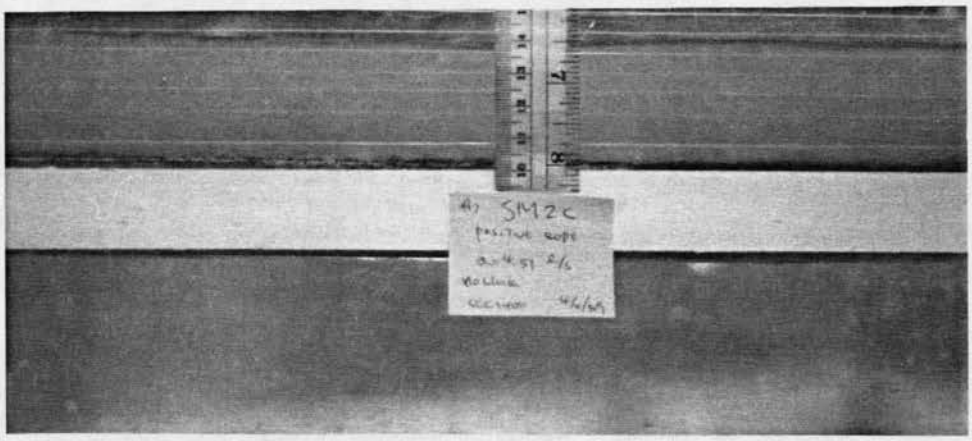

Picture 73. Run SM-2C, Step 4 (positive slope)

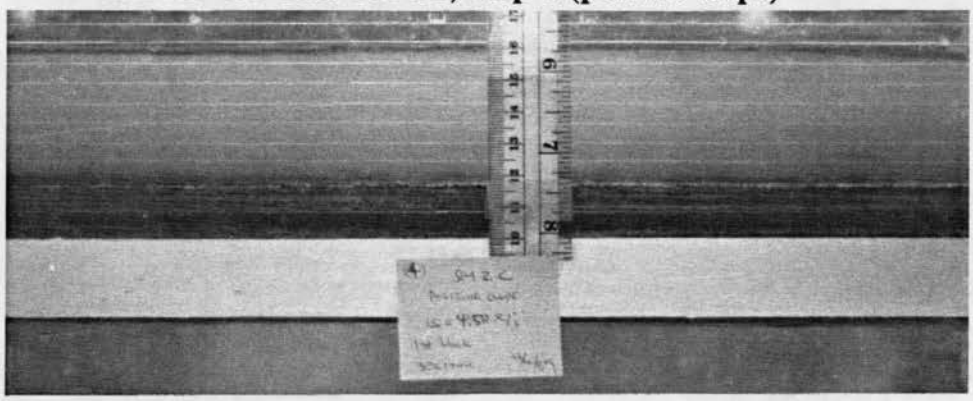

Picture 74. Run SM-2C, Step 4 (positive slope)

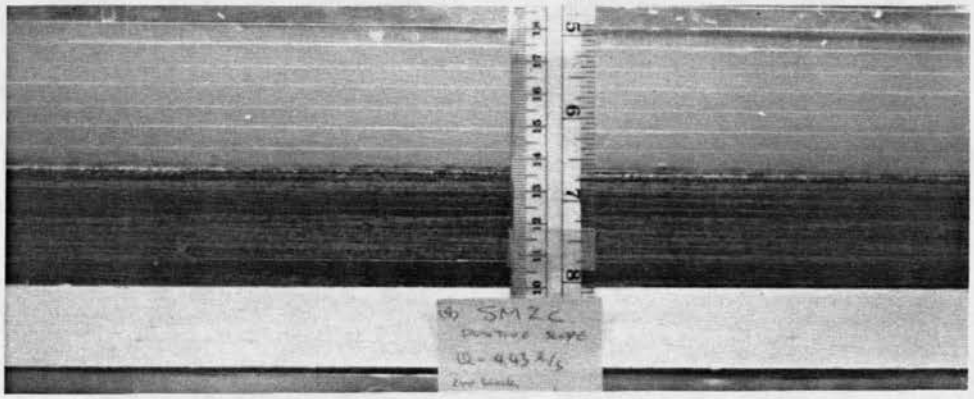

Picture 75. Run SM-2C, Step 4 (positive slope)

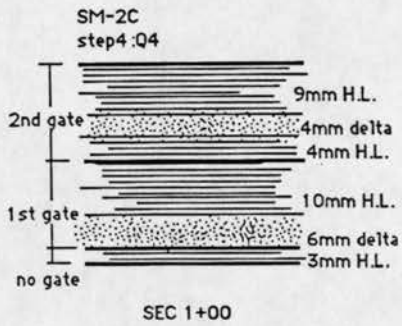

The horizontal lamination is subparallel to the underlying laminae and not parallel to the flume bed. These results are in agreement with those of Berthault (1988).

The thickness of horizontal lamination is also dependent on flow velocity (comparing 2nd gate condition, thickness increased from 6mm, 7mm, 7mm to 9mm as velocity increased). The deposition for each step is sketched on Figure 25.

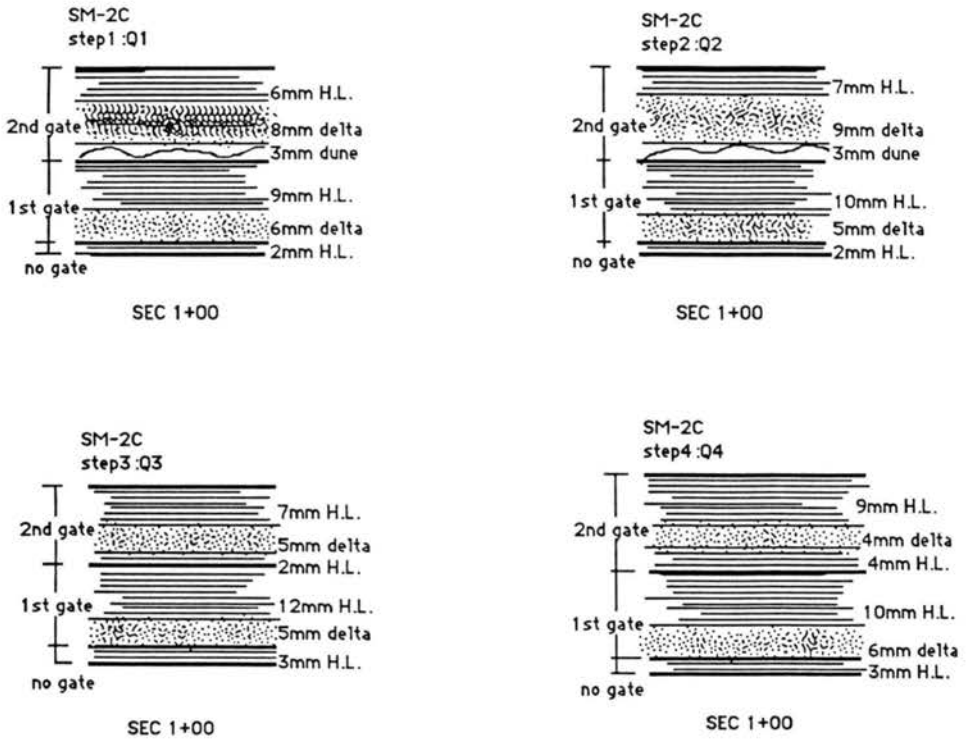

Figure 25. The deposition of SM-2C (positive slope)

3.4.4 Run SM-2D

(1) Objective of this run: Examine the influence of larger tailgate conditions on the thickness of horizontal lamination.

(2) Experimental conditions and data summary:

- Horizontal flume slope
- SM-2 sand mixture (B2040 & ERC #4), D_{50} = 0.28 mm
- Fist small gate (2cm high) and second larger gate (4cm high)
- The deposition for each step is shown on pictures as:

  Step 1: Picture 76, 77 and 78

  Picture 79, 80 and 81 (infrared pictures)*

  Step 2: Picture 82, 83 and 84
- The data for this run is summarized in Table 15 below.

* Note: we took infrared pictures for this run only. The results did not justify taking infrared photographs for the other runs and therefore color prints were shown for every run.

Table 15. Data summary for run SM-2D

Run: SM-2D (Horizontal) D_{50} = 0.28mm

Step	Gate	Q cm^3/s	h cm	Vm cm/s	Vs cm/s	Sw	Shear $dyne/cm^2$	Fr	U* cm/s	f	H. Lam mm	Delta mm
SM2D-1	no	3404	3.4	64.57	71.80	0.010	24.78	1.118	4.978	0.047	2	0
	1st	3334	3.5	61.45	67.26	0.010	23.62	1.049	4.860	0.050	10	5
	2nd	2750	3.4	52.18	62.65	0.004	9.263	0.904	3.043	0.027	4	29
SM2D-2	no	4480	3.3	87.58	99.01	0.027	61.92	1.540	7.869	0.064	7	0
	1st	4428	3.5	81.62	91.52	0.020	47.25	1.393	6.874	0.056	21	0
	2nd	4026	4.0	64.93	66.10	0.010	27.66	1.037	5.259	0.052	5	23

Q = flow discharge; h+ water depth SEC1+00; Vm = mean velocity; Vs = surface velocity; Sw = water surface slope; shear = bed shear stress; Fr = Froude number; U* = friction velocity; f = friction coefficient; H.Lam = horizontal lamination.

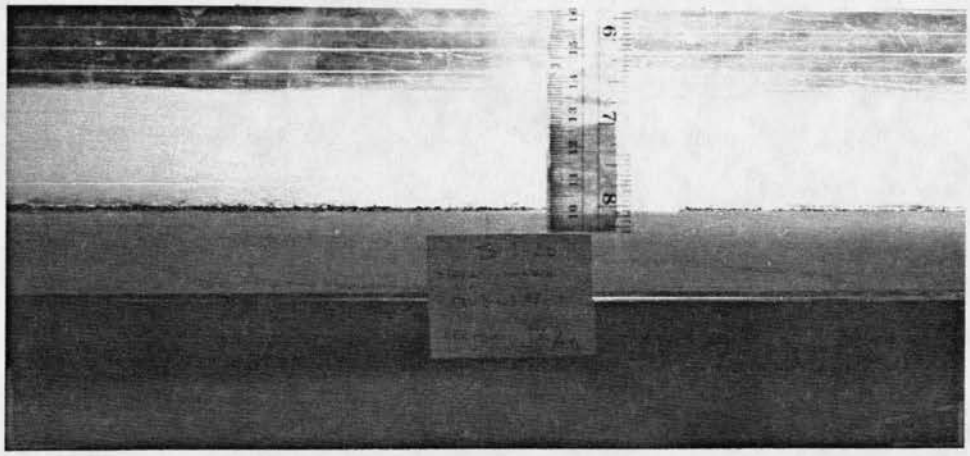

Picture 76. Run SM-2D, Step 1 (horizontal)

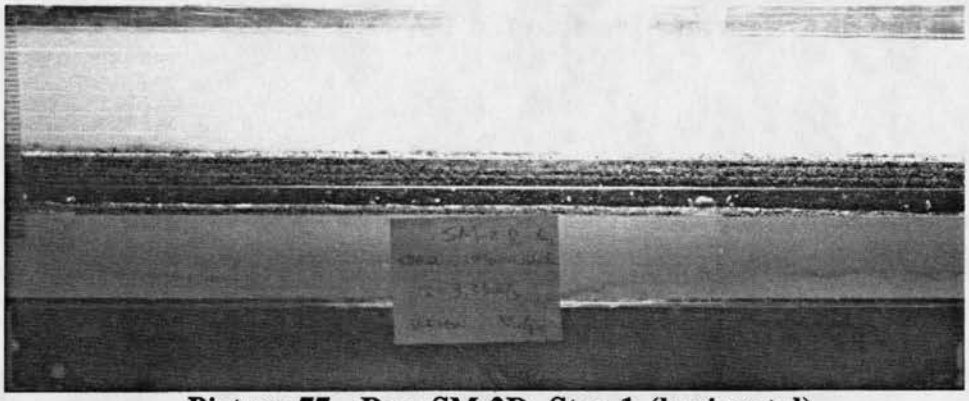

Picture 77. Run SM-2D, Step 1 (horizontal)

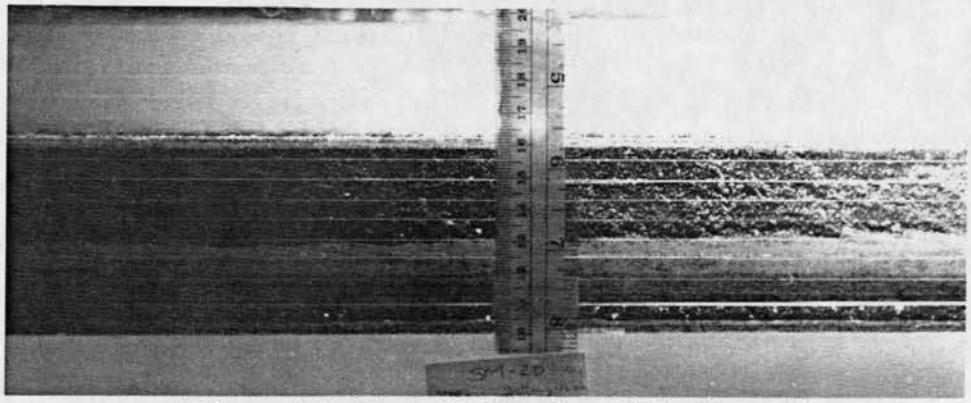

Picture 78. Run SM-2D, Step 1 (horizontal)

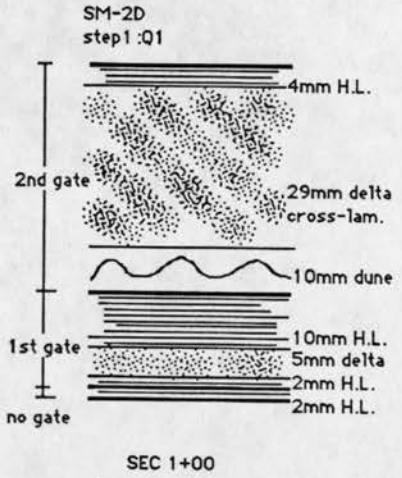

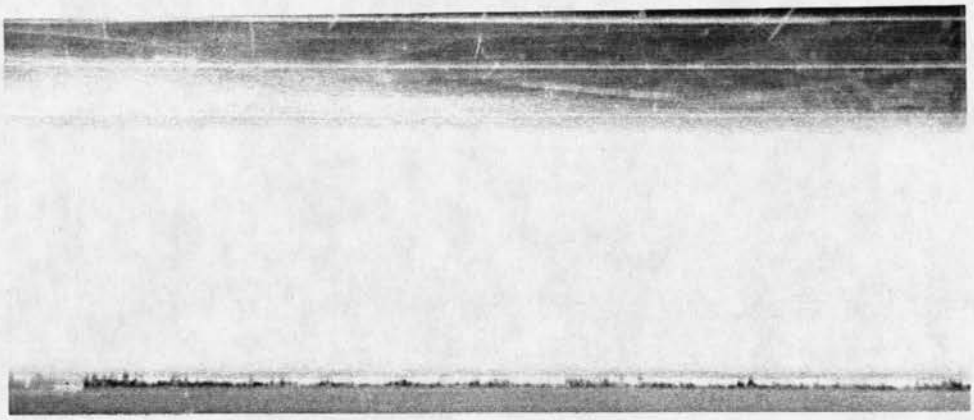

Picture 79. Run SM-2D, Step 1 (horizontal) *

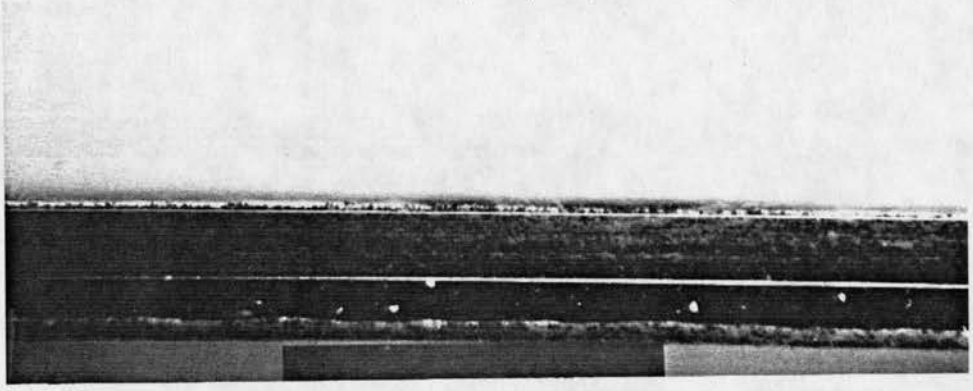

Picture 80. Run SM-2D, Step 1 (horizontal) *

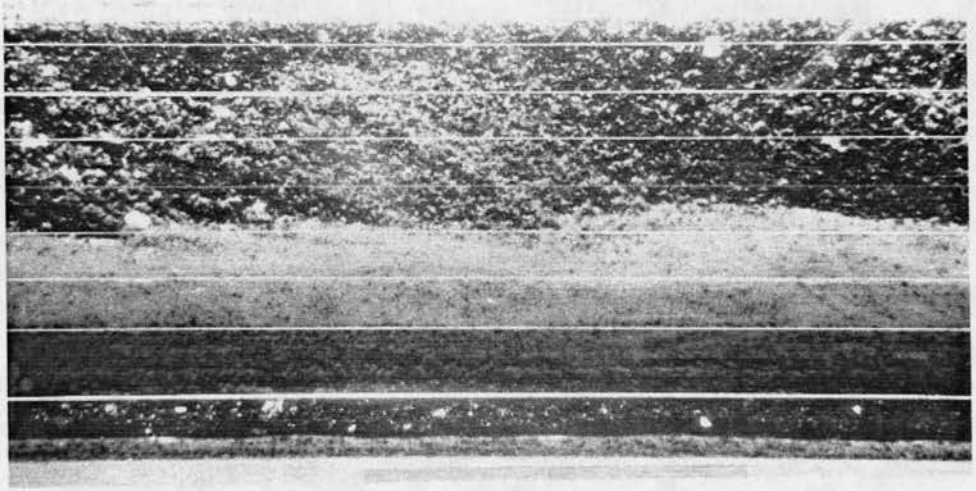

Picture 81. Run SM-2D, Step 1 (horizontal) *

* infrared pictures

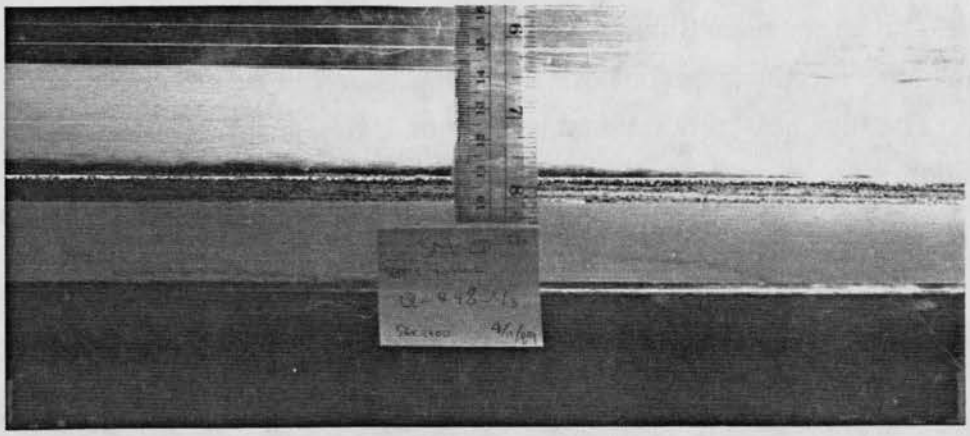

Picture 82. Run SM-2D, Step 2 (horizontal)

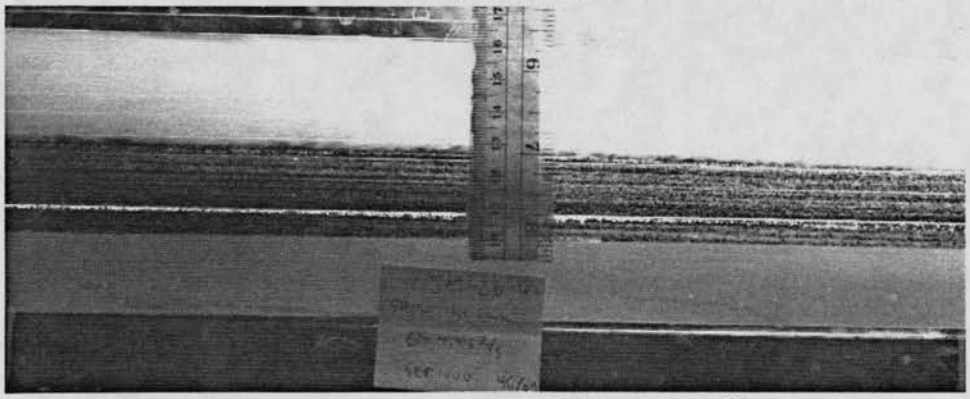

Picture 83. Run SM-2D, Step 2 (horizontal)

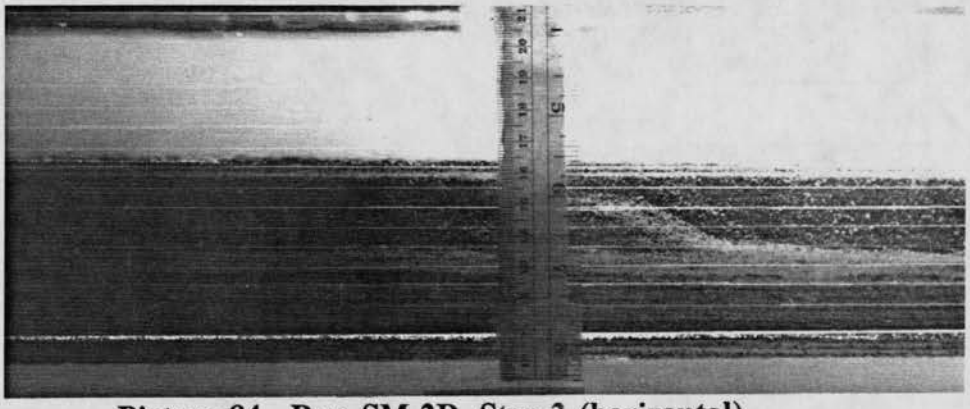

Picture 84. Run SM-2D, Step 2 (horizontal)

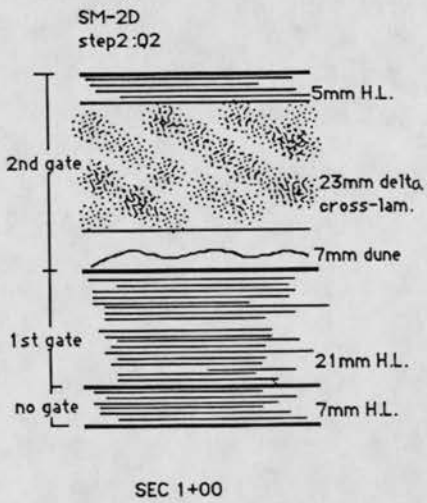

The larger second tailgate produces a thicker delta deposit. On the other hand, it does not increase the thickness of horizonal lamination but decreases it.

The thickness of horizontal lamination is dependent on flow velocity (comparing 1st gate condition, it increased from 10mm to 21mm). The deposition for each step is sketched on Figure 26.

Under larger flow velocity condition delta may not occur as in the 1st gate of step 2 (SM-2D-2).

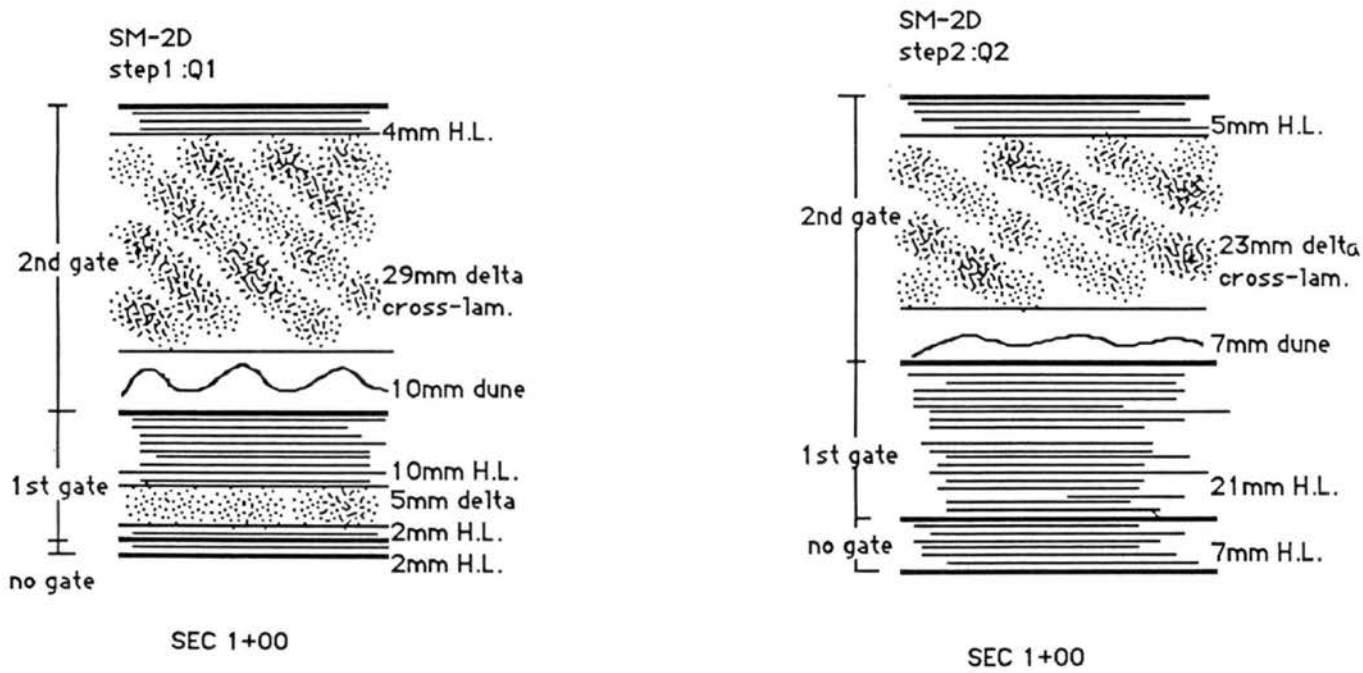

Figure 26. The deposition of SM-2D (horizontal)

3.4.5 Run SM-3A

(1) Objective of this run: Examine the thickness of horizontal lamination in a coarser sand mixture.

(2) Experimental conditions and data summary:

- Horizontal flume
- SM-3 sand mixture (B3060 & ERC #2), D_{50} = 0.62 mm
- Two small tailgates (2 cm high each).
- Two deposition for each step is shown on pictures as:

  Step 1: Picture 85, 86 and 87

  Step 2: Picture 88, 89 and 90

  Step 3: Picture 91, 92 and 93

  Step 4: Picture 94, 95 and 96
- The data for this run is summarized in Table 16 below.

Table 16. Data summary for run SM-3A

Run: SM-3A (Horizontal) D_{50} = 0.62mm

Step	Gate	Q cm^3/s	h cm	Vm cm/s	Vs cm/s	Sw	Shear $dyne/cm^2$	Fr	U* cm/s	f	H. Lam mm	Delta mm
SM3A-1	no	3727	3.5	68.70	81.53	0.014	33.08	1.173	5.571	0.056	?	0
	1st	3665	3.7	63.90	69.22	0.009	22.08	1.061	4.699	0.043	14	4
	2nd	3558	3.9	58.85	64.80	0.008	20.34	0.952	4.510	0.046	7	6
SM3A-2	no	3948	3.4	74.91	79.40	0.014	32.42	1.297	5.694	0.046	?	0
	1st	3909	3.9	64.66	71.10	0.012	30.51	1.045	5.523	0.058	11	5
	2nd	3850	3.9	63.68	63.96	0.010	25.42	1.030	5.042	0.050	11	5
SM3A-3	no	4195	3.8	71.22	83.88	0.016	39.98	1.167	6.323	0.063	8	0
	1st	4304	4.0	69.41	80.46	0.011	28.44	1.108	5.332	0.047	14	0
	2nd	4304	4.4	63.10	70.43	0.010	27.50	0.961	5.244	0.055	12	10
SM3A-4	no	5032	3.9	83.24	81.16	0.018	45.76	1.346	6.765	0.052	8	0
	1st	4764	4.2	73.17	74.42	0.015	40.04	1.140	6.327	0.059	16	3
	2nd	4939	4.5	70.81	77.52	0.010	27.90	1.066	5.282	0.044	13	4

Note: ? = lamination type not clear

Q = flow discharge; h+ water depth SEC1+00; Vm = mean velocity; Vs = surface velocity; Sw = water surface slope; shear = bed shear stress; Fr = Froude number; U* = friction velocity; f = friction coefficient; H.Lam = horizontal lamination.

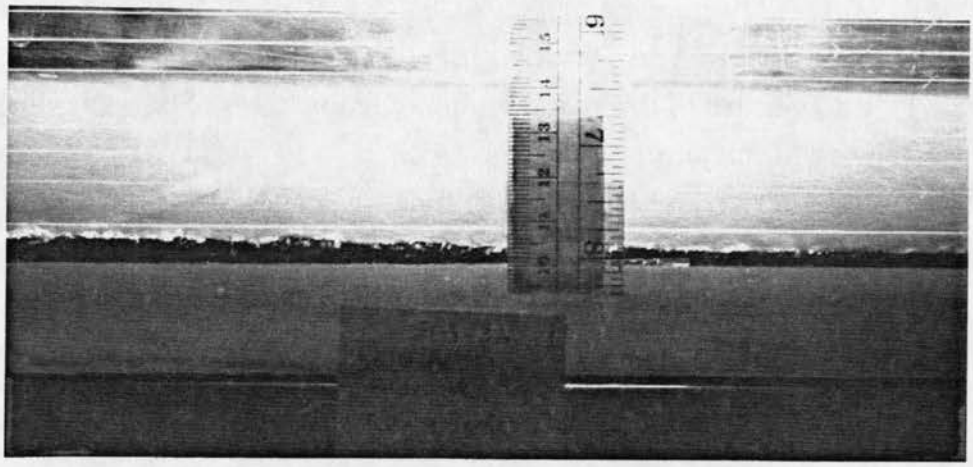

Picture 85. Run SM-3A, Step 1 (horizontal)

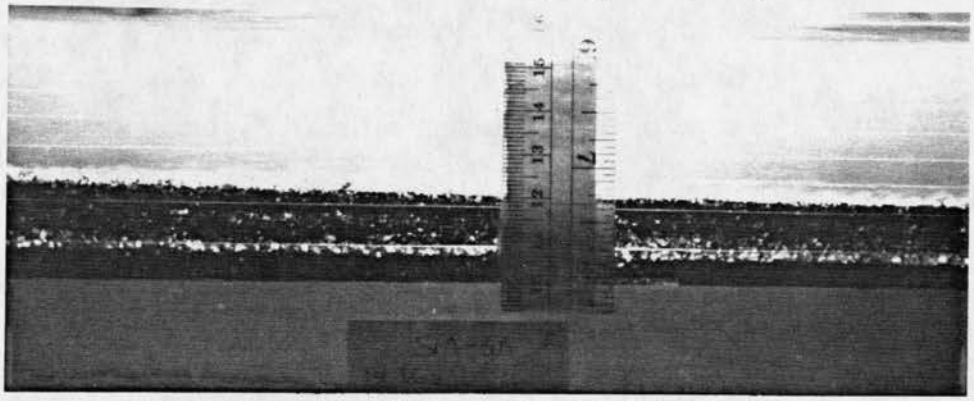

Picture 86. Run SM-3A, Step 1 (horizontal)

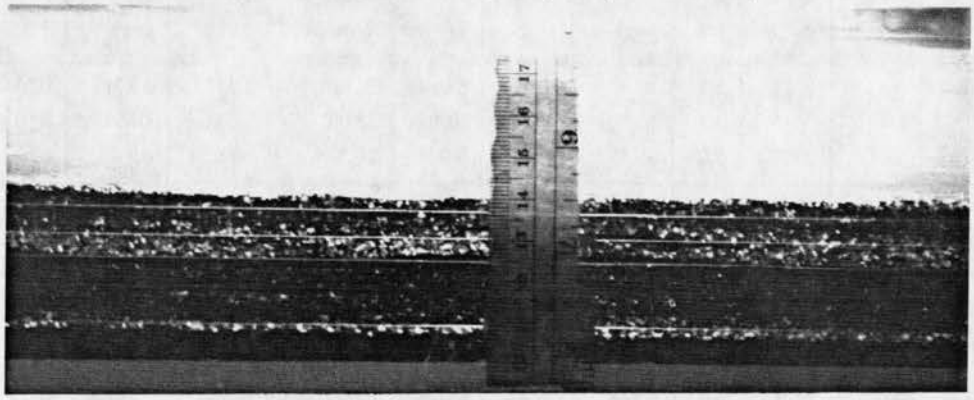

Picture 87. Run SM-3A, Step 1 (horizontal)

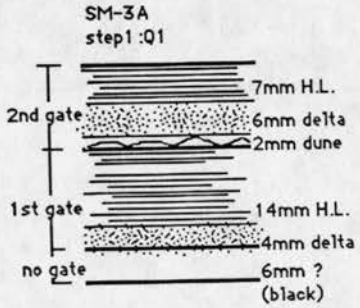

SEC 1+00

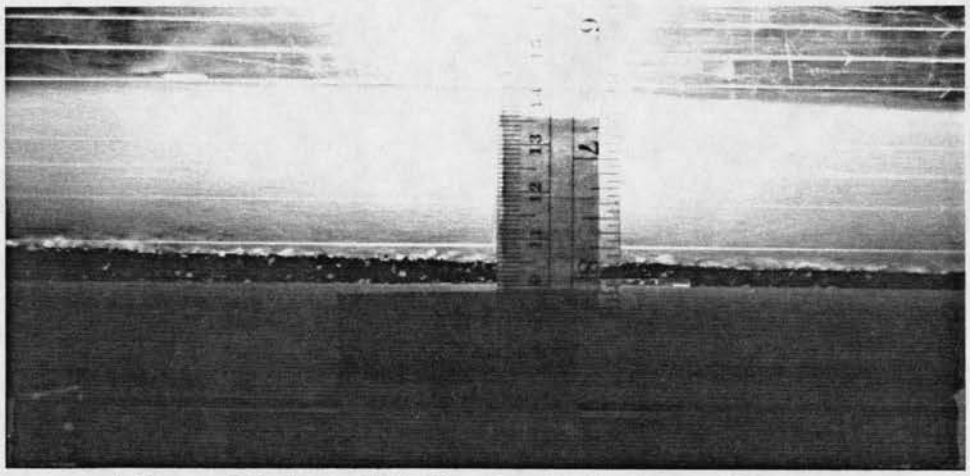

Picture 88. Run SM-3A, Step 2 (horizontal)

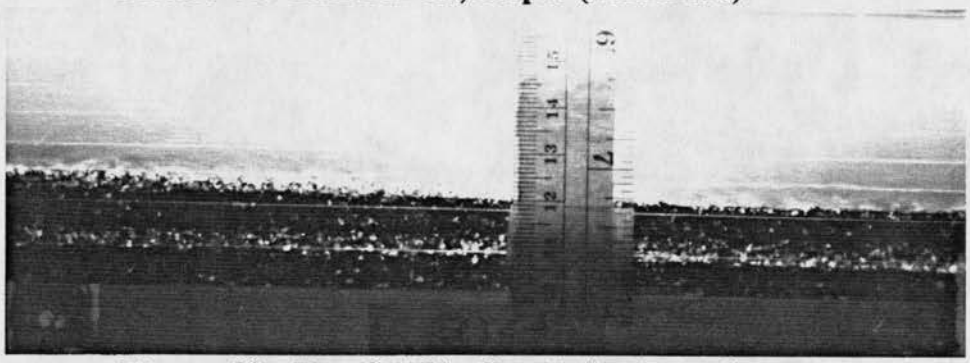

Picture 89. Run SM-3A, Step 2 (horizontal)

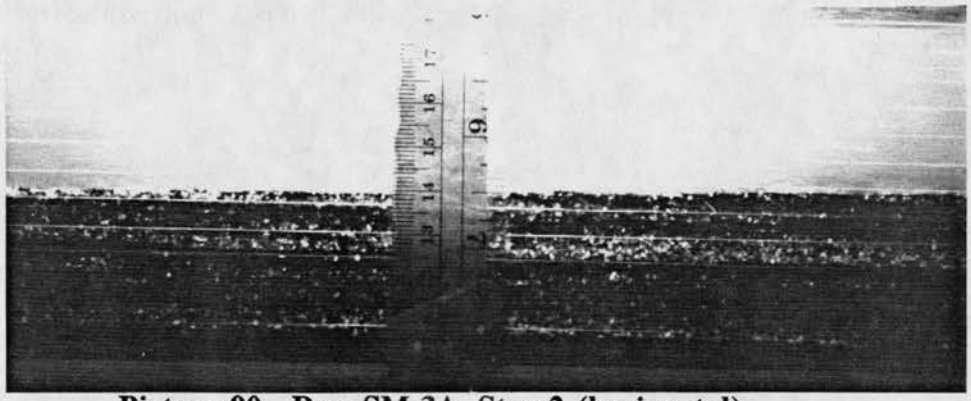

Picture 90. Run SM-3A, Step 2 (horizontal)

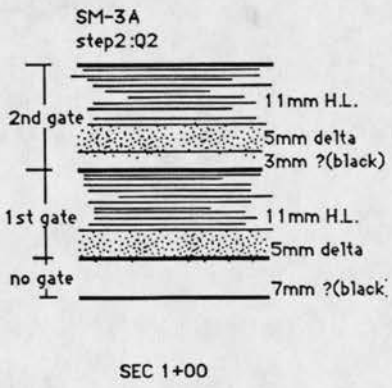

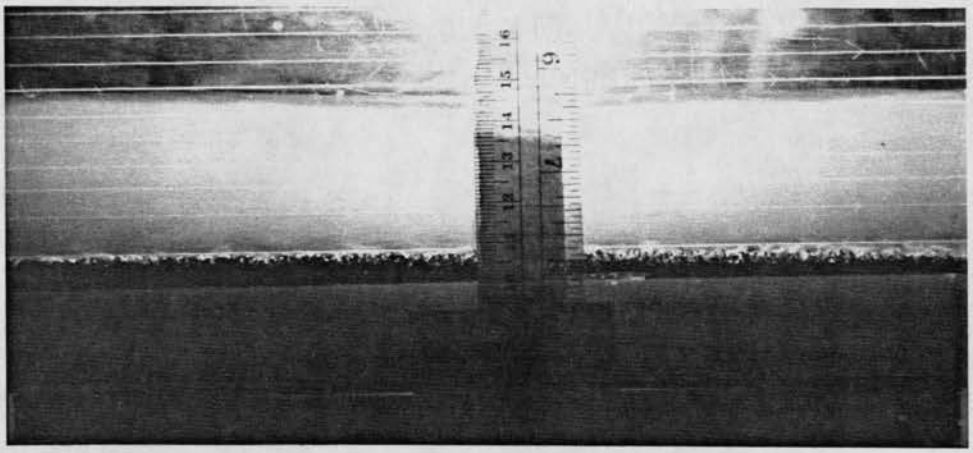

Picture 91. Run SM-3A, Step 3 (horizontal)

Picture 92. Run SM-3A, Step 3 (horizontal)

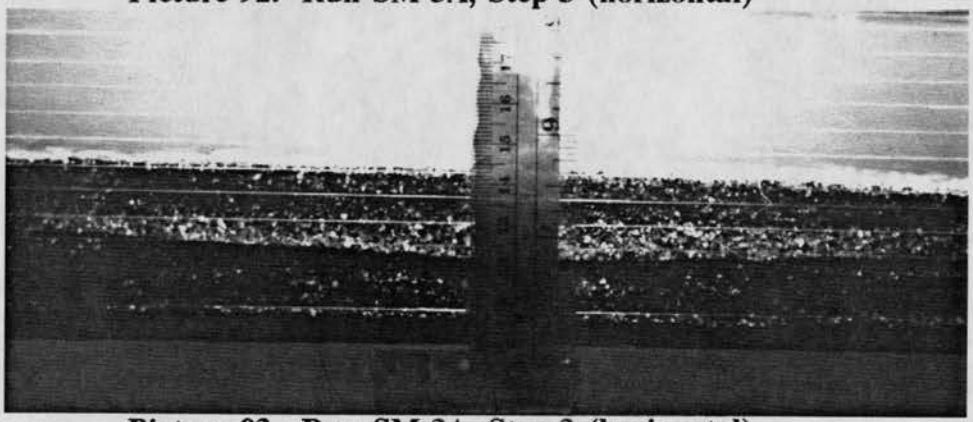

Picture 93. Run SM-3A, Step 3 (horizontal)

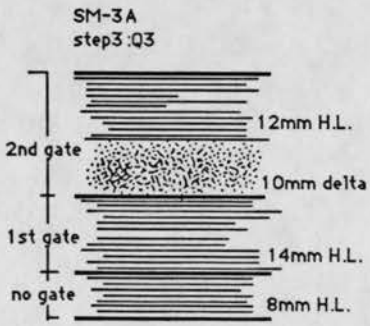

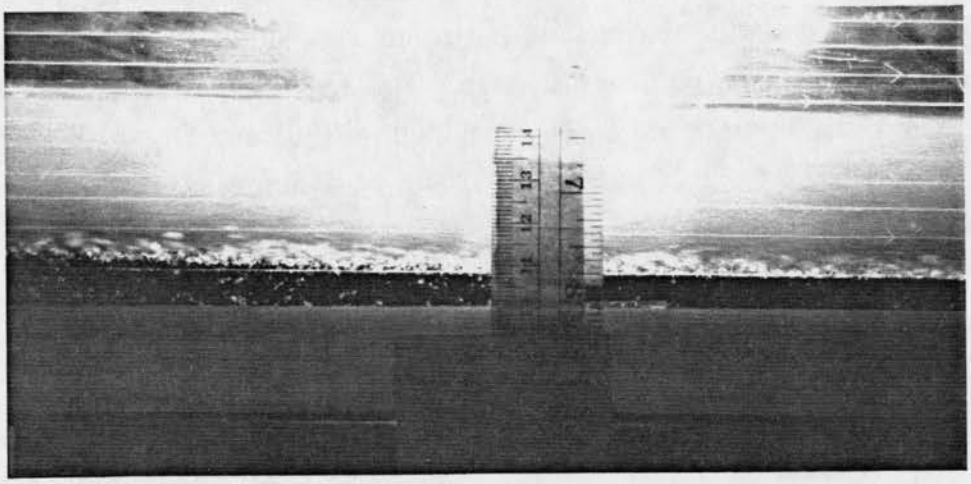

Picture 94. Run SM-3A, Step 4 (horizontal)

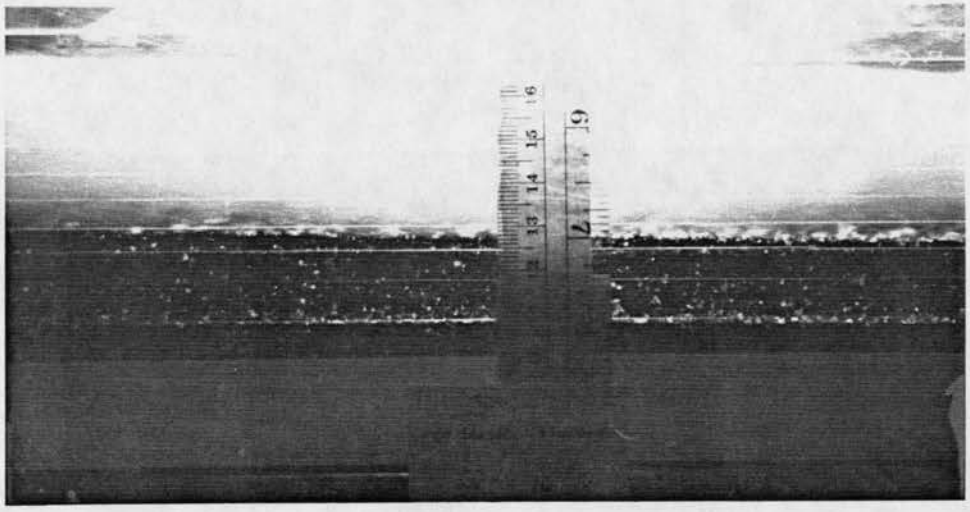

Picture 95. Run SM-3A, Step 4 (horizontal)

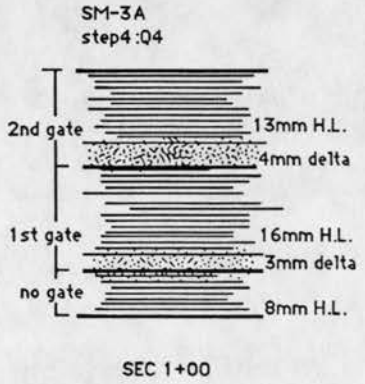

Under similar flow discharge as in the 1st gate between SM-3A-1 and SM-2B-2, the thickness of horizontal lamination in SM-3A-1 is larger than it is in SM-2B-3 (14mm and 8mm, respectively). Overall, the thickness of horizontal lamination in SM-3A is larger than others in SM-2 at a similar range of flow discharge. This may be caused by the larger difference of particle size distribution in SM-3 (D_{50} in B3060 = 0.335mm; D_{50} in ERC #2 = 1.20mm than SM-2 (D_{50} in ERC #4 = 0.16mm; D_{50} in B2040 = 0.575mm). These results are similar to those of Berthault's experiment in still water (1986).

We also observed a series of low-relief sandwaves migration during the formation of horizontal lamination (as shown in Picture 96). It is similar to the result of SM-2B and the observation of Smith's (1971) and McBride et al. (1975).

The deposition for each step is sketched on Figure 27.

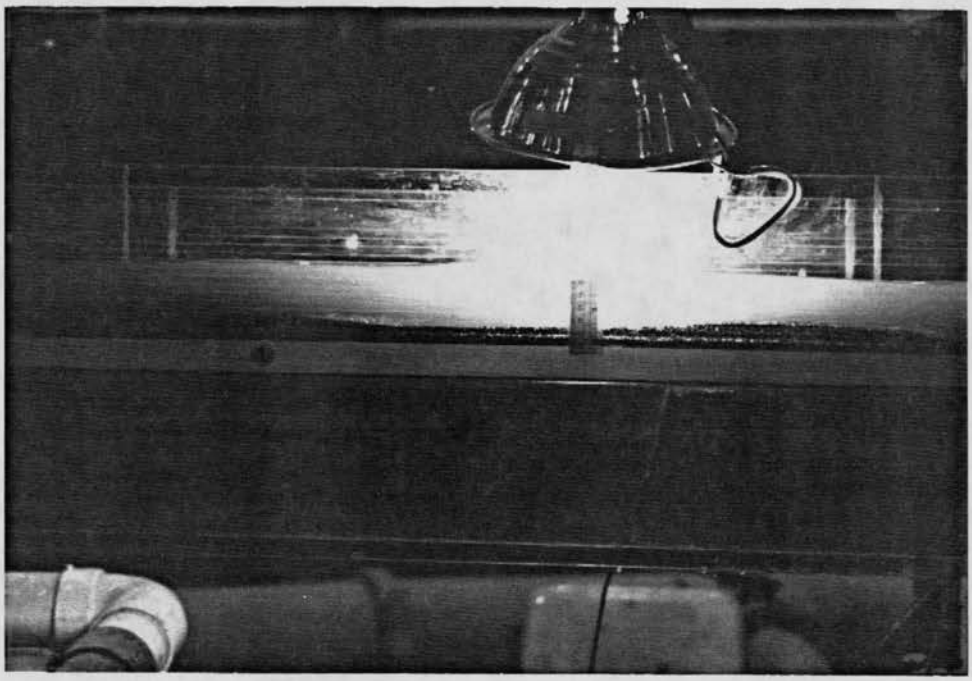

Picture 96. Low relief sandwave migration, (SM-3A, horizontal)

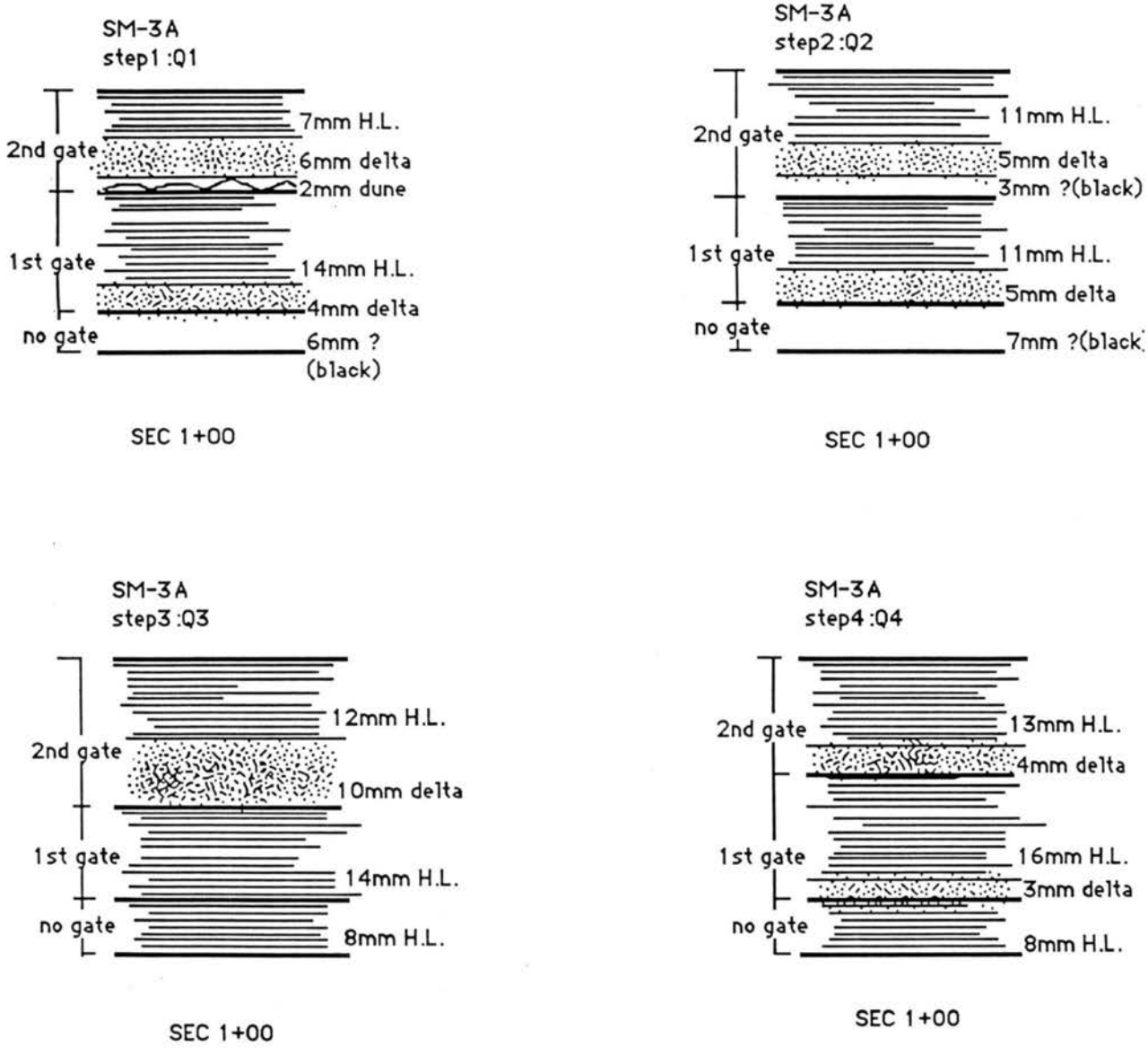

Figure 27. The deposition of SM-3A (horizontal)

3.5 Compilation of Results

The analysis of the with horizontal laminae (H-Lam) layer thickness in terms of average velocities upstream V_u and downstream V_d of the delta are compiled in Table 17. It is found that for the runs SM-2A, V_u varies slightly, but V_d and H-Lam significantly increases with discharge, while the delta thickness decreases with discharge. At a comparable discharge, the runs SM-2D show an increase in delta thickness with gate height as expected. With positive slope, runs SM-2C, the results are similar to those with horizontal slope (SM-2A) except that the thickness of deposits is less sensitive to changes in discharge. Under adverse slopes, runs SM-2B, the thickness variability with discharge is also less significant.

These results clearly show that the delta thickness increases as V_d decreases, while V_u remains fairly constant ($V_u \approx 50$ cm/s). The effect of slope shows that the variability in delta and H-Lam thickness with discharge is clear for horizontal slope, but most obvious for either positive or adverse slope.

In order to examine the variability in upstream velocity V_u, downstream velocity V_d, horizontal lamination thickness H-Lam, and delta thickness with increasing discharge, the experimental results were compiled in Table 18 for both the first and the second gate. It is very difficult to detect any significant tend in the analysis of any of these four variables.

Table 17. Compilation of experimental results for each run

Step	Q cm^3/s	h cm	V_m cm/s	V_u cm/s	V_d cm/s	H-Lam cm	Delta cm
Run:SM2A	**(Horizontal)**	**D_{50} = 0.28mm**					
SM2A-1	2650	2.9	57.55	53.20	33.25	0.27	1.9
SM2A-2	3470	3.9	57.40	47.60	40.00	0.8	0.8
SM2A-3	3949	4.0	63.69	50.00	46.30	1.1	0.4
SM2A-4	4480	4.1	70.49	54.50	52.50	1.2	0.2
Run:SM2D	**(Horizontal)**	**D_{50} = 0.28mm,**	**2nd L**				
SM2D-1	2750	3.4	52.18	46.70	26.20	0.4	2.9
SM2D-2	4026	4.0	64.93	57.50	37.60	0.5	2.3
Run:SM2C	**(P. slope**	**S = +0.005)**	**D_{50} = 0.28 mm**				
SM2C-1	2778	3.7	48.43	42.00	35.50	0.6	0.8
SM2C-2	3470	3.8	58.91	50.00	41.40	0.7	0.9
SM2C-3	4007	4.5	57.44	50.00	45.30	0.7	0.5
SM2C-4	4428	4.4	64.92	53.80	50.00	0.9	0.4
Run: SM2B	**(Adv. Slope**	**S = -0.005)**	**D_{50} = 0.28mm**				
SM2B-1	3334	4.0	53.77	45.70	36.40	0.7	1.2
SM2B-2	3601	4.1	56.66	50.00	41.50	0.6	0.9
SM2B-3	3644	4.0	58.77	50.00	42.70	0.7	0.8
SM2B-4	3988	4.1	62.75	52.50	42.10	0.8	1.2
Run:SM3A	**(Horizontal)**	**D_{50} = 0.62mm**					
SM3A-1	3558	3.9	58.85	50.00	44.00	0.7	0.8
SM3A-2	3850	3.9	63.68	49.60	45.10	1.1	0.5
SM3A-3	4304	4.4	63.10	49.60	42.00	1.2	1.
SM3A-4	4939	4.5	70.81	54.90	51.40	1.3	0.4

Table 18. Compilation of experimental results by increasing discharge

Run	Q cm^3/s	V_m cm/s	V_u cm/s	V_d cm/s	H-Lam cm	Delta cm
First Gate						
SM2A-1	2650	59.89	52.4	34.9	0.3	1.6
SM2D-1	3334	61.45	47.8	43.0	1.0	0.5
SM2A-2	3536	61.65	50.0	43.0	0.9	0.7
SM3A-1	3665	63.90	46.3	43.0	1.4	0.4
Run #2	3665	42.20	40.0	32.2	0.3	1.4
SM3A-2	3909	64.66	50.4	45.8	1.1	0.5
SM2A-3	4026	57.40	47.6	40.7	0.8	0.8
SM3A-3	4304	69.41	51.4	51.4	1.4	0.0
SM2D-2	4428	81.62	51.0	51.0	2.1	0.0
SM2A-4	4548	75.23	53.3	48.9	1.6	0.5
SM3A-4	4764	73.17	54.0	50.5	1.6	0.4
Second Gate						
Run #2	3357	40.63	37.8	33.5	0.4	0.7
SM2A-2	3470	59.40	47.6	40.0	0.8	0.8
SM3A-1	3558	58.85	50.0	44.0	0.7	0.8
SM3A-2	3850	63.68	49.6	45.1	1.1	0.5
SM2A-3	3949	63.69	50.0	46.3	1.1	0.4
SM3A-3	4304	63.10	49.6	42.0	1.2	1.0
SM2A-4	4480	70.49	54.5	52.5	1.2	0.2

IV. ANALYSIS OF DEPOSITS IN A WIDE LABORATORY FLUME

4.1 Introduction

The proposed lamination study in a wide rectangular flume extends the previous investigation in a narrow rectangular flume. This part of the study examines the possible formation of horizontal laminae under different flow conditions in a wide rectangular flume. It is the primary objective of this study to demonstrate that the results of the experiments in the narrow flume are also applicable to the wide rectangular flume.

4.2 Experimental Procedure

4.2.1 Equipment

The experiments are carried out in a broad flume: 2.20m wide, 0.16m deep, and 6.0m long, as sketched in Figure 29. With this design, both water and sediment can be recirculated whenever needed. The recirculating pipe is actually designed to recirculate the sediments trapped in the tailbox shown in Figure 29 and Picture 98, and the entrance pipe ensures a sufficient supply of water to the flume. The flow rate is controlled by two valves and measured by a Venturi tube in the recirculating pipe and an orifice in the entrance pipe. The deposition is controlled by tailgate logs which can be varied from .00m to 0.16m (see Figure 28). Details of the experiment facilities are also illustrated in Pictures 97 and 98.

4.2.2 Sediment Mixtures

The sands used in these experiments are similar to those of Julien and Chen (1989b). To simplify the problem only two types of sand, one black and one white, were used in run #1.

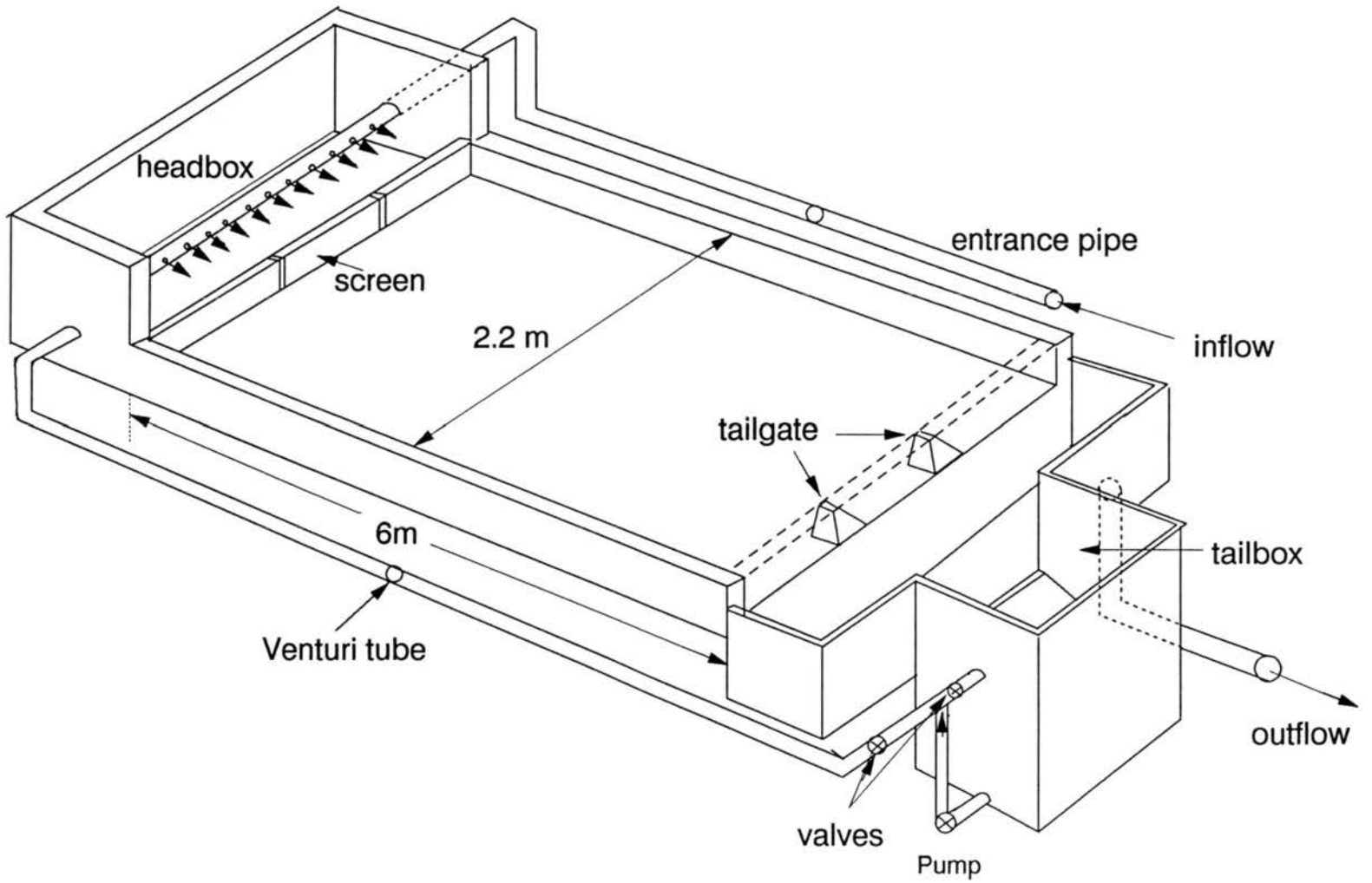

Figure 28. Wide flume used for the experiments

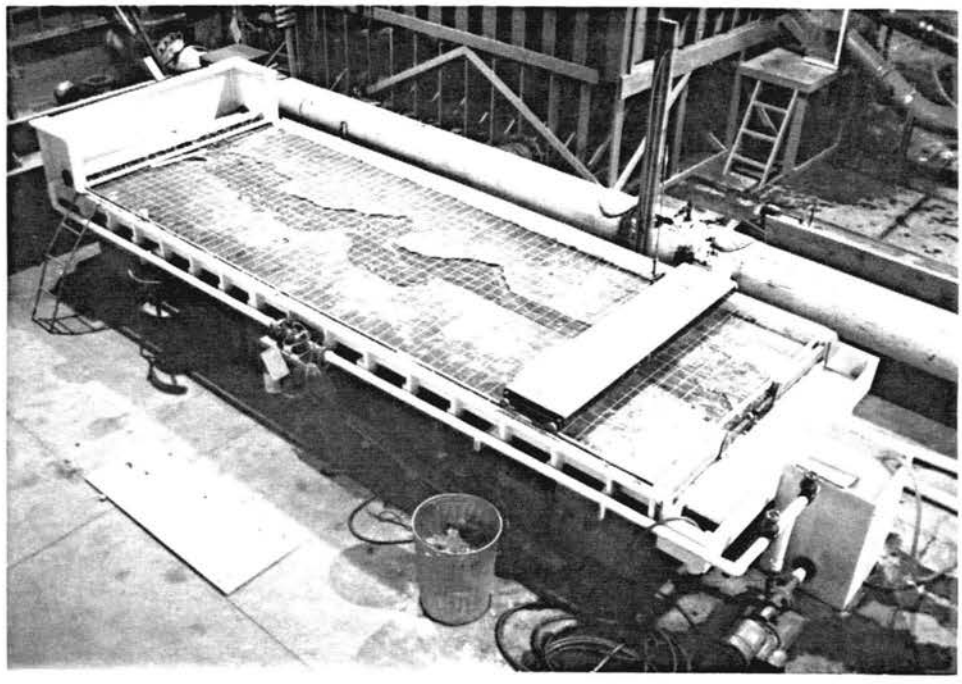

Picture 97. Wide laboratory flume

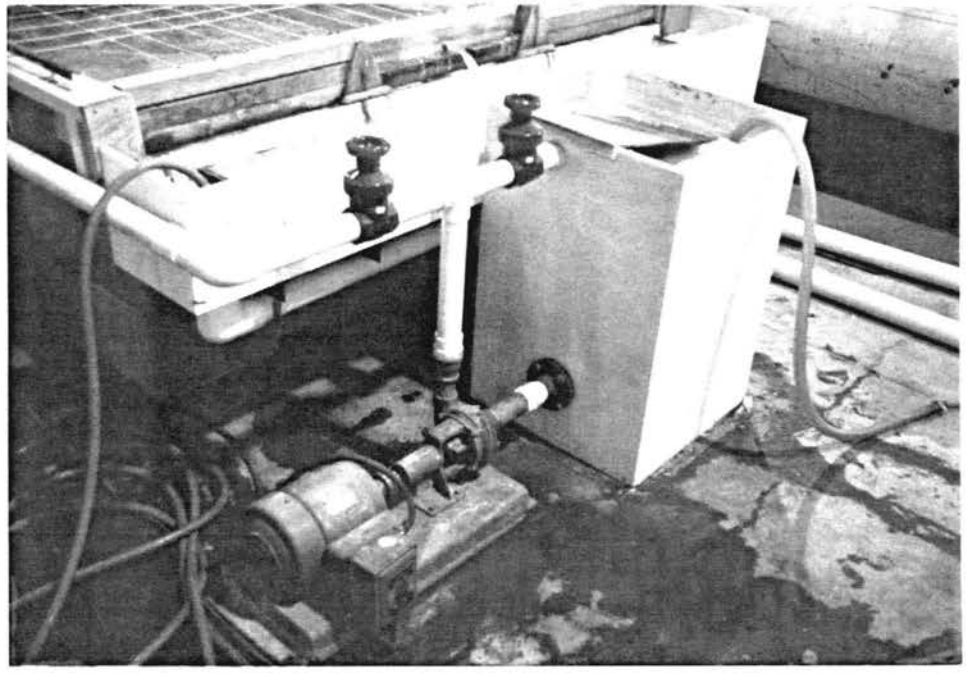

Picture 98. Detail of pump, valves and tailbox

The characteristics of these two types of sands are summarized in Table 19, and the particle size distributions are shown in Figure 30.

Table 19. Sand characteristics

Type	Color	Density	D_{10}	D_{25}	D_{50}	D_{75}	D_{90}
B3060	black	2.70	.14 mm	.205 mm	.335 mm	.55 mm	.62 mm
ERC #5	white	2.65	.084 mm	.110 mm	.130 mm	.155 mm	.180 mm

The following experiment is primarily intended to verify that the results of Julien and Chen (1989b) in a small flume are also applicable for a wide rectangular flume. Only one mixture has been examined in this experiment. It is assumed that if the results of Julien and Chen (1989b) could be reproduced for a single mixture, similar good agreement would be obtained for the other mixtures. The proportion of black and white sands in this mixture is 1:4. According to Julien and Chen's experiment, this mixture would provide excellent visualization of the laminae.

4.2.3 Procedure

At the very beginning of the experiment, a constant value of water discharge is selected and controlled by adjusting the two valves in the oncoming pipe and the recirculating pipe. Without the control of the tailgate, the sand is shoveled into the headbox shown in Picture 99 at a rate which is as uniform as possible, the turbulence generated from the water exiting the entrance pipe induces excellent mixing condition for the sand. The inflow of sediment passing the screen shown in Figure 29 is quite steady and spreads very uniformly across the entire width of the flume. When the front of the deposit approached the tailgate, the water level at the gate is raised about 5 cm by controlling the tailgate elevation, in order to increase the deposited layer thickness and provide better visualization of the laminae. At equilibrium conditions, the water surface slopes and water surface elevations at different cross-section are measured for the calculation of flow velocity and flow depth. Meanwhile, photos were taken to record the bedform configuration and the movement of sands. At the end of the experiment, the bed elevation at different cross sections is measured after shutting off the two valves and after draining the water in the flume.

After the experiment, the deposits are dried on the flume, then cut vertically at some sections both in the streamwise direction and the cross stream direction. Photographs are taken to examine the configuration of laminae.

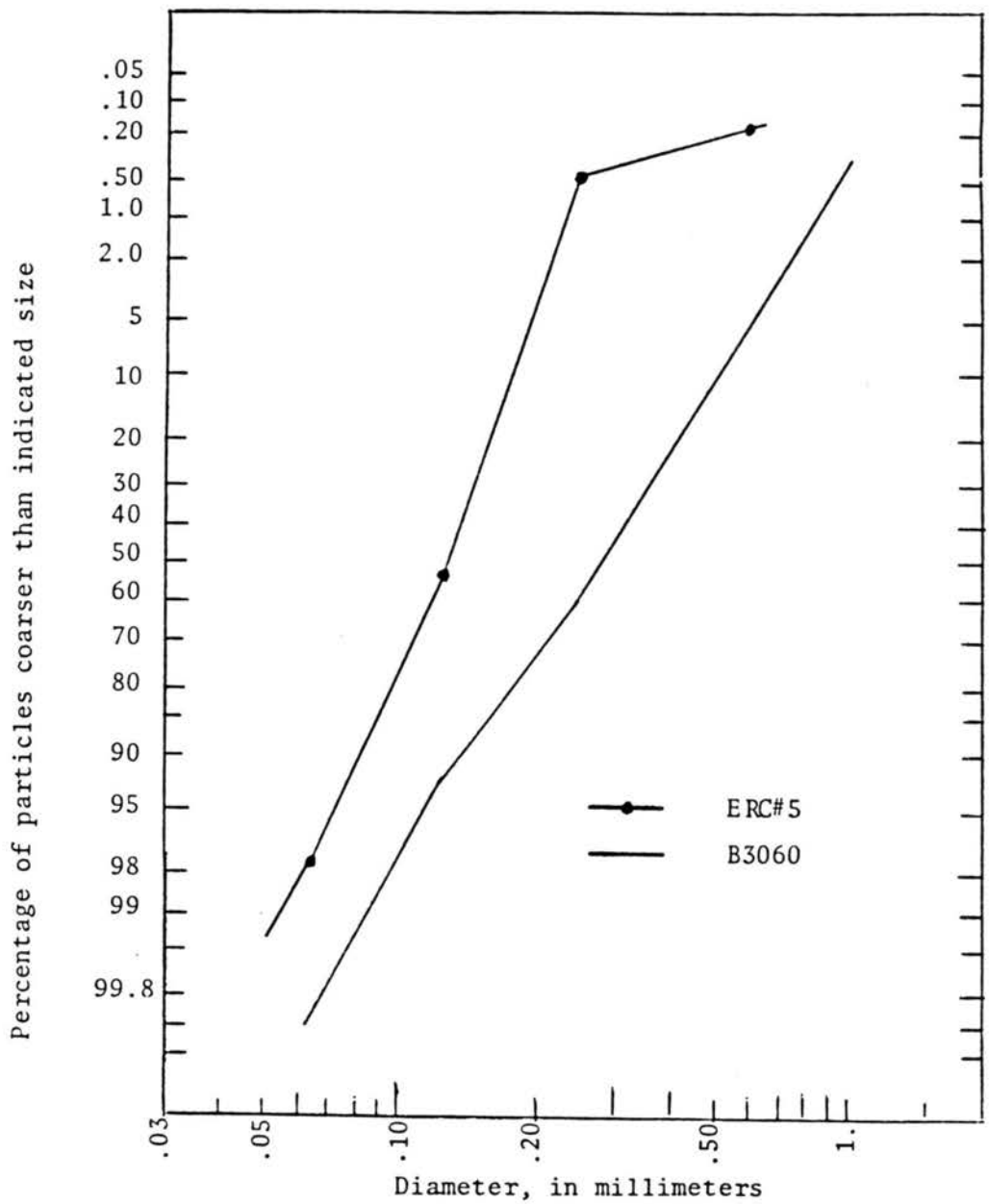

Figure 29. Particle size distributions of two sands used

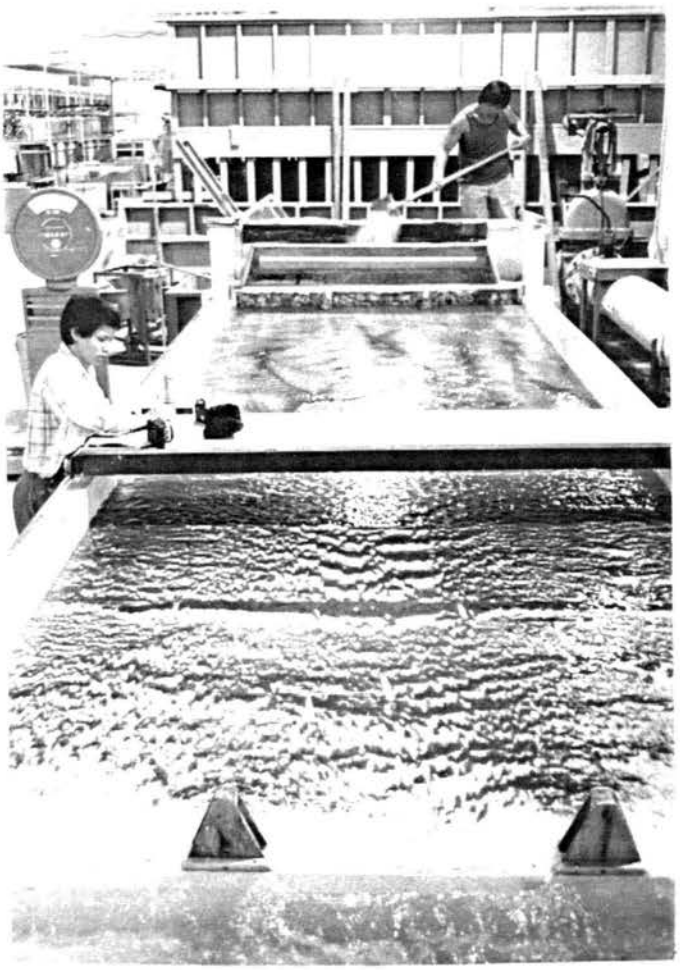

Picture 99. Sand feeding and water level measurement

4.3 Experimental Results

The hydraulic data for this run is summarized in Table 20. The flow depth and velocity are the cross-section averages. The pattern of sediment movement during aggradation was observed in Pictures 100-102. It was interesting to see that coarser grains (black) kept rolling on the surface of the deposits as it progressed downstream, although more black sand deposited near the downstream end of the flume.

Table 20. Hydraulic data summary

Gate Height cm	Q l/s	h cm	V_m cm/s	Slope	Fr	U^* cm/s	f
5.0	5.773	1.33	26	0.0081	.72	3.25	.125

Q = flow discharge; h = averaged flow depth; V_m = averaged flow velocity; Fr = Froude number; U^* = shear velocity; f = Darcy-Weisbach friction coefficient.

The lamination is examined at three places, respectively the upstream, middle, and downstream section of the flume. Their positions and the related pictures taken are illustrated in Figure 30, and the laminae are shown in Pictures 103-110.

Table 21. Description of pictures 103-110

Picture #	Position	Orientation	Comment
103	upstream	streamwise	clear lamination is observed
104	upstream	streamwise	with a distinct layer of
105	upstream	cross-section	black sand closest to
106	upstream	streamwise	the bottom of the flume
107	middle	cross-section	bottom layer has
108	middle	cross-section	more distinct
109	middle	cross-section	lamination
110	downstream	cross-section	lamination is less distinct

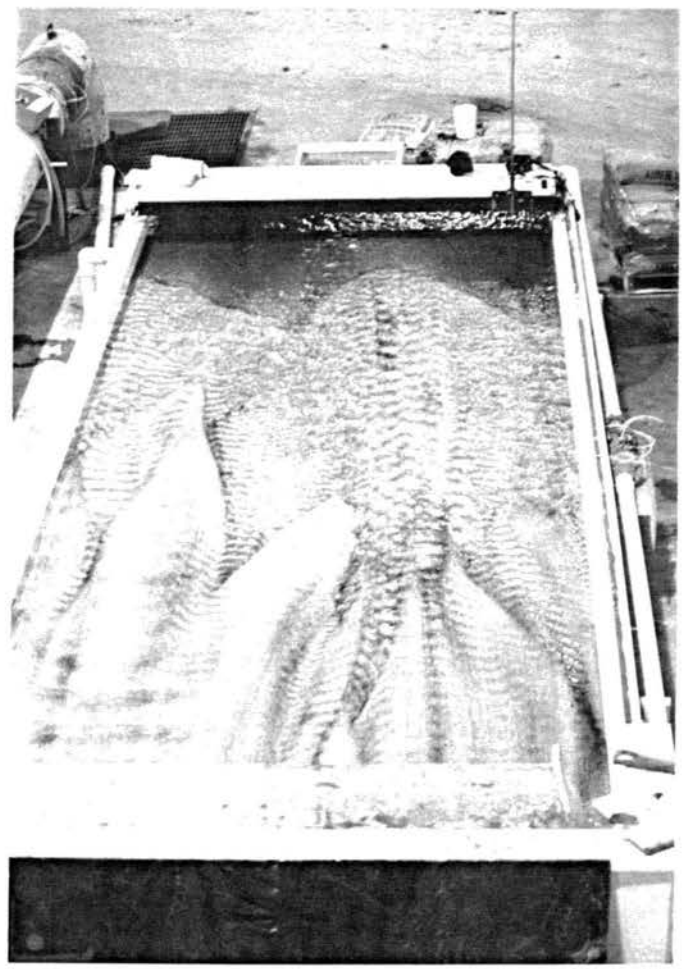

Picture 100. Formation of alluvial deposits

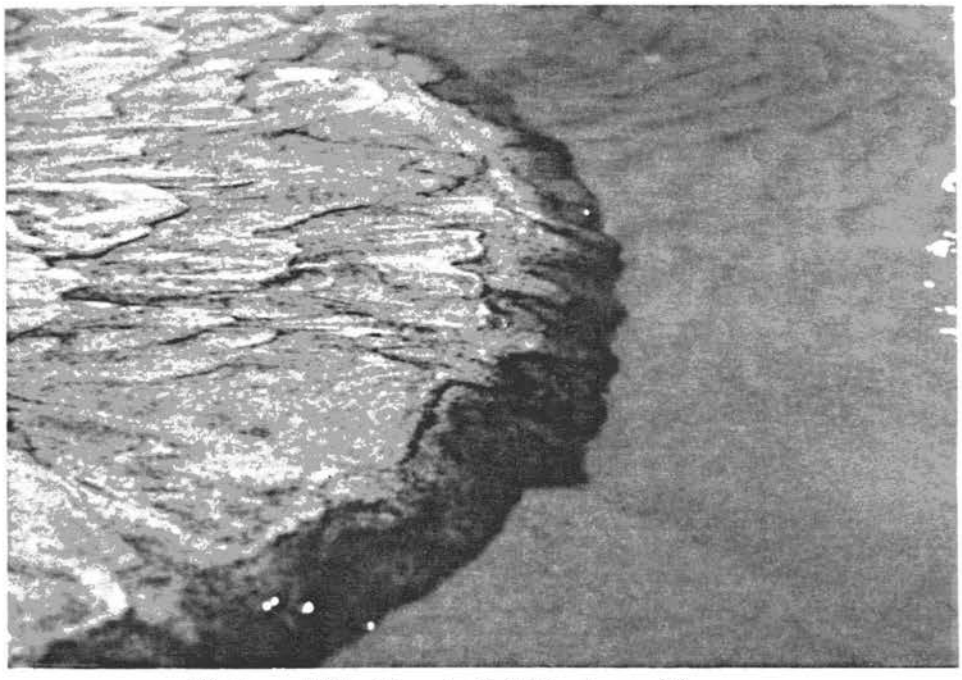

Picture 101. Front of delta deposition

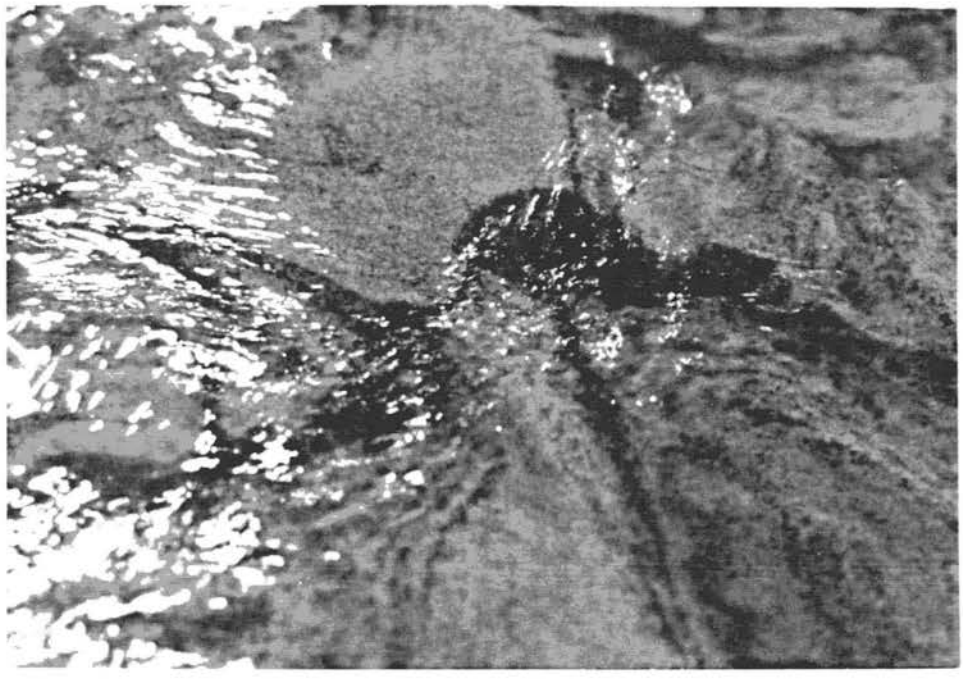

Picture 102. Rolling of black sands on the surface of the bedform

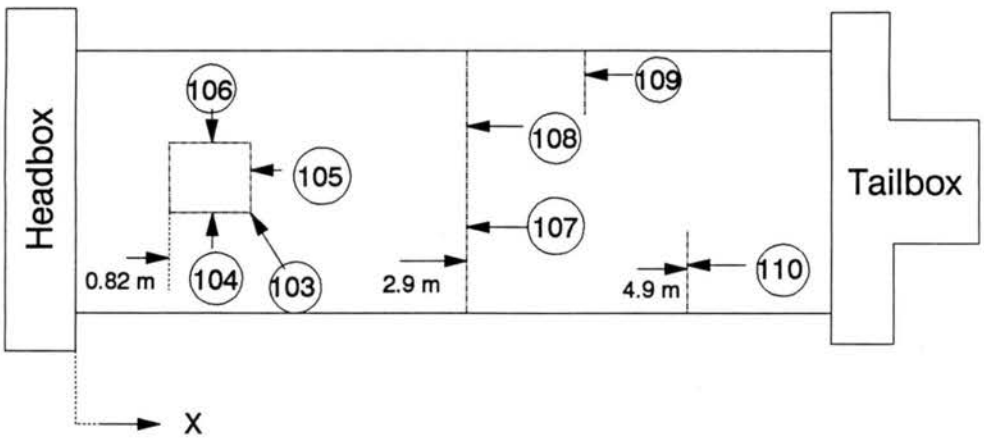

Figure 30. Location of cross-sections where deposits are examined
(Number in circle refers to the picture no., and blank arrow refers to the direction the picture is taken.)

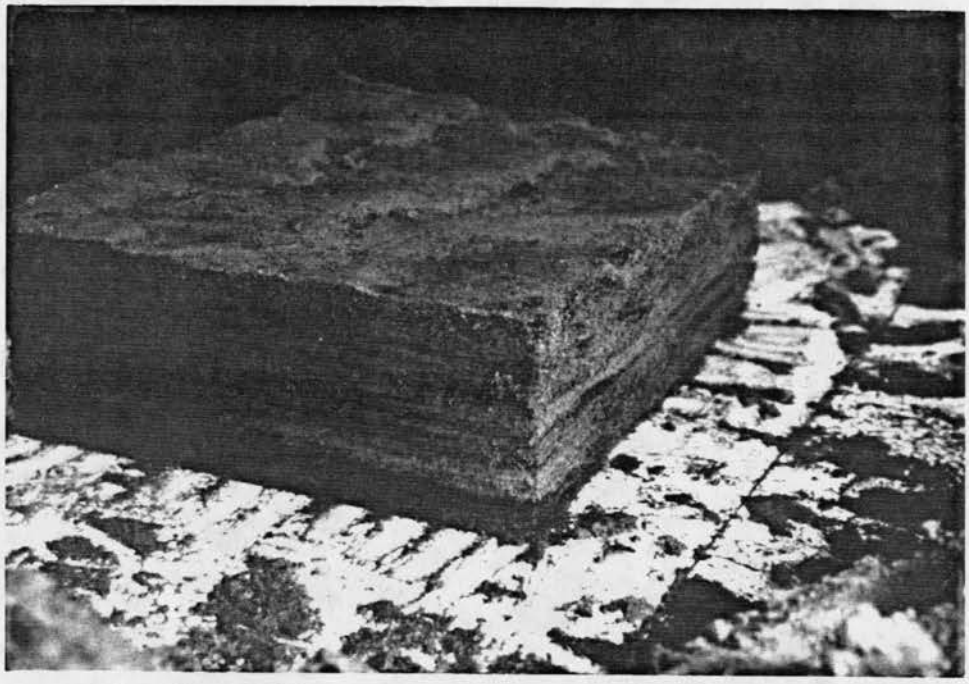

Picture 103. Upstream lamination profile

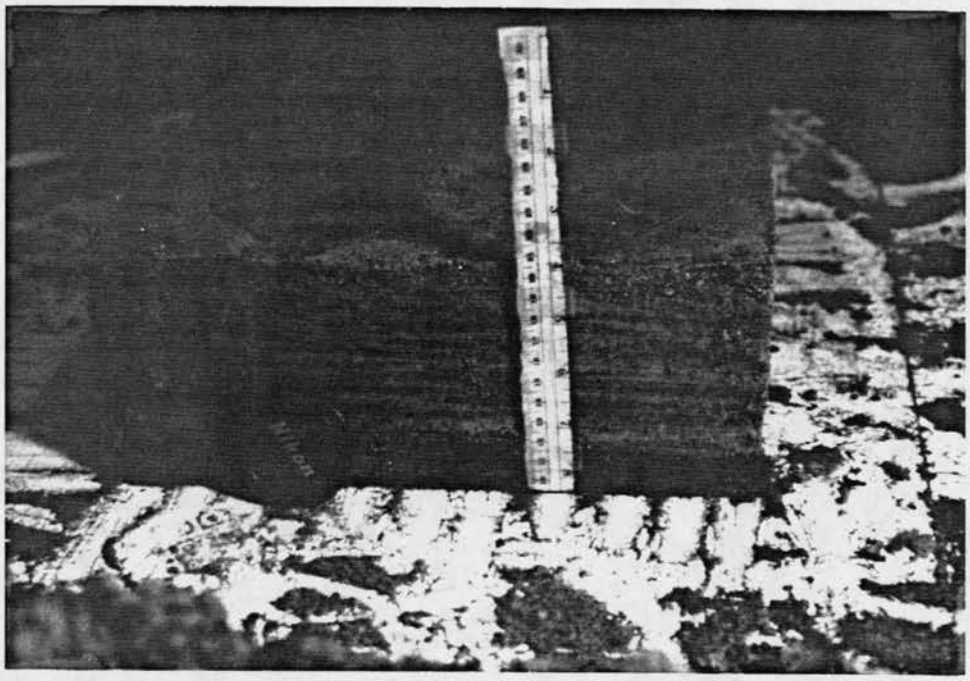

Picture 104. Upstream lamination profile

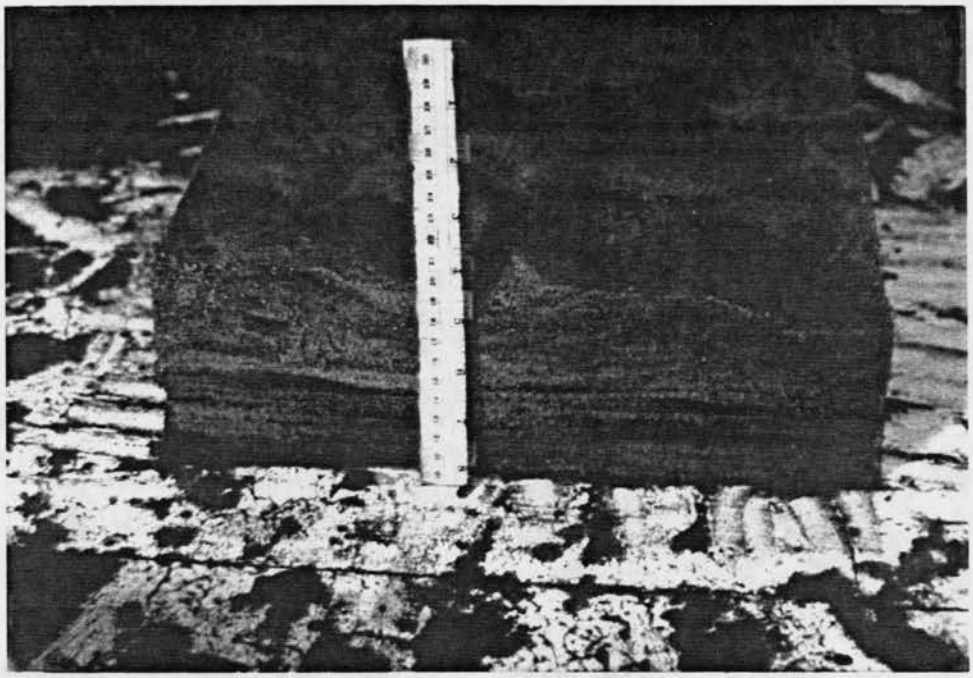

Picture 105. Upstream lamination profile

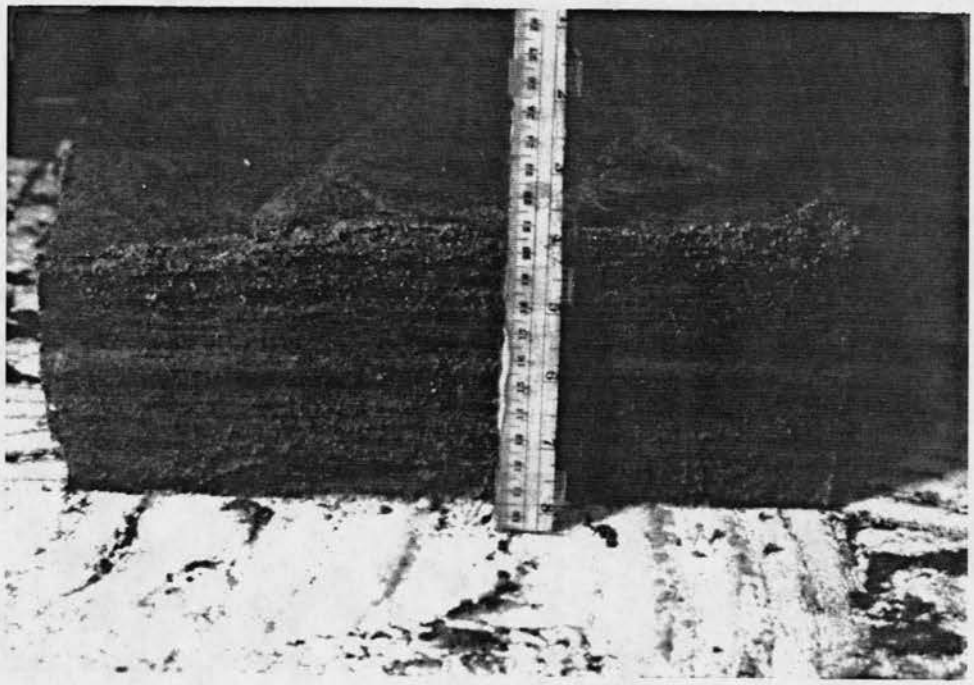

Picture 106. Upstream lamination profile

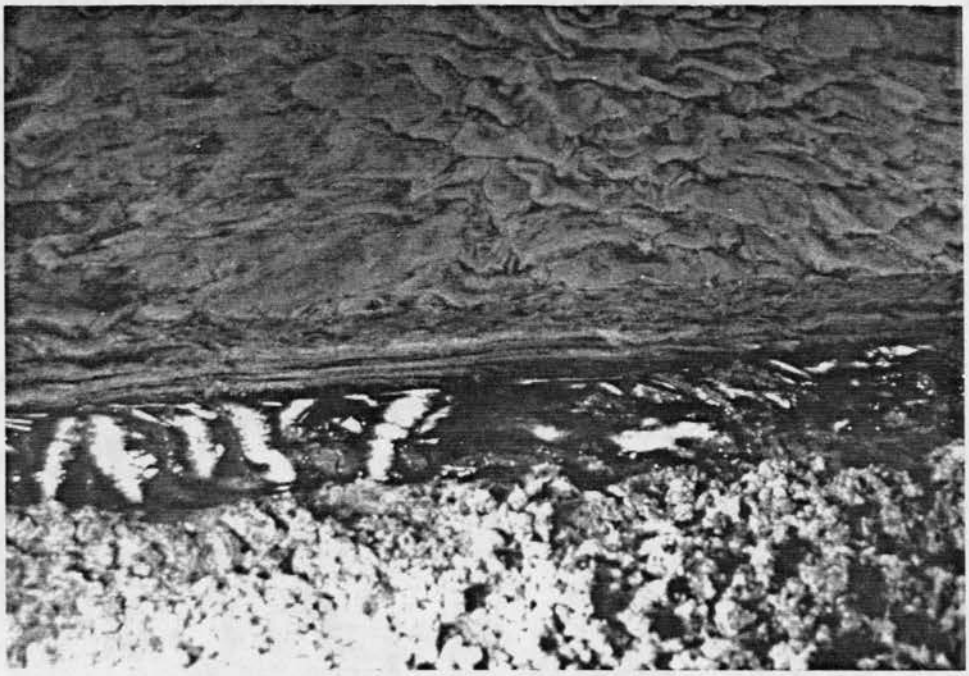

Picture 107. Middle section lamination profile

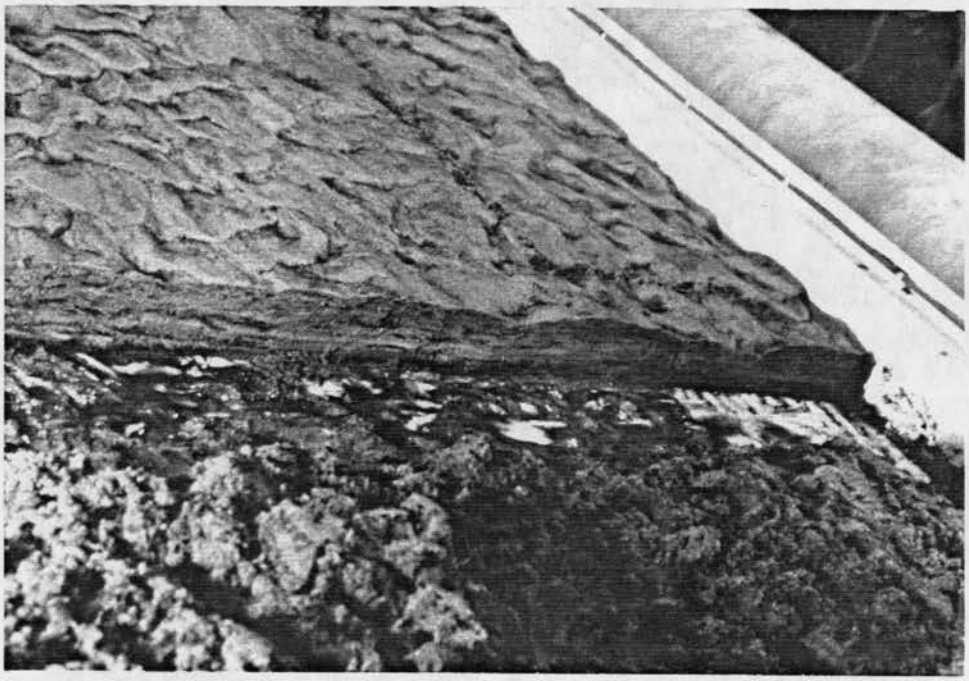

Picture 108. Middle section lamination profile

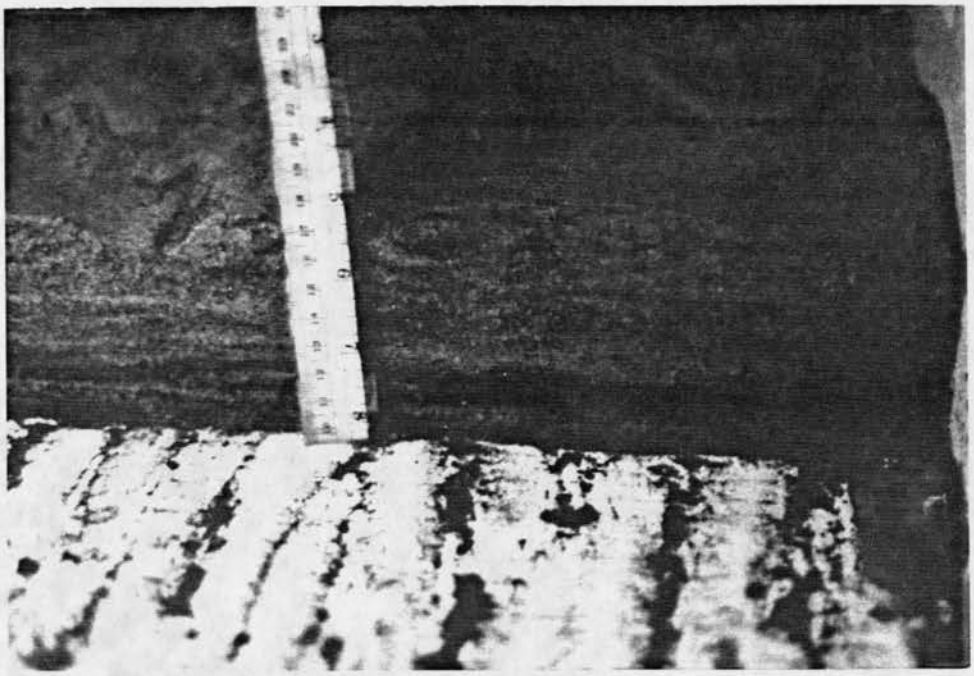

Picture 109. Middle section lamination profile

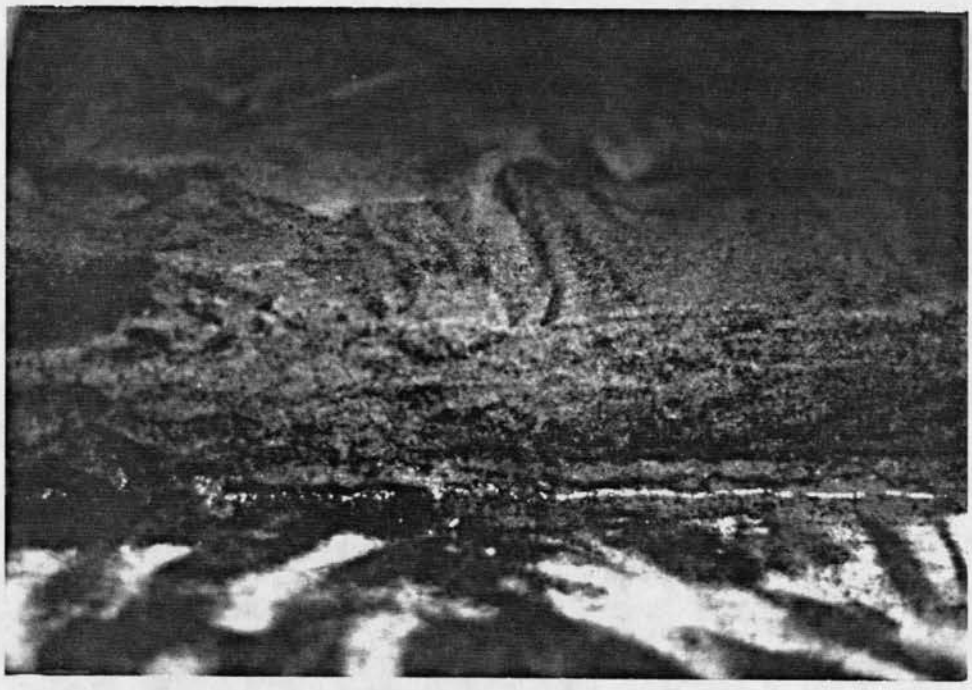

Picture 110. Middle section lamination profile

The upstream pictures (Pictures 103-106) show that there is a layer of black sand closest to the flume bed at the upstream position. This is in accordance with the observations that black sand moves at a lower shear stress than white sand. At the beginning of the test, the black sand moved further out than the white sand, and created this layer.

Pictures 107 and 108 show the laminae of the entire cross-section at the middle reach (about 2.9 meters from the headbox). The laminae are still quite distinct as compared with the laminae in the upstream. However, Picture 110 from the downstream position, does not show lamination as clear as those from upstream and middle positions, due to the decrease of flow velocity near the tailgate.

Another conclusion to be drawn from the pictures is that the lamination is more distinct at the upstream end of the flume, and less distinct at the downstream end. This may be explained in terms of lamination being the result of a sorting process. The sorting effect will be stronger for increasing velocities, and we have higher velocities at the upstream end of the flume because the slope is higher as we feed in sediments. The velocity at the downstream end of the flume will be lower, and hence a smaller sorting effect and lamination. This can also explain why the layer of black sand closest to the flume bed is less distinct than at the upstream position.

V. EXPERIMENTS ON DESICCATION OF BIJOU CREEK SANDS

5.1 Introduction

The proposed laboratory experiments in a small recirculating flume are intended to examine the depositional characteristics of Bijou Creek sand under plan bed conditions with sediment motion. This study is limited to horizontal deposition processes without bed forms. After each experiment, the sediment deposits were dried in the flume to examine the appearance of vertical cracks and stratification joints.

5.2 Experimental Procedure

5.2.1 Equipment

The experiments were carried out in a small tilting recirculating plexiglas flume: 0.15 m wide, 0.15 m deep, and 2.40 m long. The flow rate is controlled by a gate valve and measured by a calibrated Venturi orifice. The deposition of sand in the flume is controlled by two kinds of tailgate: 0.02 m high and 0.04 m high. The depth of water and deposition is measured by an affixed ruler on the sidewall of the flume. The flume slope can be adjusted by a screw jack which supports the front end of the flume.

Particular consideration in the design procedure has been given to the entrance condition of the flume. The return of water and sediment in the headwater box needs to be carefully designed in order to ensure complete mixing of the sediment particles and constant inflow of sediment under steady flow condition. The rounded entrance profile and the use of a movable plate provided excellent feeding conditions into the flume channel.

5.2.2 Sediment Mixtures

The sediment used in this experiment is natural sand from the surface of the main channel bed of Bijou Creek near Hoyt, Colorado as shown in Figure 32. The locality of this sample is also near the locality III in the investigation of McKee et al. (1967). Prior to the experiments, this natural sand has been sieved and the vegetation and pebbles were removed. The characteristics of the natural Bijou Creek sand are summarized in Table 22, and the particle-size distribution curve in shown on Figure 33.

Table 22. The Bijou Creek sand size distribution

Type	D_{10}	D_{25}	D_{50}	D_{75}	D_{90}
Bijou Creek sand	0.34 mm	0.52 mm	0.75 mm	1.10 mm	1.65 mm

The size of sand particles ranges from fine to very coarse sand, and the silt and clay content (below #230 sieve) is only 0.1 percent according to Table 23 of sediment grade scale which is modified from the classification of the Subcommittee on Sediment Terminology of the American Geophysical Union (Lane, 1947). It is similar to the grain analysis in the report of McKee et al. (1967)--"At all localities sampled, the most abundant sediment was quartz sand of fine to coarse texture. Minor amounts of silt and clay, mostly less than 2%" (p. 831).

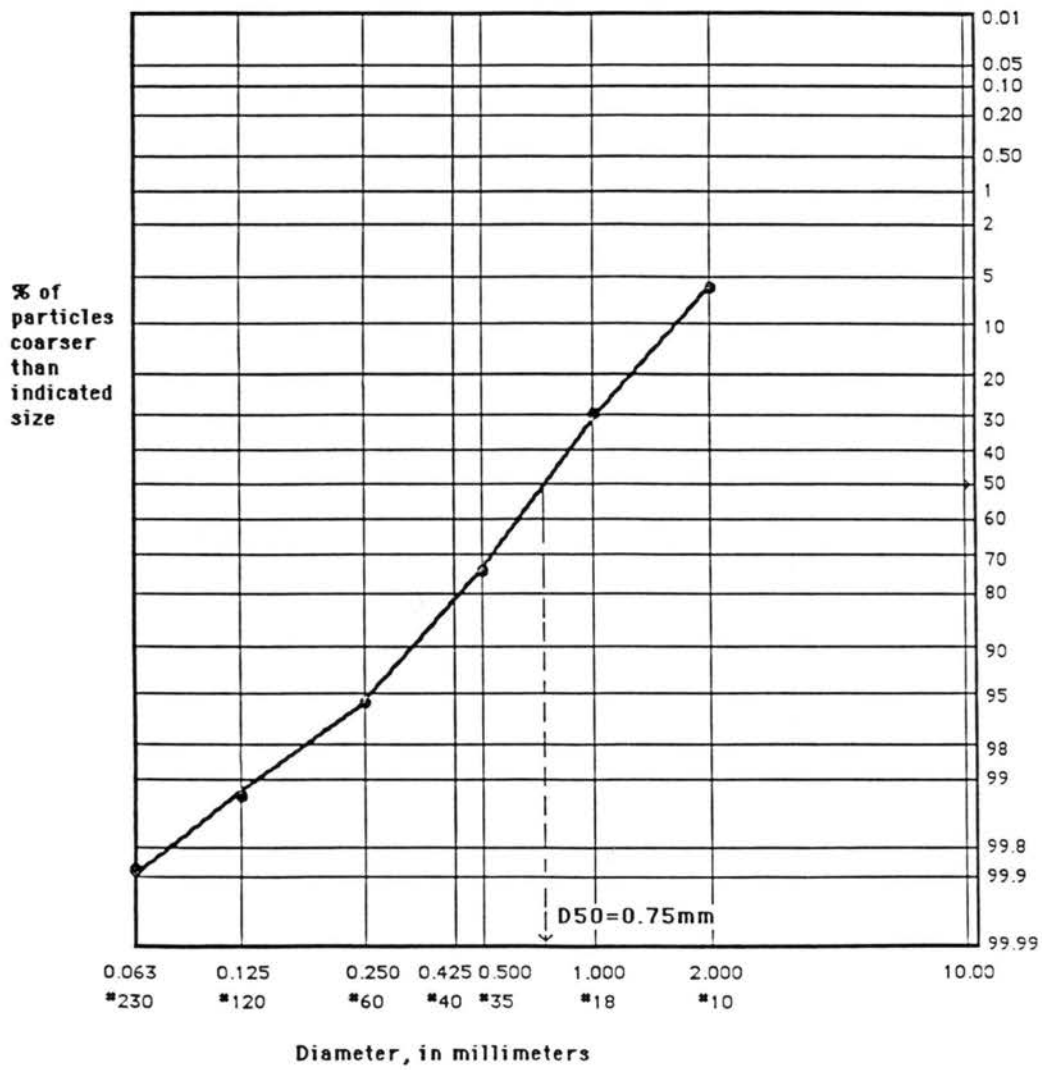

Figure 31. Particle-size distribution for Bijou Creek sand

Table 23. Sediment grade scale

Class Name	Size Range (mm)	Sieve Mesh (U.S. Standard)	Percentage
Gravel	above 2.00	above #10	6.0%
Very coarse sand	2.00 - 1.00	#18	30.0%
Coarse sand	1.00 - 0.50	#35	74.0%
Medium sand	0.50 - 0.25	#60	96.0%
Fine sand	0.25 - 0.125	#120	99.2%
Very fine sand	0.125 - 0.063	#230	99.9%
Silt and clay	below 0.063	below #230	100.0%

5.2.3 Procedure

In this experimental program, two runs are proposed for the Bijou Creek sand. Before each run, the flume slope is set horizontal and the valve is adjusted to control the flow rate which recirculates sediment and forms horizontal deposits. The flow discharge is then maintained steady during the course of each run.

For the first run (run #1) the water flows freely without gate control until the first deposition layer is formed. The first small gate (2 cm high) is then inserted at the downstream end and the second strata forms until equilibrium conditions are reached. The second gate (2 cm high) is then inserted to form the other strata superposed on the first one. During the equilibrium condition in each step we measure the discharge, depth of water, surface velocity and note the configuration of laminae deposition.

For the second run (run #2) the water flows freely without gate; the same condition as run #1. Sequentially, we put in a simple large gate (4 cm high) to form a thicker strata. However, the second gate is not introduced and the measurements are made after equilibrium conditions are reached.

After each run, solar lights (as shown in Picture 111) are set above the flume to dry the deposit of sediment for about one week. The purpose is to observe whether the sand deposit will consolidate and whether vertical cracks and stratification joints will occur or not. The reason why we are interested in the cracking phenomenon is that thin sun-cracked mud layers are often observed on the last sediments deposited during each flood--for example, the cracked surface of the Colorado River flood plain delta at Lake Mead, Arizona (McKee, 1965). In the experiments, the cross-sections are cut at SEC.1+00, and samples are taken from each strata for sieve analysis.

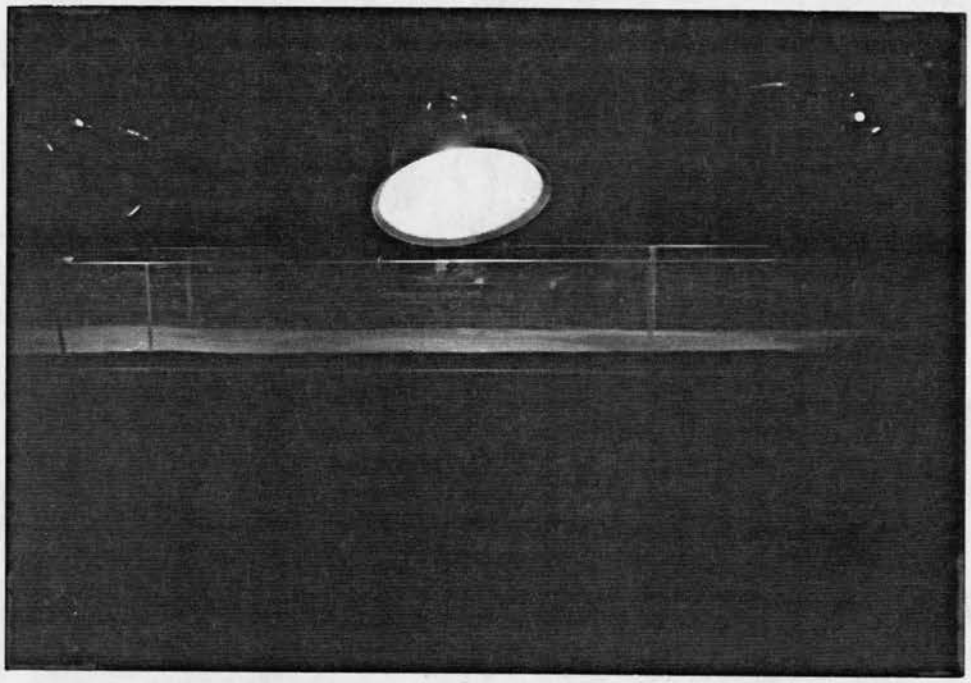

Picture 111. Lights used to dry the deposits

5.2.4 Data Measurement

During each run, several types of measurements are repeated to generate a data base of hydraulic conditions associated with observed formations of laminae and stratified deposits.

The flow discharge is measured by a Venturi orifice in which the manometer readings are transformed into discharge values through a calibrated chart. The hydraulic characteristics of flow depth and flow velocity are measured with the water surface slope. The water depth is measured with a ruler affixed on the flume sidewall at several sections including SEC.1+00. The water surface slope is determined from the difference in water surface elevations between two sections. The surface velocity is measured by the travel time of floating particles between two cross-sections. Average flow velocity is calculated from discharge and cross-section area.

The thickness of horizontal laminae deposits are measured from the ruler affixed on flume sidewall at SEC.1+00, see Picture 112-115. After each run the deposition of sediment is dried out with solar lights. The representative grain size of each stratum is measured by sieve analysis of the samples taken at cross-section SEC.1+00.

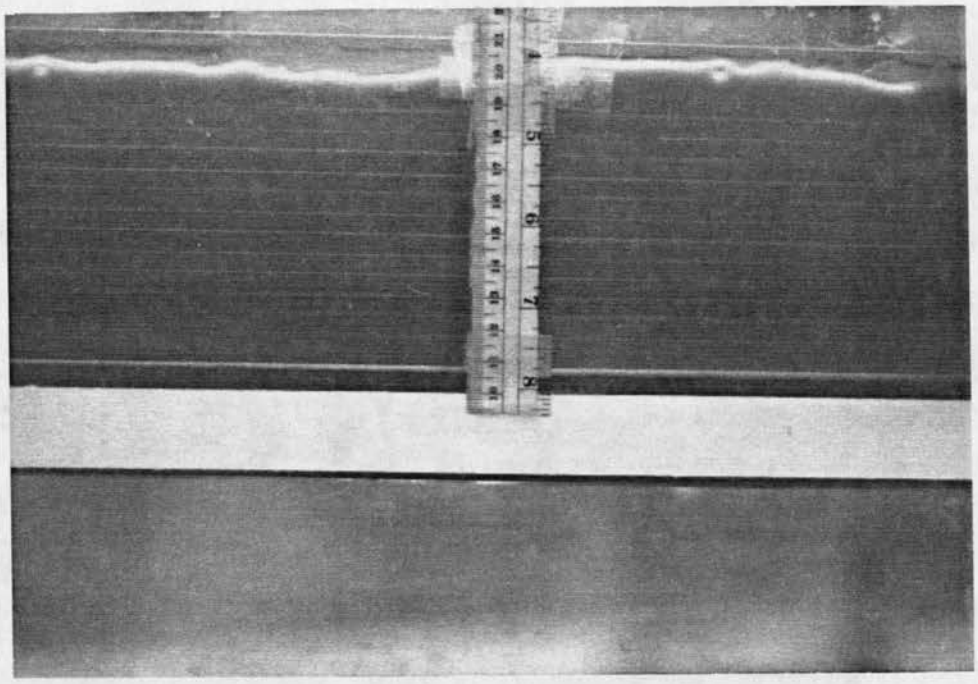

Picture 112. The propagation of the delta

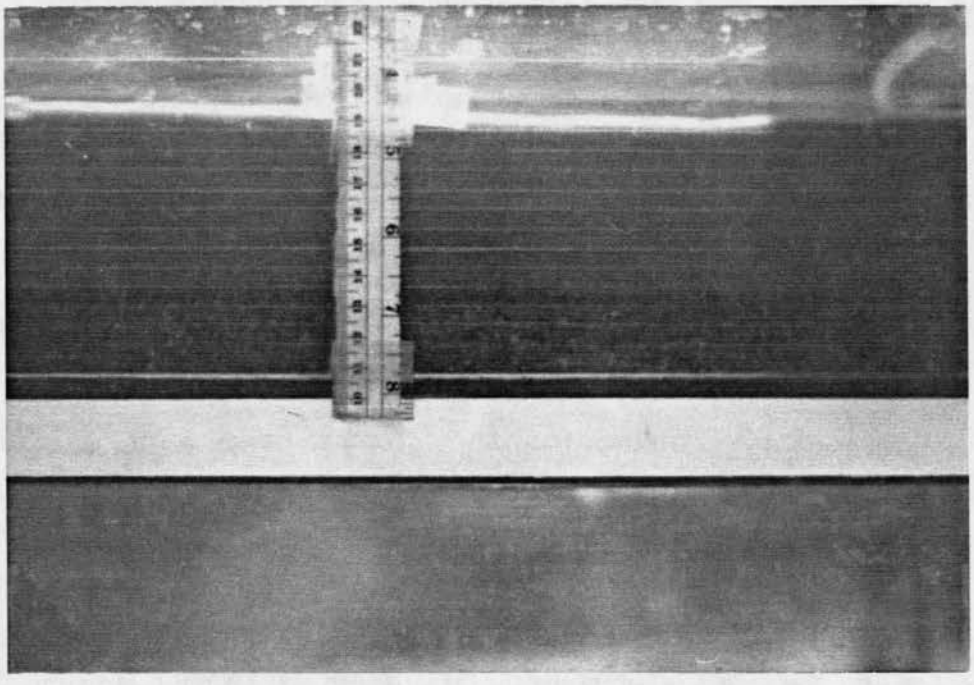

Picture 113. The downstream propagation of the delta

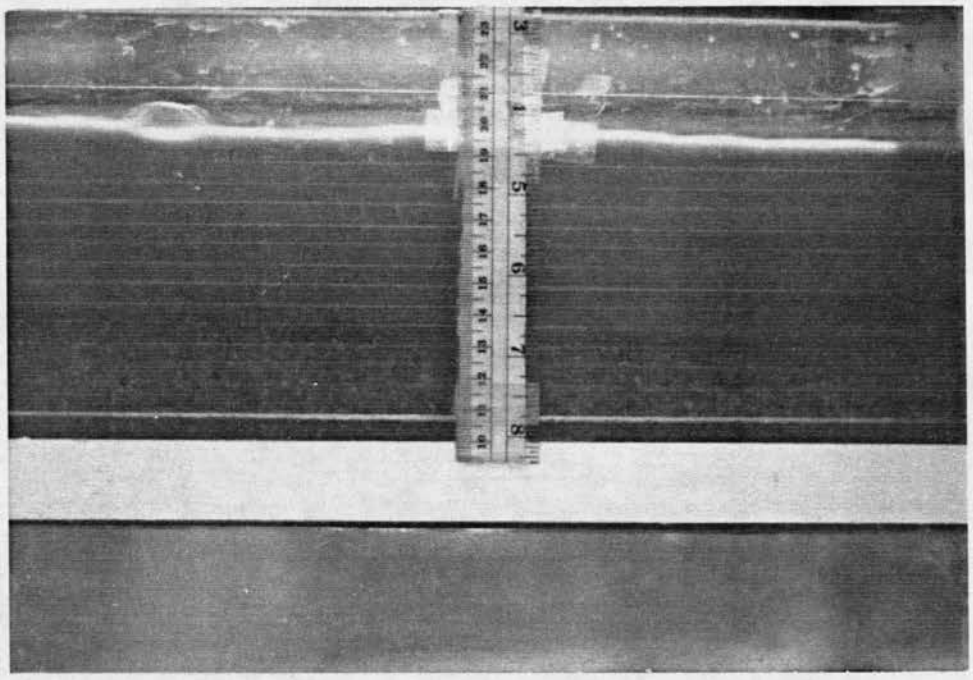

Picture 114. Deposition of fine particles

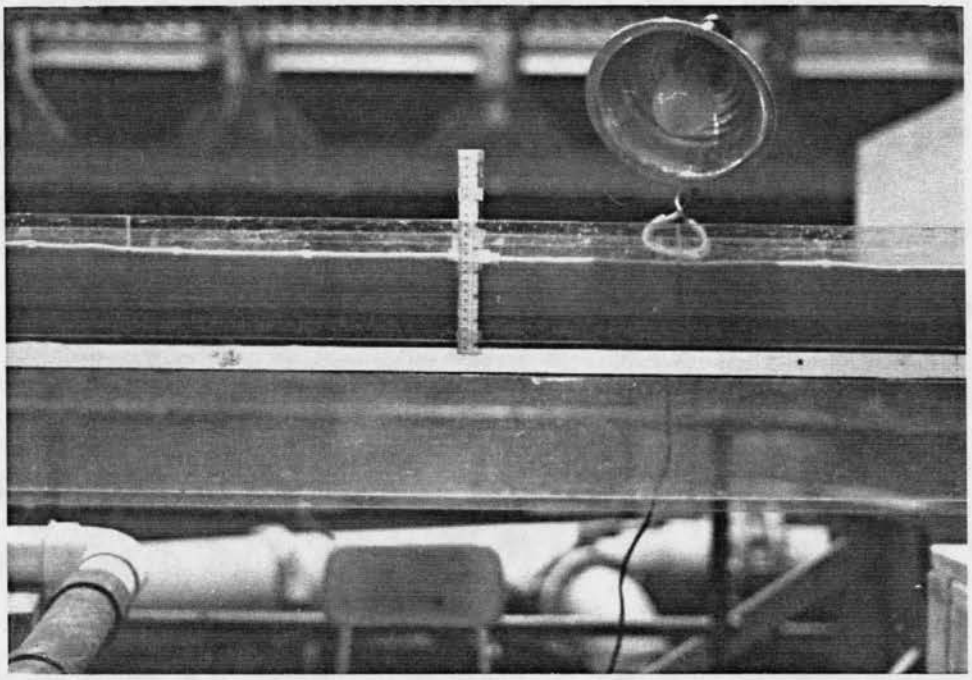

Picture 115. Low-relief sandwaves migrating downstream

5.3 Run #1

5.3.1 Experimental conditions and data summary

- Horizontal flume
- D_{50} = 0.75 mm
- Two small tailgates (2 cm high each)
- Deposition is shown in sequence on three photographs:
  without gate - Picture 116
  first gate - Picture 117
  second gate - Picture 118
- The data for this run are summarized in Table 24 below.

Table 24. Data summary for run #1

Run #1: horizontal flume, D_{50} = 0.75 mm

Gate	Q cm^3/s	h cm	V_m cm/s	V_s cm/s	S_w	Shear $dyne/cm^2$	Fr	U^* cm/s	f	H-Lam mm	Delta mm
No	3558	4.20	54.65	58.49	0.010	26.69	0.85	5.17	0.072	1	0
First	3665	5.60	42.22	55.57	0.005	15.93	0.57	3.99	0.071	3	14
Second	3357	5.33	40.63	47.35	0.006	18.57	0.56	4.31	0.090	4	7

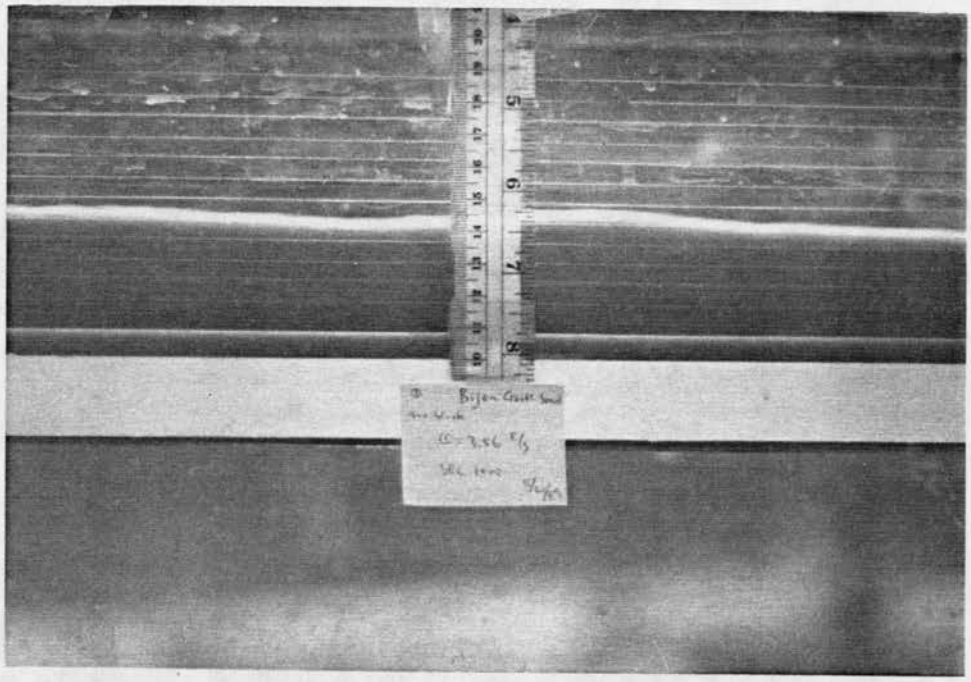

Picture 116. Deposition without gates (run #1)

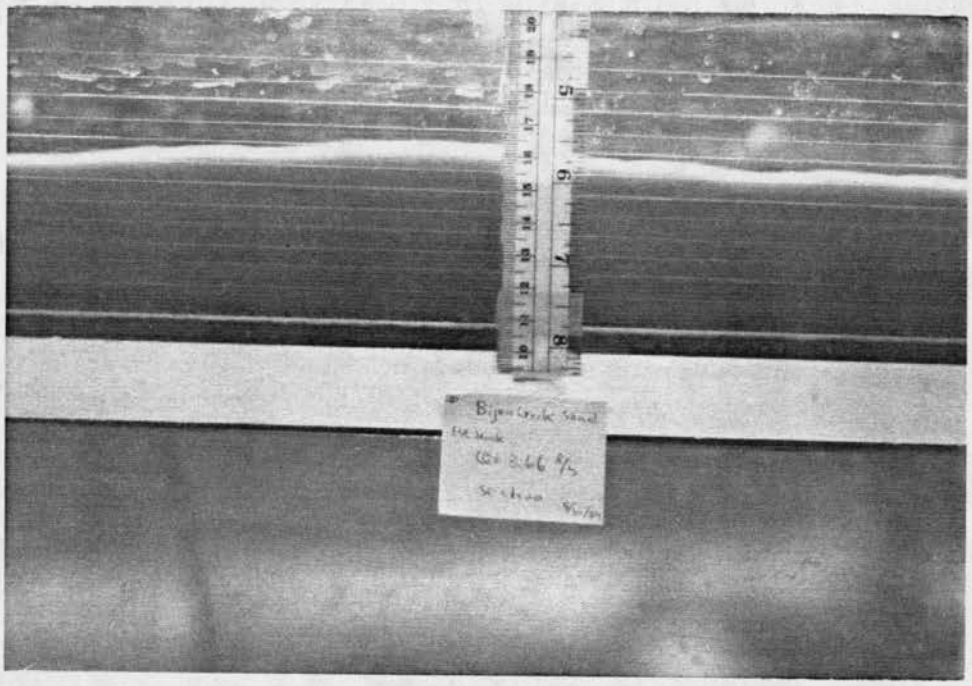

Picture 117. Deposition using one gate (2 cm high; run #1)

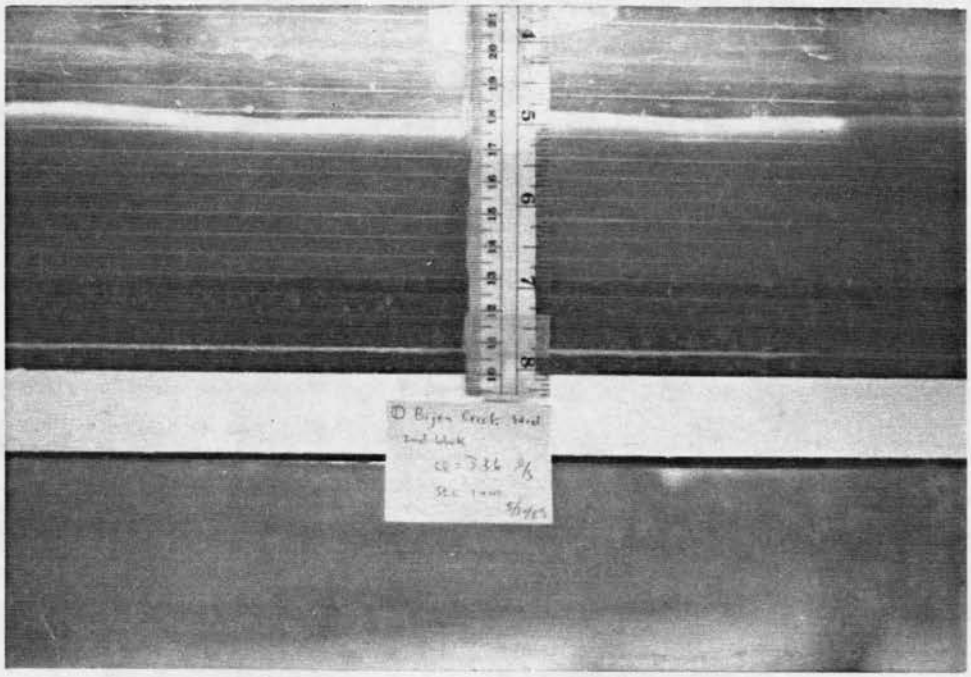

Picture 118. Deposition using two gates (2 cm high; run #1)

5.3.2 Results of Run #1

The horizontal lamination layer thickness for the second tailgate condition is a little thicker than that in the first gate condition although the velocity is reduced in the second gate condition as shown on Table 24. However, we find that the bed shear and shear velocity is a little higher in the second gate condition. We also can find similar conditions in the results of Julien and Chen (1989b) where the horizontal lamination thickness increased by increasing not only flow velocity, but also bed shear or shear velocity. Therefore, the horizontal lamination thickness seems dependent on the bed shear or shear velocity as well as flow velocity. The deposition of this run is sketched on Figure 34.

After seven days of exposition under solar lights, clear layers of finer and coarser material are shown on Picture 119. There is no vertical crack as shown on Picture 120. However, we can see horizontal cracks after we cut the cross-section at SEC.1+00 as shown on Picture 121. We can peel the separated layers of finer sands and coarser sands easily as shown on Picture 122.

Samples from each layer were taken for analysis. The particle-size distribution curves are drawn on Figure 33 for each layer. The medium grain size (D_{50}) and grade scale classification for each layer are shown on Figure 32. We also find that silt and clay content is less than 1 percent on the top finer layer. It may explain that no vertical crack appeared on the surface.

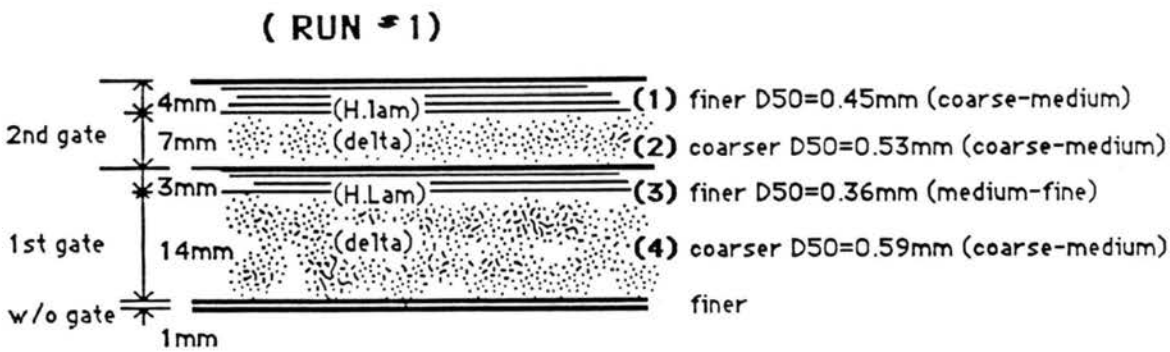

Figure 32. The deposition of Bijou Creek sand at SEC.1+00 (run #1)

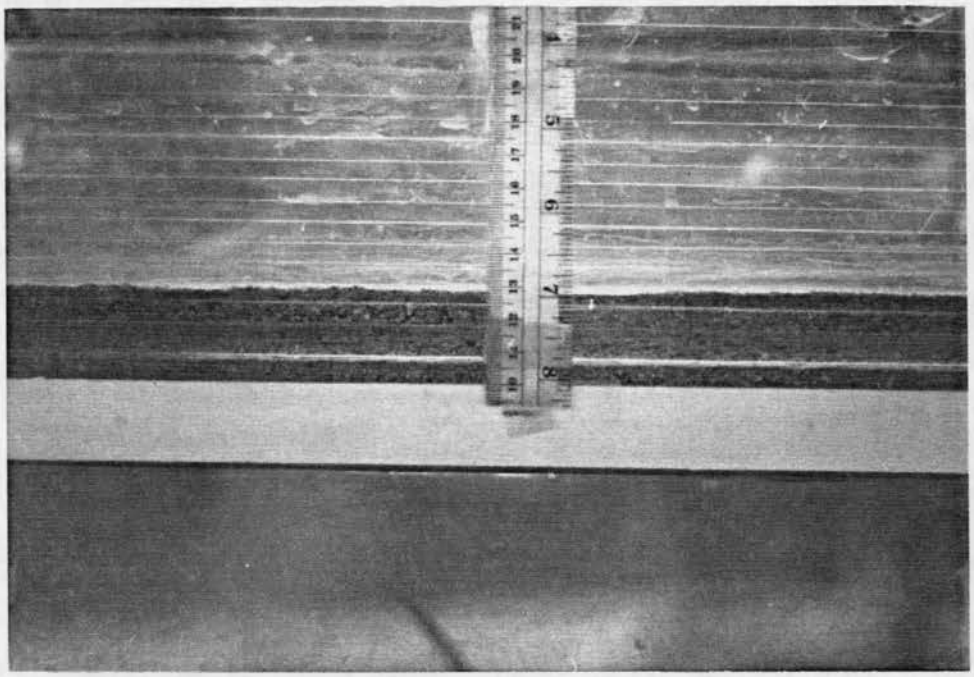

Picture 119. Clear layered deposits after drying

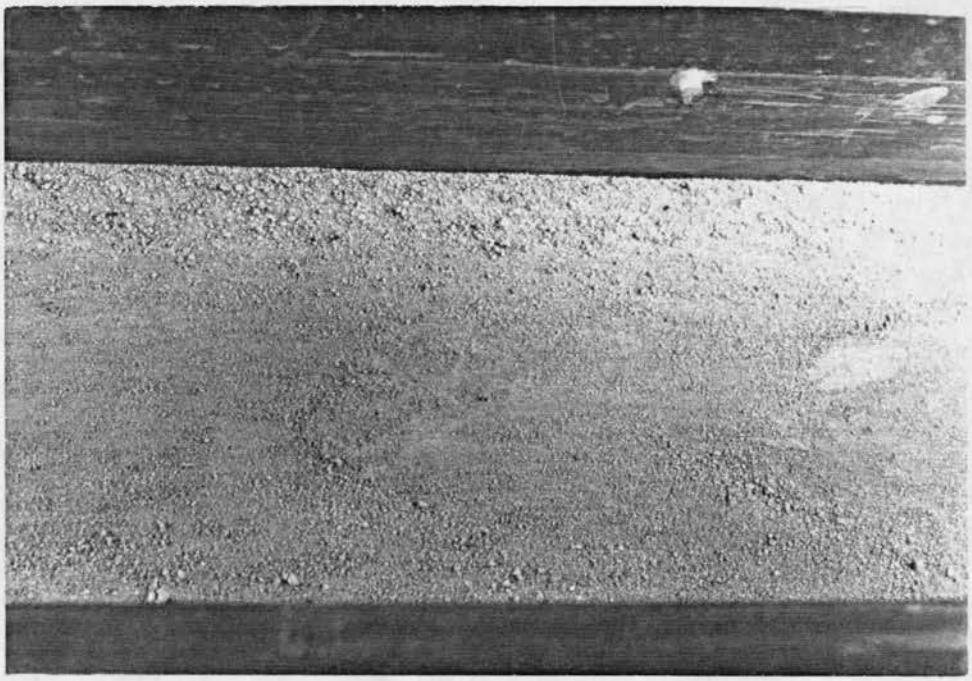

Picture 120. No vertical cracks on the top layer

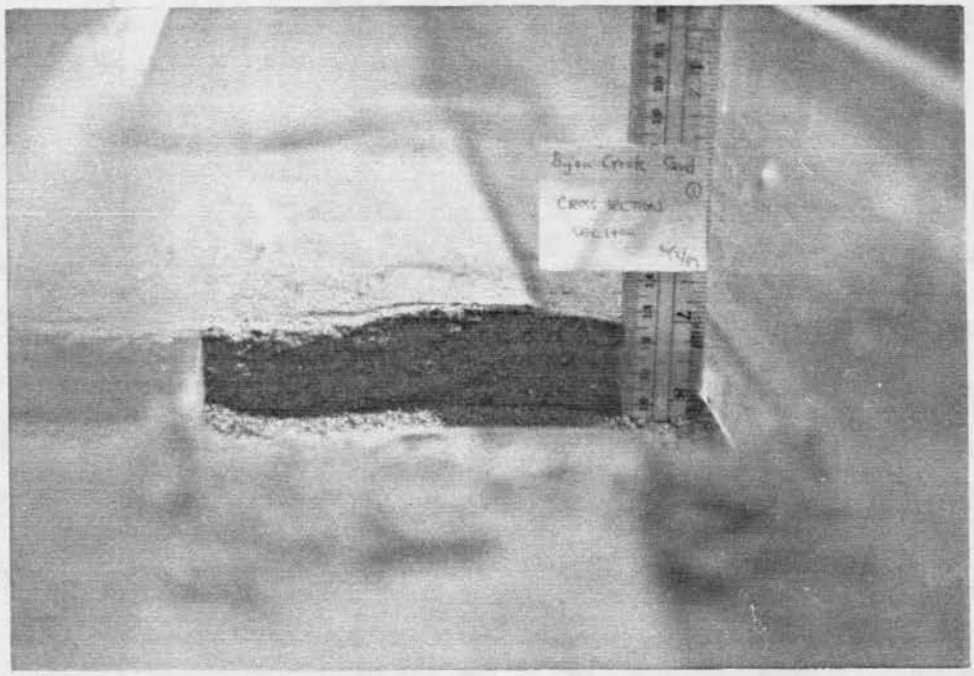

Picture 121. Cross-section at SEC.1+00

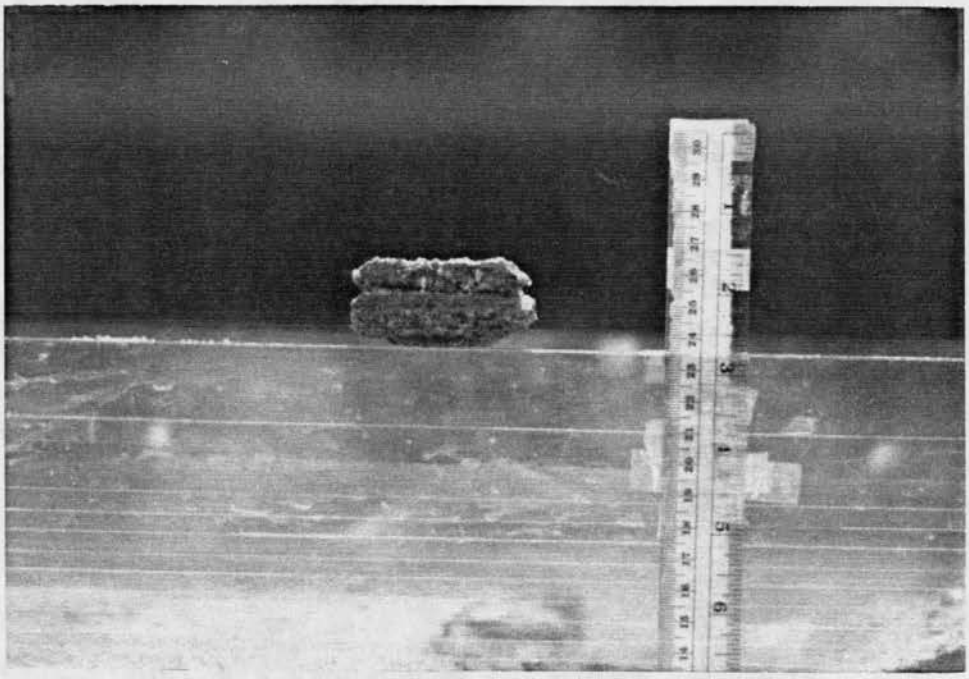

Picture 122. Separated layer can be peeled easily

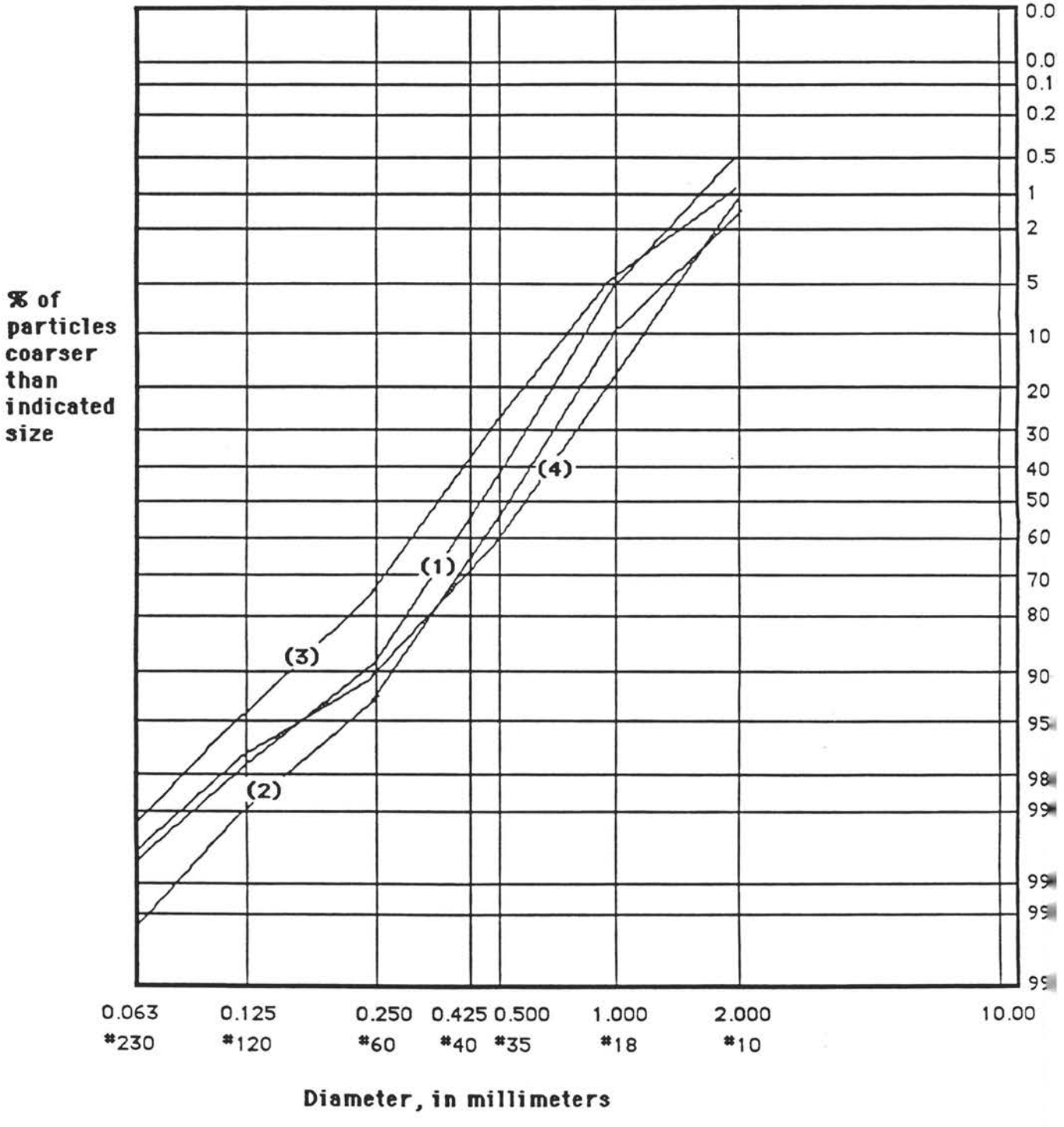

Figure 33. Particle size distribution for each stratum of run #1

5.4 Run #2

5.4.1 Experimental conditions and data summary

- Horizontal flume
- D_{50} = 0.75 mm
- One larger tailgate (4 cm high)
- Deposition is shown in sequence on three photographs:
  without gate - Picture 116
  first gate - Picture 117
  second gate - Picture 118
- The data for this run are summarized in Table 25 below.

Table 25. Data summary for run #2

Run #2: horizontal flume, D_{50} = 0.75 mm

Gate	Q cm^3/s	h cm	V_m cm/s	V_s cm/s	S_w	Shear $dyne/cm^2$	Fr	U^* cm/s	f	H-Lam mm	Delta mm
No	5272	4.07	83.56	85.45	0.016	41.84	1.32	6.47	0.048	9	0
First	5958	5.33	72.13	84.77	0.014	43.33	1.00	6.58	0.067	9	22

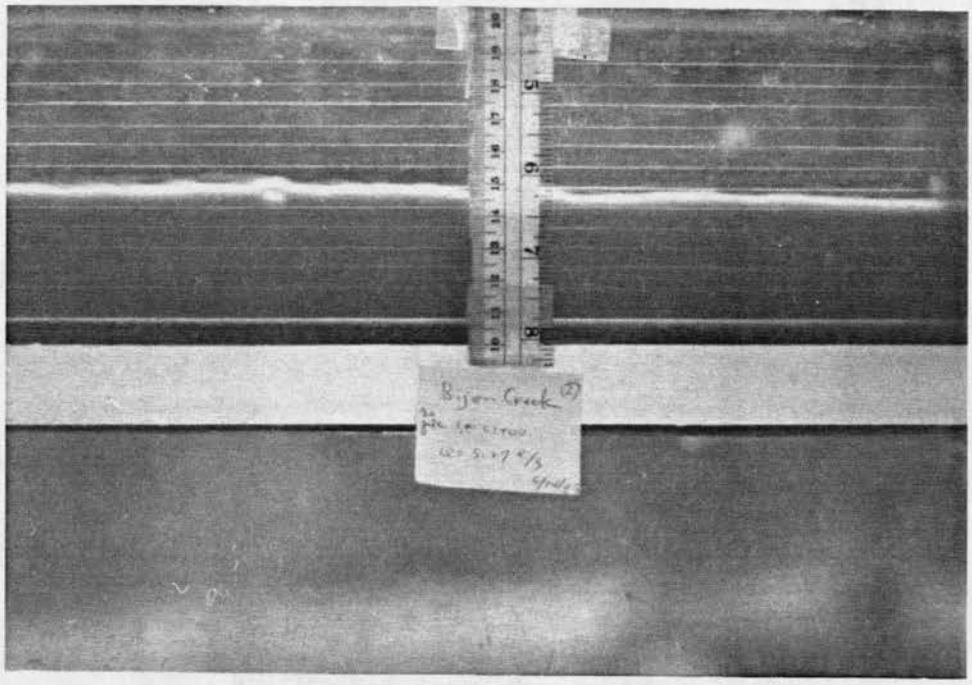

Picture 123. Deposition without gates (run #2)

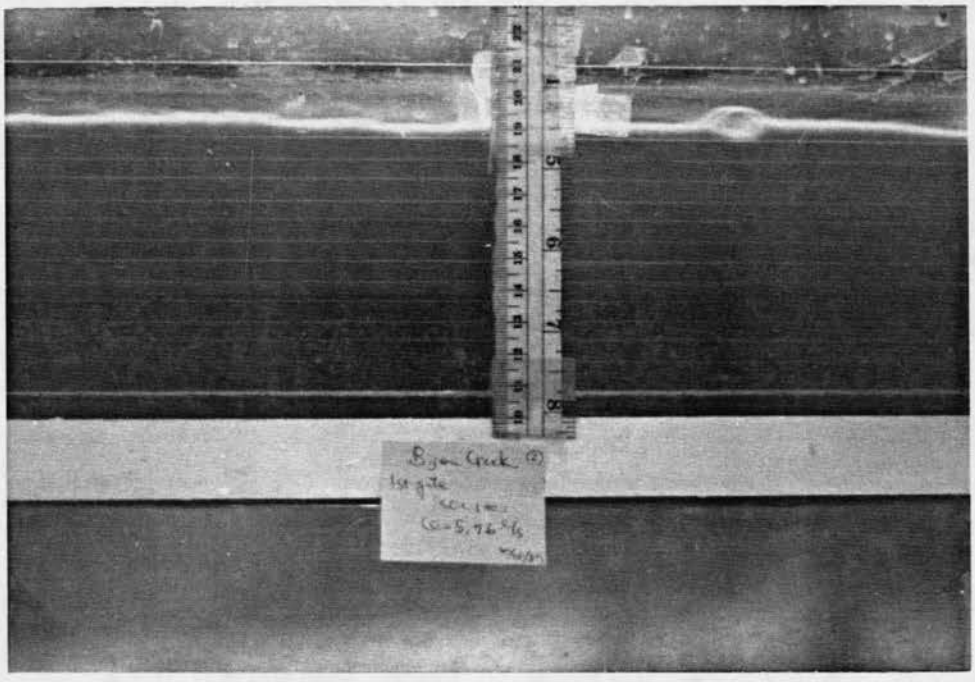

Picture 124. Deposition using one gate (4 cm high; run #2)

5.4.2 Results of run #2

Comparing the results with a larger gate versus those without a gate, we find that the larger tailgate only increases the thickness of the deltaic deposit, but not the horizontal lamination deposit. The horizontal lamination layer thicknesses are comparable during similar bed shear and shear velocity. The deposition of this run is sketched on Figure 34.

The layers of fine and coarse deposits are shown on Picture 125 after exposure to solar light for seven days. The surface layer still shows no vertical cracks (Picture 126). Horizontal cracks between each layer are seen after preparing a cross-sectional cut at SEC.1+00 (Picture 127). We can separate the layer of finer sands from the layer of coarser sands easily as shown on Picture 128.

The particle-size distribution curves of those three depositional layers are drawn on Figure 37. The medium grain size (D_{50}) and the grade scale classification for each layer are shown on Figure 34. The silt and clay content is less than 1 percent in the top layer as in run #1, which may explain why no vertical cracks are seen on the surface.

A series of low-relief sandwaves migrate under critical flow conditions (Froude number equal to unity) which is similar to the result reported by Julien and Chen (1989b).

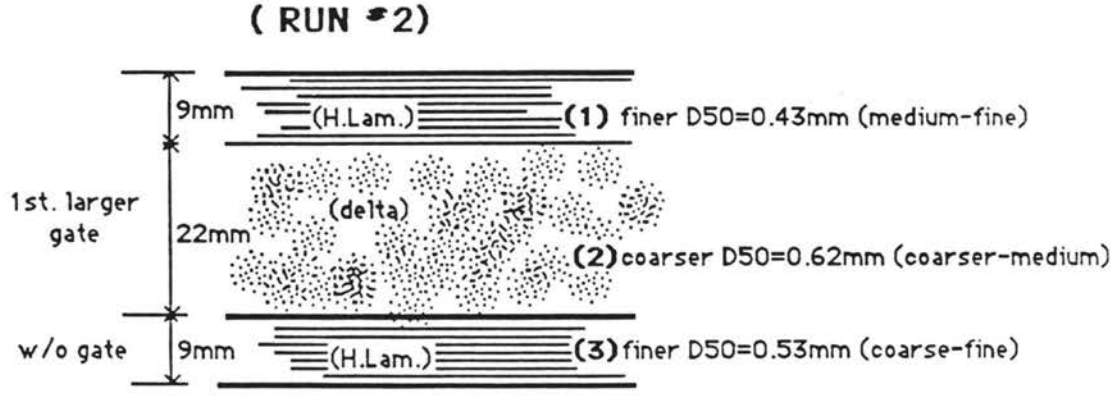

Figure 34. The deposition of Bijou Creek sand at SEC.1+00 (run #2)

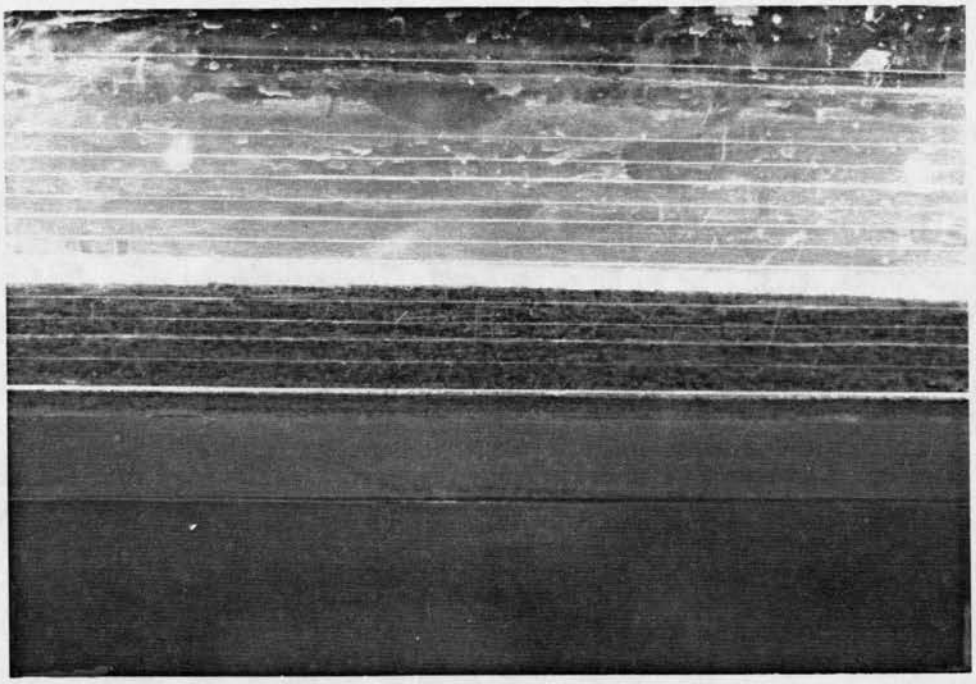

Picture 125. Clear layered deposits after drying

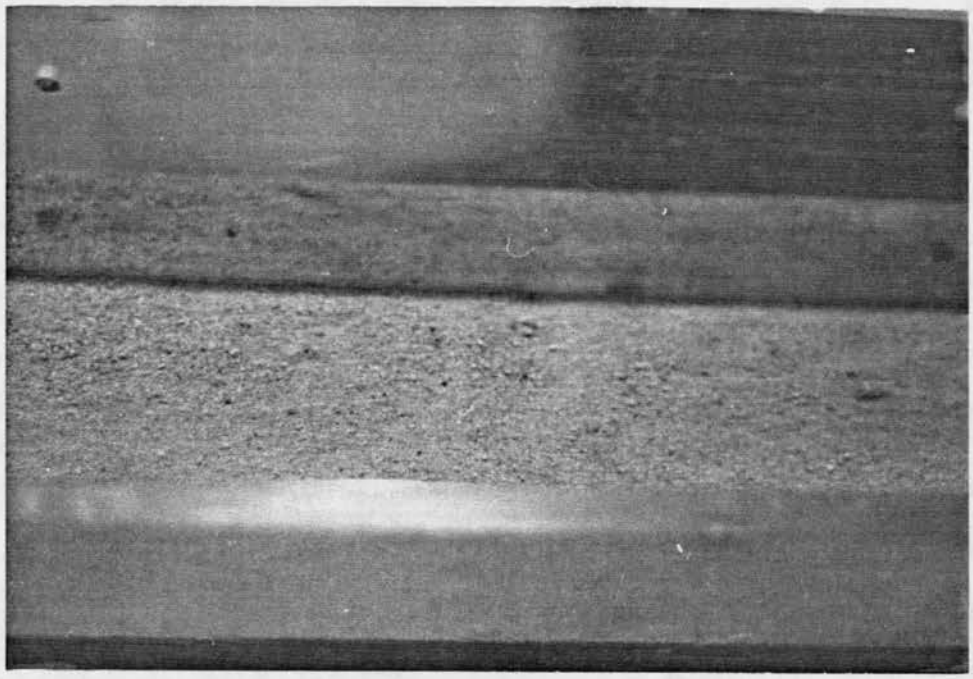

Picture 126. No vertical cracks on the top layer

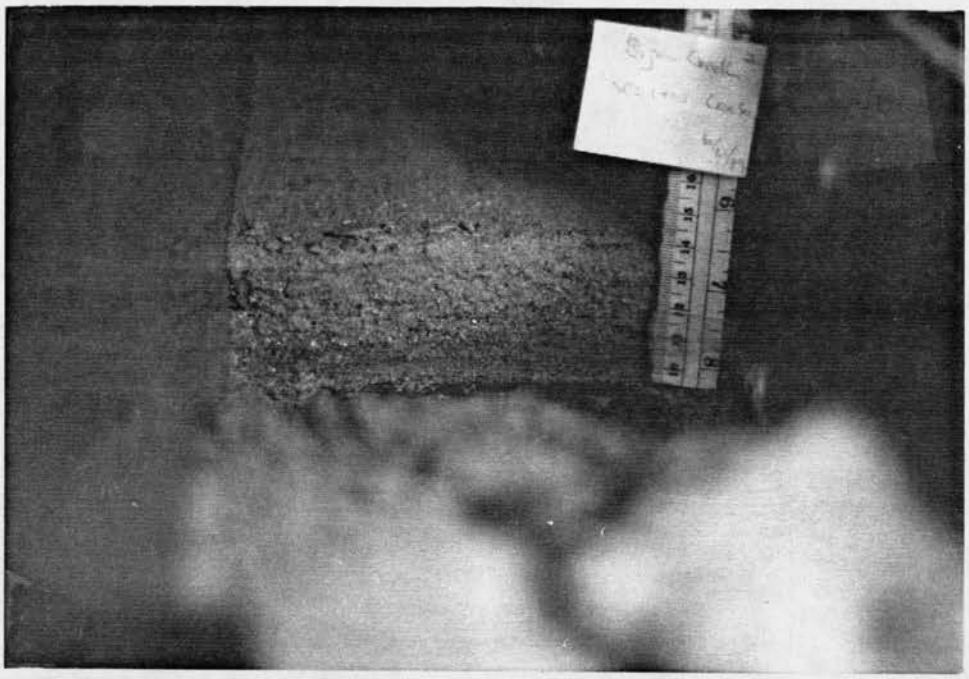

Picture 127. Cross-section at SEC.1+00
Horizontal cracks and separated layers are shown clearly.

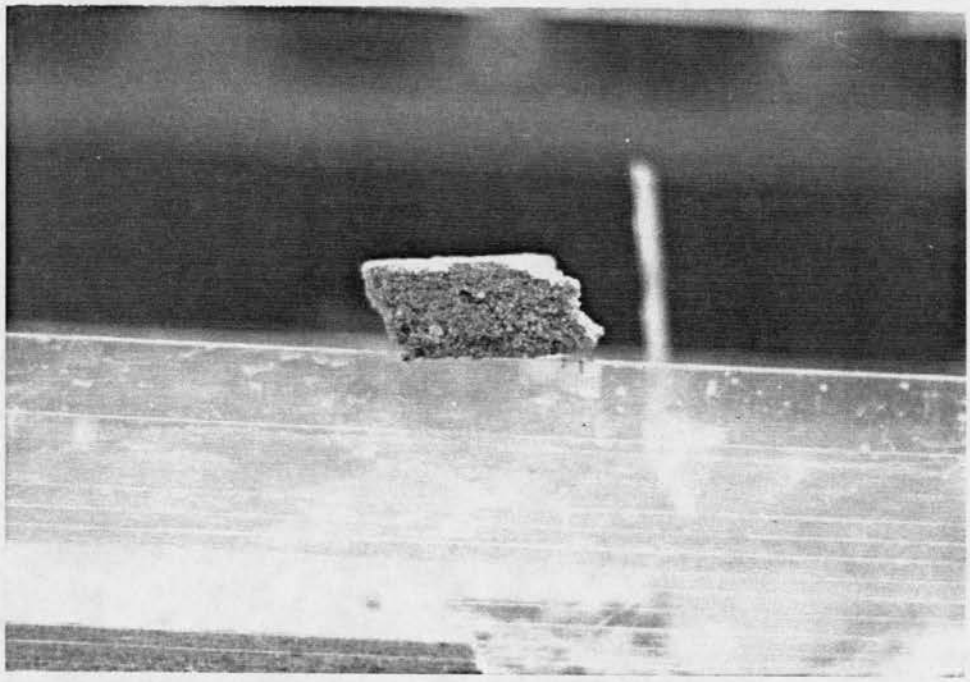

Picture 128. Separated layer can be peeled easily

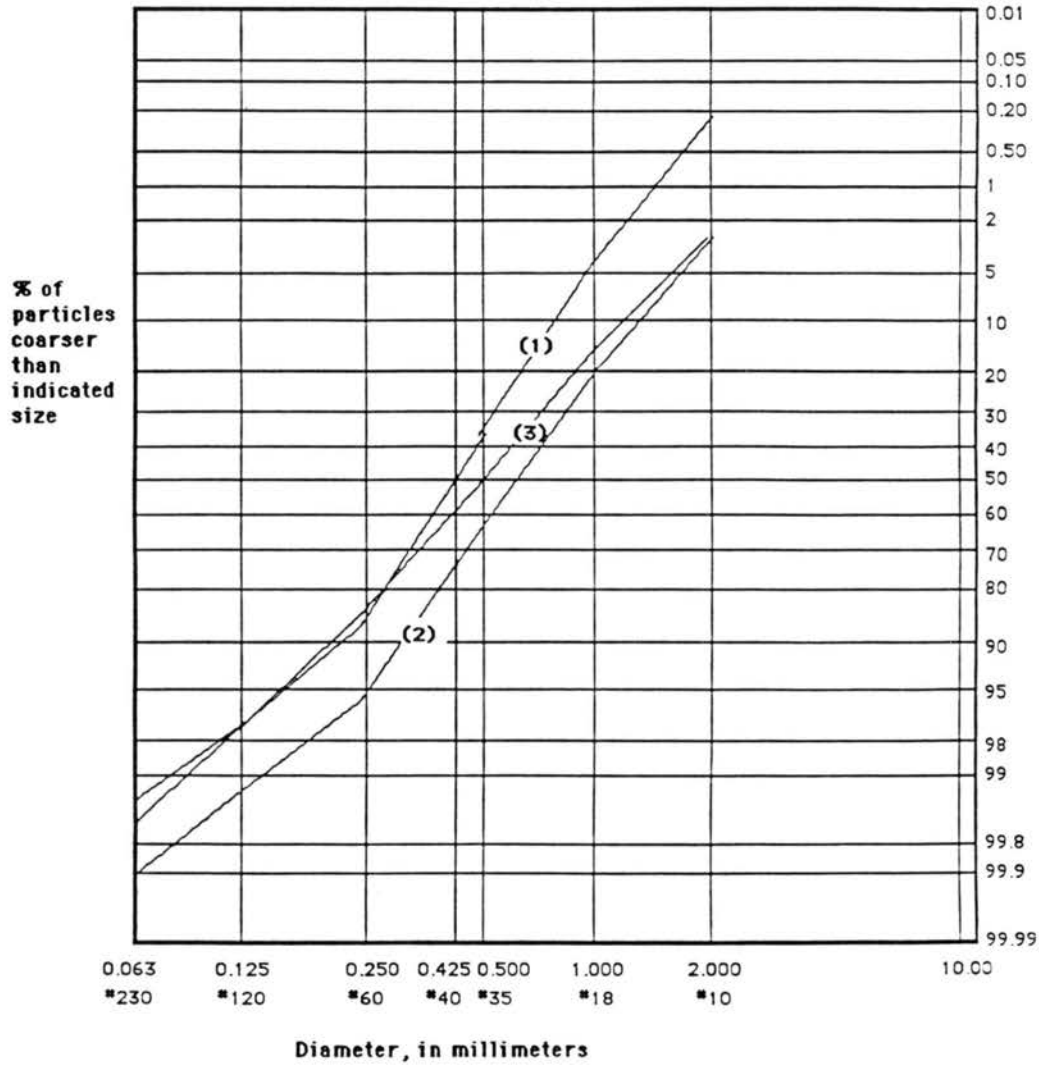

Figure 35. Particle size distribution for each stratum of run #2

VI. SUMMARY AND CONCLUSIONS

This study stems from the recent investigations of Berthault (1986, 1988). The primary objective of this experimental program is to examine the fundamental process of segregation of heterogeneous sediment mixtures under settling conditions, and under fluvial conditions of plane bed with sediment transport.

This study focuses on three primary aspects: 1) settling in air and water; 2) segregation under fluvial conditions; and 3) desiccation of alluvial deposits.

The facilities used in the Hydraulics Laboratory at the Engineering Research Center, Colorado State University, include a specifically designed settling column, a recirculating plexiglas flume, and a wide rectangular flume.

The square cylindrical plexiglas settling column allows the visualization of segregation of heterogeneous sand mixtures in air and water. Photographs are taken from the sides of the column and the characteristics of sorting of various mixtures with different densities, sizes and shapes are documented.

The recirculating plexiglass flume has been particularly designed for the analysis of lamination , stratification and desiccation processes under a wide variety of flow conditions. The flume recirculates both water and sediment in order to provide a constant supply of sediments under steady flow conditions during the course of each experiment. The slope of the channel is determined prior to each run in order to study the thickness of laminae and the angle of laminated deposits with the slope of the flume bed.

The wide rectangular flume allows the study of lamination processes under wide flow conditions not constrained by the wall effects of narrow flumes. This facility provides additional insight for processes that occurred under field conditions.

A key feature in this investigation is the use of sand mixtures with grains of different colors. Mixtures of natural black and white sediment particles of different sediment size, shape and specific gravity ensure a better visualization of the laminae besides providing an assessment of the distribution of different sediment particles.

6.1 Sedimentation in a vertical cylinder

Sedimentation experiments of heterogranular sand mixtures in air and still water have been conducted in a vertical square cylinder. With these experiments the lamination of heterogranular mixtures composed of sediments of different size, density, and shape is investigated and documented. The following conclusions can be obtained from this study.

1. Laminae can be observed under the following conditions: (1) sand mixtures of the same density but different sediment size; (2) sand mixtures of the same size but different density; or (3) sand mixtures of different density and different sediment size.

2. Laminae can be obtained both in air and water. Segregation of heterogeneous sand mixtures is the primary cause to lamination. In air, splashing of particles when they impact the surface of deposit becomes stronger as the mixture gets coarser due to higher fall velocity. However, splashing does not occur in water. In water, the least fluid turbulence created by settling of particles should be maintained. As the fall velocity of coarser particles increases such that turbulence created by the settling causes suspension of finer particles, the deposition of the mixtures becomes more uniform and no laminae can be found in the deposit. Under this circumstance, landsliding and rolling of one type of particles over the other is generally not observed.

3. Lamination is mainly caused by landsliding and the rolling of one particle over the other during sedimentation process. While the occurrence of landsliding and segregation of particles requires sufficient space, lamination would not be obtained if insufficient distance exists between the center and the walls of the cylinder. In the runs with inclined column the cylinder does not stand straight up, but is inclined at about 2-5°. These experiments show that clearer lamination is obtained at the section farther from the impact point. The thickness of laminae, however, is found not to vary with the inclination angle. On the other hand, for those runs without enough spacing, no laminae is observed. Coarser mixtures generally create splashing of particles when they impact the surface of deposit on the bottom of the cylinder, due to the high fall velocity of the particles. And this splashing of particles causes the mixing of particles around the center of the cylinder, lamination is not clearly observed within a short distance.

4. The shape of the particles in the mixture is believed to affect the lamination process. The densities of ERC #1 and the limestone #1 are about the same, but their mixing with black sand (B3060) and coal #1 gives different results. Mixtures 2 and 3 produce clear lamination, while mixtures 5 and 6 produce no lamination. Another example is from comparing mixture #1 and #10. The densities of limestone #1, B2040, and ERC #3 are about the same in these two

mixtures. The size difference of B2040 and ERC #3 in mixture #1 cannot produce lamination in either air or water, however mixture #10 can produce lamination in water although not in air. These two mixtures both produce splashing in air and landsliding in water, but, as we mentioned before, there is an obvious segregation of limestone #1 from B2040 during the landsliding in run #20 while such phenomena is not observed in run #21. This could be caused by the difference in density rather than the size. From laboratory observations, it is found that the shape of ERC #3 is more angular while the shape of limestone #1 is more rounded. However, this conclusion can only be confirmed from further experiments.

5. Heavier and coarser materials have the tendency to push lighter and finer sediment particles away from the center of the deposit. This makes it more difficult for the mixtures to form laminae. However, this type of mixture tends to produce clearer laminae in water if sedimentation is not continuous (see mixture 4).

6.2 Deposits in a narrow laboratory flume

Laboratory experiments have been conducted on the process of horizontal lamination under flat bed conditions in a narrow recirculating flume. A primary feature of the experimental program is the use of two different colors to separate the fines from the coarse sand particles. With these black and white sand mixtures, the laminae can be easily observed and documented. The horizontal lamination process has been scrutinized by analyzing four conditions of discharge for each plane bed condition. Two different mixtures are considered and the influence of tailgate size can also be determined from one run. Experiments were also conducted under various slopes including horizontal, adverse and positive slopes. A total of five runs and 18 steps is documented with measurements of discharge, flow depth, average velocity, surface velocity, water surface slope, bed shear stress, Froude number, shear velocity, resistance parameter and thickness of the delta and horizontal laminae deposits.

The results of the experimental program have been detailed, and the primary conclusions can be summarized as:

1. The thickness of the deposit of horizontal laminae increases with flow velocity. These results confirm those of Berthault (1988) taken at much lower velocity.

2. The thickness of the deposit of horizontal laminae increases with the gradation of the sediment mixtures. This result also corroborates the previous findings of Berthault under tranquil flow conditions.

3. The thickness of the delta increases with the size of the tailgate used for downstream control. The thickness of the layer of horizontal laminae remains unchanged regardless of tailwater conditions.

4. The observations of the SM-2 experiments showed that the coarser particles kept rolling on a deposit of finer particles. The most intriguing phenomenon relates to the gradual thickening of the deposits of finer particles while the coarser particles keep rolling on the surface. This phenomenon certainly contradicts any prediction from either the Shields diagram, the critical velocity criterion, or the equal mobility concept.

5. The experiments with adverse slope SM-2B indicate that the laminae do not necessarily remain parallel to the flume bed slope. Experiment SM-2C also demonstrates that they are not necessarily horizontal either. It may be more appropriate to refer to parallel lamination rather than horizontal lamination.

6.3 Deposits in a wide laboratory flume

Horizontal laminae can be reproduced in a large flume as well as in a small flume. The results show very good agreement with the previous findings of Julien and Chen (1989b), and Berthault (1988) from small flume experiment. Although we cannot conclude from these two experiments that the thickness of the laminae increases with flow velocity, the observations showed that the coarser particles (black) kept rolling on a deposit of finer particles.

An important observation is that the black sand grains move at a lower shear stress than the white grains. Considering that the black grains have larger diameter and higher density than the white grains, this contradicts the Shields diagram. It should be pointed out here that further experiments ought to be carried out in order to substantiate this intriguing observation. It must be kept in mind, however, that the observation of Julien and Chen (1989b), and the video tape of the experiment in the small flume lead to the same conclusive statement.

6.4 Desiccation of Bijou Creek sands

A primary feature of the experimental program is the use of natural sand from Bijou Creek, Colorado and investigate the features of the major deposits observed during the Bijou Creek flood in June, 1965. Laboratory experiments in a circulating flume have been conducted on the process of horizontal deposition under flat bed condition with sediment transport.

The deposition of cross-bedding under flow regime as well as horizontal laminae under upper flow regime observed in the investigation of the Bijou Creek flood by McKee et al. (1967) was reproduced by the experiment of Julien and Chen (1989a). The results of this experiment should correspond to the field observations as well.

The results of the experimental program detailed in this report can be summarized as:

1. The thickness of the horizontal lamination layer should depend on bed shear and shear velocity as much as flow velocity mentioned in the report of Julien and Chen (1989b). Further experiments should clarify which of these variables is dominant.

2. The thickness of the delta increases with the size of tailgate. The thickness of the layer of horizontal laminae remains unchanged regardless of tailwater condition.

3. The low-relief sandwaves can still be seen in the formation of horizontal lamination under critical flow condition.

4. The small content of silt and clay in the top layer of the deposits may explain why no vertical cracks have been observed at the surface of the deposits after seven days of drying under solar lamps.

5. Most important, the horizontal cracks and the consolidation of each layer makes the finer and coarser depositional layers separate easily.

6.5 Discussion on the Mechanism of Sediment Lamination

In the flume experiments with running water, the horizontal lamination of heterogranular mixtures has been explained by many theories, such as that of Paola et al. (1989). They explained that lamination resulted from the superposition of two processes: 1) high frequency erosion and deposition due to turbulence; and 2) migration of low-amplitude bed forms that is neither upper-regime nor lower-regime solely. From experiments in still and running water in vertical cylinder, Berthault (1986, 1988) concluded that a clear segregation of particles of the same size within the deposited mixture is the genesis of the lamination, and this segregation resulted from spontaneous periodic and continuous grading process, which took place immediately following the deposit of the heterogranular mixture. The thickness of formed laminae increased as the difference between the size of particles becomes greater in still water, and increased with flow velocity of running water. The present experiments surely have support to this hypothesis. From these experiments, either in air or in still water, laminae formed only

under the circumstance that landsliding occurs as sedimentation progresses. Needless to say, this landsliding creates an ideal condition for grading or sorting of sediment particles of different size, density, and shape.

Landsliding (grading or sorting of mixture) is related to the cone formed by the deposit which is in turn apparently affected by the size of particles in the mixture. For fine particles, the fall velocity in air or in water is small, little splashing of particles occurs when they impact the surface of deposits. This type of sedimentation created a well-formed cone at the center of the cylinder. As the particle size increases, the size of the cylinder probably should increase to compensate for the increase of splashing distance of coarser particles if landsliding is to occur.

Density differences between mixing particles also play an important role in the formation of laminae. Generally, the lighter particles in the mixture are pushed away from the point of impact towards the wall of the cylinder while heavier particles stay in the center. Again, the formation of laminae depends on whether landsliding occurs or not. In cases where landsliding and segregation of particles occurs, lamination is observed. The lamination of this type of mixture is still quite uniform, although the layers are apparently thicker (see Pictures 27 and 28). Since the fall velocity of lighter particles is much smaller than that of heavier particles in water, any discontinuity of sediment supply during the process will cause the formation of a layer of lighter material on top of the heavier materials, due to the longer suspension of lighter particles in the water. The thickness of this layer depends on the settling rate.

The shape of particles is assumed to influence the process of lamination, since the internal friction coefficients of different shaped particles are different. This is demonstrated by comparing mixtures 2 and 5 (run #2 and #6) where ERC #1 and limestone #1 have different shapes, while the other type of material is the same (B3060). Unfortunately, this hypothesis cannot be confirmed because the shape of particles in this experiment is not carefully measured. Further experiments should take this parameter under consideration.

A review of the hypotheses explaining the formation of laminae in Table 1 reveals that, of the two mechanisms most commonly cited (turbulence and migration of low relief bedforms), none seems fully satisfactory to explain our observations. It is clear from the experiments in air that turbulence, saltation, and burst and sweep cycles are not sufficient to explain lamination in a vertical cylinder. The statement becomes even stronger in the light of recent experiments by P. Habib (see Appendix I) whose experiments in vacuum showed the formation of laminae even when there is no surrounding fluid. In vacuum, turbulence effects are non existent and therefore one must reject the following explanations based on: velocity pulsations and fluctuations (Kuenen, 1953, 1957; Sanders, 1965; and Pettijohn, 1957, 1975); turbulent currents (Ksiazkiewicz,

1952; Unrug, 1959; and Wood and Smith, 1959); sorting action of turbulent vortices (Ten Haaf, 1956); laminae boundary layers (Hsü, 1959); small turbulent eddies (Bouma, 1962; and Lombard, 1963); pulsating sediment supply due to large scale eddies (Allen, 1964, 1984); and burst and sweep cycle (Bridge, 1978; Hesse and Chough, 1980; Bridge and Best, 1988; and Paola et al., 1989).

The authors are also suspicious about hypothesis requiring small amplitude bedforms for the formation of laminae. The "like-seeks-like" process proposed by Moss (1963) and Kuenen (1966) also involves interaction with the saltating carpet and such processes were not observed in our settling experiments. Bridge (1978) also severely criticized the "like-seeks-like" principle.

In summary, from our investigations, the most likely mechanism giving the segregation of heterogeneous sand mixtures can be explained as follows. Starting from a uniform mixture of coarse and fine particles sketched in Figure 36a, only the lateral motion of the mixture in any direction is necessary to induce the sorting of particles. Through lateral motion, the fine particles find their way through the interstices of the coarse particles and reach the bottom of the moving layer while the coarse particles start rolling on top of the fine particles (Figure 36b). After a certain time, the fine particles are found at the bottom of the moving layer while the coarse particles remain on top (Figure 36c). In order to obtain lamination, it is important that the fines be sufficiently small to fall between the interstices of the coarse particles, and also, the coarse particles must be able to roll on top of the small ones. A set of complementary experiments have been detailed in Appendix B in order to experimentally confirm this process. It is shown on Pictures B-1 through B-24 that the segregation of particles in heterogeneous mixtures can be obtained without turbulence and without low amplitude bedforms.

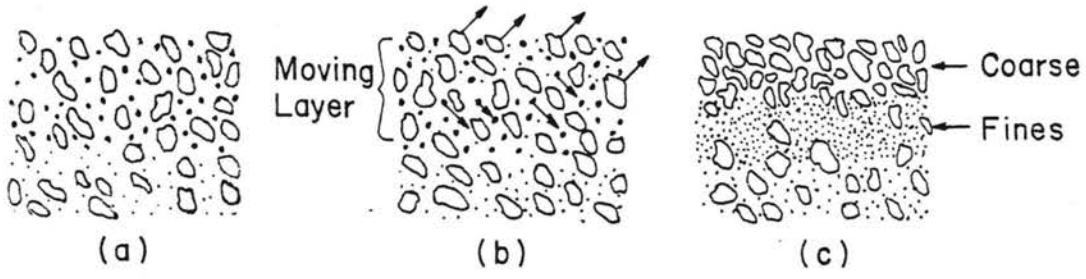

Figure 36. Proposed explanation of the lamination process

The problem of upward coarsening versus upward fining is probably more a matter of where the reference level is taken (i.e. the base of fine particles or the base of coarse particles).

This process becomes more complex when particles of different densities and shapes are considered. In general, very light material has a tendency to remain in suspension for a longer period of time, whereas the shape of particles may be of secondary importance.

It is acknowledged that other processes, such as turbulence, burst and sweep cycles, and interaction between suspended load and bed load can further complicate the lamination process, but, lamination is found to be essentially the result of mechanical interaction between particles of different size, shape and density.

6.6 Overall Conclusions

It can be concluded that the two primary processes described in the recent literature, to explain lamination namely the turbulent burst and sweep cycles, and the migration of low amplitude bedforms, are challenged by our experiments. Lamination is observed in air, as well as in water, where turbulence is almost nonexistent.

Moreover, the fact that lamination becomes clearer at a larger distance from the center of the core contradicts the assumption based on turbulence because turbulence is almost nonexistent at the edge of the settling column. The second process of migration of small amplitude bedforms has been observed in some of our experiments in the small flume. This process, however, does not explain everything. Some cases of lamination cannot be explained by the small amplitude bedwave migration such as the case of settling in the vertical column.

From all these experiments, the best possible explanation of the lamination process involves the motion of a layer of heterogeneous sediments. Through lateral movement, the finer particles fall within the interstices of the rolling coarser particles. The coarse particles then roll on top of the fines and microscale separation of the particles is then obtained. This natural segregation only requires the lateral motion of a sediment mixture. Small amplitude bedforms can cause lamination though it is not a necessary condition. For instance, a thin layer of sediments could be in lateral motion without any bedform configuration, and be conducive to the formation of laminae, as experimentally verified in Appendix B.

Our experiments also clearly demonstrate the formation of stratified deposits in which, under steady flow conditions and a continuous supply of sediments of different sizes, the deposition process involves the formation of a delta comprised of coarse particles between two layers of laminated deposits of finer particles. This process has been repeatedly verified in the

laboratory. It is important to understand the time sequence of the formation of these deposits which demonstrates that laminated deposits progress vertically upward while the deltaic formation process laterally in the downstream direction. The resulting stratified deposits are quite similar to those reported by McKee et al. (1967) on Bijou Creek.

Finally, the desiccation experiments indicate that after drying, the Bijou Creek sand deposits in laboratory flumes, a fracturation of the crusty deposit is possible along horizontal planes corresponding to the changes in sediment structure. For instances the planes between coarse and fine particles are particularly conducive to horizontal fractures. On the other hand, no vertical cracks were observed in our experiments, which may be explained by the low content in clay particles of the Bijou Creek sand.

In summary, these experiments demonstrate the feasibility of analyzing lamination processes, stratification processes, and fracturation processes in the laboratory. Our experiments were carried out under conditions representative of natural field environments and the results may explain natural processes observed in geomorphological and geological formations.

VII. BIBLIOGRAPHY

Allen, J.R.L., 1963. "The classification of cross stratified units with notes on their origin," Sedimentology, V. 2, pp. 93-114.

Allen, J.R.L., 1964. "Primary current lineation in the Lower Old Red Sandstone (Devonian), Anglo-Welsh basin, "Sedimentology, V. 3, pp. 89-108.

Allen J.R.L., 1970. Physical Processes of Sedimentation, Am. Elsevier Publ. Co., New York, 248 p.

Allen, J.R.L., 1971. "Some techniques in experimental sedimentology," J. Sed. Petrol., V. 41, pp. 695-702.

Allen, J.R.L., 1971. "A theoretical and experimental study of climbing-ripple cross-lamination with a field application to Uppsala Esker," Geogr. Annn., V. 53A, pp. 157-187.

Allen, J.R.L., 1980. "Sandwaves: a model or origin and internal structure", Sed. Geol., V. 26, pp. 281-328.

Allen, J.R.L., 1982. Sedimentary Structures--Their Character & Physical Basis, V. 1, Elsevier Sci. Publ. Co., New York, 593 p.

Allen, J.R.L., 1984. "Parallel lamination developed from upper-stage plane bed: a model based on the large coherent structures of turbulent boundary layer," Sediment. Geol., V. 39, pp. 227-242.

Allen, J.R.L., 1985. "Loose-boundary hydraulics and fluid mechanics: selected advances since 1961," in (P.J. Brenchley etc., ed.), Sedimentology-Recent Development and Applied Aspecs, Blackwell Publs., pp. 7-28.

A.S.C.E., 1975. Sedimentation Engineering, A.S.C.E. manual and report on Engineering Practice No. 54, New York, 745 p.

Ashley, G.M., Southard, J.B. & Boothroyd, J.C., 1982. "Deposition of climbing-ripple beds: a flume simulation," Sedimentology, V. 29, pp. 67-79.

Berthault, G., 1986. "Sedimentology-experiments on lamination of sediments," C.R. Acad. Sci. Paris, t303, Serie II. No. 17, pp. 1569-1574.

Berthault, G., 1988. "Sedimentation of heterogranular mixture--experimental lamination in still and running water," C.R. Acad. Sci. Paris, t306, Serie II, pp. 717-724.

Bouma, A.H., 1962. Sedimentology of Some Flysch Deposits; a Graphic Approach to Facies Interpretation. Elsevier, Amsterdam, 168p.

Bridge, J.S., 1978. "Origin of horizontal lamination under turbulent boundary layer," Sediment. Geol., V., 20, pp. 1-16.

Bridge, J.S., 1987. "Horizontal laminae formed under upper flow regime plane bed conditions: a discussion," J. Geol., V. 95, 281 p.

Bridge, J.S. & J.L. Best, 1988. "Flow, sediment transport and bedform dynamics over the transition from dunes to upper-stage planebeds: implications for the formation of planar laminae," Sedimentology, V. 35, pp. 753-763.

Briggs, L.I. & G. V. Middleton, 1965. "Hydromechanical principles of sediment structure formation," in (G.V. Middleton, ed.), Primary Sedimentary Structure and their Hydrodynamic Interpretation, Spec. Publs. Sco. Econ. Paleont. Miner., Tulsa, No. 12, pp. 5-16.

Brush, L.M., 1965. "Experimental work on primary sedimentary structures," in (G.V. Middleton, ed.), Primary Sedimentary Structure and their Hydrodynamic Interpretation, Spec. Publs. Sco. Econ. Paleont. Miner., Tulsa, No. 12, pp. 17-24.

Cheel, R.J. & G.V. Middleton, 1986a. "Measurement of small scale laminae in sand-sized sediments," J. Sed. Petrol., V. 56, pp. 547-548.

Cheel, R.J. & G.V. Middleton, 1986b. "Horizontal laminae formed under upper flow regime plane bed conditions," J. Geol., V. 94, pp. 489-504.

Coleman, J.M. & S.M. Gagliano, 1965. "Sedimentary structures: Mississippi River deltaic plain," in Primary sedimentary structures and their hydrodynamic interpretation: Soc. Econ. Paleon. & Miner. Spec. Publ. 12, pp. 133-148.

Collins, J.D. & D.B. Thompson, 1982. Sedimentary Structures, George Allen & Unwin, London, 194 p.

Fairbridge, R.W. & J. Bourgeois, 1978. The Encyclopedia of Sedimentology, Dowden, Hutchinson & Ross, Inc., Pennsylvania, 901 p.

Frostick, L.E. & I. Reid, 1977. "The origin of horizontal laminae in ephemeral stream channel-fill," Sedimentology, V. 24, pp. 1-9.

Guy, H. P., D. B. Simons and E. V. Richardson, 1966. "Summary of Alluvial Channel Data from Flume Experiments: 1956-1961," U.S. Geological Survey, Prof. Paper 462-I, 96 p.

Harm, J.C. & R.E. Fahnestock, 1965. "Stratification, bed forms and flow phenomena (With an example from the Rio Grande)," in (G.V. Middleton, ed.), Primary Sedimentary Structure and their Hydrodynamic Interpretation, Spec. Publs. Sco. Econ. Paleont. Miner., Tulsa, No. 12, pp. 84-115.

Harm, J.C., Southard, J.B., Spearing, D.R. & R.G. Walker, 1975. Depositional Environments As Interpreted From Primary Sedimentary Structures & Stratification Sequences, Sco. Eco. Paleont. Miner., Short course No. 2 (April, 1975), Texas, 161 p.

Hesse, R. & S.K. Cough, 1980. "The Northwest Atlantic Mid-Ocean Channel of the Larador Sea: II. Deposition of parallel laminated levee muds from the viscous sublayer, " Sedimentology, V. 27, pp. 697-711.

Hjulstrom, F., 1935. "The Studies of the Morphological Activity of Rivers as Illustrated by the River Fyris," Bull. of the Geol. Inst., University of Upsda, pp. 292-327.

Hsu, K.J., 1959. "Flute- and groove-casts in the prealpine flysch, Switzerland," Am. J. Sci., V. 257, pp. 529-536.

Hunter, R.E., 1977. "Terminology of cross-stratified sedimentary layers and climbing-ripple structures", J. Sed. Petrol., V. 47, pp. 697-706.

Hunter, R.E., 1985. "Subaqueous sand-flow cross-strata," J. Sed. Petrol., V. 55, pp 886-894.

Jopling, A.V., 1965. "Laboratory study of the distribution of grain size in cross-bedded deposits," in (G.V. Middleton, ed.), Primary Sedimentary Structure and their Hydrodynamic Interpretation, Spec. Publs, Sco. Eco. Paleont. Miner., Tulsa, No. 12, pp. 53-65.

Jopling, A.V., 1967. "Origin of laminae deposited by the movement of ripples along a streambed: a laboratory study," J. Geol., V. 75, pp. 287-305.

Jopling, A.V. & R.G. Walker, 1968. "Morphology and origin of ripple-drift cross-lamination, with examples from the Pleistocene of Massachusetts," J. Sed. Petrol., V. 38, pp. 971-984.

Julien, P.Y., 1987. "Erosion and Sedimentation," teaching guide for CE-716, Erosion and Sedimentation. Engineering Research Center, Colorado State University.

Julien, P.Y. & Y.Q. Lan, 1989. "Experimental Formation of Alluvial Channel in Wide Rectangular Flume," Civil Engineering Report, CER89-90PYJ-YQL2, Department of Civil Engineering, Colorado State University, Fort Collins, CO, 29 p.

Julien, P.Y. & Y.Q. Lan, 1990. "Sedimentation of Heterogranular Mixtures in a Vertical Cylinder," Civil Engineering Report, CER89-90PYJ-YQL13, Department of Civil Engineering, Colorado State University, Fort Collins, CO, 48 p.

Julien, P.Y. & Y.C. Chen, 1989a. "A short report about the experiment of lamination in a small flume," Unpublished Report, Colorado State University.

Julien, P.Y. & Y.C. Chen, 1989b. "Experimental study of horizontal lamination in a recirculating flume," Civil Engineering Report CER88-89PYJ-YCC14, Colorado State University, Fort Collins, CO, 63 p.

Julien, P.Y. & Y.C. Chen, 1989. "Experimental Study of the Deposition and Drying of Bijou Creek Sand in a Recirculating Flume," Civil Engineering Report, CER89-90PYJ-YCC4, Colorado State University, Fort Collins, CO, 35 p.

Ksiazkiewicz, M., 1952. "Graded and laminated bedding in the Carpathian flysch," Ann. Soc. Geol. Polgne., V. 22, pp. 399-499.

Kuenen, Ph.H., 1953. "Significant features of graded bedding, "Bull. Am. Assoc. Pet. Geol., V. 74, pp. 523-545.

Kuenen, Ph.H., 1957. "Sole markings of graded greywacke beds," J. Geol., V. 65, pp. 231-258.

Kuenen, Ph.H., 1966. "Experimental turbidite lamination in a circular flume," J. Geol., V. 74, pp. 523-545.

Kuenen, Ph.H. & H. W. Menard, 1952. "Turbidity currents, graded and non-graded deposits," J. Sed. Petrol., V. 22, pp. 86-96.

Lane, E.W., 1947. "Report of the subcommittee on sediment terminology," Transactions, Am. Geop. Union, V. 28 No. 6, Washington, D.C., pp. 936-938.

Langford, R. & B. Bracken, 1987. "Medano Creek, Colorado, a model for upper flow regime fluvial deposition," J. Sed. Petrol., V. 57, pp. 863-870.

Lombard, A., 1963. "Laminities: a structure of flysch-type sediments," J. Sed. Petrol., V. 33, pp. 14-22.

McBride, E.F., R. G. Shepherd & R.A. Grawley, 1975. "Origin of parallel, near-horizontal laminae by migration of bed forms in a small flume," J. Sed. Petrol., V. 45, pp. 132-139.

McKee, E.D., 1965. "Experiments on ripple lamination," in (G.V. Middleton, ed.), Primary Sedimentary Structures and their Hydrodynamic Interpretation, Spec. Publs. Sco. Econ. Plaeton. Miner., Tulsa, No. 12, pp. 66-83.

McKee, E.D., Crosby, E.J. & H.L. Berryhill, Jr., 1967. "Flood deposits, Bijou Creek, Colorado, June, 1965," J. Sed. Petrol., V. 37, pp. 829-851.

McLaughlin, T.G., 1946. "Geology and groundwater resources of parts of Lincoln, Elbert, and El Paso counties, Colorado," Colorado Water Conser. Board Bull., 1, 139 p.

Middleton, G.V. ed., 1965. Primary Sedimentary Structures and their Hydrodynamic Interpretation, Spec. Publs. Sco. Econ. Plaeton. Miner., Tulsa, No. 12, 265 p.

Middleton, G.V., 1965. "Antidune cross-bedding in a large flume," J. Sed. Petrol., V. 35, pp. 922-927.

Moss, A.J., 1962. "The physical nature of common sandy and pebbly deposits, part I," Am. Jour. of Sci., V. 260, pp. 337-373.

Moss, A.J., 1963. "The physical nature of common sandy and pebbly deposits, part II," Am. Jour. Sci., V. 261, pp. 197-243.

Otto, G.H., 1938. "The sedimentation unit and its use in field sampling," J. Geol., V. 46, pp. 569-582.

Paola, C., S.M. Wiele & M.A. Reinhart, 1989. "Upper-regime parallel lamination as a result of turbulent sediment transport and low-amplitude bed forms," Sedimentology, V. 36, pp. 47-59.

Pettijohn, F.J., 1957. Sedimentary Rocks, Harper and Row, New York, N.Y., 2nd ed., 718 p.

Pettijohn, F.J., 1975. Sedimentary Rocks, Harper and Row, New York, N.Y., 3rd ed., 628 p.

Pettijohn, F.J., Potter, P.E. & R. Siever, 1987. Sand and Sandstone, Springer-Verlag, New York, 553 p.

Potter, P.E. & F.J. Pettijohn, 1977. Paleocurrents and Basin Analysis, 2nd ed., Springer-Verlag, Berlin, 296 p.

Robin, D.M. & R.E. Hunter, 1982. "Bedform climbing in theory and nature," Sedimentology, V. 29, pp. 121-138.

Robertson, J.A. & C.T. Crowe, 1985. "Engineering Fluid Mechanics," Houghton Mifflin Co.

Sanders, J.E., 1965. "Primary sedimentary structures formed by turbidity currents and related re-sedimentation mechanisms, " In: G.V. Middleton, ed., Primary Sedimentary Structures and their Hydrodynamic Interpretation, Soc. Econ. Paleontol. Mineral. Spec. Publ., V. 12, pp. 192-329.

Selley, R.C., 1988. Applied Sedimentology, Academic Press Limited, San Diego, California, 446 p.

Shields, A., 1936. "Anwendung de Ahnlichkeitsmechanik und der Turbulenzforschung auf die Geschiebebewegung," Mitteilungen der Preussischen Versuchsanstalt fur Wasserbau und Schiffbau, Berlin, Germany, translated to English by W.P. Ott and J.C. van Uchelen, California Institute of Technology, Pasadena, CA.

Smith, N.D., 1971. "Pseudo-planar stratification produced by very low amplitude sandwave," J. Sed. Petrol., V. 41, pp. 69-73.

Ten Haaf, E., 1956. "Significance of convolute lamination," Geol. Mijnbouw, V. 18, pp. 188-194.

Unrug, R., 1959. "On the sedimentation of the Lgota beds, Biesle area, Western Carpathians," Rocz. Pol. Tow. Geol., V. 29, pp. 218-223.

Walker, R.G., 1965. "The origin and significance of the internal sedimentary structures of turbidities," Proc. Yorksh. Geol. Soc., V. 35, pp. 1-32.

Williams, G.D., 1970. "Flume width & water depth effects in sediment transport experiment," Prof. Pap. U.S. Geol. Surv., 562-H, 37 p.

Wood. A. & A.J. Smith, 1959. "Sedimentation and sedimentary history of the Aberystwyth Grits (Upper Llandoverian)," Q. J. Geol. Soc. London, V. 114, pp. 163-195.

Wright, M.D., 1959. "The formation of cross-bedding by a meandering or braided stream," J. Sed. Petrol., V. 29, pp. 610-615.

APPENDIX A

Experiments carried out at the Ecole Polytechnique in Paris by M.P. Habib on segregation of mixtures under partial vacuum.

...YTECHNIQUE - ÉCOLE NATIONALE SUPÉRIEURE DES MINES DE PARIS - ÉCOLE NATIONALE DES PONTS ET CHAUSS

LABORATOIRE DE

MÉCANIQUE DES SOLIDES

UNITÉ ASSOCIÉE AU C. N. R. S.

Palaiseau, le 25 Septembre 1989

École polytechnique
91128 Palaiseau cedex
téléphone : (1) 69.41.82.00
télex : Écolex 601596 F
LB/PH2509A.L89

Monsieur Guy BERTHAULT X45
28 Boulevard Thiers
78250 MEULAN

Mon cher Camarade,

Je n'ai pas grand chose à te donner comme résultat bien que j'ai fait quelques essais.

1) J'ai refait l'expérience de déversement à sec du mélange de poudres et j'ai reproduit la figure 1 de ta note au CR à l'ACSC de 1986. Il s'agit en fait d'une simple ségrégation : lorsqu'on déverse des grains de tailles différentes, il se produit un granoclassement, les gros dévallant la pente alors que les petits s'arrêtent. Je ne sais pas s'il existe une bonne explication de ce phénomène (qui est désagréable par exemple quand on déverse du béton frais). Il est d'usage de dire qu'il n'y a pas ségrégation quand les petits grains peuvent se placer dans les interstices entre les gros. Ce qui se produit lorsque les dimensions des petits sont inférieures ou au plus égales au dixième des gros. Les poudres que tu m'as adressées (400 à 500 μ et 60-100 μ) sont donc susceptibles de ségrégation ; les lignes observées dans l'allonge à robinet en verre ne sont pas des laminaes mais des traces de colerette en pied de talus.

2) J'ai refait l'expérience de la formation de laminations par déversement dans l'eau aux vitesses que tu m'as indiquées et j'ai obtenu la même chose que la figure 2 de ta note de 1986. Mais le débit que tu m'as indiqué est un débit très faible, trop faible pour provoquer les mouvements turbulents visibles dans l'eau de la sédimentation dont je te parlais dans ma lettre du 18 Décembre 1986 (page 2 § 6).

Si on augmente le débit des turbulences de ce type apparaissent, mais alors les laminaes ne se forment plus. Et mon interprétation est par terre en particulier parceque les gros grains de 4/10 sédimentent avec une très grande vitesse en eau calme. En tout cas, ce qui se passe est exactement le contraire de ce que je prévoyais dans ma lettre du 25 Février 1987!

3) Il me semble donc que les phénomènes (1) et (2) ci-dessus n'ont rien de commun. Le premier dans l'air correspond à une simple ségrégation des grains roulant le long d'une pente. Il n'y a pas d'interaction dans l'air pendant la chute. Dans le vide, il n'y en a pas non plus et la ségrégation se produit de la même façon après la chute et sur le talus : là aussi ma prévision du 9 Février 1987 est erronée, mais cette fois je crois comprendre pourquoi.

De toutes façons, tout cela n'est pas bien brillant et ne fait pas avancer beaucoup ton problème. Il me semble tout de même qu'il peut y avoir une interaction entre les gros grains au cours de la sédimentation dans l'eau même si on ne voit pas de turbulence dans le fluide.

Je suis désolé de ces résultats qui ne t'apportent rien mais je te prie de croire que cela m'a beaucoup intéressé de refaire tes expériences.

Reçois, mon cher Camarade, l'expression de mes sentiments cordiaux.

P. HABIB

ÉCOLE POLYTECHNIQUE - ÉCOLE NATIONALE SUPÉRIEURE DES MINES DE PARIS - ÉCOLE NATIONALE DES PONTS ET CHAUSSÉES

LABORATOIRE DE

MÉCANIQUE DES SOLIDES

UNITÉ ASSOCIÉE AU C. N. R. S.

École polytechnique
91128 Palaiseau cedex
téléphone : (1) 69.41.82.00
télex : Écolex 601596 F

PH/MAW

Palaiseau, le 9 Octobre 1989

Monsieur Guy BERTHAULT
28, boulevard Thiers
78250 MEULAN

Mon Cher Camarade,

Je me suis mal exprimé dans ma lettre du 25 Septembre. J'ai effectivement fait la manip d'écoulement à sec du mélange de poudres dans l'air et dans un vide (modéré) avec le même résultat, c'est-à-dire avec apparition d'une ségrégation des grains, les gros roulant sur la pente et formant une colerette le long de la paroi du tube en verre d'une éprouvette graduée.

Bien entendu les fins arrivent aussi en bas de la pente mais par une série de mini accidents de surface, mi-glissement de terrain, mi-avalanche, comme ceux qui sont déclenchés par le fourmilion au fond de son entonnoir pour attraper les petites bêtes qui passent par là.

Ces petits glissements recouvrent les colerettes et le granoclassement est fait. Bien entendu dans l'eau et sans courant latéral (ce qui était mon cas) les strates se forment horizontalement et non en cône comme à sec.

Bien cordialement.

P. HABIB

APPENDIX B

Laboratory Experiments on Segregation of Mixtures.

A complementary set of experiments has been conducted to investigate the segregation of sediment particles of the mixtures used in the present research. In this experiment, a piece of transparent plexiglas of 30 X 40 cm^2 is used. A small amount of sand mixture is poured onto the plate glass and then the glass is agitated gently for about five minutes in a horizontal direction along the plane of the plexiglas. Segregation of sand particles is observed without any turbulence or low amplitude bedforms. Pictures are then taken above and below the plexiglass to illustrate the pattern of sand segregation. A device shown in Picture B-1 makes it convenient for taking pictures from underneath. Table B-1 summarizes the results from the experiment.

Pictures B-2 through B-4 were taken from the segregation of a mixture (ERC #1 and B2040), which is very similar to the mixture SM-2 used in the lamination experiments conducted in the small flume. In this mixture, there is no size overlap between the black sands and the white sands. This experiment demonstrates that it is very easy to separate these two types of particles with the coarser black particles (B2040) on top (see Figures B-2 and B-3), and the finer white particles (ERC #1) underneath (see Figure B-4). The clear segregation of particles is easily observed in this experiment.

Different results are observed for mixtures #1 to #11 used in the first part of this report. The pattern of particle segregation generally includes three types: 1) no segregation; 2) top and bottom layers; and 3) parallel segregation. If the sizes of the two particles in the mixture are similar, no clear segregation is observed, for instance, Pictures B-5 and B-6 for mixture #1, Pictures B-13 and B-14 for mixture #5, and Pictures B-17 and B-18 for mixture #8. Segregation of particles always takes place if the two types of particles in the mixture have different sizes or densities. It appears that mixtures of particles with different densities lead to parallel segregation (see Pictures B-7, B-8, B-15 and B-16), while mixtures of particles with different sizes lead to top and bottom segregation (see Pictures B-21 through B-24).

Table B-1. Summary on Segregation of Sand Particles in Mixtures

Mixture #	Mixture Content	Observation	Pictures
Test	ERC#1 & B2040	Clear segregation. Black particles on top and white particles on bottom.	B-2, B-3, B-4
1	ERC#3 & B2040	No apparent segregation.	B-5, B-6
2	ERC#1 & B3060	Clear segregation. Black on top and white on bottom.	B-7, B-8
3	ERC#1 & coal#1	Clear segregation. Black on top and white on bottom. Parallel configuration normal to the direction of motion.	B-9, B-10
4	ERC#3 & coal #3	Clear segregation. Coal on top and other on bottom. Parallel configuration normal to the direction of motion.	B-11, B-12
5	limestone#1 & B3060	No clear segregation of sand particles.	B-13, B-14
6	limestone#2 & coal#1	Clear segregation. Black on top and white on bottom.	B-15, B-16
8	ERC#2 & coal#1	No clear segregation is observed.	B-17, B-18
9	limestone#1 & coal#2	Clear segregation. Black on top. Configuration normal to the direction of motion.	B-19, B-20
10	limestone#1 & B2040	Clear segregation. Black particles on top. No configuration observed.	B-21, B-22
11	B3060 & ERC#3	Clear segregation. Black particles on bottom and white on top.	B-23, B-24

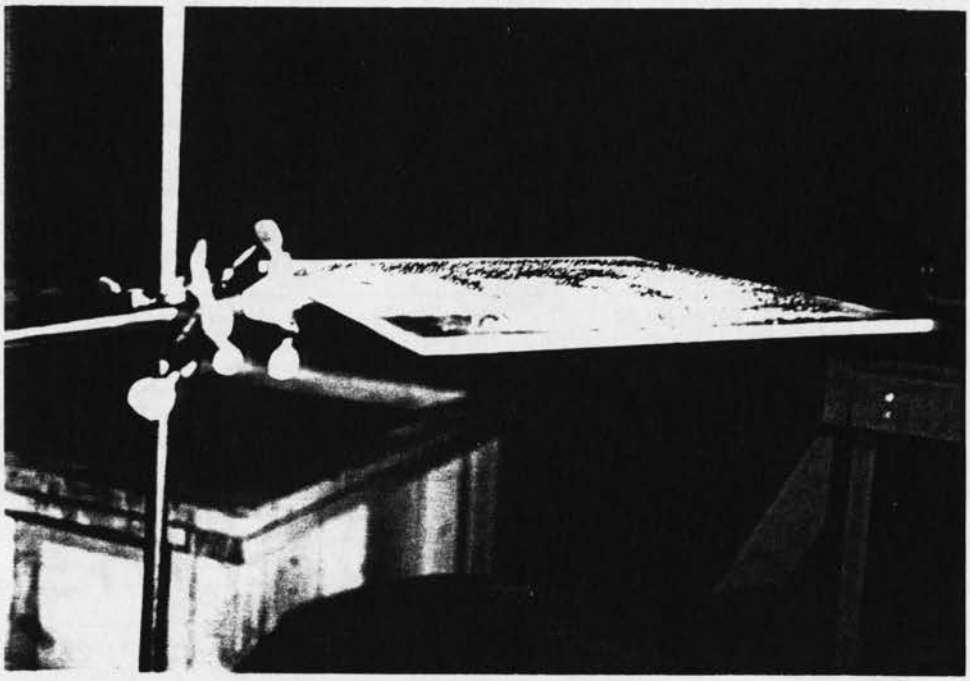

Picture B-1. Experimental set up

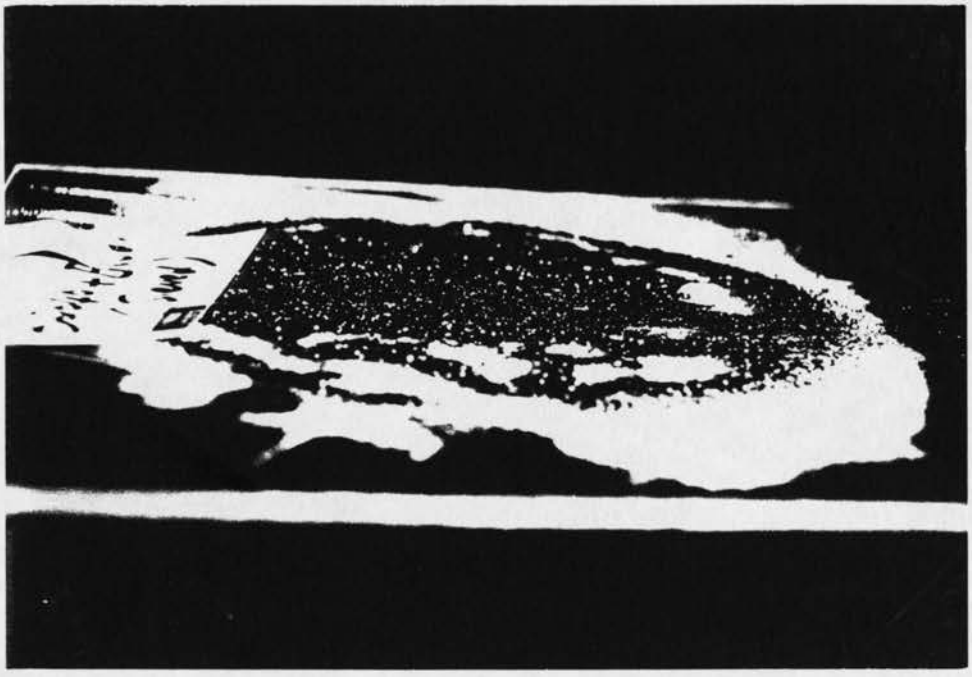

Picture B-2. Detail view of particle segregation in front

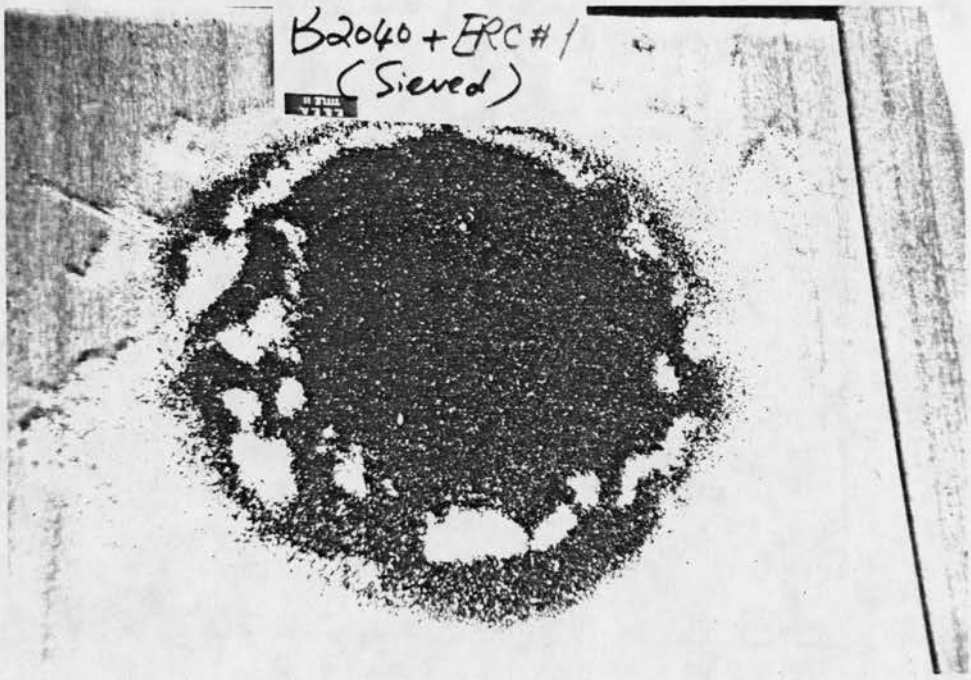

Picture B-3. Clear segregation of a mixture (ERC#1 & B2040) from above

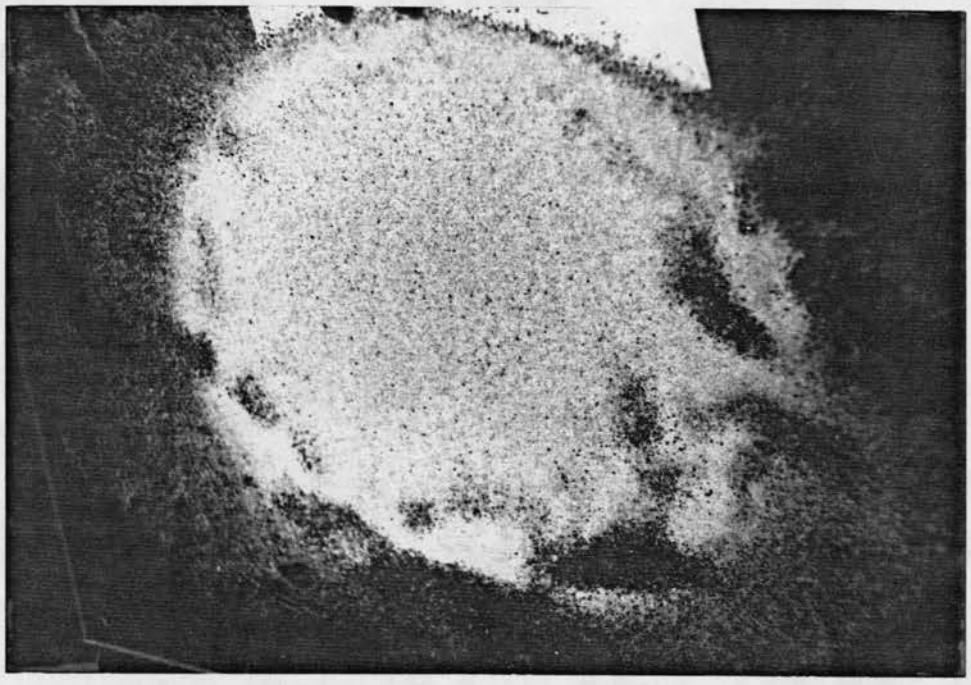

Picture B-4. Clear segregation of a mixture (ERC#1 & B2040) from underneath

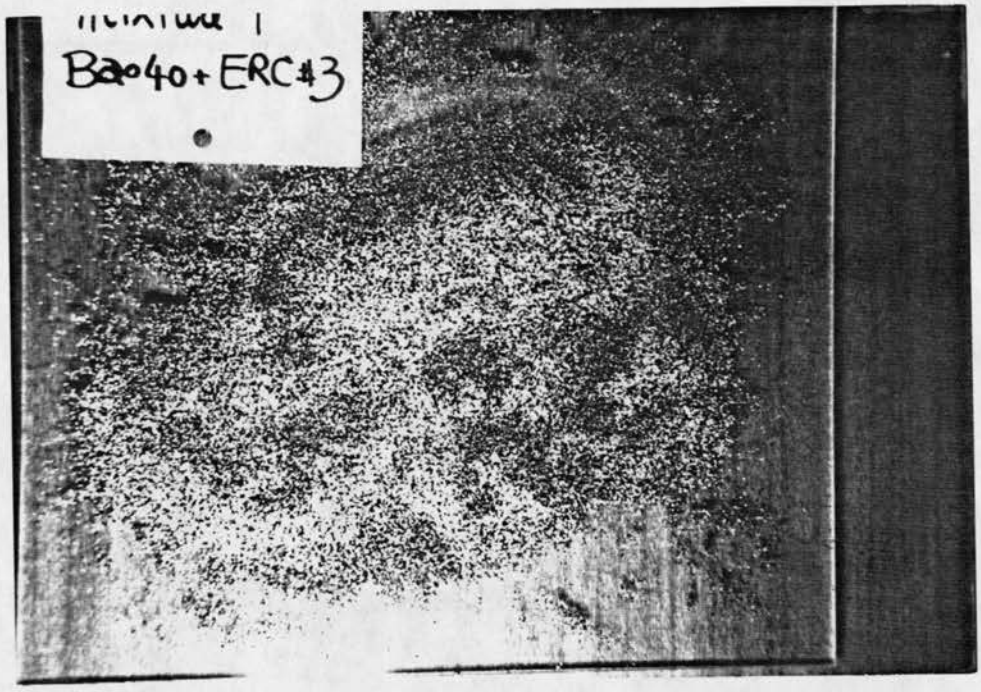

Picture B-5. No clear segregation of mixture #1 from above

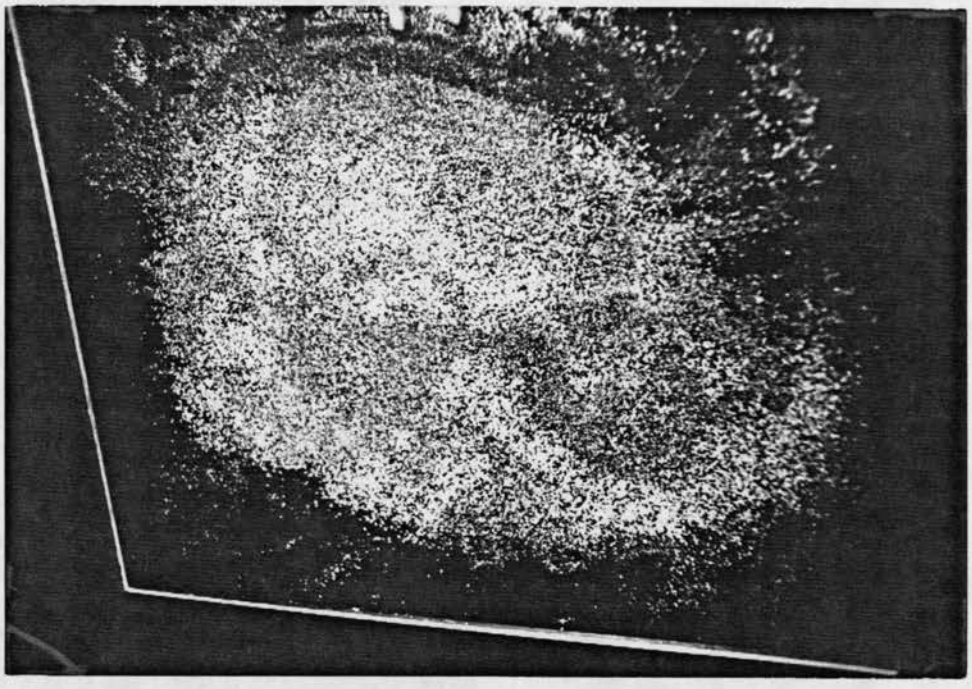

Picture B-6. No clear segregation of mixture #1 from underneath

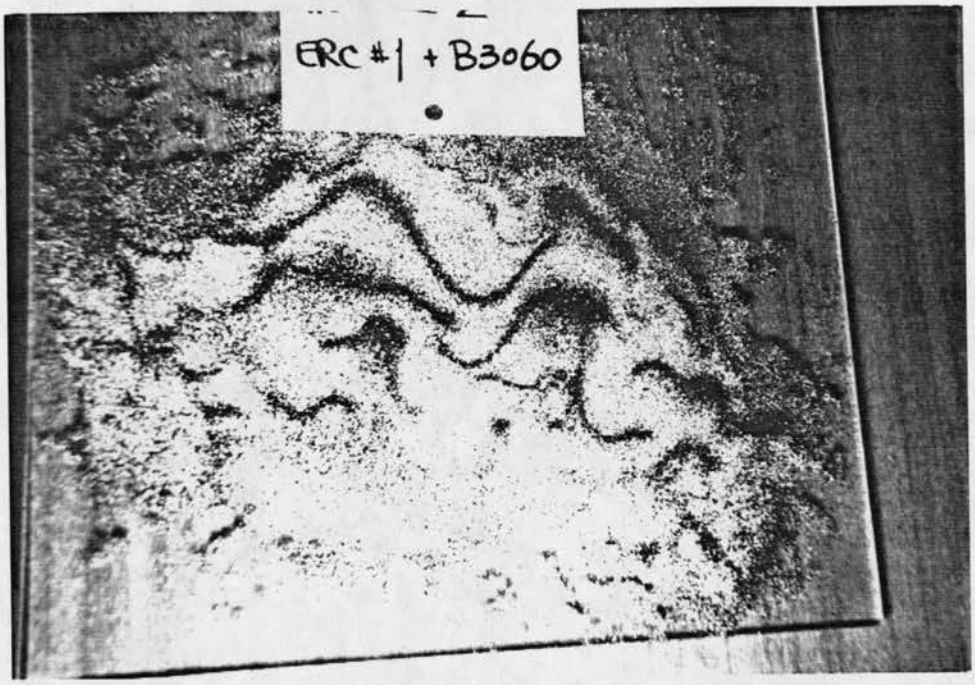

Picture B-7. Parallel segregation of mixture #2 from above

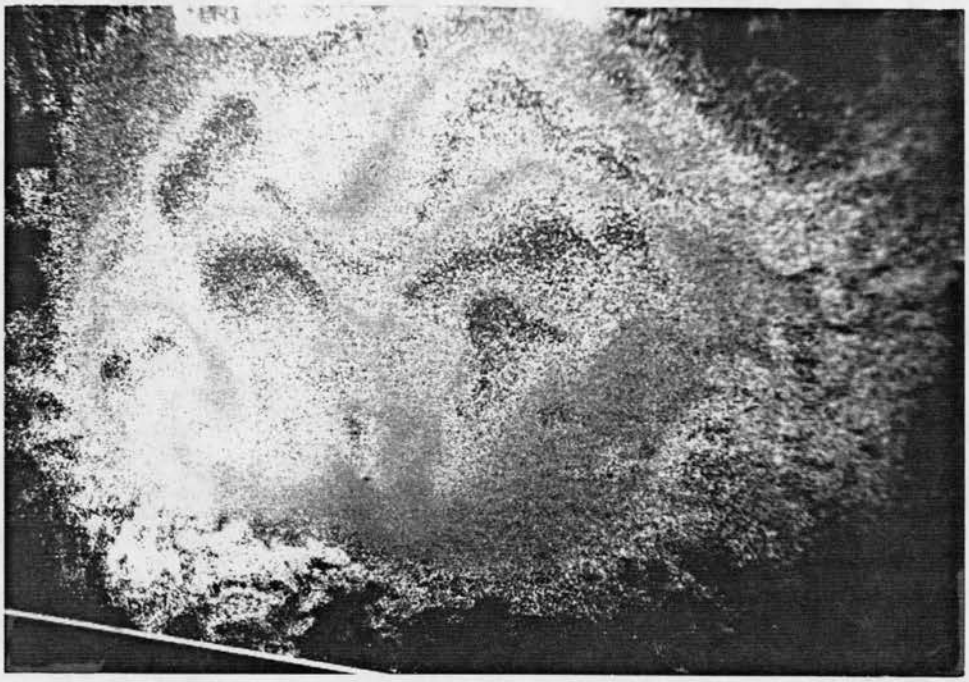

Picture B-8. Parallel segregation of mixture #2 from underneath

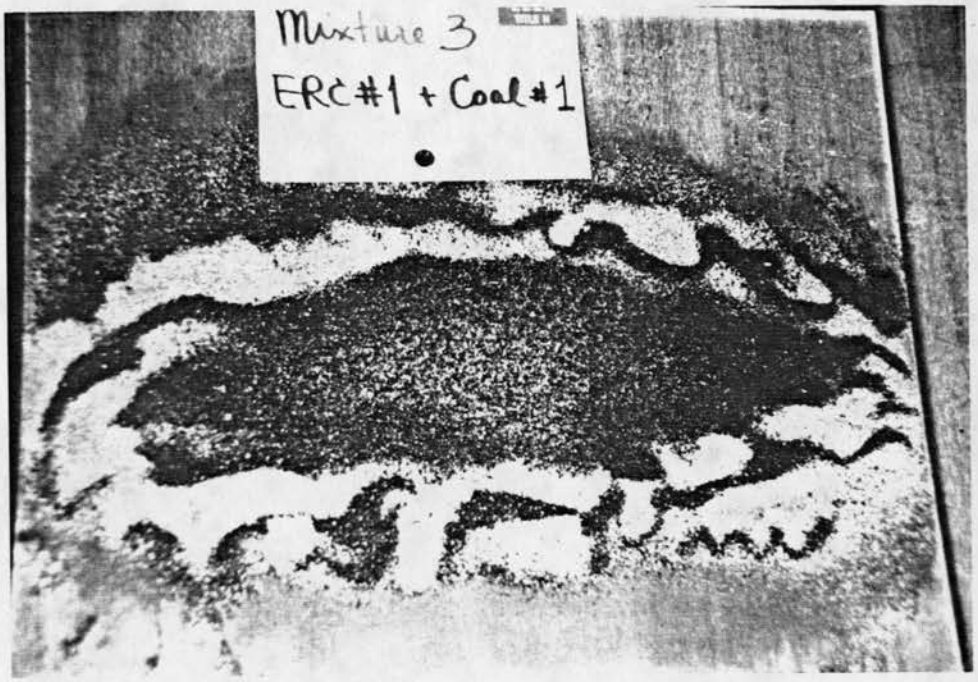

Picture B-9. Clear segregation of mixture #3 from above

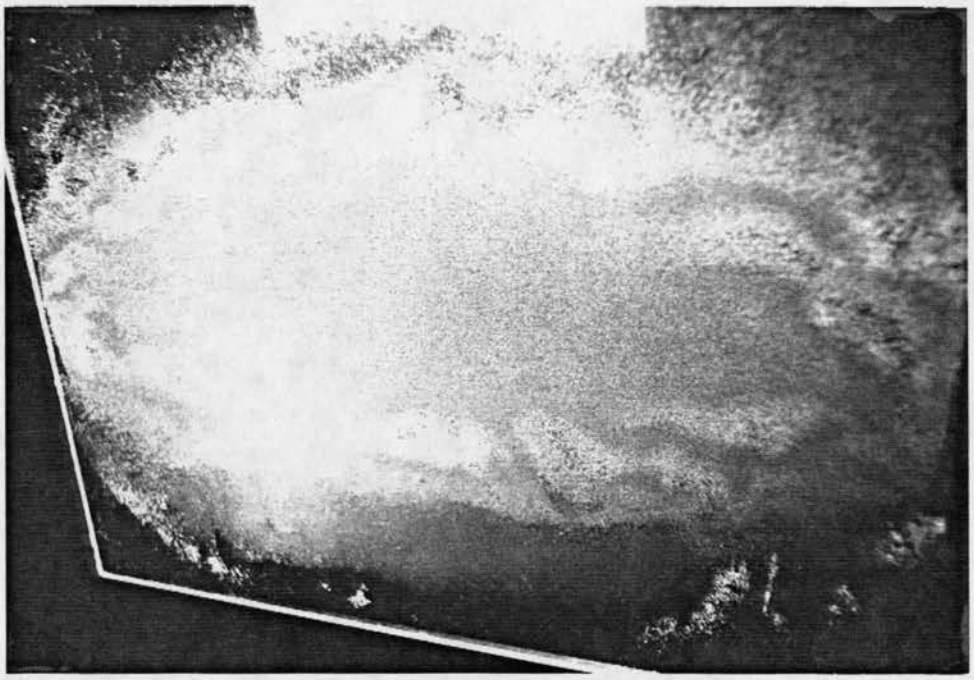

Picture B-10. Clear segregation of mixture #3 from underneath (white sands on bottom)

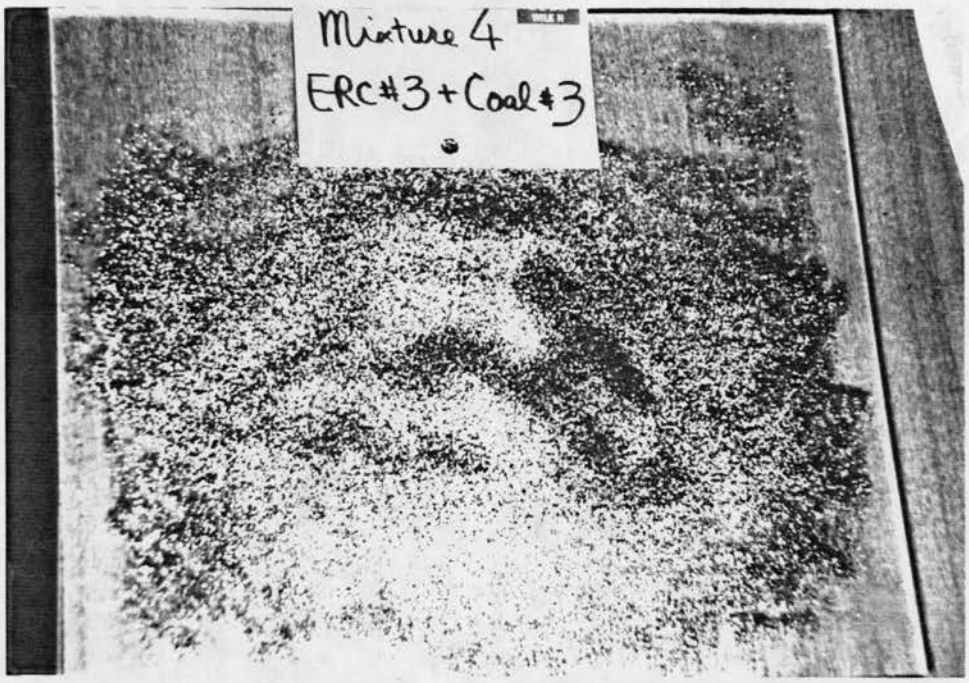

Picture B-11. Parallel segregation of mixture #4 from above

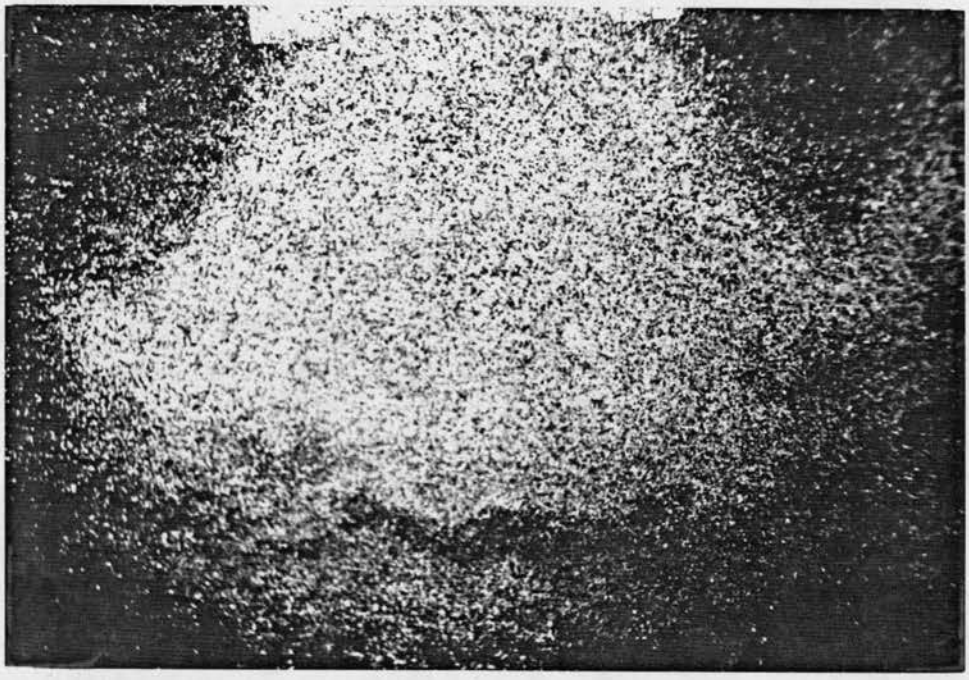

Picture B-12. Parallel segregation of mixture #4 from underneath

Picture B-13. No clear segregation of mixture #5 from above

Picture B-14. No clear segregation of mixture #5 from underneath

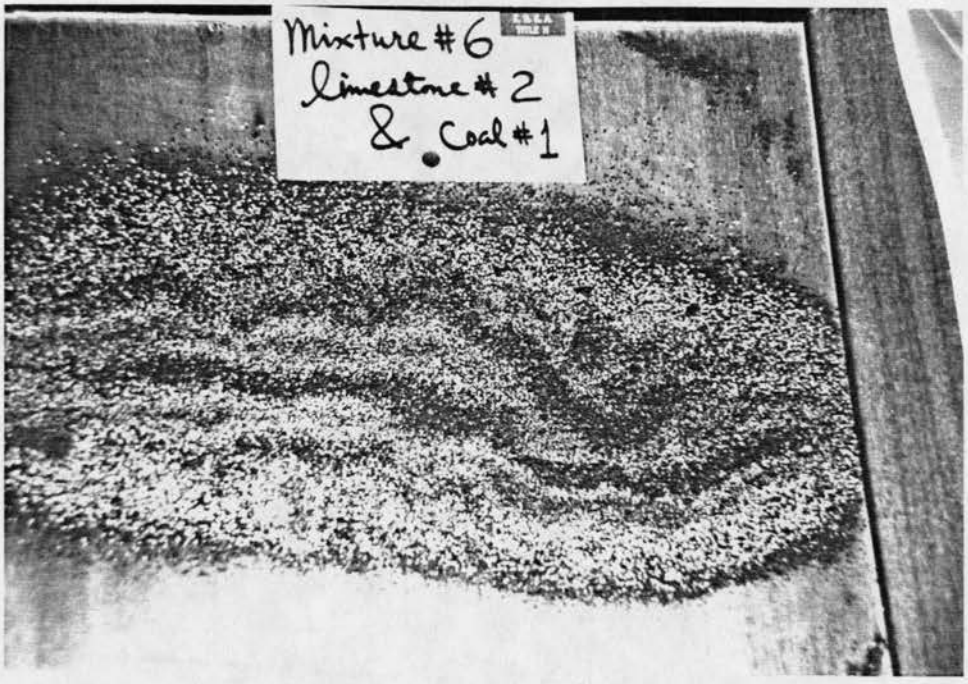

Picture B-15. Parallel segregatin of mixture #6 from above

Picture B-16. Parallel segregation of mixture #6 from underneath

Picture B-17. Black particles on top from mixture #8 (view above)

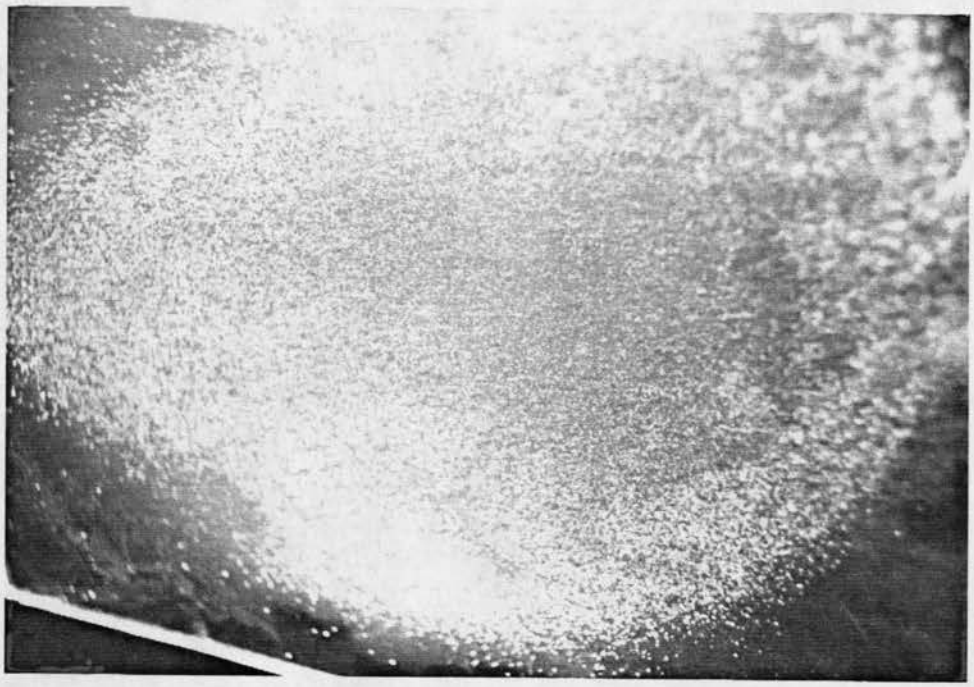

Picture B-18. White particles on bottom from mixture #8 (view underneath)

Picture B-19. Black particle on top from mixture #9 (view above)

Picture B-20. White particles on bottom from mixture #9 (view underneath)

Picture B-21. Black particles on top from mixture #10 (view above)

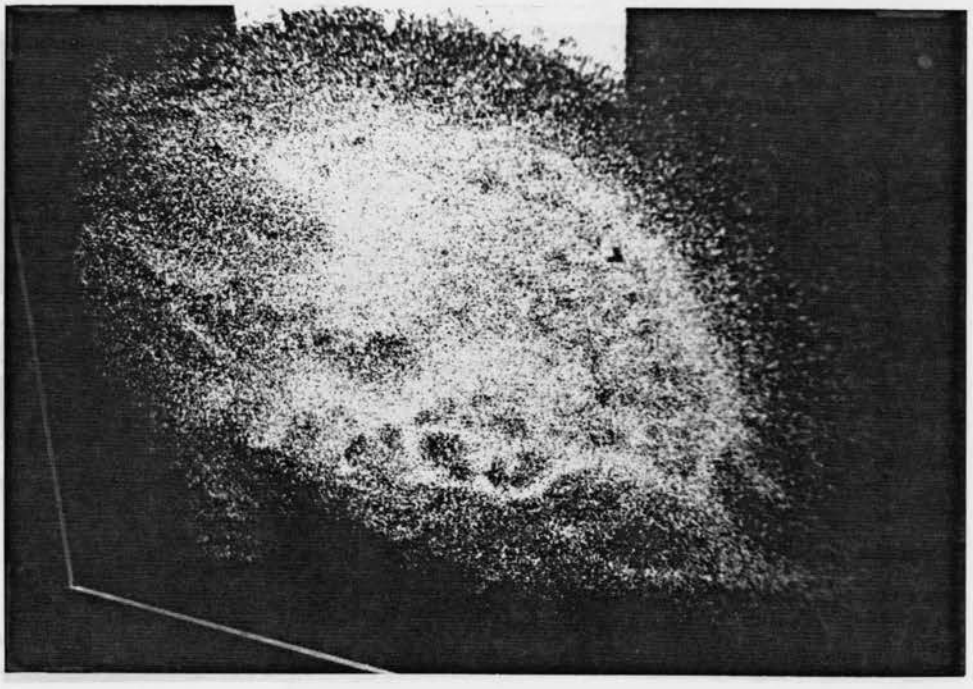

Picture B-22. White particles on bottom from mixture #10 (view underneath)

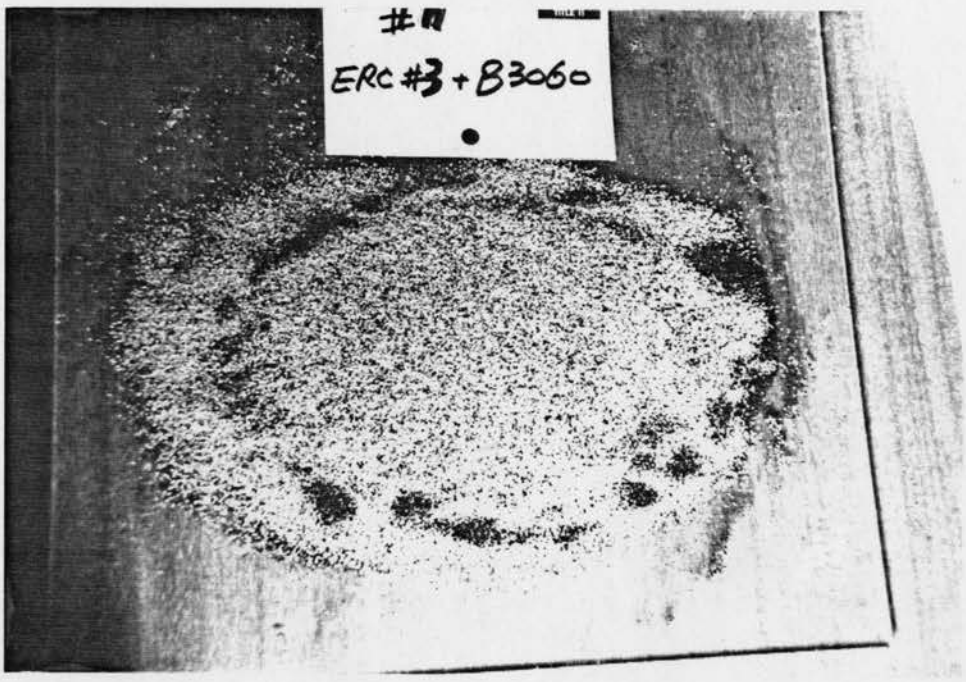

Picture B-23. White particles on top from mixture #11 (view above)

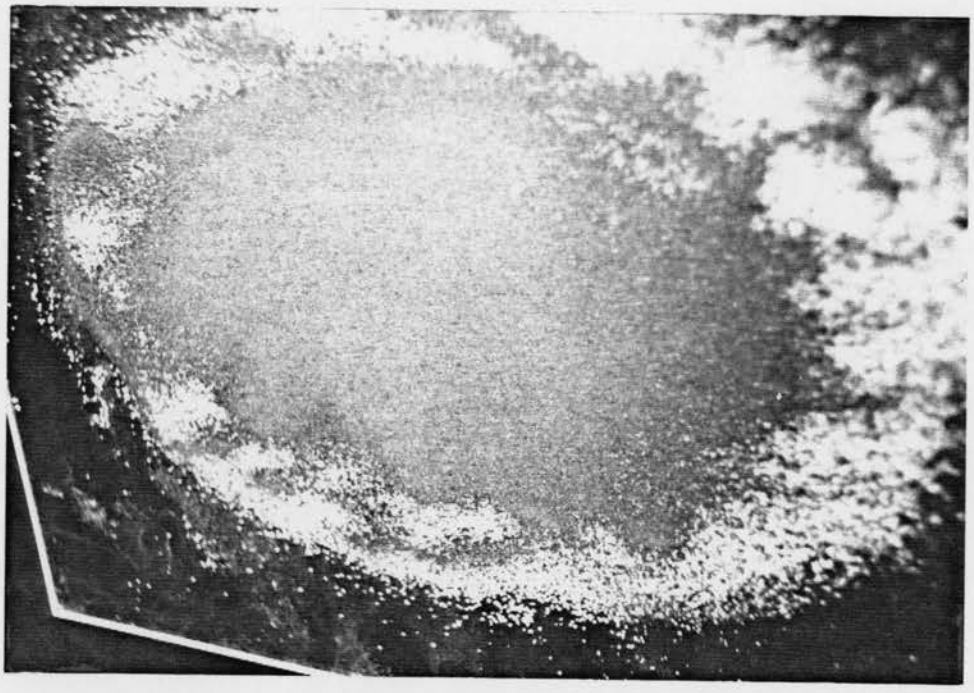

Picture B-24. Black particles on bottom from mixture #11 (view underneath)

APPENDIX C - Comments from M. G. Berthault

As the instructor of these experiments, namely in the flume model of the Bijou Creek Flood, I would, as did McKee in the conclusion of his report, infer from them, some lessons about stratigraphy. Let us imagine a man, having only notions about stratigraphy, discovering, in a few years, our canal, in inclined position. He would observe through its lateral sides, a desiccated deposit, showing an alternated superposition of deltas of large particles, and of laminae, parallel to the slope of the flume, in which he would distinguish some fractures, themselves parallel to the slope.

Identifying each delta, each laminae to a sedimentary layer deposited during an interval of time, horizontally, and uniformly in the flume, he would apply to them the principle of superposition saying: "Each layer is older than the one which recovers it, and younger than the one it recovers," and the principle of continuity: "Each layer is of the same age in every point." From the obliquity of the deltas and laminae, he would deduce that the flume had inclined because of subsidence. About the fractures, he will say they resulted from interruptions of the sedimentation, provoking an induration of their inferior surfaces. As regards the duration of the deposit, he will assimilate each millimetric laminae to an annual varve. As the deposit has a thickness of 5 cm, he will estimate its minimum duration at 50 years, ignoring the sedimentary interruptions.

We know, for we have witnessed the experiments, that such an interpretation would be wrong. We have seen, at the same time, and at each instant, a deposit, up the flume, of laminae of the upper level, down the flume, those of the lower level, and between the two, the large particles of the delta. Thus, a sedimentary layer, deposited within a given interval of time, includes parts of inferior and superior laminae, and of the intermediate delta (Figure 22 of this report). Neither the laminae, nor the delta, thus, are distinct and successive layers. But, in proportion the deposit forms, thickening at the same time from the bottom to the top and up to down the flume, the superposition of laminae and delta is spreading towards the lower part of the flume, and upwards, each time a gate is introduced, reducing the speed of the flow.

Of course, we cannot say that the delta is younger than the inferior laminae and older than the superior laminae since the superior laminae upstream t_1 were deposited before the particles of the delta in middle portion t_2, which themselves were deposited before the particles of the inferior laminae downstream t_3.

We cannot say also that the delta is of the same age at every point since it prograded in time from up to down the flume. Consequently, the principle of segregation and continuity are inapplicable to the laminae and delta of our experiments. Besides, we know that the flume was inclined at the moment of the experiment, and that any subsidence occurred. We know that the fractures result from the desiccation, and that this has occurred any sedimentary interruption. At last, we know that 20 minutes were sufficient for the deposit.

Those who, two centuries ago, founded stratigraphy, reasoned as our man. They observed in sedimentary rocks, banks, lithologically homogenous (sandstone, clay, limestone, etc...), shared in strata, characterized by a repetitive graded-bedding, generally decreasing, and fractures or joints of stratification. They identified these superposed strata with successive sedimentary layers, intermittent because of the joints. And where they are inclined, they infer tectonic subsidences. Then they applied to strata the principle of superposition and continuity evident for layers, and scaffolded the geological column, its hundreds of millions of years, which lets appear a succession of fossilized species including their evolution, according to the theory of Darwin.

Therefore, there are good reasons to raise fundamental questions again regarding identification and consequences in sedimentology. Considering these recent observations and experiments which unveil some physical factors governing stratification in continuous sedimentation (segregation of particles according to their size, flow speed, incidence of slope, and desiccation), these factors should be considered to settle the stratigraphic concept on a more solid basis.

What I say completes what, one century ago, the sedimentologist Johannes Walther(*) had observed as regards to superposed marine banks which are, at the same time, beside each other on the ocean bottom, from which is born sequential analysis.

Thanks to MM Julien and Lan who have successfully completed these experiments.

G. Berthault

(*) *Walther, Johannes, 1893-1894, "Einleitung in die Geologie als historische Wissenschaft: Jena", Verlag van Gustav Fisher, 3 vols., 1055 p.*

Sédimentologie/*Sedimentology*

Sédimentation d'un mélange hétérogranulaire. Lamination expérimentale en eau calme et en eau courante

Guy BERTHAULT

Résumé — Ces expériences montrent qu'en eau calme, le dépôt en continu d'un sédiment hétérogranulaire, donne naissance à des *laminae* disparaissant avec l'accroissement de la hauteur de chute des grains dans l'eau, et apparemment de leur taille. La lamination se forme suivant l'inclinaison de la partie supérieure du dépôt. En eau courante, apparaissent dans le dépôt plusieurs types de lamination, voisins les unes des autres, parfois superposés.

Sedimentation of a heterogranular mixture. Experimental lamination in still and running water

Abstract — *The experiments demonstrate that in still water, continuous depositing of heterogranular sediments gives rise to laminae which disappear progressively as the height of the fall of particles into water, and apparently their size, increase. Laminae follow the slope of the upper part of the deposit. In running water, many closely related types of lamination appear in the deposit, even superimposed.*

Abridged English Version — I. INTRODUCTION. — The author has previously performed experiments on lamination of sediments, resulting from a periodic graded-bedding subsequent to deposit [1], that contribute to the explanation of lamination of various sediments and sedimentary rocks. These sedimentation experiments were conducted in still water with a continuous supply of heterogranular material. A deposit was obtained, giving the illusion of successive beds or laminae. These laminae were the result of a spontaneous, periodic and continuous grading process which took place immediately following the deposit of the heterogranular mixture. The thickness of the laminae appeared to be independent of the sedimentation speed but increased with extreme differences in the size of the particles in the mixture.

Where a horizontal current was involved, thin laminated superposed layers developing laterally in the direction of the current were observed. The object of the new complementary experiments described hereafter was to study, first in still water, the influence of the height of the fall of particles into water, and the influence of a slope on lamination in the deposit; secondly, in running water, at a higher rate of particle discharge than in the initial experiment, the incidence on the structure of the deposit.

These experiments were undertaken at the request of the author, by MM. Penquer, Guillaume and Bertinier, at the "Institut de Mécanique des Fluides de Marseille".

II. EXPERIMENTS. — 1. *Influence of the height of the fall on lamination in calm water.* — The first series of experiments was effected by a mixture of two types of sand, one white calibrated between 20-80 μ, the other, coloured with methylene blue with the calibrations increasing in size. It was poured from a variable speed screw distributor into a rectangular tube 200 × 150 mm × 4,7 mm deep, filled initially with 2 m of water, then with 4,7 m.

The proportions were varied: 1/3 for the coloured and 2/3 for the white sand at 2 m; 1/4-3/4 at 4,7 m. The flow varied from 35 to 170 cm^3/5 min., at 2 m, and at 4,7 m, it remained constant at 40 cm^3/min., then more slowly at 200-400 cm^3/hr.

Note présentée par Georges MILLOT.

0249-6305/88/03060717 $2.00

It was observed that the lamination in the deposit was present at 2 m, in any case, but at 4,7 m, it was only present with the highest flows, and disappeared as the flow diminished and the size of the coloured particles increased. This tended to prove that the disturbance of water, here caused by the falling particles, was a necessary factor to the segregation to take place into large and small particles giving an appearance of lamination (*Figs.* 1, 2 and 3).

2. *Influence of a slope on lamination in calm water.* — In the second series of experiments, the direction of the lamination formed in the sediments falling on a slope was observed. An aquarium was used, having the same dimensions as the PVC tube. The depth of water was 1,10 m. Successive experiments were performed on a slope of 6°, and then 15° (*Fig.* 4).

Laminae are parallel to the slope of the upper part of the deposit.

3. *Incidence of current water on lamination.* — The third series of experiments was performed in a recirculating flume: 10 m long × 29 cm deep × 0,5 m wide, equipped with a lateral transparent viewing window to observe the structure of the deposit. The water discharge could vary from 16 to 70 l/sec. At a speed from 0,4 m/sec. on, many closely related types of lamination, horizontal and cross, sometimes superimposed, appeared in the structure of the deposit, the configuration of which being dunes and ripples (*Figs.* 5, 6 and 7). On the upper surface of ripples, lamination could be observed (*Fig.* 8). The dip of cross-lamination seemed to depend upon the height of water above the deposit, therefore upon all parameters varying with it.

III. Conclusions. — 1. *Confirmation of experimental lamination.* — These experiments, in calm and running water, confirm that the continuous deposit of a heterogranular sediment can give rise to horizontal and cross lamination, provided that a minimum disturbance of water is involved. In calm water, laminae are horizontal or parallel to the dip of the upper part of the deposit induced by a basic slope. No penetration of coloured grains through the surface of the deposit was observed during these experiments, contrary to the observations made by the author during one of his initial experiments, which was certainly accidental.

In running water, horizontal and cross laminae were observed placed together and sometimes superimposed.

2. *Discussion of the possible mechanism of lamination.* — H. Campbell [2] has demonstrated that a dry flow of a mixture of powders gave rise to a segregation of particles of the same size. Such segregation, in calm and running water is induced by the disturbance of water, however slight. Lamination resulting from such segregation can therefore result either from the correlation between turbulence of water and the concentration at the level of the deposit, or from instability phenomena resulting from the sedimentary fall of a hyperconcentrated mixture, or from the conjugation of these two factors.

3. *Prospects.* — These results should be compared with flume experiments by Guy [3] and Williams [4], the object of which was not the study of structure, despite some remarks on it, but the configuration of the deposit. They should also be compared with the observations by McKee [5] of structures of sediment deposits from the Bijou Creek flood, where horizontal and cross laminae, similar to those of these experiments, can be observed. Thus, it would be necessary to pursue such experiments in larger flumes to reproduce flow sedimentation and study the variations of deposit structure with all determining parameters. These experiments, no doubt, can help to a better understanding of laminar sedimentation, both in deposits and in sedimentary rocks.

I. INTRODUCTION. — L'auteur avait précédemment réalisé des expériences sur la lamination des sédiments par granoclassement périodique en cours de dépôt [1]. Ces expériences montraient que, en eau calme, le dépôt en continu d'un sédiment hétérogranulaire, donne naissance à des *laminae*, donnant l'illusion de lits successifs mais résultant en fait d'un granoclassement périodique : leur épaisseur semble indépendante de la vitesse de sédimentation, mais croît avec l'écart des tailles extrêmes des particules sédimentaires. En présence d'un courant d'eau horizontal, on voit des couches fines laminées superposées se développer latéralement dans le sens du courant. C'était une contribution à l'explication de la lamination dans nombre de sédiments et roches sédimentaires.

Les nouvelles expériences complémentaires dont il est rendu compte ici, ont pour but d'étudier, d'abord en eau calme, l'influence de la hauteur de chute sédimentaire, et de la pente, sur la lamination; ensuite, en eau courante, à débit nettement plus élevé que dans les expériences précédentes, l'incidence de ce débit sur la structure du dépôt.

Ces expériences ont été réalisées à la demande de l'auteur par MM. G. Salaun-Pinquer, Docteur-ès-Sciences, R. Guillaume, Maître de Conférences, M. Bertinier, Docteur de l'Université Aix-Marseille-II, à l'Institut de Mécanique des Fluides de Marseille, 1, rue Honnorat, 13003 Marseille.

II. INFLUENCE DE LA HAUTEUR DE CHUTE SUR LA LAMINATION EN EAU CALME. — Un mélange de deux sables, l'un blanc, de calibre 20-80 μ, l'autre coloré au bleu de méthylène, de calibre croissant, est émis par un distributeur à vis au-dessus de la surface de l'eau remplissant un tube PVC, de 4,7 m de hauteur, et de section rectangulaire 200 × 150 mm.

1. *Hauteur de chute de 2 m.* — (*a*) Mélange 30% sable bleu 250-315 μ, 70% sable blanc. Trois débits sont utilisés successivement dans la même expérience : 35, 100 et 170 cm^3/5 mn.

(*b*) Même mélange avec du sable bleu 315-400 μ. Trois débits voisins des précédents. Dans ces deux expériences, on observe trois couches superposées (*fig.* 1) présentant des *laminae* millimétriques assez régulières, d'autant plus nettes que le débit croît.

2. *Hauteur de chute de 4,7 m.* — (*a*) Mélange d'environ 25% de sable bleu et 75% sable blanc. Quatre expériences sont effectuées à débit constant : 40 cm^3/mn, avec quatre calibres croissants de sable bleu. Pour le sable bleu 200-250 μ, on observe des *laminae* millimétriques, d'une netteté moyenne (*fig.* 2). Pour les sables 250-315 μ et 315-400 μ, les *laminae* sont irrégulières, très peu nettes, et assez fines aux endroits où elles apparaissent. Pour le sable 400-500 μ, elles disparaissent pratiquement.

(*b*) Trois nouvelles expériences sont effectuées à des débits plus faibles, pour voir si les *laminae* apparaissent ou non dans le dépôt. Mélange 1/3 sable bleu 400-500 μ, 2/3 sable blanc. Débit 230 g/h. Pas de *laminae*. Débit 500 g/h. Pas de *laminae* (*fig.* 3). Mélange 1/3 sable bleu 150-212 μ, 2/3 sable blanc. Débit 230 g/h. Pas de *laminae*.

3. *Interprétation.* — La conclusion des essais sur l'influence de la hauteur de chute d'un mélange hétérogranulaire sur la formation de *laminae* est assez délicate. En effet, la lamination en eau calme, est un phénomène qui semblait tout à fait crédible, dans la mesure où cette dernière, bien que peu nette, apparaissait lors des expériences à $h = 2$ m, hauteur qui *a priori* semble suffisante pour que les effets dus à l'émission soient en grande partie amortis; or, les résultats sont différents suivant que l'on opère à 2 ou 4,7 m. Deux explications sont alors possibles :

— ou bien, effectivement, les mouvements tourbillonnaires induits par l'émission ponctuelle ne s'amortissent qu'à une distance supérieure à 2 m, et alors l'apparition de la lamination est étroitement liée à la présence d'une « agitation » du fluide porteur;

— ou bien, quoique les conditions d'expériences (débit, proportions) soient voisines, la répartition verticale des concentrations en sable fin dans le tube est modifiée par la hauteur d'eau : il est possible que les remontées fluides provoquées par l'émission maintiennent en suspension en partie du sable blanc, et ce très loin de la surface de dépôt au niveau duquel le rapport des concentrations sable blanc/sable bleu serait alors fortement diminué. Cependant, lors d'une telle expérience à $h=2$ m, la concentration moyenne en sable blanc au niveau du dépôt est une fonction croissante du temps, tout autant qu'à ce niveau le flux vertical de ce sable est inférieur au flux massique à l'émission. Or, à $h=2$ m, il apparaît une lamination peu après le début de l'expérience, ce qui tend à réfuter l'hypothèse, à $h=5$ m, d'une concentration en sable blanc, au niveau du dépôt, insuffisante pour que la lamination apparaisse.

Toutefois, la série d'expérience effectuée à $h=5$ m semble prouver que l'énergie dissipée par la chute d'un mélange hétérogranulaire de sables suffit à elle seule à affecter le dépôt d'un caractère anisotropique, tendant vers un classement granulométrique horizontal, sans pour autant qu'on puisse affirmer qu'il y a lamination.

D'autre part, l'apparition de *laminae* semble d'autant plus probable que la concentration totale en sable est élevée.

Ces diverses remarques nous conduisent à penser que la lamination, quand elle apparaît, est due en partie : soit à la corrélation entre une agitation turbulente du fluide et la concentration au niveau du dépôt, soit à des phénomènes d'instabilité dus à la chute sédimentaire d'un mélange hyperconcentré, soit à la conjugaison des deux phénomènes précités.

III. Influence de la pente sur la lamination en eau calme. — Le dépôt est effectué sur une surface inclinée pour examiner l'effet sur la lamination. On utilise un aquarium à quatre faces transparentes : section identique à celle du tube PVC; fond à pente variable (6° et 15°); hauteur d'eau 1,10 m.

1. *Pente de* 6°. — (*a*) Mélange 25 % sable bleu 315-400 μ, 75 % sable bleu 20-80 μ. Une lamination apparaît, peu nette, en pente, sur les faces latérales, et pratiquement invisible sur les faces avant et arrière. De plus, on relève un effet de cône, donc des effets de glissement des sables, montré par la différence d'épaisseur entre les dépôts en bas et en haut de pente. A cette hauteur de chute sédimentaire, la taille des gros grains utilisés ici est la limite supérieure permettant d'obtenir des *laminae*.

(*b*) Le même mélange avec sable bleu 250-315 μ. Une lamination apparaît assez nette, sauf en bas de pente. Sur les faces latérales, la lamination est, au degré près, parallèle à la pente.

2. *Pente de* 15°. — Mêmes mélanges, résultats similaires (*fig.* 4).

3. *Interprétation.* — La pente de la surface de base du dépôt influe peu sur la lamination et semble même la favoriser. Les premières lamines se forment parallèlement au support. Dans tous les cas, la dernière lamine se forme suivant l'inclinaison du dépôt précédent. L'angle de ces deux plans est d'autant plus faible que la taille des grains et la pente sont plus faibles.

IV. Sédimentation en eau courante. — 1. *Introduction.* — Cette étude a pour but la mise en évidence des phénomènes de lamination interne résultant d'une sédimentation hétérogranulaire se produisant au sein d'un écoulement liquide.

2. *Matériel utilisé.* — Les expériences sont effectuées dans le canal de l'Institut de Mécanique des Fluides, modifié pour la circonstance. Longueur 10 m, largeur ramenée à

Fig. 1. – Laminations à 2 m de profondeur, débit 35 à 170 cm^3/ 5 mm.

Fig. 1. – Laminations under 2 m of water, discharge 35 to 170 cm^3/5 m.

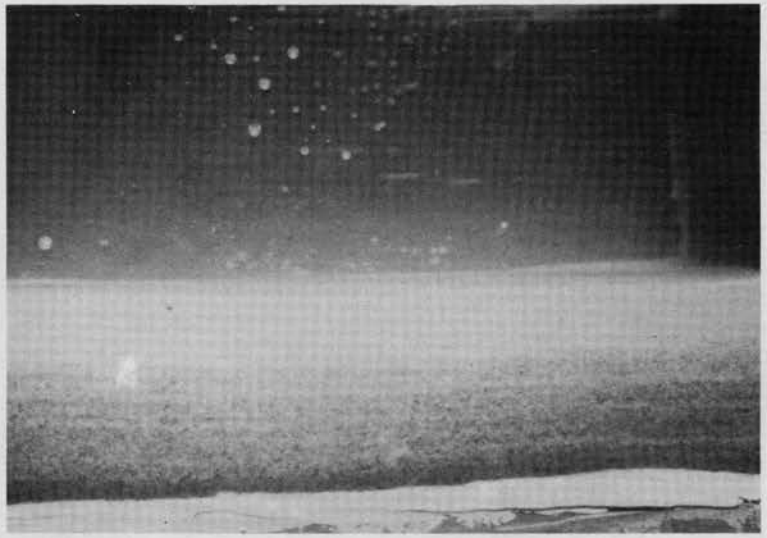

Fig. 2. – Laminations à 4,7 m de profondeur, débit 40 cm^3/mm.

Fig. 2. – Laminations under 4.7 m of water, discharge 40 cm^3/mm.

Experiences en tube/*Experiments in tube*

Fig. 3. – Absence de lamination à 4,7 m de profondeur, débit 400 cm^3/h.

Fig. 3. – No lamination under 4.7 m, discharge 400 cm^3/h.

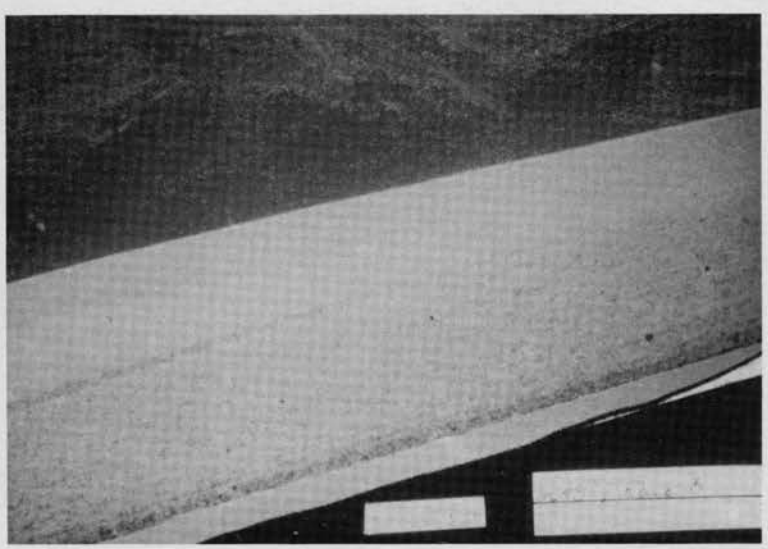

Fig. 4. – Lamination parallèle à une pente de 15°.

Fig. 4. – Lamination parallel to a slope of 15°.

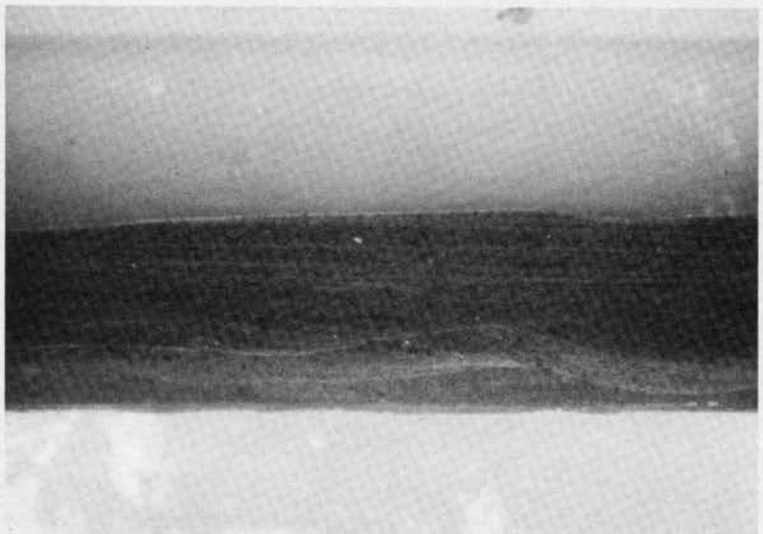

Fig. 5. – Lamination oblique surmontée de laminae horizontales.

Fig. 5. – Cross laminated ripples surmounted by horizontal laminated.

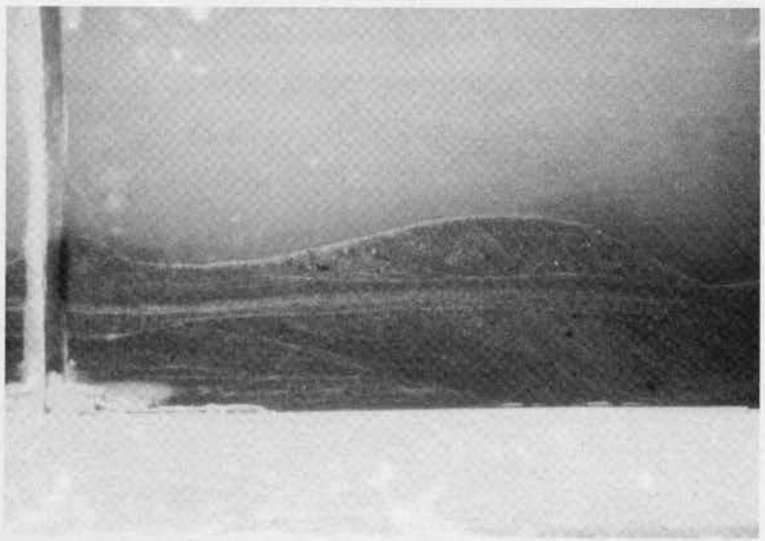

Fig. 6. – Laminations obliques séparées par une couche de laminae horizontales.

Fig. 6. – Cross laminated ripples splitted by a layer of horizontal laminae.

Expériences en canal/*Experiments in flume*

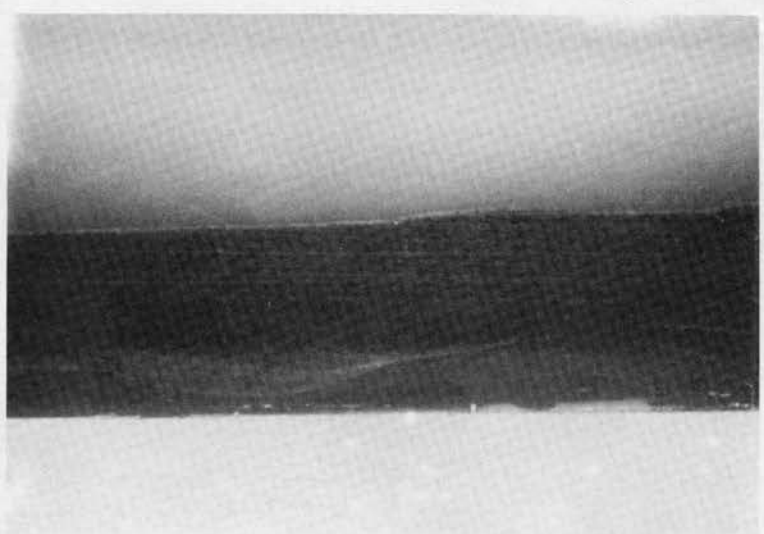

Fig. 7. – Lamination oblique surmontée de laminae horizontales.

Fig. 7. – Cross laminated ripples surmounted by horizontal laminated.

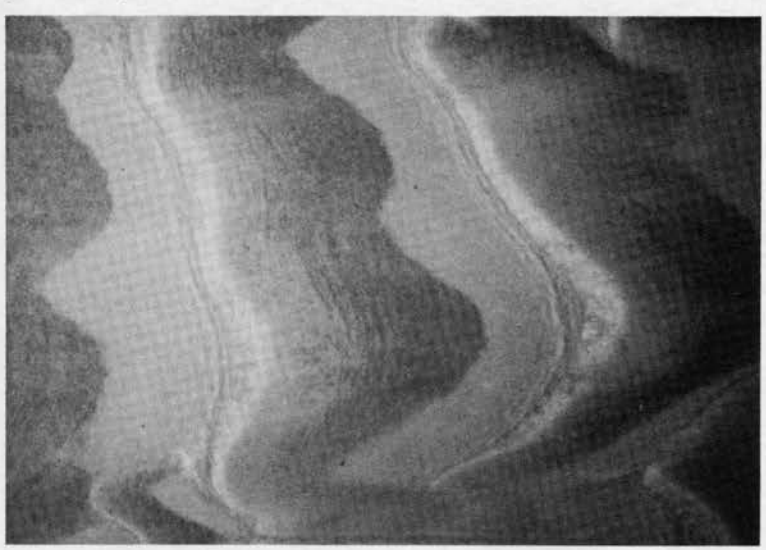

Fig. 8. – Rides laminées vues du haut du canal.

Fig. 8. – Cross laminated ripples seen from above.

0,5 m en fixant au milieu du canal, une paroi vitrée permettant l'observation latérale du dépôt. Profondeur : 29 cm. Pente : $1{,}2.10^{-3}$. Coefficient de perte de charge linéaire : 0,016 (fond lisse). Une vanne équipant une pompe Flight permet de faire varier le débit d'eau de 16 à 70 l/s. Un tube de Pitot placé sur chariot, permet la mesure des vitesses en tout point d'écoulement. La vérification des valeurs obtenues s'effectue par la mesure de la vitesse surfacique à l'aide d'un flotteur. L'épaisseur de la lame est repérée à l'aide de règles apposées verticalement contre la paroi vitrée. L'émission des sables est réalisée par une trémie située en amont au-dessus du canal.

3. *Expériences de lamination interne.* — Deux expériences sont conduites :

(*a*) Un mélange de 120 kg de sable bleu 100-150 μ et 240 kg de sable blanc 20-80 μ, est émis de la trémie en 3 h.

(*b*) Un mélange de 80 kg de sable bleu 150-210 μ et 240 kg de sable blanc 20-80 μ est émis en 2 h 30 mn.

Les caractéristiques de l'écoulement en début d'expérience sont :

— Vitesse moyenne U, obtenue par exploration du plan vertical médian du canal : (A) 38,4 cm/s, (B) 39,6 cm/s. Vitesse surfacique : (A) et (B) 40 cm/s. Hauteur d'eau maximale : (A) 9,9 cm, (B) 8,8 cm. Hauteur d'eau moyenne h : (A) 9,7 cm, (B) 8,9 cm. Hauteur d'eau minimale : (A) 9,5 cm, (B) 9 cm.

On en déduit : — débit $Q=U.h.1$: (A) $18{,}6.10^{-3}\,m^3.s^{-1}$, (B) $17{,}6.10^{-3}\,m^3.s^{-1}$.

— Coefficient de perte de charge linéaire $\Lambda=8.g.h.1.i/U^2(2H+1)$ = (A) 0,045, (B) 0,039.

— Nombre de Reynolds $R=Uh/v$ = (A) 37 250, (B) 35 240.

— Nombre de Froude $F=U\sqrt{gh}$ = (A) 0,394, (B) 0,424.

— Puissance du courant $P=U\tau$ = (A) $0{,}44\,J.m^{-2}.s^{-1}$, (B) $0{,}416\,J.m^{-2}.s^{-1}$

τ étant la tension tangentielle critique des grains de sable dans l'eau.

Ces caractéristiques varient en cours d'expérience : l'épaisseur du dépôt augmentant, la hauteur de la lame d'eau diminue et la vitesse augmente.

On observe, dans les deux cas, plusieurs types de laminations, obliques et horizontales, voisines les unes des autres, parfois superposées (*fig.* 5, 6 et 7), parfois désordonnées.

4. *Expériences de visualisation des* laminae *à la surface du dépôt.* — Quatre expériences sont conduites avec du sable blanc seul. Après la deuxième expérience, le dépôt obtenu est formé de dunes dont la dessication partielle fait apparaître une alternance de raies sèches et humides, vues de dessus, qui semble résulter d'un classement répétitif oblique.

La même expérience est répétée cette fois avec le même mélange de sables bleu et blanc de l'expérience (*b*), à la vitesse de 0,4 m/s. Le dépôt se déssèche, après vidange du canal. Il est constitué de rides à la surface desquelles, vues de dessus, on voit des *laminae* (*fig.* 8).

5. *Interprétation.* — L'inclinaison des *laminae* semble dépendre de la hauteur d'eau surmontant le dépôt, donc des paramètres qui la détermine. Par ailleurs, la lamination interne semble affleurer en surface, dans le cas des rides.

V. Conclusions générales. — 1. *Confirmation de la lamination expérimentale.* — Ces expériences tant en eau calme que courante, confirment que le dépôt en continu d'un sédiment hétérogranulaire, peut donner naissance à des *laminae*, à condition qu'une agitation minimale de l'eau existe. En eau calme, elles peuvent être soit horizontales, soit parallèles à la pente du dépôt, même à une certaine profondeur. En eau courante, elles

sont horizontales ou obliques. L'obliquité semblant dépendre de la hauteur de la lame d'eau au-dessus du dépôt.

2. *Infirmation de l'observation de l'enfoncement des plus gros grains dans le dépôt.* — Au cours de ces expériences, un tel enfoncement n'a pas été observé, comme l'auteur l'avait vu lors d'une de ses expériences, ce qui ne pouvait qu'être accidentel.

3. *Discussion des mécanismes possibles de la lamination.* — H. Campbell [2] a démontré que l'écoulement à sec de mélanges de poudres, produit une ségrégation des particules de même calibre. Ces expériences montrent qu'elle se produit également dans l'eau, à condition que celle-ci présente une agitation minimale; la lamination qui en résulte est due, soit à la corrélation entre une agitation turbulente du fluide, et la concentration au niveau du dépôt, soit à des phénomènes d'instabilité dus à la chute sédimentaire d'un mélange hyperconcentré, soit à la conjugaison des deux phénomènes précités.

En eau courante, l'orientation de la lamination semble conditionnée par la hauteur d'eau au-dessus du dépôt, où elle peut affleurer, donc, par les paramètres influant sur elle.

4. *Leçon à tirer.* — Ces expériences en canal sont à comparer à celles de Guy [3] et Williams [4] ayant pour objet l'étude de la configuration du dépôt en fonction de ces paramètres et non de sa structure, bien que quelques observations sur elle figurent dans leurs comptes rendus. Il serait donc nécessaire d'étudier, dans des canaux plus grands, les variations de la structure en fonction de ces paramètres, en sédimentation continue. Modélisant une sédimentation fluviatile, on pourrait ainsi mieux connaître la genèse de la structure des dépôts correspondants, tels qu'ils furent par exemple observés par McKee [5], et plus généralement, approfondir notre connaissance de la sédimentation laminaire.

Note reçue le 8 février 1988, acceptée le 16 février 1988.

RÉFÉRENCES BIBLIOGRAPHIQUES

[1] G. BERTHAULT, *C. R. Acad. Sci. Paris*, 303, série II, 1986, p. 1569-1574.
[2] M. CAMPBELL et W. C. BAUER, *Chemical Engineering*, 73, 1966, p. 179-185.
[3] H. P. GUY, D. B. SIMONS et E. V. RICHARDSON, *U.S. Geol. Surv*, Prof Paper 462-1, 1967, 96 p.
[4] G. P. WILLIAMS, *U.S. Geol. Surv*, Prof. Paper 562-B, 1967, 31 p.
[5] E. MCKEE, *Journal of Sedimentary Petrology*, 37, 1967, p. 820-851.

28, *boulevard Thiers*, 78250 *Meulan*.

SÉDIMENTOLOGIE. — *Expériences sur la lamination des sédiments par granoclassement périodique postérieur au dépôt. Contribution à l'explication de la lamination dans nombre de sédiments et de roches sédimentaires.* Note de **Guy Berthault,** présentée par Georges Millot.

Ces expériences montrent que, en eau calme, le dépôt en continu d'un sédiment hétérogranulaire, donne naissance à des *laminae*, donnant l'illusion de lits successifs, mais résultant en fait d'un granoclassement périodique : leur épaisseur semble indépendante de la vitesse de sédimentation, mais croît avec l'écart des tailles extrêmes des particules sédimentaires. En présence d'un courant d'eau horizontal, on voit des couches fines laminées superposées se développer latéralement dans le sens du courant.

SEDIMENTOLOGY. — Experiments on lamination of sediments, resulting from a periodic graded-bedding subsequent to deposit. A Contribution to the explanation of lamination of various sediments and sedimentary rocks.

These sedimentation experiments have been conducted in still water with a continuous supply of heterogranular material. A deposit is obtained, giving the illusion of successive beds or laminae. *These* laminae *are the result of a spontaneous, periodic and continuous grading process, which takes place immediately, following the deposit of the heterogranular mixture. The thickness of the* laminae *appears to be independent of the speed of sedimentation but increases with extreme differences in the size of the particles in the mixture. Where an horizontal current is involved, thin laminated superposed layers developping laterally in the direction of the current are observed.*

I. INTRODUCTION. — Les *laminae* sont traditionnellement définies par les géologues comme des strates de faible épaisseur, inférieure au centimètre. Le grand traité de Augustin Lombard [1], donne les définitions suivantes : « Le litage groupe l'ensemble des structures qui caractérisent les roches sédimentaires à l'intérieur d'une strate. C'est la disposition interne des strates suivant des niveaux lithologiquement distincts, les lits ou *laminae* (p. 147) ». « Une strate est une unité de sédimentation comprise entre deux surfaces limites. Elle consiste en un dépôt de sédiments de structures diverses mais accumulé pendant une phase continue (p. 166) ». Au sujet de la genèse, Lombard [1] écrit : « L'origine des *laminae* planes et parallèles est attribuée à des courants lors du dépôt (p. 148) ». « Les répétitions du granoclassement dans une strate, semblent résulter de pulsations successives dans l'écoulement de la masse du sédiment (p. 158) ». Toutefois Lombard [1] remarque : « Kuenen (1966) a reproduit ces *laminae* sans faire intervenir des pulsations de courants; elles se forment pendant des décélérations (p. 248) ».

Je me suis demandé si la présence d'un courant était indispensable à la formation des *laminae* et si celles-ci ne pouvaient pas résulter également d'une sédimentation continue, même en eau calme, et non pas d'un dépôt couche par couche.

II. EXPÉRIENCES FONDAMENTALES. — Pour éprouver cette hypothèse, j'ai réalisé trois expériences très simples.

1. J'ai fait un mélange composé en volume de 25 % de sable dont le calibre est compris entre 0,3 et 0,4 mm, coloré au bleu de méthylène, et de 75 % de poudre siliceuse dont le calibre varie de 20 à 80 μm. J'ai alors versé le *mélange à sec*, en 10 mn, dans une allonge à robinet d'une capacité de 2 l. La figure 1 montre que se forme dans l'allonge un cône de déjection qui résulte de la chute constante du mélange, et qui monte dans le ballon. *Simultanément* apparaissent à la base du cône, des séquences granoclassées sensiblement horizontales, de sable bleu à la base, surmonté de poudre siliceuse de 2,5 mm d'épaisseur environ. Un rapprochement saisissant peut être fait avec l'écoulement à sec, de mélanges de poudres [2]. Il est montré expérimentalement une ségrégation des particules de même calibre.

0249-6305/86/03031569 $ 2.00

2. 5 kg de ce même mélange sont placés dans l'entonnoir d'un distributeur à vis qui permet l'écoulement continu du mélange à vitesse variable, dans une éprouvette à pied de 2 l remplie d'eau. A la vitesse de 140 g/h, 400 g de mélange s'écoulent. On obtient un dépôt laminé. L'épaisseur des *laminae* est sensiblement constante et de 2,5 mm environ. Une coupe pratiquée dans le dépôt asséché montre les *laminae*.

3. Pour mieux observer le mécanisme lui-même de la lamination, l'expérience précédente a été refaite, mais l'eau fut également colorée au bleu de méthylène.

La figure 2 montre que la partie tout à fait supérieure du dépôt est plus claire que le dépôt lui-même. Elle forme un anneau constitué en majorité de poudre siliceuse, au sein de laquelle on voit les grains de sable bleus s'enfoncer. Au fur et à mesure que cet anneau s'épaissit, un lit mince de sable bleu apparaît en son sein. Il constitue la base d'une nouvelle *lamina*. Et ainsi de suite.

Telle est la genèse de cette lamination, qui résulte bien d'une ségrégation de particules de même calibre au sein du mélange déposé. Il s'agit d'un *granoclassement dans le dépôt lui-même*, après qu'il fut sédimenté, et non d'une superposition de couches.

III. Étude des variations de l'épaisseur des *laminae* avec la vitesse de sédimentation. — Sont utilisés : un sable de calibre compris entre 0,135 et 0,400 mm, coloré au bleu de méthylène et une poudre siliceuse calibrée entre 20 et 40 μm.

1. *Variation de la vitesse de sédimentation de la poudre siliceuse.* — Dans une éprouvette de 2 l, sont mis successivement, en suspension dans l'eau, des lots de 50, 100, 200 et 300 cm^3 de poudre siliceuse. Le temps de sédimentation croît en fonction de ces volumes en suspension. Dans chacune de ces suspensions, on laisse s'écouler de l'allonge, un même volume de 80 cm^3 de sable, en un même temps de 5 mn. L'épaisseur des *laminae* reste constante, d'environ 2,5 mm.

2. *Variation de la vitesse de sédimentation du sable.* — Une même suspension de 200 cm^3 de poudre siliceuse dans 2 l d'eau, reçoit successivement 40, 80 et 120 cm^3 de sable en 5 mn. L'épaisseur des *laminae* produites reste invariable, d'environ 2,5 mm.

3. *Variations simultanées des vitesses de sédimentation du sable et de la poudre siliceuse.* — On laisse s'écouler un mélange composé de 25% de sable et de 75% de poudre siliceuse, du distributeur à vis, dans une éprouvette de 2 l, remplie d'eau, à la vitesse de 140 g/h, puis à vitesse double et triple. La figure 3 montre que l'épaisseur des *laminae* est restée constante.

4. *Première conclusion.* — L'épaisseur des *laminae* est indépendante de la vitesse de sédimentation, dans les limites expérimentales.

IV. Variation de l'épaisseur des *laminae* avec le calibre des particules. — 1. *Variation avec le calibre des grosses particules.* — Une même suspension de 200 cm^3 de poudre siliceuse calibrée entre 20 et 80 μm, dans une éprouvette de 2 l d'eau, reçoit en 5 mn, successivement 100 cm^3 de sable de calibre croissant. L'épaisseur des *laminae* croît avec le calibre S, de la façon suivante : $0{,}125 < S < 0{,}160$ mm : 2 mm; $0{,}200 < S < 0{,}250$ mm : 2 mm; $0{,}315 < S < 0{,}400$ mm : 2,5 mm; $0{,}500 < S < 0{,}630$ mm : 2,7 mm; $0{,}630 < S < 0{,}800$ mm : 3 mm; $0{,}800 < S < 1$ mm : non mesurable.

2. *Variation avec le calibre de la poudre fine.* — On laisse s'écouler en 5 mn, successivement, six mélanges composés de 100 cm^3 d'un même sable calibré entre 0,3 et 0,4 mm, et de 200 cm^3 de poudres siliceuses et sables, de calibre croissant. L'épaisseur des *laminae* croît avec le calibre de la poudre fine, mais faiblement de la façon suivante : $S < 4$ μm :

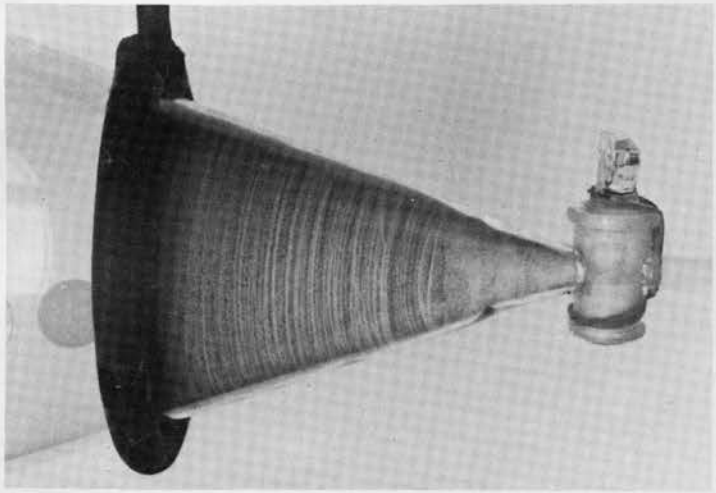

Fig. 1. – Laminations résultant d'un écoulement à sec.
Fig. 1. – Laminations resulting from flowing of dry sediment.

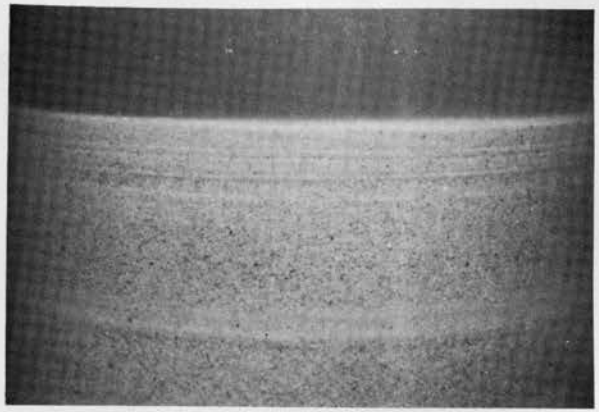

Fig. 2. – Laminations résultant d'un écoulement dans l'eau.
Fig. 2. – Laminations resulting from flowing in water.

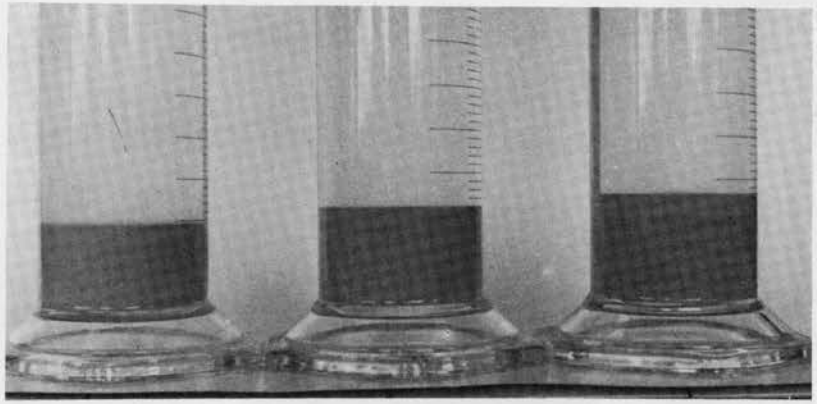

Fig. 3. – L'épaisseur des *laminae* est indépendante de la vitesse de sédimentation.
Fig. 3. – The thickness of laminae *is independent of the speed of sedimentation.*

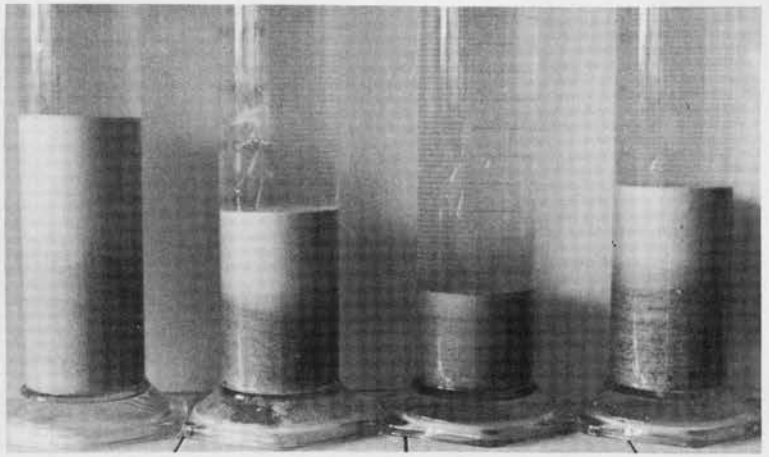

Fig. 4. – L'épaisseur des *laminae* croît avec l'écart extrême des tailles des particules.
Fig. 4. – The tickness of laminae *increases with wide difference in the size of the particles.*

Fig. 5. – Échantillon de diatomite.

Fig. 5. – Sample of diatomite.

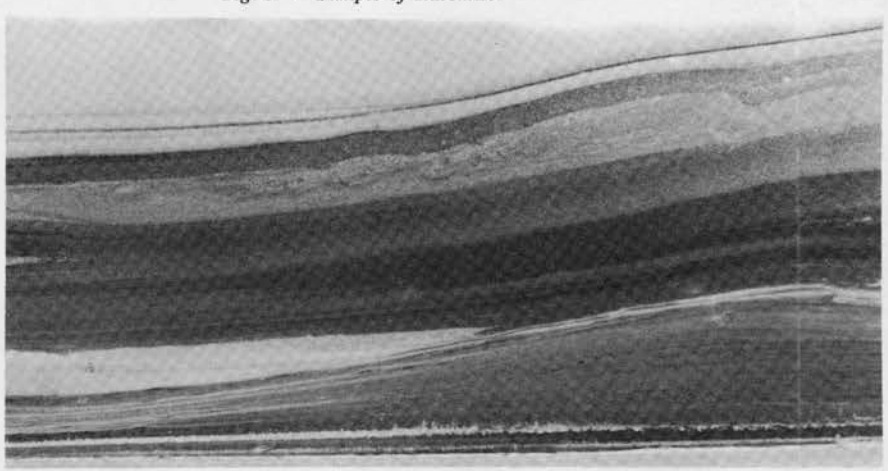

Fig. 7. – Laminations résultant d'un courant d'eau latéral.

Fig. 7. – Laminations resulting from a lateral water flow.

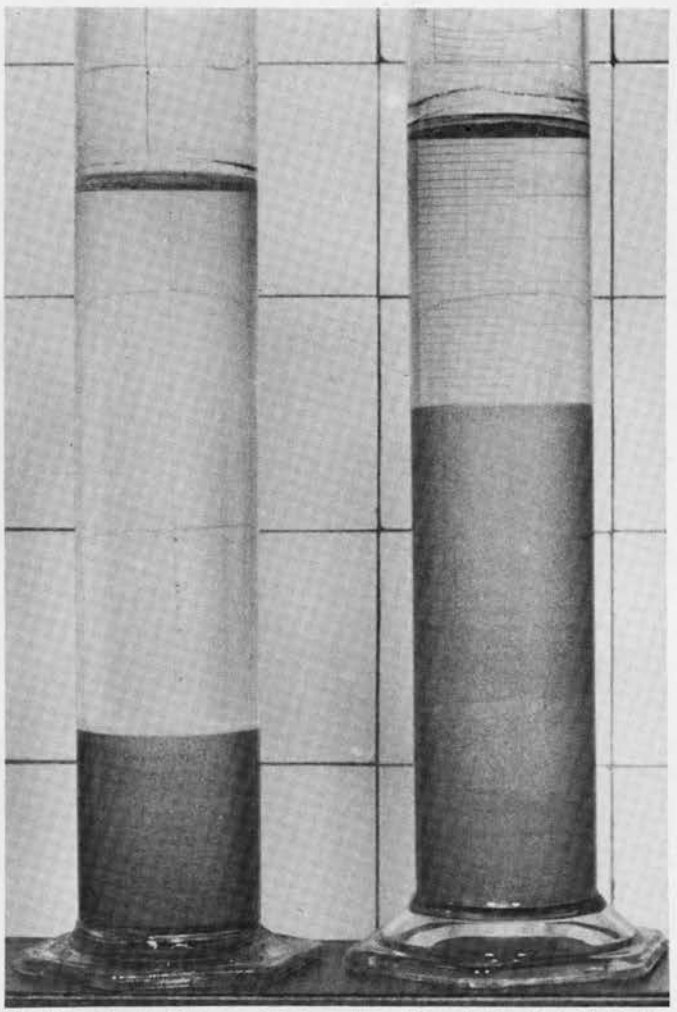

Fig. 6. – Laminations produites par la resédimentation de la diatomite.

Fig. 6. – Laminations resulting from the resedimentation of the diatomite.

2,5 mm; $20<S<40$ µm : 3,5 mm; $63<S<80$ µm : 2,5 mm; $80<S<100$ µm : 2,5 mm; $125<S<160$ µm : 2,7 mm; $200<S<250$ µm : 2,7 mm.

3. *Variation avec l'écart des tailles extrêmes des particules de sable.* — On laisse s'écouler de l'allonge, des sables dont l'écart croît avec la taille des grosses particules, celle des petites demeurant constante. La figure 4 montre la croissance de l'épaisseur des *laminae* avec l'écart, selon les données suivantes : $4\ \mu m<S<0{,}4$ mm : 5 mm; $4\ \mu m<S<0{,}63$ mm : 6 mm; $4\ \mu m<S<0{,}8$ mm : 8 mm; $4\ \mu m<S<1$ mm : 1 cm. Trois essais avec des écarts supérieurs : 1,25, 1,6 et 2 mm, ont produit une lamination visible mais irrégulière.

4. *Deuxième conclusion.* — L'épaisseur des *laminae* croît avec l'écart des tailles extrêmes des particules.

V. Expérimentation sur des roches sédimentaires naturelles laminées. — Nombre de sédiments, fluviatiles et marins, et de roches sédimentaires naturelles, présente cet aspect microstratifié que l'on désigne de noms divers : *laminae*, lamines, laminites, varves, sous varves, etc. Et ces types de lamination sont attribués à des dépôts successifs effectués couche par couche. Une question se pose aussitôt : certaines de ces *laminae* naturelles ne sont-elles pas explicables par le mécanisme ici démontré? Ce pourquoi notre méthode expérimentale est appliquée aux roches sédimentaires naturelles suivantes :

1. *Un sable de Fontainebleau bariolé présente une lamination de l'ordre de 3 mm.* — Effrité, il montre une granulométrie comprise entre 0,1 et 0,3 mm. Placé dans le distributeur à vis, on le laisse s'écouler à la vitesse de 50 g/h dans 2 l d'eau. La lamination originelle est reproduite, régulière, et avec une épaisseur sensiblement égale.

2. *Une diatomite d'Auvergne est laminée* (fig. 5). — Effritée, elle est passée au cyclone pour séparer les particules d'un calibre supérieur à 80 µm, avec vérification au microscope que les tests ne sont pas brisés. Colorée, la fraction la plus grosse est mélangée à la fraction fine et livrée au distributeur à vis avec trois vitesses : 50, 100, puis 150 g/h pendant des temps identiques. La lamination apparaît dans le dépôt et ne varie pas avec la vitesse d'écoulement. La lamination originelle est reproduite avec une épaisseur comparable (*fig.* 6).

La réponse à notre question est donc affirmative nonobstant les cas où il est démontré que la lamination résulte de dépôts saisonniers [3].

VI. Incidence d'un courant latéral. — A une extrémité d'un aquarium de dimensions : 80, 25 et 40 cm, on adapte, au niveau de l'eau du récipient rempli, une platine qui reçoit à la fois un courant d'eau horizontal, prélevé dans l'aquarium par une pompe à faible débit, et la même diatomite tombant à 80 g/h.

La sédimentation a duré 15 jours, en continu, sauf une interruption. On voit de fines couches laminées superposées (*fig.* 7) se développer latéralement dans le sens du courant, qui se distinguent par une gradation de teintes due visiblement à des charges différentes de grosses particules colorées.

VII. Conclusions. — Ces expériences étudient le dépôt en continu et en eau calme, d'un sédiment hétérogranulaire. 1. Il est observé que le matériel déposé s'organise spontanément, aussitôt après son dépôt, en lamines granoclassées périodiques, qui donnent l'illusion de minces couches successives. 2. L'un des traits principaux de ces lamines qui s'organisent dans le dépôt lui-même, est leur régulière périodicité. 3. L'épaisseur de ces lamines se mesure en millimètres; elle ne dépend pas de la vitesse de sédimentation, mais de l'écart des tailles extrêmes des particules mélangées. 4. Lorsque le dépôt se produit

dans un courant d'eau, le phénomène de lamination après dépôt se produit également. Le courant en modifie la géométrie, mais il n'en est pas la cause. 5. Ces lamines granoclassées périodiques ressemblent aux lamines ou varves observées dans la nature, qui sont interprétées comme une superposition de couches saisonnières ou annuelles. Mais leur origine est toute différente : structuration périodique après dépôt. 6. La question se pose d'étudier nombre de formations laminées ou varvées, en fonction de ce mécanisme de structuration physique, obtenu expérimentalement.

VII. CONCLUSIONS. — *The continuous deposit of a heterogranular sediment in still water was studied. 1. It was noted that the deposited material organised itself immediately after deposition into periodic graded laminae giving the appearance of successive beds. 2. One of the more striking features of these laminae formed in the sediment itself was their regular periodicity. 3. The thickness of the laminae is measured in millimetres. It is independent of the speed of sedimentation and varies according to the extreme difference in the size of the mixed particles. 4. When deposition took place in a water flow, the lamination phenomenon was also observed. The geometry of lamination was modified by the water flow, but the latter was not the cause of the modification. 5. The periodic graded laminae were similar to the laminae or varves observed in nature which are interpreted as a superposition of seasonal or annual beds. Their origin, however, was quite different arising from periodic structuring after deposit. 6. The question now is to study a number of laminated or varved formations in relation to this mechanism for physical structuring obtained from experimentation.*

The complete translation in english of the reprint can be obtained by request from the author.

Reçue le 3 novembre 1986.

RÉFÉRENCES BIBLIOGRAPHIQUES

[1] A. LOMBARD, *Séries sédimentaires, Genèse, Évolution*, Masson, Paris, 1972, 425 p.
[2] H. CAMPBELL et W. C. BAUER, *Chemical Engineering*, 73, 1966, p. 179-185.
[3] J. C. GALL, *Mém. Serv. Carte géol. Als. Lorr.*, 34, 1971, p. 126-128.

28, *boulevard Thiers*, 78250 *Meulan*.